UNIVERSIDADE D
COIMBRA

Akel Ferreira Kanaan

IONIC LIQUID BASED FUNCTIONALIZED MATERIALS FOR THE DEVELOPMENT OF MULTI-RESPONSIVE ELECTROACTIVE HYDROGELS

Tese no âmbito do doutoramento em Engenharia Química orientada pelo Professor Doutor Hermínio José Cipriano de Sousa e Doutora Ana Maria Antunes Dias e apresentada ao Departamento de Engenharia Química da Faculdade de Ciências e Tecnologia da Universidade de Coimbra

Novembro de 2020

Akel Ferreira Kanaan

Ionic liquid based functionalized materials for the development of multi-responsive electroactive hydrogels

A Thesis submitted for the degree of Doctor in Philosophy in Chemical Engineering

Coimbra 2020

UNIVERSIDADE D
COIMBRA

Financial support by:

"Do not be afraid of your difficulties. Do not wish you could be in other circumstances than you are. For when you have made the best of an adversity, it becomes the stepping stone to a splendid opportunity."
– Helena Blavastky

"*Eu vivo na Terra, no presente, e não sei o que sou. Sei que não sou uma categoria. Não sou uma coisa, um nome. Pareço ser um verbo, um processo evolutivo, uma função integral do Universo."*
– Richard B. Fuller

"Il faut bien que je supporte deux ou trois chenilles
si je veux connaître les papillons."
– Antonie de Saint-Exupéry

Acknowledgements/ Agradecimentos

Ao meu orientador Doutor Hermínio C. de Sousa por ter depositado confiança e ter acreditado em meu trabalho. Gostava de agradecer ao encorajamento, motivação, princípios e visão profissional que o senhor passou para mim desde o princípio deste doutoramento.

À minha coorientadora Doutrora Ana M. A. Dias pela grande atenção e dedicação de tempo depositadas em mim na realização deste trabalho. Obrigado pela paciência e consentimento para comigo durante todas nossas reuniões nas quais eu lhe apresentava somente “mistérios”.

A todos profissionais que ajudaram a mim e aos meus orientadores a concretizar esta tese, nomeadamente Doutora Ana Paula Piedade, Doutor Christopher Brett, Doutora Madalina Barsan, Doutora Carmen Alvarez-Lorenzo e Doutor Angel Concheiro.

À minha família pelo enorme amor recebido o qual foi fundamental para minha estabilidade emocional durante todo o doutoramento. Sou grato a vocês pelos ensinamentos que me foram passados, carinho, atenção e dedicação.

Ao meu companheiro André Marques por todo o companheirismo, amor, apoio e amizade recebidos os quais fortaleceram-me imenso nesta minha fase de vida.

Aos meus queridos amigos Camila Dariva, Manuel Rodrigues, Sónia Ribeiro e Roseli Dariva por todo companheirismo, amor, carinho e apoio nas horas mais difíceis e nas menos difíceis também.

Aos meus amigos e companheiros desta grande jornada Sofia Marceneiro, Luísa Filipe, Rita Chin, Rafael Botelho e Usman Syed por todo o companheirismo, apoio e momentos de descontração que foram essenciais para meu desempenho profissional.

Aos meus amigos do yoga Miriam Jorge, Suzana Soares, Marco Miranda, Sissi Gomes, Cristina, Maria João, Maurem, Inês Gaspar, Eduardo e Gonçalo Sousa por todo carinho, fraternidade, apoio espiritual e filosófico que me proporcionaram.

Aos alunos e colegas de laboratório Gustavo Marques, Andreia Madeira, Andreia Antunes, Bárbara Valente e Patrícia Ribeiro pelo aprendizado compartilhado.

Aos meus amigos do departamento de engenharia mecânica Catarina Pinho, Micaela Sousa, Cristina Borges e Patrícia Rodrigues por todo apoio moral e emocional concedido.

Aos técnicos José Santos (senhor "Zé") e Manuel Leitão da Silva por toda ajuda na confeção de todas as "geringonças" que foram necessárias em meus experimentos.

Às profissionais Maria João, Ana Borba, Luciana Tomé, Patrícia Coimbra, Gláucia Medeiros, Madi Gica e Joana Gonçalves por toda ajuda concedida.

Ao CNPq pela Bolsa de Doutoramento concedida (200808/2014-1).

Ao departamento de engenharia química (DEQ) pela disponibilização do espaço e dos equipamentos necessários para o desenvolvimento desta tese.

Um agradecimento especial para a força cósmica Universal da fonte criadora a qual permitiu-me desfrutar desta experiência única e também trilhar este caminho com força de espírito e determinação.

De uma maneira geral, agradeço a todos por tudo que de alguma forma contribuíram para minha evolução e amadurecimento como profissional e como pessoa.

Abstract

The main objective of the present thesis was the development and characterization of novel electroactive ionic liquid-based polycationic hydrogels. These materials were obtained by the functionalization of natural-origin and/or synthetic polymers with an ionic liquid-based vinyl monomer (functionalized at the cation) by two different approaches, namely by the formation of semi-interpenetrating polymer networks (s-IPNs) and by copolymerization with a non-charged comonomer. Through this doctoral work, three different multi-responsive systems were developed targeting a broad range of applications, such as, drug delivery devices, bioseparators, soft actuators, tissue engineering scaffolds, iontophoretic patches and wound dressings.

The first approach was employed to obtain multi-responsive s-IPNs hybrid structures based on natural polymers (starch and chitosan) and homopolymers/copolymers of poly(1-butyl-3-vinylimidazolium chloride) (poly(BVImCl) and poly(2-hydroxyethyl methacrylate-co-1-butyl-3-vinylimidazolium chloride) (poly(HEMA-co-BVImCl)). In the case of the starch-based s-IPNs, results demonstrated that the sorption/release capacity of these hydrogels towards L-tryptophan (used as a model biomolecule) could be adjusted depending on the intensity of the applied DC voltage and/or sorption/release medium. It was also confirmed that the process employed to dry the hydrogels (oven and freeze-drying) has a major influence on the conductivity of the materials and that freeze-drying induced higher conductivity values. Furthermore, biological tests demonstrated that the prepared s-IPNs were able to guarantee fibroblasts viability. These newly obtained hybrid materials demonstrated to have potential to be employed for bio-separation processes and for the sustained delivery of specific charged-biomolecules. In the case of the chitosan-based s-IPNs it was demonstrated that the prepared hybrid hydrogels presented enhanced mechanical

properties, water swelling capacities (at different pH and ionic strengths) and sorption capacities towards charged molecules when compared to pristine chitosan. Obtained s-IPN hydrogels also demonstrated to have modulated lidocaine hydrochloride permeation/delivery profiles at low current densities (0.56 mA/cm^2) and as a function of their charge density. Moreover, biological tests showed that the prepared s-IPN hydrogels were non-hemolytic and presented potential hemostatic capability. These "smart" s-IPNs presented advantageous properties for the design of topical iontophoretic patches and/or hemostatic agents.

The second approach was employed to obtain multi-responsive electro-actuating hydrogels based on poly(HEMA-co-BVImCl) copolymers. Studies were performed to evaluate the influence of surface properties on the actuating behavior of the hydrogels in different aqueous media, with different pH and ionic strength values. The different surface properties were obtained by simply employing different mold subtracts, with different hydrophobicities (namely Teflon® and glass) during the copolymer free radical polymerization in aqueous media. Obtained results demonstrated that hydrogels synthesized on Teflon® molds presented the highest electro-actuation capacity in aqueous media, with equivalent bending motion on both directions according to the polarization applied. Moreover, it was also noticed that hydrogels surface charge density and water swelling capacity could be modulated depending on the type of mold utilized during polymerization. Resulting soft stimuli-responsive materials can be regarded as "smart" platforms for the design of soft actuators and cell culture scaffolds for biomedical applications.

Overall, this PhD thesis allows concluding that the functionalization of natural and/or synthetic polymers with ILs represents a viable and efficient strategy for the

development of multi-responsive electroactive materials for applications in biomedicine, (bio)separation and electrochemistry.

Keywords: ionic liquid-based copolymers; ionic liquid-based s-IPNs; polysaccharides; stimuli-responsive hydrogels; electro-active hydrogels; electro-assisted sorption/release; electro-mechanical actuation.

Resumo

O objetivo principal desta tese foi o desenvolvimento e caracterização de novos hidrogéis eletroativos policatiónicos à base de líquidos iónicos. Esses materiais foram obtidos pela funcionalização de polímeros de origem natural e/ou sintéticos com um monómero vinílico à base de líquidos iónico (funcionalizados no catião) por meio de duas diferentes abordagens, nomeadamente redes poliméricas semi-interpenetradas (s-IPNs) e copolimerização com um comonómero não carregado. Durante a realização do trabalho, foram desenvolvidos três sistemas multi-responsívos diferentes visando uma vasta gama de aplicações, por exemplo, dispositivos para a entrega de fármacos, bioseparadores, atuadores *soft*, *scaffolds* para engenharia de tecidos, pensos para iontoforese e para tratamento de feridas.

A primeira abordagem consistiu na obtenção de s-IPNs híbridos multi-responsívos à base de polímeros naturais (amido e quitosano) e homopolímeros/copolímeros de poli(cloreto de 1-butil-3-vinilimidazólio) (poli(BVImCl) e poli(metacrilato de 2-hidroxietila-co-cloreto de 1-butil-3-vinilimidazólio) (poli(HEMA-co-BVImCl)). No caso dos hidrogéis s-IPNs à base de amido, os resultados demonstraram que a capacidade de sorção/entrega de L-triptofano, usado como biomolécula modelo, poderia ser otimizada consoante a diferença de potencial aplicada e/ou o tipo de meio utilizado na sorção/libertação. O processo de secagem utilizado nos hidrogéis (secagem em estufa e liofilização), provou ter uma influência significativa na condutividade dos materiais estudados, sendo que os foram sujeitos ao processo de liofilização apresentaram valores superiores de condutividade. Concomitantemente, a viabilidade de fibroblastos na presença dos s-IPNs foi comprovada com recurso a testes biológicos. Desta forma, os materiais híbridos e inovadores desenvolvidos nesta abordagem demonstraram potencial para serem

utlizados em processos de biosseparação e para entrega contínua de biomoléculas carregadas específicas. No caso dos s-IPNs à base de quitosano, foi demonstrado que os hidrogéis híbridos desenvolvidos apresentaram melhores propriedades mecânicas, capacidades de entumecimento em água (em diferentes condições de pH e força iónica) e capacidades de sorção para moléculas carregadas, quando comparados com o quitosano puro. Os s-IPNs exibiram perfis modulares de permeação/entrega de lidocaína, a baixas intensidades de corrente (0.56 mA/cm^2), em função da respetiva densidade de cargas. Além disso, após testes biológicos, os hidrogéis s-IPN provaram ser não-hemolíticos e hemostáticos. Estes s-IPNs "inteligentes" apresentaram propriedades vantajosas para a preparação de pensos tópicos para iontoforese e/ou pensos hemostáticos.

A segunda abordagem estudada foi baseada na obtenção de copolímeros electroactuators híbridos multi-responsívos à base de hidrogéis de poli(HEMA-co-BVImCl). A influência das propriedades de superfícies no comportamento de atuação dos hidrogéis em diferentes meios aquosos (com diferentes valores de pH e força iónica), foi avaliada. Diferentes propriedades de superfície foram obtidas pela simples utilização de diferentes moldes com hidrofobicidade distintas, nomeadamente Teflon® e vidro, durante a copolimerização por polimerização radicalar livre, em meio aquoso. Os resultados demonstraram que os hidrogéis preparados em moldes de Teflon® apresentaram superior capacidade de eletroatuação em meio aquoso, com atuação mecânica equivalente em ambas direções, de acordo com a polaridade aplicada. Para além disso, foi também verificado que a densidade de carga na superfície dos hidrogéis e a capacidade de entumecimento em água pode ser modulada de acordo com o tipo de molde utilizado durante a polimerização. Os materiais responsivos a estímulos podem

ser equiparados a plataformas “inteligentes” para a produção de atuadores *soft* e *scaffolds* para cultura celular em aplicações biomédicas.

Em suma, a presente tese de doutoramento permitiu concluir que a funcionalização de polímeros naturais e/ou sintéticos, com ILs, representa uma estratégia viável e eficiente para o desenvolvimento de materiais eletroativos multi-responsívos para aplicações na biomedicina, biosseparação e eletroquímica.

Palavras-chave: copolímeros à base de líquidos iónicos; s-IPNs à base de líquidos iónicos; polissacarídeos; hidrogéis multi-responsívos; hidrogéis eletroativos; sorção/libertação eletro-assistida; atuação eletromecânica.

List of publications

The thesis is based on the following papers:

Kanaan, A. F.; Barsan, M. M.; Brett, C. M. A.; Alvarez-Lorenzo, C.; Concheiro, A.; de Sousa, H. C.; Dias, A. M. A. Sustainable electro-responsive semi-interpenetrating starch/ionic liquid copolymer networks for the controlled sorption/release of biomolecules. Published in ACS Sustainable Chemistry & Engineering, 2019 (DOI: 10.1021/acssuschemeng.9b01071).

Kanaan, A. F.; Piedade, A. P.; de Sousa, H. C.; Dias, A. M. A. Effect of mold assemblies-induced interfaces in the mechanical actuation of electro-responsive ionic liquid-based polycationic hydrogels. Published in Applied Materials Today, 2020 (DOI:10.1016/j.apmt.2020.100711).

Kanaan, A. F.; Piedade, A. P.; de Sousa, H. C.; Dias, A. M. A. Semi-interpenetrating chitosan/ionic liquid polymer networks as electro-responsive biomaterials for potential wound dressings and iontophoretic applications. Submitted to Materials Science and Engineering: C, 2020.

Contribution to meetings

Kanaan, A. F.; Barsan, M. M.; Brett, C. M. A.; Alvarez-Lorenzo, C.; Concheiro, A.; de Sousa, H. C.; Dias, A. M. A. Semi-interpenetrating polymer networks based on starch/ionic liquid copolymers for the electro-assisted adsorption of biomolecules. ILMAT IV - 4. International Conference on Ionic Liquid-based Materials. Santiago de Compostela, Spain, October 24th to 27th, 2017.

Kanaan, A. F.; Valente, B. S. R.; de Sousa, H. C.; Dias, A. M. A. Superabsorbent polyelectrolytes using ionic liquids electro-responsive comonomers. ILMAT IV - 4. International Conference on Ionic Liquid-based Materials. Santiago de Compostela, Spain, October 24th to 27th, 2017.

Dias, A. M. A.; **Kanaan, A. F.**; Marceneiro, S.; Alvarez-Lorenzo, C.; Concheiro, A.; Brett, C. M. A.; de Sousa, H. C. Different strategies for the functionalization of biopolymers with ionic liquids for the development of multi-responsive biomaterials, ISBMS - International Symposium on Bioinspired Macromolecular Systems, Aveiro, Portugal, November 6th to 8th, 2017.

Kanaan, A. F.; Barsan, M. M.; Brett, C. M. A.; Alvarez-Lorenzo, C.; Concheiro, A.; Piedade, A. P.; de Sousa, H. C.; Dias, A. M. A. Ionic liquid-based multi-stimuli responsive materials for biomedical applications, Encontro com a Ciência e Tecnologia em Portugal, Lisboa, Portugal, July 8th to 10th, 2019.

Kanaan, A. F.; Ribeiro, P.; Piedade, A. P.; de Sousa, H. C.; Dias, A. M. A. "Smart" electro-active hydrogels based on ionic liquid copolymers for biomedical applications. Noite Europeia dos Investigadores, Coimbra, Portugal, September 27th, 2019.

List of contents

List of figures

List of tables

List of acronyms

^{13}C-NMR	Solid-state ^{13}C nuclear magnetic resonance
AB	Acetate buffer
AC	Alternating current
ACD	Acid citrate-dextrose solution
AIBA	2,2'-Azobis (2-methylpropionamidine) dihydrochloride
AIBN	2,2′-Azobis(2-methylpropionitrile)
APIs	Active pharmaceutical ingredients
APS	Ammonium persulfate
BB	Bicarbonate buffer
BCI	Blood clotting index
BG	Bromocresol green
$BVIm^+$	1-butyl-3-vinylimidazolium cation
BVImCl	1-butyl-3-vinylimidazolium chloride
CFU	Colony formation units
Cl^-	Chloride anion
CPE_{dl}	Non-ideal double layer capacitance
CPE_{pol}	Polarization capacitance
CS	Low molecular weight chitosan
D_1	Short-time diffusion coefficient
D_2	Long-time diffusion coefficient
DC	Direct current
DCS	Chitosan deprotonated with NaOH
DDA	Degree of deacetylation

DMEM	Dulbecco’s modified Eagle’s medium
DMTA	Dynamic mechanic thermal analysis
DSC	Differential scanning calorimetry
EA	Elemental analysis
EAP	Electroactive polymer
EDL	Electrical double layer
EIS	Electrochemical impedance spectroscopy
EtOH	Ethanol
FTIR-ATR	Attenuated total reflection Fourier transform infrared
full-IPN	Full-interpenetrating polymer networks
G^*	Complex shear modulus
G’	Storage modulus
G’’	Loss modulus
G-G	Poly(HEMA-co-BVImCl) samples prepared in between glass molds
Hb	Hemoglobin
HEMA	2-hydroxyethyl methacrylate
I	Ionic strength
ILs	Ionic liquids
IPNs	Interpenetrating polymer networks
IUPAC	International Union of Pure and Applied Chemistry
k	Kinetic constant
l	Thickness of hydrogel sample
LH	Lidocaine hydrochloride monohydrate

M_∞	Absolute cumulative amount of drug released at infinite time
MBA	*N,N'*-methylenebis(acrylamide)
MCM-41	Mesostructured silica nanoparticles
MO	Methyl orange
M_t	Absolute cumulative amount of drug released at time *t*
n	Release exponent
NTf_2^-	Bis(trifluoromethylsulfonyl)imide anion
PAc	Polyacetylene
PANI	Polyaniline
PB	Phosphate buffer
PBS	Phosphate buffered saline
PILs	Poly(ionic liquids)
PMMA	Poly(methyl methacrylate)
pNiPAAm	Poly(*N*-isopropylacrylamide)
poly(HEMA)	Polymerized HEMA
poly(HEMA-co-BVImCl)	Copolymer of HEMA and BVImCl
PPy	Polypyrrole
PTh	Polythiophene
PVDF	Poly(vinylidene fluoride)
RBCs	Red blood cells
R_{ct}	Charge-transfer resistance
RH	Relative humidity
RTILs	Room Temperature Ionic Liquids
R_Ω	Cell resistance

SEM-EDX	Scanning electron microscope coupled with energy dispersive X-ray spectroscopy
semi-IPNs/s-IPNs	Semi-interpenetrating polymer networks
s-IPN/CS/Co-PIL	Semi-interpenetrating polymer network based on chitosan functionalized with poly(HEMA-co-BVImCl)
s-IPN/CS/PIL	Semi-interpenetrating polymer network based on chitosan functionalized with poly(BVImCl)
s-IPN/CS/poly(HEMA)	Semi-interpenetrating polymer network based on chitosan functionalized with poly(HEMA)
s-IPN/St0.5	Semi-interpenetrating polymer network based on starch (0.5 % w/v) functionalized with poly(HEMA-co-BVImCl)
s-IPN/St1.0	Semi-interpenetrating polymer network based on starch (1.0 % w/v) functionalized with poly(HEMA-co-BVImCl)
St	Starch
t	Time
$T_{5\%}$	Temperature at which the weight loss of the sample is 5% (wt)
tan δ	Loss factor
T_g	Glass transition temperature
T-G	Poly(HEMA-co-BVImCl) samples prepared in between Teflon® and glass molds
TGA	Thermogravimetric analysis

T_{onset}	Temperature at which thermal degradation of the sample starts to occur
T_{peak}	Maximum degradation temperature from DTG curves (obtained from first derivative of weight loss vs temperature)
Triton® X-100	4-(1,1,3,3-Tetramethylbutyl)phenyl-polyethylene glycol
TRIZ	Trizma base buffer
Try	L-tryptophan
T-T	Poly(HEMA-co-BVImCl) samples prepared in between Teflon® molds
WCA	Water contact angle
WSC	Water swelling capacity
WSE	Water swelling equilibrium
Wt_{150^oC}	Weight loss (%) at 150 ºC
WVS	Water vapor sorption
Z_w	Warburg diffusional resistance
θ^o	Bending angle

Scope, motivations, objectives, and thesis organization

According to recent predictions, an exponential increase of the world population is expected in the next few decades, especially from the emerging countries. A fallout of this increase in the global population is the inevitable increase in the number of cases of several diseases that demand proper and specific medical treatment. Biomedicine is a scientific research field that aims to design advanced and task-specific devices to provide better healthcare services. In order to achieve it, the development of new biomedical systems having fast response, low cost, multi-task capability and non-invasive properties is pivotal.

Multi-stimuli responsive hydrogels, often called as “smart” hydrogels, represent a class of materials which can be employed in several biomedical applications, for instance, as controlled drug delivery systems, soft actuators, biosensors, and tissue engineering scaffolds. “Smart” hydrogels can undergo significant physicochemical modifications in response to specific local environmental changes such as electrical current, pH, ionic strength, and temperature. These features allow this class of materials to be employed in distinct and complex environments such as those found in different parts of the human body.

The soft and rubbery nature of hydrogels as well as their high water swelling capacity make them resemble natural tissues. Efforts have been made to develop competitive hydrogels based on natural polymers such as polysaccharides. Nevertheless, and despite of the intrinsic advantages of polysaccharides such as starch and/or chitosan, which include their biocompatibility, biodegradability, non-toxicity, low price etc., the fact is that they present poor thermomechanical properties, and any/slow responsiveness to environment changes. In order to overcome these issues, and to enhance/promote stimuli sensitiveness of these materials, functionalization

strategies (e.g. semi-interpenetrating polymer networks and copolymerization) with ionic liquids can be employed.

Ionic liquids (ILs) represent a group of organic/inorganic salts which have melting temperatures below 100 ºC. They exhibit unique properties such as low vapor pressure, high ionic conductivity and thermal stability. However, ILs may present a certain level of toxicity for human life and for the environment.

Electroactive hydrogels represent a suitable interface between human's metabolic system and electronic devices. The functionalization of biocompatible biopolymers and/or synthetic polymers with ILs represents an efficient approach to design novel electroactive hybrid platforms which are highly attractive to the biomedical and pharmaceutical scientific fields due to their improved physicochemical, thermomechanical, toxicological and multi stimuli-responsive properties. Nevertheless, the functionalization of natural-origin and/or synthetic polymers with ILs targeting biomedical applications still represent a poorly explored research field.

The scientific challenge of this doctoral thesis was the development of electroactive multi-stimuli responsive IL-based copolymers and/or IL-based semi-IPNs and the study of the effects of ILs functionalization on the thermomechanical, toxicological and electroactive properties of the obtained hybrid polycationic materials. To achieve this goal, biocompatible natural and/or synthetic polymers were functionalized with ion conducting vinyl functionalized ionic liquids, envisaging the development of novel electroactive multi-stimuli responsive hydrogels. The subsequent resulting hybrid polycationic hydrogels, containing fixed and pH independent charge density, were electroactive and presented fast response over changes in media's ionic strength, relative humidity and electrical current. This allows them to be employed for different biomedical applications such as controlled drug release/sorption systems,

biosensors, cell growing/differentiation scaffolds, soft actuators, bio-separators, iontophoretic patches and hemostatic wound dressings, etc.

This PhD thesis is divided into five chapters (1–5). Chapter 1 was dedicated to a brief introduction of the main topics covered within this thesis. In summary, it presents the current "State-of-the-Art" of multi-stimuli responsive hydrogels comprising electro-responsive IL-based materials towards electrochemical applications. Their mechanisms of response, main applications, growing interest into the biomedical field and limitations were also highlighted.

Chapter 2 reports the development and characterization of semi-interpenetrating polymer networks (semi-IPNs) of starch and copolymers of poly(HEMA-co-BVImCl). The underlying motivation of this work was to prepare ion conducting and biocompatible hydrogels with modulated electro-assisted sorption/desorption profiles of biomolecules envisaging a broad range of applications, namely as wastewater treatment systems, bioseparators and sustained drug delivery platforms. The key scientific challenges of this work included: i) to analyze the effect of the ionic liquid onto the electro-assisted sorption and desorption capacity of the s-IPNs towards charged biomolecules and onto their cytocompatibility; ii) to study the influence of the amount of ionic liquid and polysaccharide onto the electrical current and ionic strength responsiveness of the developed hydrogels; iii) to study the effect of the drying method (oven-drying and freeze-drying) onto the morphological, physicochemical, electrochemical and stimuli-responsive properties of the synthesized materials.

Chapter 3 was focused on the development and characterization of soft electro-actuators based on crosslinked poly(HEMA-co-BVImCl) copolymer hydrogels. The main objective of this work was to obtain electroactive IL-based copolymers with tunable electro-actuating response and surface properties induced by the type of mold

employed during their synthesis. The key scientific challenges along this work included: i) to evaluate and comprehend the influence of hydrogels surface properties onto their electro-actuating capacity; ii) to evaluate the effect of the chemical nature of the mold substrates employed during free radical polymerization in aqueous media on the properties on the IL-based copolymer hydrogels; iii) to study the mechanical response of the hydrogels under electrical stimulus (with different applied electrical current intensities) and in different aqueous media (with distinct ionic strength values).

Chapter 4 details the development and characterization of multi-responsive semi-IPN hydrogels based on chitosan and poly(BVImCl) or poly(HEMA-co-BVImCl) homopolymers/copolymers. The main objective of this case study was to prepare an electroactive, pH-responsive, hemocompatible and hemostatic hybrid biomaterial envisaging potential biomedical applications, namely as iontophoretic patches and hemostatic dressings. The main scientific challenges of this work included: i) to evaluate the influence of the IL-based homopolymer/copolymers onto the physicochemical, mechanical, electrical and biological properties of chitosan-based hydrogels; ii) to evaluate the electro-assisted permeation/release capacity of the prepared hydrogels towards charged biomolecules under the presence of low current densities.

Finally, Chapter 5 addresses the major conclusions that were drawn from the development of the aforementioned work as wells as suggested future work.

Chapter 1

State of the art

1.1 Innovative stimuli-responsive hydrogels for biomedical applications

Hydrogels are defined as 3D polymeric networks that can absorb (retain) large amounts of water or biological fluids (up to thousands of times their dry weight) which increase their biocompatibility and biodegradability. This capacity also allows hydrogels to act as platforms to carry several molecules, namely drugs, proteins, amino acids, etc. Due to their soft nature and hydrophilic character they have received significant biomedical interest.[1] Hydrogel's porosity and rubbery consistency closely simulates living tissues and contributes to minimize the irritation of biological tissues. Hydrogels are commonly based on natural polymers (e.g. pectin, carrageenan, collagen, chitosan, dextran, agarose, hyaluronic acid, etc.), synthetic polymers (e.g. polyethylene glycol, polyhydroxyethyl methacrylate, polylactic acid, polyacrylic acid, polyvinyl alcohol, polyacrylamide, etc.) and combinations of both natural and synthetic polymers and composites.[1,2] Depending on the route of fabrication, hydrogels can be classified as physical/reversible and chemical/permanent gels. The former results from electrostatic, hydrophobic and Van-der-Waals network interactions while the latter results from covalently crosslinked networks.[3] These soft materials can be further processed in different shapes, such as films, rods, disks, and microparticles, which enables their usage for a variety of applications including contact lenses, wound healing dressings, drug delivery systems, tissue engineering scaffolds and hygiene products.[2-5]

Hydrogels can be formulated to respond to an external stimulus giving rise to an interesting sub-class of hydrogels called "smart" or stimuli-responsive hydrogels which are materials that respond to different external or internal stimuli (e.g. temperature, pH, light and electrical

field) trough changes in their structure (e.g. swelling, shrinking and/or bending).[6] The major advantage of stimuli-responsive hydrogels over conventional ones (non-responsive) is that it is possible to tune/control several of their physicochemical properties by changing the conditions (e.g. pH, ionic strength, temperature, etc.) of the environment in which they will be employed. Figure 1.1 schematizes the stimuli-responsive mechanism of commonly employed "smart" hydrogels. Poly(*N*-isopropylacrylamide) (pNiPAAm) is the classical example of a thermoresponsive hydrogel which exhibit a volume phase transition at approximately 32 ºC.[7,8] Its thermoresponsive mechanism results from hydrophobic and hydrophilic transitions upon heating. When medium temperature is below 32 ºC, hydrogen bond interactions between water molecules and the hydrophilic amide groups of pNiPAAm dominate increasing its water solubility. In contrast, for temperatures above 32 ºC, hydrogen bonds between amide groups and water become weaker leading to the association of pNiPAAm chains through hydrophobic interactions, resulting in the release of water from the hydrogel (phase separation) and consequently, to polymer contraction (deswelling) (Figure 1.1A).

pH-responsive hydrogels (Figure 1.1B) are those that contain weak acidic or basic groups in their chemical structure which originate pH dependent ionizable pendant groups, as for instance poly(acrylic acid)[9] and chitosan.[10] The principle that governs their response lies on the dissociation/association (deprotonation/protonation) of hydrogen ions to specific functional groups (e.g. carboxyl and amine groups), depending on the pH of the media, which alters the osmotic pressure of the hydrogel.[11] Considering a polycationic hydrogel, pendant basic groups (e.g. amine groups) become protonated at acidic media (higher charge density), increasing the electrostatic repulsion among protonated chains. Consequently, the osmotic pressure gradient between the charged polymeric environment and the aqueous environment augments (higher at the aqueous media and lower at the polymeric environment) resulting in

hydrogel swelling as the water molecules (from the aqueous media) diffuse towards the hydrogel in order to balance the osmotic pressure ("dilute" the higher charge density). At alkaline media, amine groups become deprotonated, reducing the osmotic pressure gradient (between the polymeric environment and the aqueous media) resulting in hydrogel deswelling. Finally, for polyanionic hydrogels its swelling/deswelling behavior also follows the osmotic pressure gradient mechanism presented earlier, however in opposite conditions. Pendant acidic groups (e.g. carboxyl groups) become protonated/deprotonated at acid/alkaline environment resulting in hydrogel deswelling/swelling.

In the case of light-responsive hydrogels (Figure 1.1C), they are commonly prepared by the incorporation of light-sensitive functional groups such as azobenzenes that undergo *trans*/*cis* isomerization in the presence of UV light (360/440 nm, respectively).[12] For instance, a given light-responsive hydrogel complexed with *β*-cyclodextrins undergo changes in *β*-cyclodextrins/azobenzenes stacking (upon light irradiation) which lead to reversible structural alterations in the hydrogel's polymeric chains.[7] Consequently, these reversible structural alterations allow to tune the gelation and swelling/deswelling state of the hydrogel. Upon visible light irradiation at 440 nm, loosely held polymeric chains become constraint (due to *β*-cyclodextrins/azobenzenes complex formation) resulting in a polymeric matrix with higher mechanical integrity and lower interchain free volume and thus, lower swelling. At UV light stimulus (360 nm) the *β*-cyclodextrin/azobenzene complex is broken resulting in a polymeric matrix with weak mechanical integrity, higher interchain free volume and thus, higher swelling.

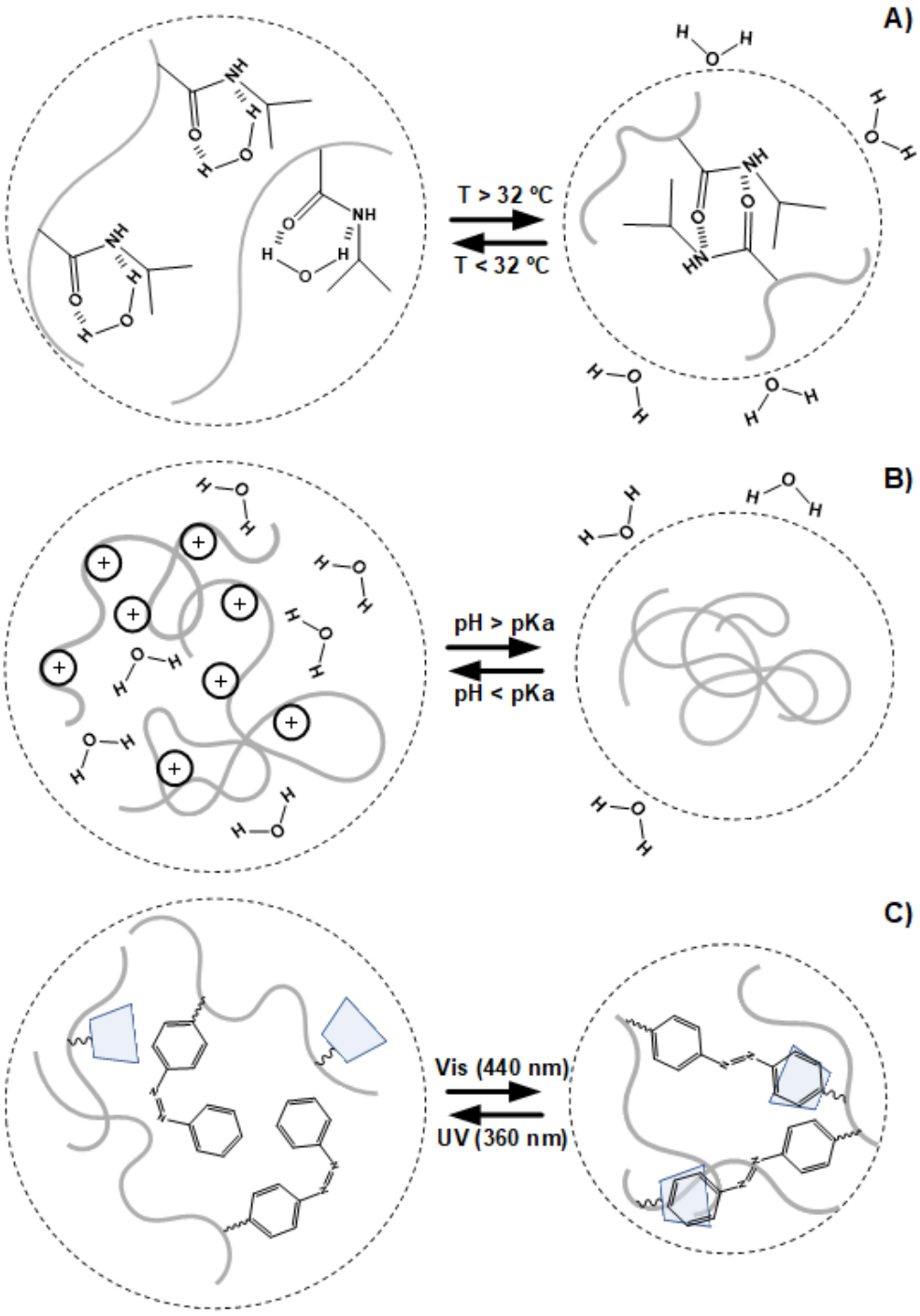

Figure 1.1 Schematic representation of the stimuli-responsive mechanism of temperature-sensitive (A), polycationic pH-sensitive (B) and light-sensitive (C) "smart hydrogels". (Adapted from the literature)[7,8]

In recent years, an effort has been made to expand the field of stimuli-responsive materials. In this context, electro-responsive hydrogels have been attracting significant scientific and

technological interest, especially for biomedical applications, due to their potential to be applied in the development of advanced electronic devices such as sensors, soft actuators, artificial muscles, conducting tissue engineering scaffolds and electro-assisted drug delivery systems.[13]

1.1.1 Current trends in the development of electro-responsive systems

Conductive materials can be divided in two main groups depending on the type of charge transport, namely the group of electron-conducting and ion-conducting materials. Polyaniline (PANI), polypyrrole (PPy), polythiophene (PTh) and its derivatives and polyacetylene (PAc) are classical examples of electron-conducting materials (Figure 1.2A).[14] The conductivity of these materials results from a specific backbone structural configuration which alternates single and double bonds (Figure 1.2B). Differently from single bonds, that present only strongly localized σ-bonds, double bonds also contain weaker localized π-bonds, whose *p*-orbitals overlap with each other creating a more easily delocalized pathway that allows electrons to flow more freely between atoms of the materials' backbone. In order to achieve high conductivity, these polymers are submitted to 'doping' processes which consist in the removal or addition of electrons from/to the polymeric chain by using dopants (e.g. hydrochloric acid, dodecylbenzenesulphonic acid and lauric acid) thus creating a delocalized charge (Figure 1.2C). In order to relocate this charge, a distortion of the crystal lattice (arrangement of the atoms in a material) is obtained. This results in a loosely held, however localized, electron surrounded by a crystal lattice distortion (polaron). Depending of the polarity applied to the material, the dopant is attracted towards the anode or the cathode, traveling through the polymer chain disrupting the stable conjugated backbone allowing the conduction of electrons in the form of charge carriers such as polarons.[14,15] The electrical

conductivity of these polymers alone is found to be in the range 10^{-2}–10^{5} S/cm depending on their chemical nature.[16]

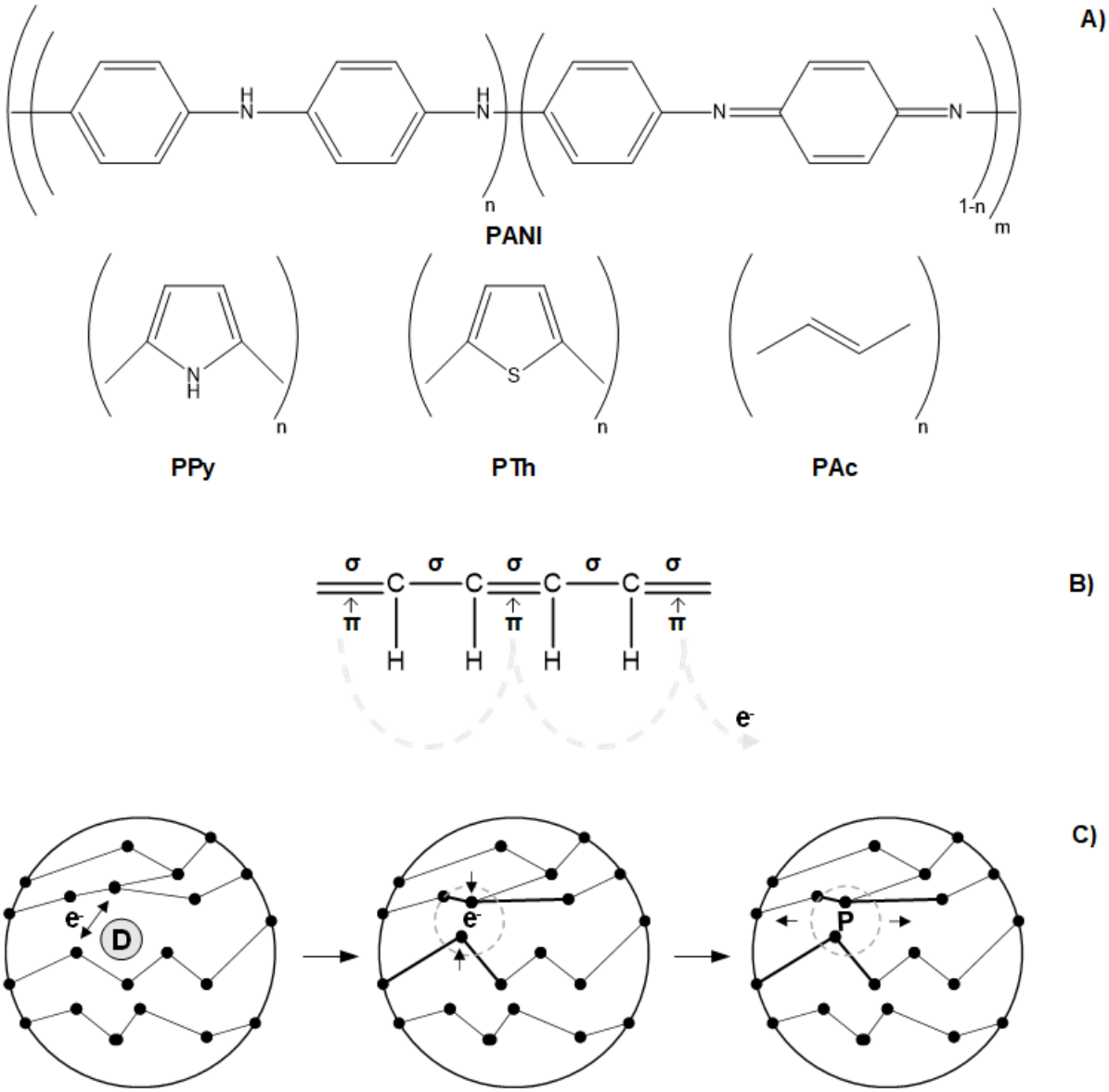

Figure 1.2 Repeat units of classical electron conducting materials (A); Illustration of the conducting mechanism on a conjugated backbone (B); Scheme of electron conduction mechanism after doping (C).

(Adapted from the literature)[14]

Generally, these conducting polymers present poor mechanical properties (e.g. brittleness and lack of flexibility) and high hydrophobicity (e.g. low degree of swelling and insolubility) which limits their usage when biomedical applications are envisaged. The conjugation of these materials with other polymers (e.g. poly(2-hydroxyethyl methacrylate), polyacrylamide, polylactic acid, alginate, collagen etc.) can be regarded as a strategy to overcome these drawbacks and to obtain a gel-like conducting polymer-based system.[14,17] Nevertheless, this approach can lead to an overall decrease in the electronic conductivity for these systems to values lower than 2 S/cm.[17]

Conductive polymer-based materials have been recently employed for different biomedical applications as tissue engineering scaffolds, drug delivery systems and actuators.[14,16-18]

Conductive polymer-based electroactive scaffolds have been regarded as suitable substrates for several tissue engineering applications including neural and cardiac tissue regeneration.[16,17] These scaffolds act as an interface between cells and the electric stimulus where their conducting nature can enhance cell-to-cell/cell-to-substrate interaction which ultimately, regulates cell attachment, communication, growth, and migration.[16,17]

Drug delivery systems based on electron-conductive polymers are usually obtained by loading the conductive polymer-based matrix with an ionic model drug. The drug delivery mechanism under electrical stimulus depends on the redox state of the doped conducting polymer and of the charge of the employed drug.[19] Upon applied electrical stimulus, the redox state of the doped conducting polymer changes and electrons are gained (reduction) or lost (oxidation). For instance, in the case of a doped conducting polymer loaded with a cationic drug, through oxidation reactions the resultant positively charged polymer electrostatically repels the cationic drug out of the polymeric matrix leading to drug release (Figure 1.3A).[13,19]

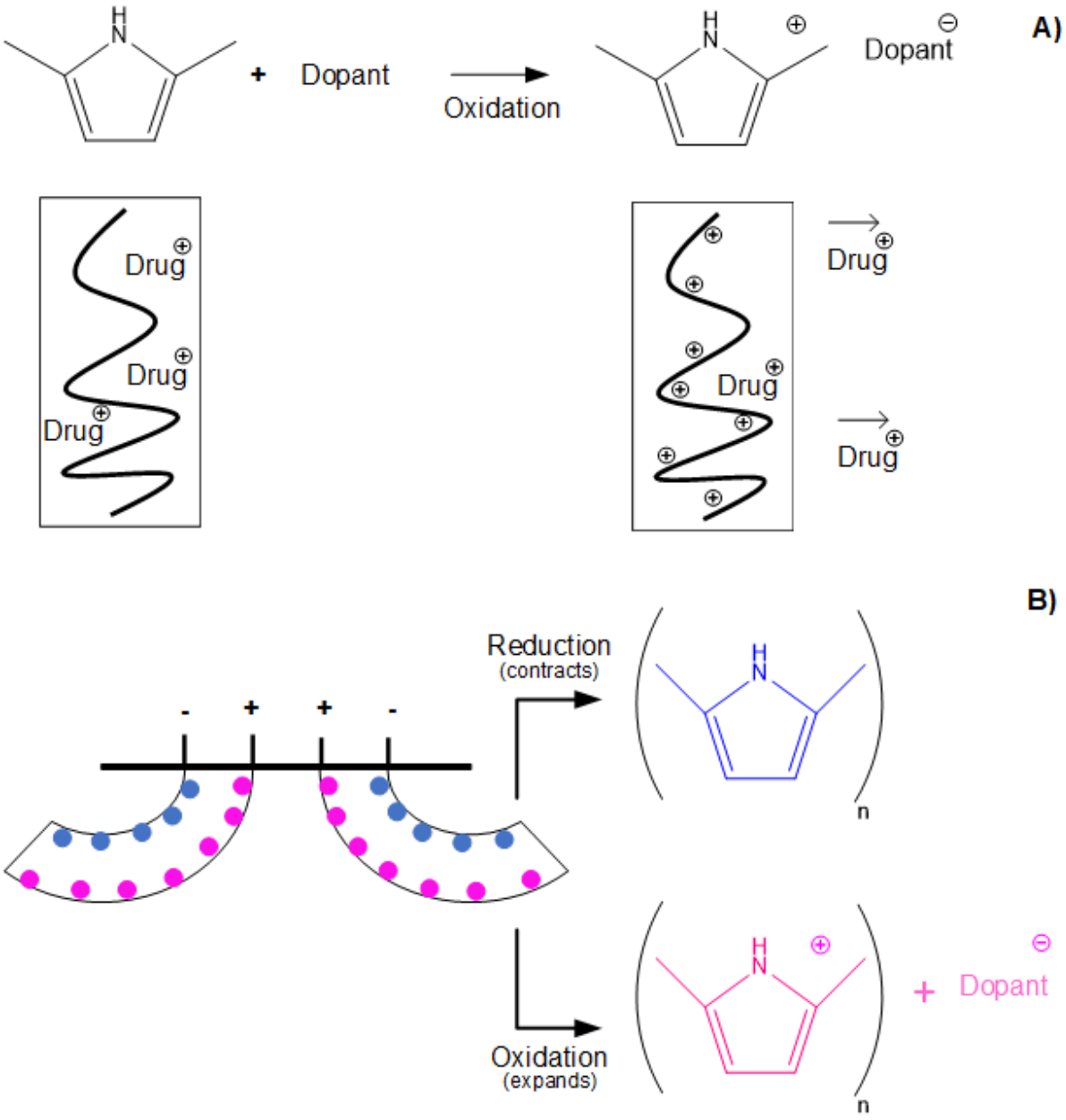

Figure 1.3 Schematic representation of drug delivery (A) and electro actuation (B) mechanisms of electron-conducting polymer taking PPy as an example.

(Adapted from the literature)[13,19,20]

Conducting polymers have also been studied for the development of electro actuators for biomedical applications.[21] The actuation response of these systems is driven by complex electrochemical redox reactions that take place at the polymer/electrodes interface upon the

application of an electrochemical potential. In the case of a conducting polymer embedded in an electrolyte solution, electrons are transferred between the polymer and the electrodes leading to changes in the polymer oxidation state. For instance, PPy is oxidized (becoming positively charged) at the anode side attracting anions (in order to compensate charge imbalance) resulting in polymer expansion. On the other hand, PPy is reduced at the cathode side (becoming neutral) giving up ions and thus, resulting in polymer contraction.[20] This difference in volume variation (expansion at the anode side/contraction at the cathode side) leads to the bending motion, in this case towards the cathode (Figure 1.3B).The direction of the bending motion can be controlled by redox reactions (following the mechanism previously mentioned) as a function of the applied polarization.

Ion-conducting hydrogels are regarded as the next generation of electro-responsive materials acting as electronic-organic bridging interfaces that can narrow the boundary between humans and machines. The growing interest in these materials for biomedical applications results from the fact that a large number of metabolic processes in the human body (e.g. central nervous system, muscular system, digestive system, etc.) are mainly regulated by electronic/ionic processes.[22]

The ionic conducting mechanism for this class of electroactive materials result from the diffusion of mobile ions under the presence of an electrical stimulus (Figure 1.4). These mobile ions act as charge carriers resulting in ionic conductivity. Typical examples of ion-conducting materials include double-ion conductors and single-ion conductors.

Double-ion conductor hydrogel-based materials are commonly composed of a polymeric matrix (e.g. poly(vinyl alcohol), poly(vinyl chloride), poly(methyl methacrylate) etc.) loaded with electrolytes such as sodium chloride and lithium chloride.[22,23]

Hydrogel-based double-ion conductors are been explored for the development of stretchable, self-healing and electro-responsive materials for different applications, namely as sensors, capacitors and batteries.[24-27]

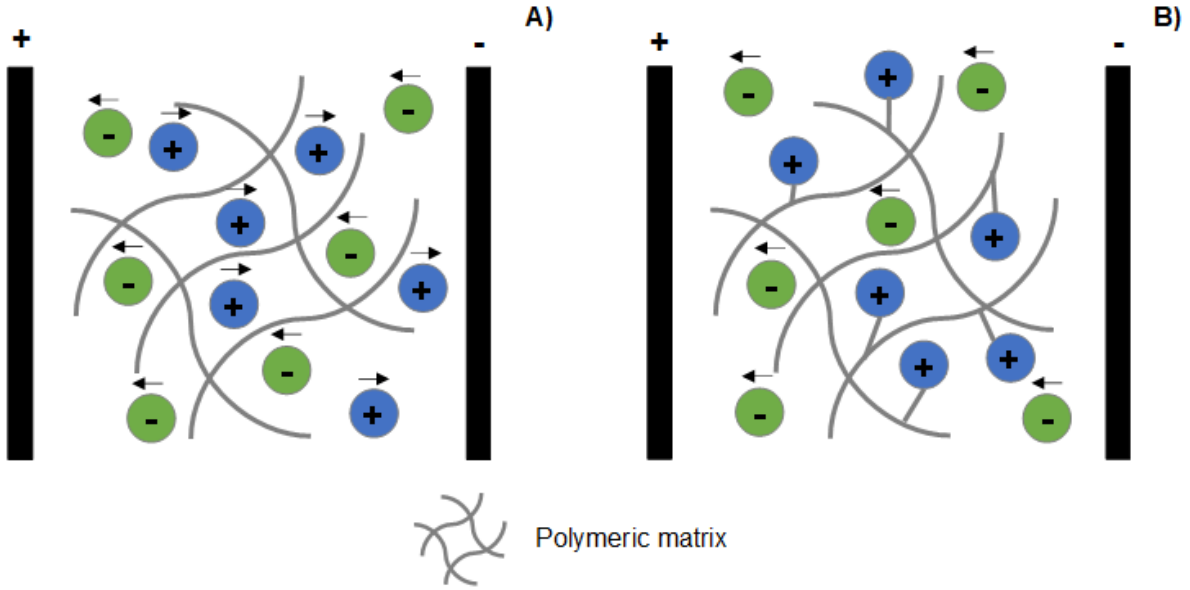

Figure 1.4 Illustration of the ionic conductivity mechanism in double-ion conductors (A) and single-ion conductors (B) (considering a polycation) under the presence of an electrical field.

Single-ion conductors hydrogels are mainly constituted by polyelectrolytes. Natural polysaccharides, such as chitosan and alginate, and synthetic polymers, such as poly(acrylic acid) and Nafion®, are examples of single-ion conductors whose ion conducting mechanism results from the transport of counterions in solution under electrical stimulus.[28-32]

This class of electro-active materials have been investigated for different applications, namely as self-healable supercapacitors,[33] mechanical sensors,[34] "smart" coatings[35] and cell-growth tissue engineering scaffolds.[36]

The ionic conductivity of polyelectrolytes has been also explored for the development of electro-assisted drug delivery systems.[37,38] Several variables can be employed to control the delivery/release of ionic/neutral molecules via electrical stimulation, including the

experimental setup (position of the electrodes and of the hydrogel), nature of the hydrogel, degree of crosslinking, media's ionic strength, charge of the drug, magnitude of applied electrical stimulus etc.[19,39] Neutral and/or ionic molecules (having the same charge as the polyelectrolyte matrix to avoid polyelectrolyte-drug ionic interactions) can be released from polyelectrolyte-based hydrogels under electrical stimulus via different mechanisms such as forced convection (release of the drug due to hydrogel's deswelling along with water syneresis), release upon hydrogel's erosion and, electrophoresis coupled with electroosmosis.[39] Besides their electro-responsiveness commonly employed polyelectrolytes are also pH-responsive due to the presence of ionizable groups along their polymeric backbone. Under electrical stimulus water undergo electrolysis (equation 1.1)[40] which allows tuning the charge of the polyelectrolyte hydrogels by altering local pH and thus, influencing the drug release mechanism.

Anode (+) (Oxidation)	$2H_2O \rightarrow O_2 + 4H^+ + 4e^-$	pH ↓	(1.1)
Cathode (-) (Reduction)	$2H_2O + 2e^- \rightarrow H_2 + 2OH^-$	pH ↑	

For instance, pH-responsive polycationic hydrogels undergo anisotropic deswelling/shrinking on the cathode (Figure 1.5A). Due to water electrolysis the pH increases at the vicinity of the cathode where it leads to the deprotonation of cationic groups reducing hydrogel's interchain free-volume (by lowering the polymeric chains' electrostatic repulsion) and, consequently hydrogel deswelling which squeezes out the drug by forced convection mechanism.[39] Electro-assisted hydrogel's erosion is another approach that can be employed to tune the release of molecules from a hydrogel attached to an electrode. In this case, a polyelectrolyte complex hydrogel previously loaded with a given drug erodes due to local pH changes (Figure 1.5B).

At the cathode's vicinity the local pH increases causing the deprotonation of ionic groups from the polycationic counterpart of the polyelectrolyte complex leading to the disruption of the electrostatic interactions of the polyelectrolyte complex and, resulting in drug release.[39]

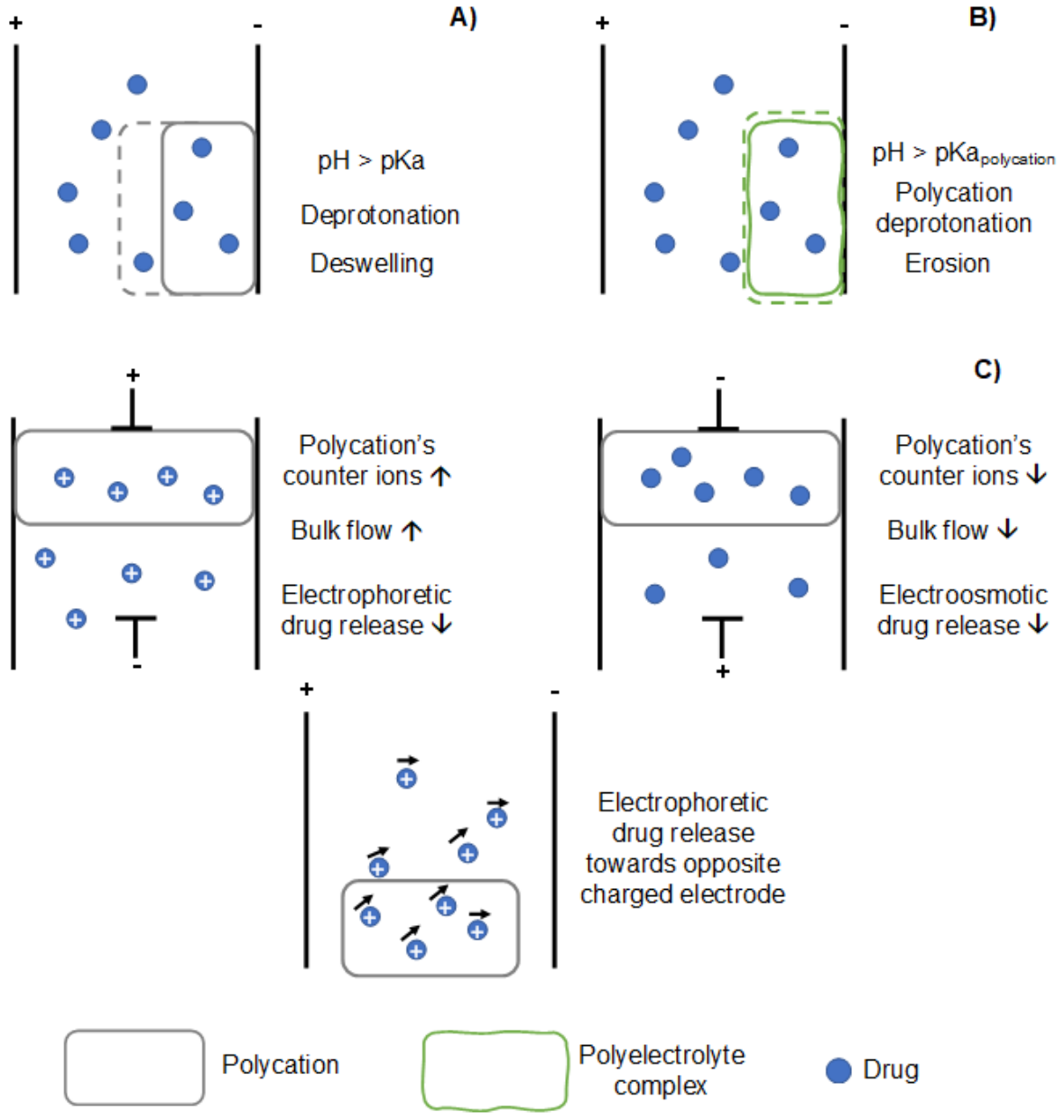

Figure 1.5 Illustration of electro-assisted drug delivery mechanisms for hydrogels based in polyelectrolytes: (A) forced convention mechanism; (B) hydrogel's erosion mechanism and (C) electrophoresis/electroosmosis mechanisms.

(Adapted from the literature)[39,41,42]

Finally, electro-assisted drug release from hydrogels can also be given by means of electrophoresis/electroosmosis mechanisms (Figure 1.5C). Briefly, electrophoresis is the migration of charged species in solution towards the oppositely charged electrode while electroosmosis is the bulk flow oriented by the diffusion of hydrogel's counter ions.[39,41] When the hydrogel is disposed in between the electrodes the electro-assisted drug delivery is given by the electrophoretic flow where the ionic drugs migrate towards the oppositely charged electrode.[42] In the case of an anodal drug release, cationic drugs are repelled by the anode and migrate towards the cathode due to the electrophoretic flow. Neutral drugs can be delivered by means of electroosmotic flow where the bulk flow is given at the same orientation of polyelectrolyte hydrogel's counter ions. Under electrical stimulus, free counter ions (from the polyelectrolyte matrix) migrate towards oppositely charged electrode dragging water molecules in the process (bulk flow), resulting in electroosmotic delivery from cathode-to-anode or anode-to-cathode orientation regarding polycations or polyanions, respectively.[39,41]

Polyelectrolytes can be further explored for the design of electroactive actuators, also known as ionic electro-active polymer actuators (ionic EAPs). These materials have the capacity to convert electrical energy into mechanical actuation[43] presenting precise response under fine and tunable control of the applied stimuli (e.g. intensity and duration of the applied electrical current).[44,45] In specific cases, ionic EAPs are also entitled as ionic polymer metal composites (IPMCs) which consist of a sandwich structure comprised of a hydrated ionic exchangeable membrane (typically a polyanion such as Nafion®) in between two conductive electrodes that are coated with noble metals such as Au, Ag and Pt.[46,47]

There are several variables that affect the electroactive responsiveness of these materials including the: experimental set up, electrical current intensity and orientation, operation

temperature, polyelectrolyte's charge density, actuator's composition/formulation, crosslinking density, etc.

The electro-assisted mechanical displacement (bending) of these ionic hydrogel actuators is governed by the following main mechanisms: Coulomb,[48] electroosmosis,[49] electrochemical,[50] and dynamic enrichment/depletion[51] mechanisms. Taking as example a polycationic hydrogel, the Coulomb mechanism[48] describes the bending displacement as the net force exerted by the external electrical stimulus on mobile counter ions and on fixed ions (causing a stationary current inside the hydrogel) pulling the polyelectrolyte towards the cathode (Figure 1.6A). The electroosmosis mechanism[49] describes the bending actuation as the electrophoretic diffusion of hydrated mobile counter ions inside the gel leading to local swelling resulting in bending towards the cathode (Figure 1.6B). The electrochemical mechanism[50] relies on the pH changes at the electrodes' vicinities that alters the redox state of the hydrogel affecting its swelling behavior resulting in bending motion towards cathode (Figure 1.6C). Finally, the dynamic enrichment/depletion mechanism describes the mechanical actuation as a result of the osmotic pressure gradients formed due to the dynamical accumulation or depletion of ions on both surfaces of the gel at the solution interface.[51] These osmotic pressure differences change the swelling/shrinking capacity of the gels at the vicinity of their surfaces resulting in bending towards the anode (Figure 1.6D).

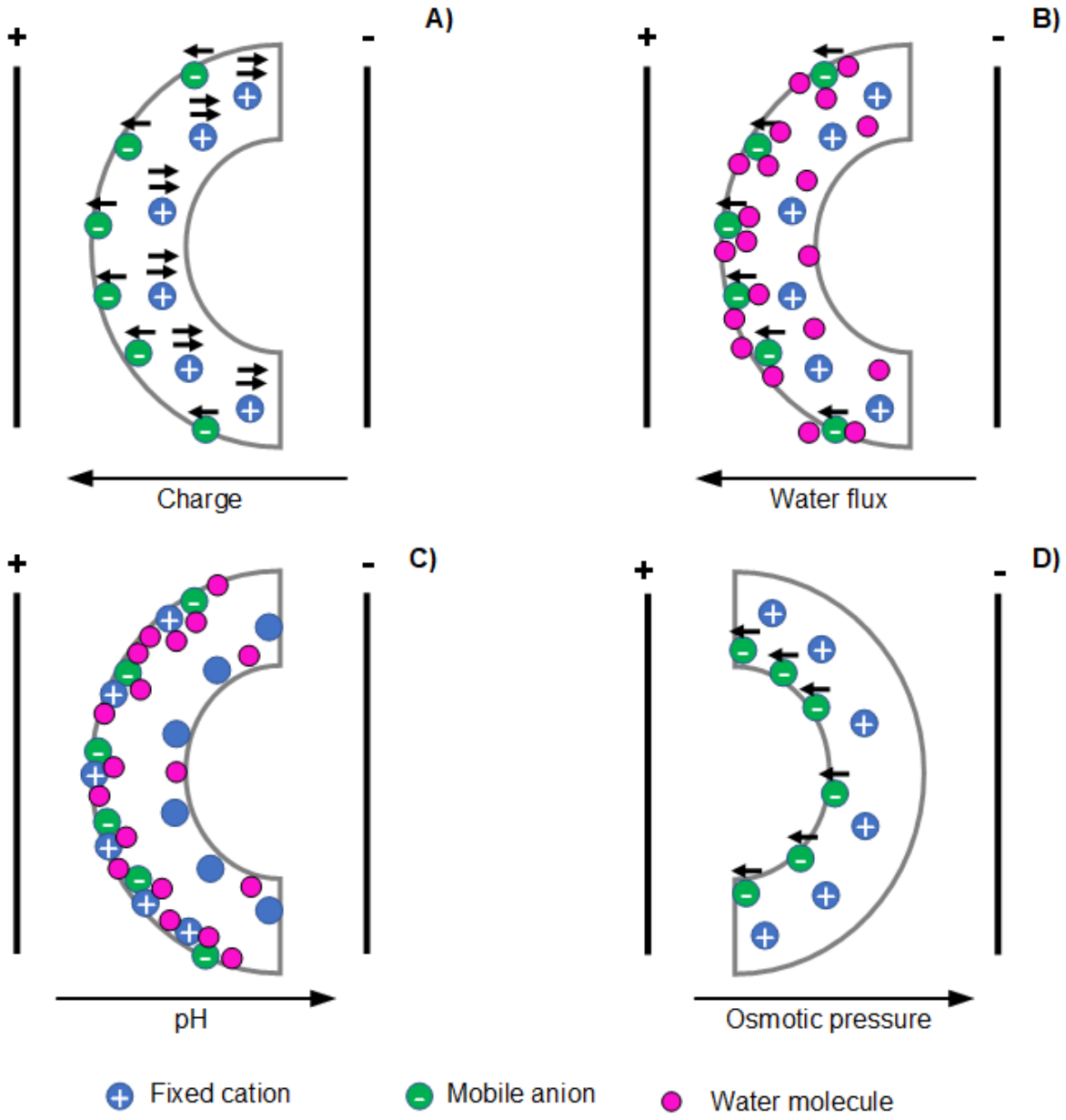

Figure 1.6 Illustration of bending mechanisms for polycationic actuators: Coulomb mechanism (A); Electroosmosis mechanism (B); Electrochemical mechanism (C) and enrichment/depletion mechanism (D).

(Adapted from the literature)[32,52,53]

Ionic EAPs have been recently applied in the design of robotic devices,[54] soft actuators,[55,56] and electroactive systems for biomedical applications, namely drug delivery platforms[57] and tissue engineering scaffolds.[58]

1.2 From ionic liquids (ILs) to polymerized ionic liquids (PILs): novel and competitive electro-responsive systems

Ionic liquids (ILs) are a remarkable class of compounds defined as salts composed by organic/inorganic cations and/or anions with a melting point lower than 100 ºC. Ionic liquids which present a melting point lower or equal to room temperature are also known as Room Temperature Ionic Liquids (RTILs).[59,60] The low melting points of RTILs result from their lack of symmetry (often due to large cationic cores) and low-energy conformation which prevents the formation of a stable crystal lattice.[61] Figure 1.7 presents the most commonly employed ILs cations and anions.

ILs have been receiving increasing attention from the academy since the nineties due to their unique properties, namely negligible vapor pressure, ionic conductivity, thermal and chemical stability, non-flammability, wide-liquid range of solvation ability and antimicrobial and antibiofilm activity.[62-65]

There is a large range of possibilities to synthesize ILs, through variations of the cation/anion pairs which allows tuning their physical, chemical, and biological properties towards specific applications.[66-68] This feature gave to ILs the status of “tailor-made” or “task-specific” compounds by estimating that the number of possible cations/anions combinations can raise up to 10^{18}.[69]

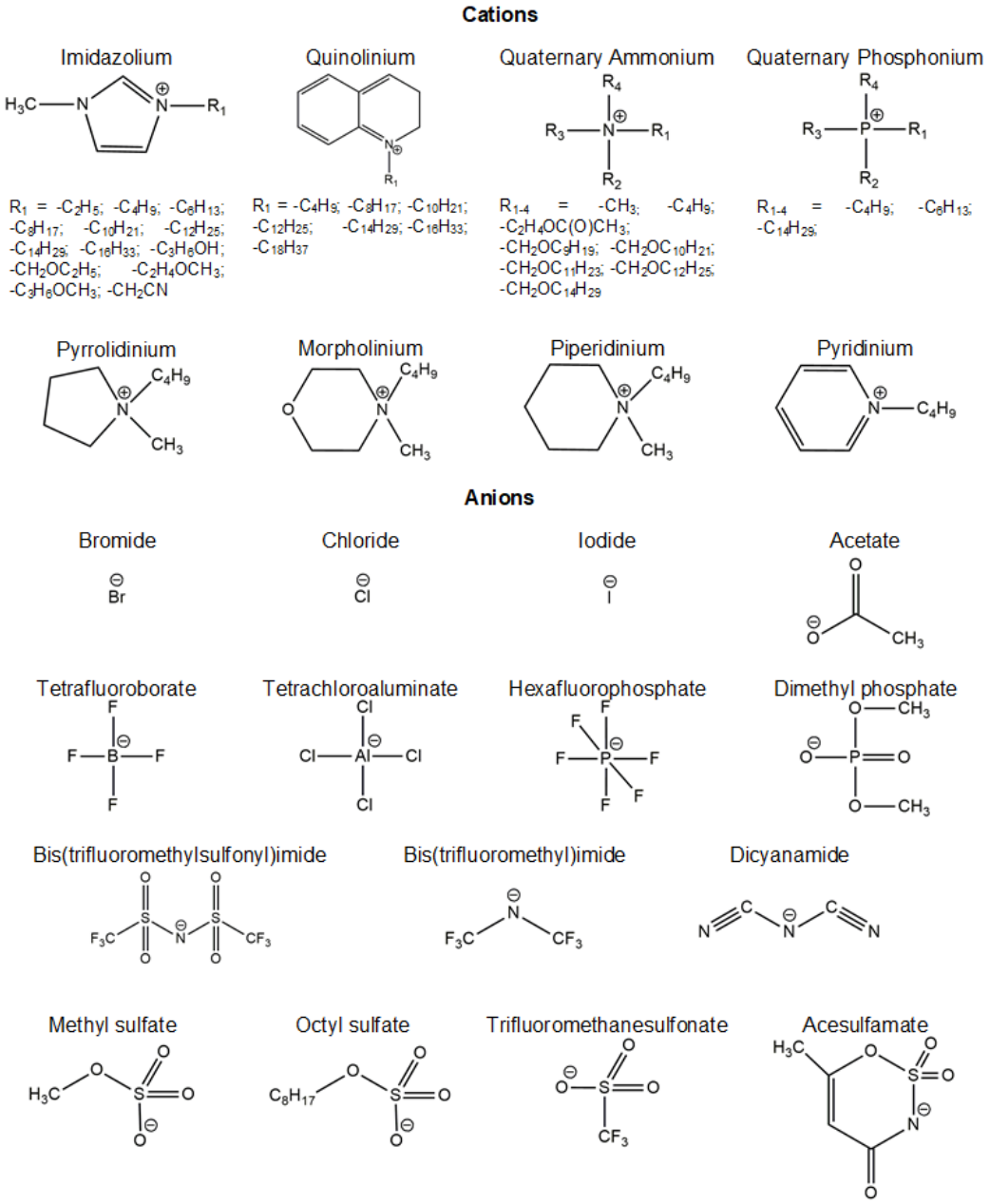

Figure 1.7 Most common cations and anions employed to prepare tailor-made ILs. (Adapted from the literature)[70,71]

ILs have been often classified as "green compounds" because of their low volatility (negligible vapor pressure) and recyclability and consequently they have been proposed as viable alternatives to traditional volatile organic compounds (VOCs). Nevertheless, and also due to their low volatility and chemical stability, ILs can persist in the environment occasioning several contaminations in rivers, sediments and soils. Therefore the classification

of ILs as green solvents cannot be generalized and it has been under scrutiny since ILs intrinsic toxicity to the environment and living organisms was reported.[70,72-74] There are several factors that influence the toxicity of ionic liquids such as: cation and anion nature; alkyl chain length; sort of microorganism/cell line/enzyme to be tested and toxicological evaluation methodology employed. Among these, IL's chemical structure (alkyl chain length and head group) plays a key role in their toxicity level against different living entities, for instance aquatic organisms (e.g. *Vibrio fischeri* bacteria, *Skeletonema marinoi* diatom, *Daphnia magna* plankton and *Scenedesmus obliquus* microalgae), bacteria (e.g. *Escherichia coli* and *Staphylococcus aureus*) and different cells lines (e.g. corneal cells (HCE), HeLa cells and catfish ovary cells (CCO)).[72-75] Generally, the increase in cation/anion alkyl chain length leads to an increase in ILs' hydrophobicity/lipophilicity which enhances the interactions between IL moiety and the lipidic bilayer and hydrophobic domain of the cells. These cell membrane-ILs interactions result in higher swelling of the cell, disrupting the membrane and exposing its cellular content resulting in cell death, and consequently higher IL toxicity. The type of cation head group also affects the toxicity of ILs. Toxicity decreases accordingly to the cationic head family as follows: phosphonium > pyridinium ≈ imidazolium > pyrrolidinium.[72,73] This trend may be due to differences in hydrophobicities of each cation head group where more hydrophobic cations (e.g. phosphonium) present higher levels of toxicity following the same mechanism explained earlier.

Due to their unique properties ILs have been explored for a variety of applications over the years (Figure 1.8) including: as solvent media to dissolve organic and inorganic substances as well as polysaccharides such as cellulose, chitin, chitosan, starch and xanthan gum,[76-80] electrochemical sensors,[81] separation techniques,[82,83] electrochemical storage devices,[84] conducting ion gel,[29,85] plasticizers,[86,87] batteries and solar cells,[88] antimicrobial agents,[89]

design of herbicidal agrochemicals[90] and in pharmaceutical and medicinal applications for the synthesis of novel active pharmaceutical ingredients (APIs).[91,92]

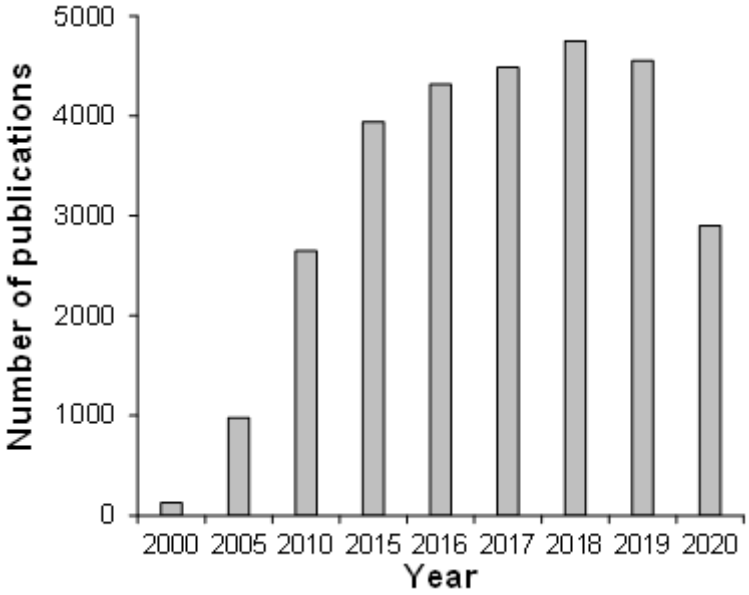

Figure 1.8 Number of publications related with ionic liquids (ILs). Data obtained from the "Web of Science" (2000 – September 2020) for all literatures (Keyword: "ionic liquids").

1.2.1 IL-based electro-responsive materials

The unique synergy between the properties of polymeric networks and those of ILs can result in advanced electroactive materials for several applications, including electromechanical actuators,[93] batteries,[94] capacitors,[95] tissue engineering scaffolds,[96] etc.

Several studies have demonstrated the possibility to endow and/or to enhance the ionic conductivity of different polymer matrices by loading the host polymeric matrix with ILs. An ionic liquid phase dispersed within a solid continuous phase is defined as an ionic liquid gel or ionogel. Ionogels comprise the properties of the IL, such as ionic conductivity, negligible vapor pressure with the structural benefits from the solid phase.[97] The mechanism of charge transport of those systems is similar to that of double-ion conductors presented earlier which is based on the free movement of ionic species (diffusion of cations and anions) under

electrical stimulus. In general, the ionic conductivity of ionogels, composed of different polymeric matrixes (e.g. poly(acrylic acid), poly(vinyl alcohol), poly(*N*-isopropylacrylamide) etc.) and ionic liquids (e.g. imidazolium-, piperidinium-based ionic liquids etc.), are comprehended in the range of (~10^{-3} – 10^{1} mS/cm).[85,86,95,96,98-105] The ionic conductivity of these systems depends on several variables, namely the intensity of the interactions between the IL ions and the polymer matrix, nature of cation/anion of the IL, IL concentration, IL's alkyl chain length, temperature, crosslinking density of the polymeric matrix and glass transition temperature (T_g).[85,86,95,96,98-102,104-108]

The effect of the IL-polymer interactions in the ionic conductivity of ionogels was demonstrated for different acrylate-based polymer gels and imidazolium-based ionic liquids. Compared to the neat IL, the ionic conductivity of the ionogel decreases as the polymer loading increases (for a fixed amount of ionic liquid) due to the physical presence of the polymer chains that hamper the diffusion of ions under the electrical stimulus.[98,100,108] The effect of the nature of the IL's anions on the ionic conductivity of ionogels was demonstrated to be regulated by the molecular size of the anion and its electrostatic affinity for the cation. Different IL gels containing phosphonium- or imidazolium-based ILs bearing distinct counter ions (Tf_2N^-/Cl^- and $CF_3SO_3^-$/FSI^-, respectively) demonstrated that larger counter ions (e.g. Tf_2N^- and $CF_3SO_3^-$) dissociate more easily from the cationic head group under the presence of an electrical stimulus, which results in higher ionic conductivity.[86,99,102] A linear direct correlation between the IL concentration and the ionic conductivity was demonstrated for ionogels comprised of poly(vinylidene fluoride) and poly(vinyl alcohol)-poly(2-hydroxyehtyl methacrylate) double networks loaded with imidazolium-based ILs.[95,96] However, the ionic conductivity of ionogels can be increased up to a certain threshold due to ion competition and agglomeration within the polymeric matrix.[106] The effect of the IL's alkyl chain length onto the ionic conductivity of ionogels was demonstrated for systems based on chitosan and

poly(*N*-isopropylacrylamide) loaded with imidazolium- and phosphonium-based ILs having different alkyl chain lengths. Higher ionic conductivities were observed for ionogels loaded with ILs with shorter alkyl chain lengths due to the lower viscosity of these ILs which facilitates ions diffusion under electrical stimulus.[101,107] A linear correlation was also found between the operation temperature and the ionic conductivity of ionogels loaded with distinct ILs (e.g. imidazolium- and pyrrolidinium-based ionic liquids). Higher temperatures led to higher ionic conductivities due to an increase in the segmental motion of the polymeric matrix that allows the ions to diffuse more freely.[85,95,104] On the contrary, ionogels based on poly(methyl methacrylate) loaded with imidazolium-based IL showed an inverse correlation between the crosslinking degree of the polymer and the ionic conductivity of the ionogels. The higher the crosslinking degree, the lower the ionic conductivity due to the decrease of the free volume of the ionogel matrix which hinders ions diffusion under electrical stimulus.[100] Finally, it was demonstrated that the ionic conductivity of ionogels loaded with piperidinium- and imidazolium-based ILs increases as the T_g of the ionogels decreases. This result was explained based on the plasticizing effect of ILs onto the polymeric matrix which reduces intra- and/or inter-polymer chain interactions (lowering the T_g) which enhances the diffusion of IL ions under electrical stimulus resulting in higher ionic conductivity.[102,105]

ILs can be employed as ion sources for the design of soft actuators. Due to their low vapor pressure (as mentioned earlier), ILs have been applied for the development of more efficient electro-actuating systems since conventional actuators utilize electrolyte solutions that evaporate during usage which compromise the mechanical actuation of the actuator overtime in response to an electrical stimulus.

Several IL-based electro-active systems were reported in the literature for the development of 'smart' actuators.[99,102,103,109] The bending mechanism behind these systems is based on ion migration (diffusivity) and formation of an electrical double layer (EDL) at the

ionogel/electrode interface. Figure 1.9 illustrates the actuation response of a system comprised of an IL-based soft ionic gel sandwiched between two electrodes. The bending response can be explained by the electroosmosis actuation mechanism discussed above.[49] Briefly, ions (cations and anions) diffuse towards oppositely charged electrodes accumulating at the gel/electrode interface, resulting in the formation of an EDL. This leads to the formation of a uniaxial stress gradient along the gel prompting the expansion at the cathode and a contraction at the anode (due to size differences between IL ions: considering cations bigger than anions) which results in bending towards the anode.

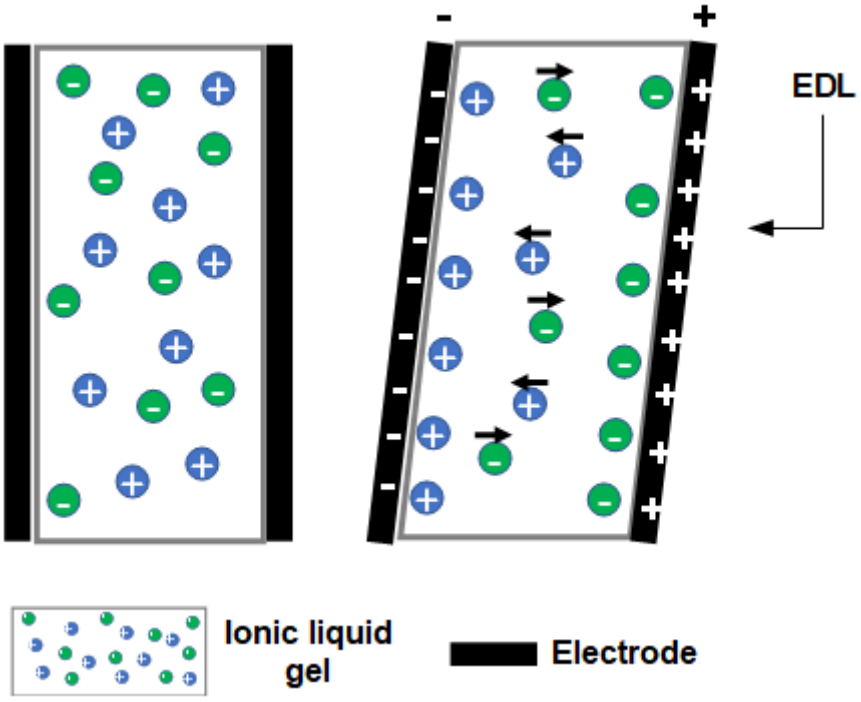

Figure 1.9 Illustration of the mechanical actuation mechanism of an IL-based electro-actuator. (Adapted from the literature)[99,110]

The bending actuation response can be tuned by changing variables such as the alkyl chain length and the cation/anion type of the IL, the intensity and polarity of the applied electrical stimulus, the tortuosity of the polymer matrix, etc.[93,102,109,111] The influence of the alkyl chain length of the IL cation on the bending response of poly(vinylidene fluoride) (PVDF) gels

loaded with imidazolium-based ILs was shown to decrease as the alkyl chain length of the IL cation increases. This is due to the augment of the IL viscosity which hinders ion diffusion within the polymer matrix.[109] Nevertheless, in some systems the augment in the alkyl chain length lead to a decrease in Young's modulus of the gel, increasing its flexibility resulting in higher bending displacements.[111] The effect of the anion type in the bending actuation response of PVDF gels loaded with imidazolium-based ILs bearing different counterions (e.g. Cl^- and NTf_2^-) was previously reported.[109] Results showed that one directional bending motion was observed when employing smaller anions (e.g. Cl^-) due to significant size asymmetry between the cation head group and the anion. Under electrical stimulus, more anions diffuse towards the oppositely charged electrode (when compared to cations diffusion) which results in an ionic gradient along the actuator and thus, in an unidirectional displacement towards the cathode. The bending response increased with the intensity of the applied voltage which enhances ion mobility within the polymer matrix resulting in higher and faster electromechanical displacement.[102,109] By inverting the polarization, the bending actuation occurs towards the opposite direction.[111] Finally, and as previously discussed, the physicochemical nature of the polymer matrix influences the ionic conductivity of IL gel, and consequently its mechanical response. The electromechanical actuation of less tortuous polymer matrixes its higher because ion diffusion under electrical stimulus is enhanced.[102]

Recently, it was reported that the main challenges and future trends regarding IL-based electro-sensitive materials relies on the fabrication of more stable actuators; on the design of electroactuators based on ILs and natural polymers; on the 3D printing of IL-polymer composites and on the study of the cytotoxicity of these electroactive systems fostering their usage for different biomedical applications.[97,112]

Most of the IL-based electro-responsive systems reported so far focused the design of electrochemical devices such as fuel cells, batteries, and robotic devices. Nevertheless, these

systems are not attractive when they are envisaged to be applied in aqueous media since IL leaching may occur and compromise the functionality of the electro-active system. An alternative approach to overcome this issue consists in the polymerization of IL-based monomers to obtain IL-based polyelectrolytes known as poly(ionic liquids) (PILs).

1.2.2 Poly(ionic liquids) (PILs): broadening the application of ionic liquids

As task specific compounds, ILs can be functionalized with vinyl bounds on the cation, on the anion or on both the cation and the anion, allowing the synthetizes of IL-based polyelectrolytes (polycation, polyanions and polyzwitterions, respectively) by free radical polymerization reactions of the IL-based monomers. Poly(ionic liquid)s (PILs) represent a unique sub-class of polyelectrolytes having improved mechanical stability, processability (coatings and films) and durability when compared to pure ILs.[113] They combine some properties of the IL monomeric units (e.g. high ionic conductivity, negligible vapor pressure, non-flammability, thermal and chemical stability) with those of polymers (e.g. viscoelastic properties, 3D structure, mechanical stability, versatility and easy functionalization).[114] PILs are versatile materials since their physicochemical and electrochemical properties (e.g. water solubility, ion conductivity etc.) can be tuned by simply procedures such as counterion exchange. PILs-based materials have been intensively employed as gas separation membranes[115,116] and as electroactive systems such as batteries,[117-119] fuel cells,[120] capacitors[121,122] and electro-active actuators.[123,124] More recently explored PILs were also explored as antimicrobial materials[125] and tissue engineering scaffolds for biomedical applications.[96]

Figure 1.10 permits to conclude that the number of publications of PILs-based materials have been increasing along the years suggesting a promising future for these materials.

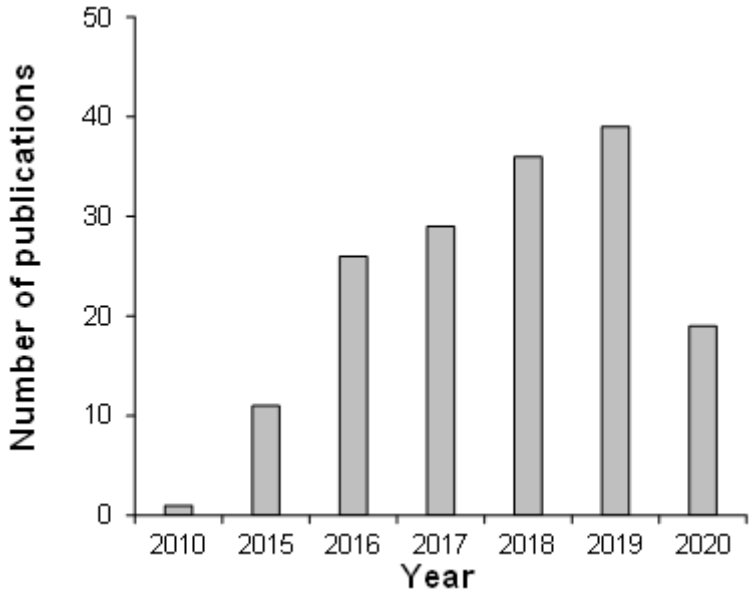

Figure 1.10 Number of publications related with poly(ionic liquids) (PILs). Data obtained from the "Web of Science" (2010 – September 2020) for all literatures (Keyword: "poly(ionic liquids)").

There are several polymerization methodologies reported in the literature that can be used to polymerize ILs, namely through ring-opening metathesis polymerization, step-growth polymerization, electrochemical polymerization, polycondensation and the conventional free radical polymerization. The latter is by far the most frequently employed methodologies because it is efficient and easy to be implemented.[113] A main drawback that results from the polymerization of ILs is that it leads to a decrease in the ionic conductivity of the resultant PIL due to an overall decrease in the density of mobile ions. In fact, ILs can be regarded as double-ion conductors and PILs as single-ion conductors. In general, PIL-based materials present ionic conductivities up to ~ 1 mS/cm.[126] There are some variables that can affect PILs' ionic conductivity including: the nature of the constituent monomeric IL (type of anion/cation), the length of the alkyl chain of the PIL, charge density, operation temperature and relative humidity, material's water content, purity of the poly(ionic liquid), presence and length of spacers, etc.[113,118,126-128] The effect of the cation/anion type and of the alkyl chain

length of the monomers employed to obtain a given PIL, the effect of the PILs' charge density and of the operation temperature on the ionic conductivity of PILs follows a similar trend as that explained earlier for ion conducting ionogels.[121,127-130] The effect of external variables such as the relative humidity in the ionic conductivity of PILs was demonstrated for ammonium-based PILs. The increase in the external relative humidity led to an increase in the water content of the gel (due to its hygroscopic nature). As the PIL's ions become hydrated (surrounded by water molecules), an increase in ionic hydrodynamic radius in attained which reduces the cation-anion Coulomb interactions and thus, facilitating the counterion diffusion within the polyelectrolyte resulting in higher ionic conductivity.[128,131] The effect of purity on the ionic conductivity of PILs is related to the amount of unreacted IL monomers inside the polymeric structure that remained after synthesis without any further purification processes (e.g. precipitation, dialysis etc.). Unreacted IL monomers increase the density of free ions within the PIL matrix which induces higher charge transport under electrical stimulus and thus, higher ionic conductivity.[130] Finally, the effect of spacers on the ionic conductivity of PILs can be evaluated by following two main different strategies, namely by varying the spacer length between the polymer backbone and the ionic liquid head group (Figure 1.11A) or by copolymerization of IL monomers with generic comonomers (Figure 1.11B). It was demonstrated that the ionic conductivity of several imidazolium-based PILs increases as the spacer length increases[132] and when neutral comonomers (e.g. acrylate-based monomers) are employed.[133] In both cases, PILs' ionic conductivity its enhanced due to the overall augment in the polymer chain flexibility (lowering the T_g) that facilitates counterion diffusion under electrical stimulus.[113,126]

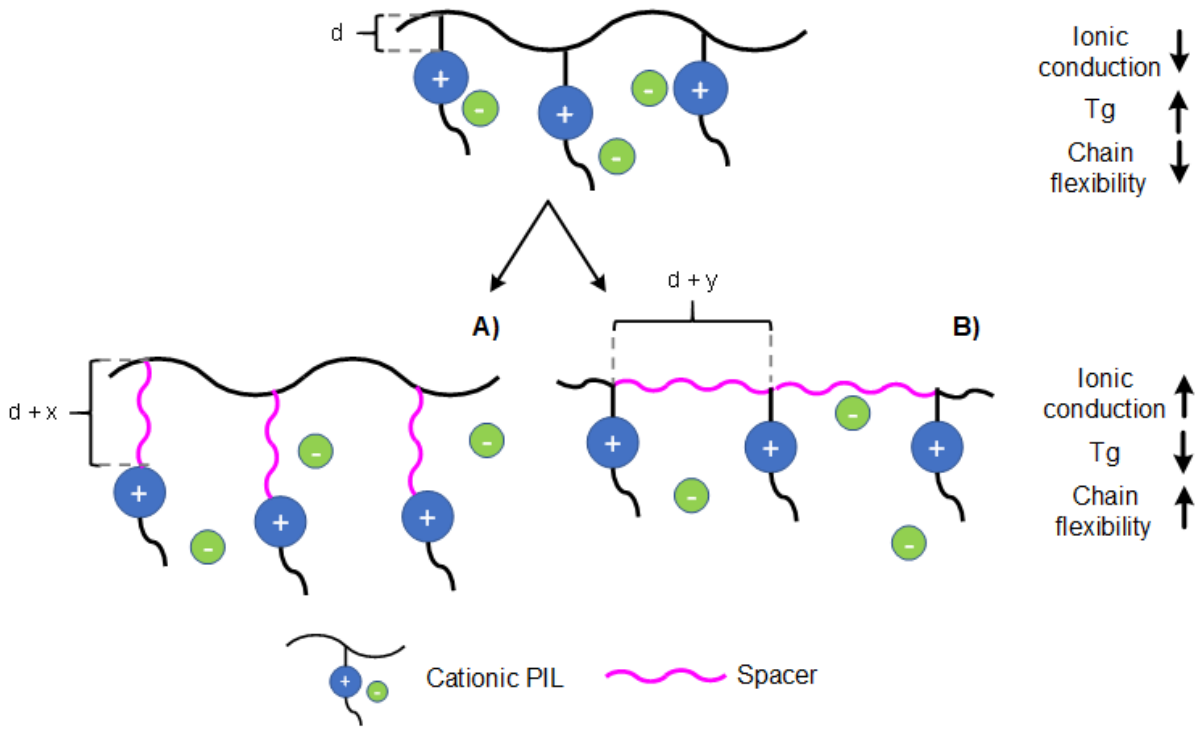

Figure 1.11 Schematic illustration of the effect of spacers in the ionic conductivity of PILs based on increasing the spacer length between the polymer backbone and the IL head group (A) and on the copolymerization of the IL-based monomers with generic comonomers (B). (Adapted from the literature)[113,126,132,133]

1.3 Functionalization of polymers with ionic liquids: methods and principles for the design of multi-stimuli-responsive materials

Over the last years, much effort has been taken to engineer "smart" multi-responsive hydrogels presenting improved functionalities such as fast response to an applied stimulus, high mechanical stability, biodegradability, biocompatibility, and low cost. In order to accomplish these set of properties, polymer functionalization approaches are required.

Functionalization is a powerful tool which envisages to attribute new properties and/or to improve specific properties of a given material, as for instance its thermomechanical stability, multi-stimuli-responsiveness, biodegradability, biocompatibility, ion conductivity, antimicrobial activity, chemical resistance, hydrophobicity/hydrophilicity, by combining the

properties of two or more distinct materials.[134] Different functionalization techniques can be employed for this purpose and the most commonly used are illustrated in Figure 1.12.

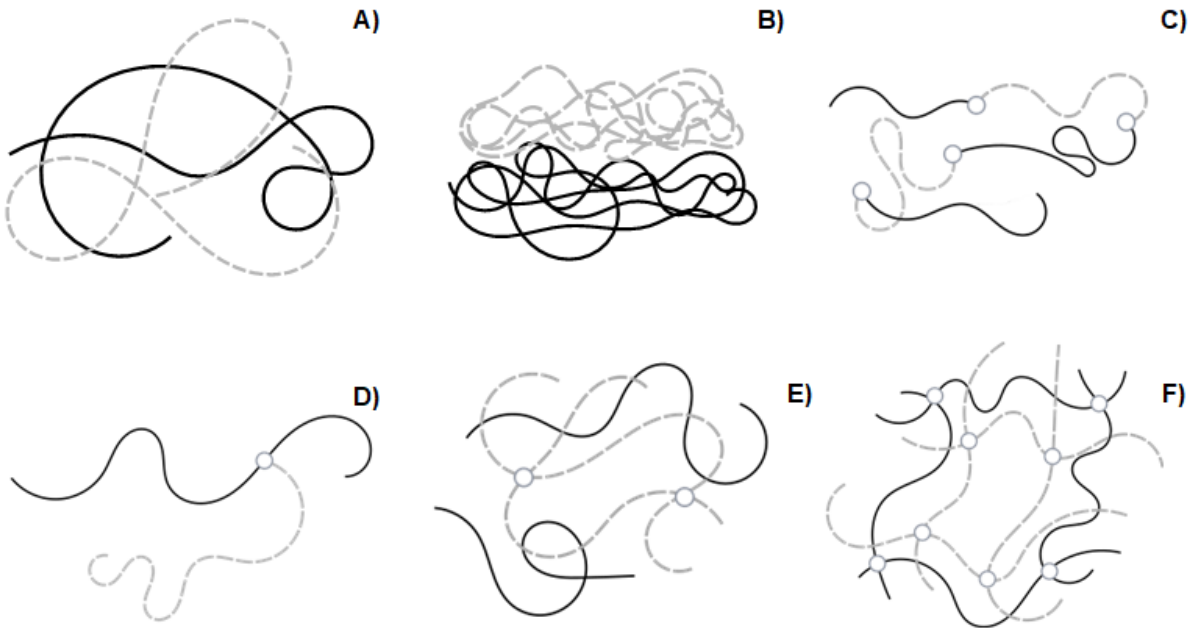

Figure 1.12 Schematic illustration of polymer functionalization strategies: blending (A), coating (B), copolymerization (C), grafting (D), semi-IPN (E) and full-IPN (F). Polymer 1 (▬), Polymer 2 (- - -) and crosslinks (○).

(Adapted from the literature)[135]

A simple functionalization strategy consists in polymer blending. Polymer blends results from the physical mixture/combination *in situ* of two or more polymers and/or additives (e.g. plasticizers, inorganic particles/compounds etc.).[136] Polymer blended systems do not have any chemical crosslinks among the polymeric chains/additives and they are stabilized by secondary forces (e.g. hydrogen bonding interactions) and/or physical entanglements (Figure 1.12A).

Layer-by-layer coating assembly is a common method that allows the fabrication of thin films onto a given substrate (Figure 1.12B). Traditional approaches for layer-by-layer

assembly include dip-coating, spin-coating and spray-coating.[137] which often consist in a sequential deposition of oppositely charged materials (polyelectrolytes, colloids etc.) onto a substrate.[138]

Another simple and common functionalization approach is the crosslinking strategy which allows to tune the physicochemical, mechanical, and structural properties of a given material. In general, a crosslinked material is commonly obtained by chemical (e.g. covalent bonding) and physical (e.g. ionic/electrostatic interactions, hydrogen bonding etc.) crosslinking strategies.[139,140]

Copolymerization (Figure 1.12C) results from the polymerization of two or more different monomers simultaneously.[141] It is an advantageous tool to fabricate diverse materials just by changing the nature and the amount of the comonomer units that are present in the final copolymer. Copolymers can be classified in four different types depending on the organization of their repeating units, namely as A) statistical copolymers: when the distribution of the monomer repeating units along the copolymer chain follows some statistical law (Figure 1.13A); B) random copolymers: when the distribution of the monomer units along the copolymer chain occurs randomly (Figure 1.13B); C) alternating copolymers: when the distribution of the monomer units along the copolymer chain occurs at regular equimolar amounts (Figure 1.13C); D) block copolymers: when the copolymer results from the combination of two long interrupted sequences of homopolymer oligomers (Figure 1.13D).

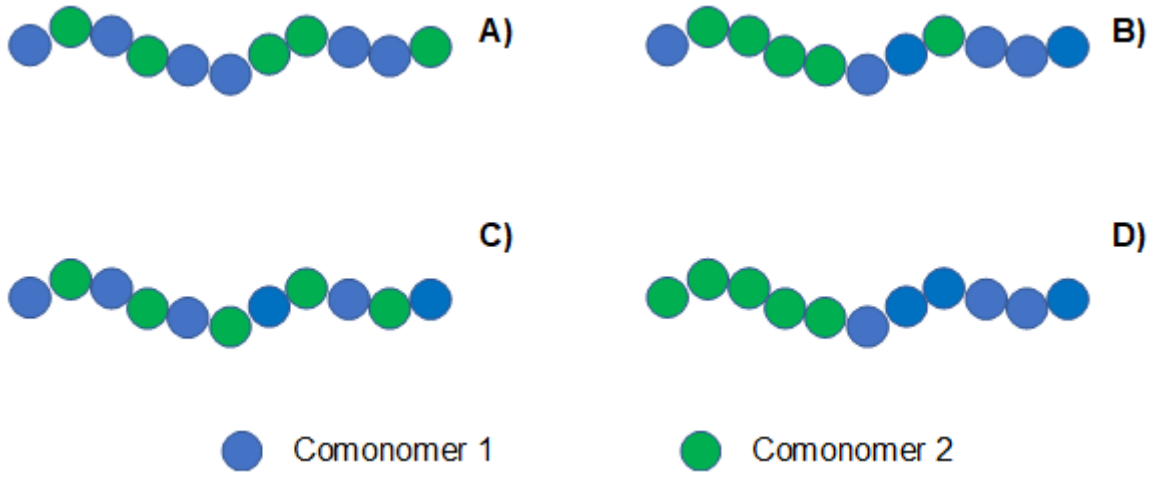

Figure 1.13 Types of copolymers structures.

(Adapted from the literature)[142]

Copolymers can be further classified as homogeneous or heterogeneous. Homogeneous copolymers usually present one T_g while heterogeneous copolymers present two or more T_gs, depending on the nature and number of comonomers employed.[143]

Grafting is a technique that connects, via covalent bonds, a given functional molecule, or a polymer chain, onto the backbone of another polymer chain (Figure 1.12D). It is a versatile method commonly employed to modify natural-based polymers (e.g. cellulose, guar gum, chitosan, dextran, hyaluronic acid and starch) with synthetic polymers to obtain materials presenting improved thermal and chemical stability, ionic conductivity and mechanical strength.[134] Grafting copolymerization can be performed by chemical, physical, physicochemical, and biological approaches which are induced by free radical initiator/redox systems, radiation, plasma and enzymatic methods, respectively.

The chemical method is the most frequently employed one and it relies on the use of chemicals, known as free radical initiators, to generate reactive sites on the main polymer backbone. Potassium permanganate, potassium persulfate, ceric ammonium nitrate and the

Fenton's reagent are the most commonly employed initiators to graft vinyl/acrylic/ester groups onto polymer backbones.[144]

Depending on the employed approach, grafting can be further classified as "grafting onto" and "grafting from". "Grafting onto" consists in the attachment of a previously polymerized molecule onto a target polymer backbone. "Grafting from", which is the most common approach, occurs when the target polymeric backbone contains reactive sites (e.g. radicals, vinylic groups) that allow further growing of a new pendant polymer chain from the polymeric backbone (Figure 1.14).[145,146]

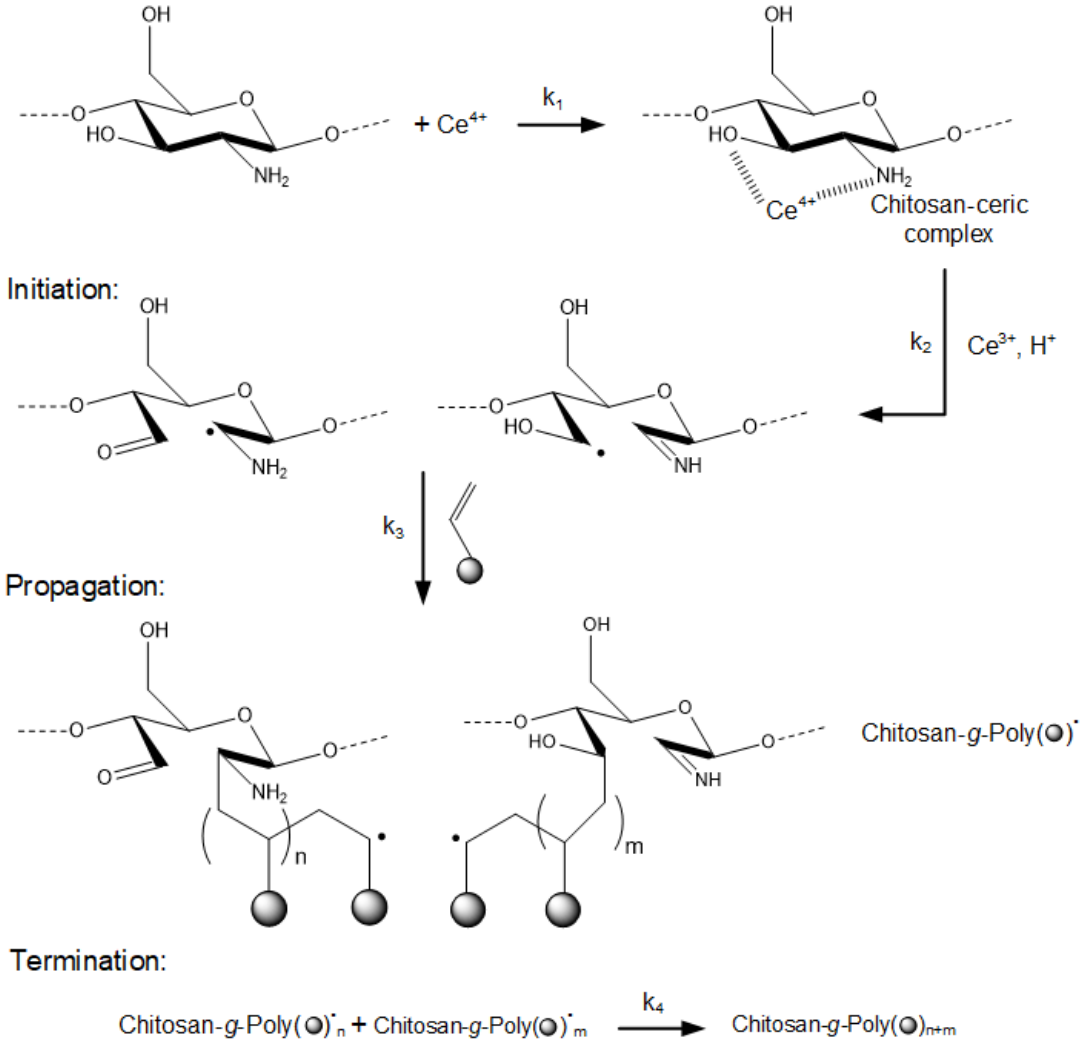

Figure 1.14 Illustration of ceric-induced grafting reaction mechanism of a generic monomer onto chitosan.

(Adapted from the literature)[144]

The formation of semi-interpenetrating polymer networks (semi-IPNs) and full-interpenetrating polymer networks (full-IPNs) (Figure 1.12E and 1.12F, respectively) is a functionalization approach that relies on the synergetic interplay between each polymer that constitutes the network. The International Union of Pure and Applied Chemistry (IUPAC) defines IPN (or full-IPN) and semi-IPN as follows: an IPN is "a polymer comprising two or more networks which are at least partially interlaced on a molecular scale but not covalently bonded to each other and cannot be separated unless chemical bonds are broken"; a semi-IPN is obtained when one of the polymers is crosslinked whilst the second one remains in the linear form. Its formal definition is "a polymer comprising one or more networks and one or more linear or branched polymer(s) characterized by the penetration on a molecular scale of at least one of the networks by at least some of the linear or branched macromolecules".[147] Comparing semi-IPNs (also known as pseudo-IPN) with full-IPNs, the former comprise linear/branched polymers that are only dispersed in the polymeric network without forming a further crosslinked interpenetrating polymer network, and which can be separated without breaking any chemical bonds. In the case of full-IPNs two or more polymers interact (not crosslinked to each other) at a molecular level (e.g. via hydrogen bonds/Van der Waals forces interactions) and cannot be separated unless chemical bonds are broken.[148]

Interpenetrating polymer networks can be produced by the sequential or by the simultaneous pathways. Semi-IPNs can only be obtained by the sequential pathway while full-IPNs can be obtained by either sequential or simultaneous methods (Figure 1.15). Moreover, they can be obtained from the polymerization of monomers or from polymers already formed. In the first case, and according to the sequential pathway, monomers A in solution are polymerized and crosslinked in order to prepare the first network (polymer A). Then, the monomers B are loaded in the previously prepared crosslinked network (polymer A) and further polymerized. When the second network is crosslinked a full-IPN is attained. In the second case (sequential

pathway from polymers) semi-IPNs are obtained by soaking a crosslinked polymer network (polymer A) with a non-crosslinked polymer (polymer B). Once again, full-IPNs are obtained by this procedure if polymer B is further crosslinked. Free radical polymerization is the easiest and consequently the most commonly used method to prepare full-IPNs/semi-IPNs by the *in situ* sequential pathway.

Regarding the simultaneous pathway, full-IPNs are obtained by mixing the monomers/polymers (A and B) together with their respective crosslinking agents and the polymerization/crosslinking reactions take place simultaneously (without interfering in one another). Full-IPNs prepared via simultaneous pathway are often accomplished when each polymer networks is obtained from different polymerization mechanisms (e.g. polymer A – condensation and polymer B – free radical polymerization) in order to avoid the formation of secondary polymeric structures (e.g. copolymers). The advantage of the simultaneous pathway over the sequential one is that the former originates complex structures with higher degree of intermixing.[135,149]

In order to differentiate IPNs from polymer blends and grafted copolymers some considerations must be taken: IPNs differ from polymer blends and polymer grafting since polymer blends are simple physical mixtures of two or more components without any chemical crosslinking between them while polymer grafting involves a chemical modification by inserting new functional groups/polymeric structures on a given polymeric backbone.[150]

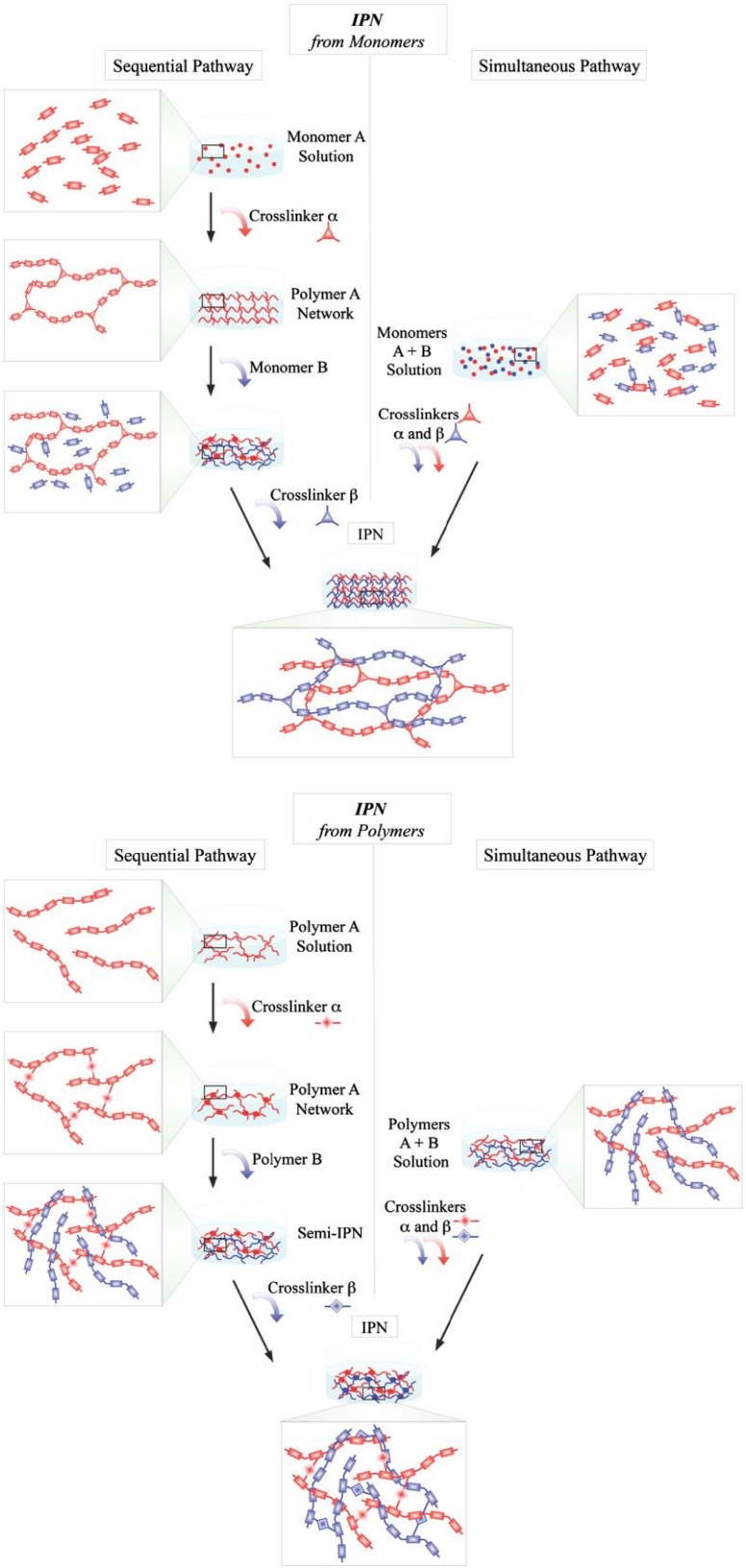

Figure 1.15 Schematic representation of sequential and simultaneous pathway of a semi-IPN and full-IPN formation. Generic monomer/polymers (A and B). Generic physical/chemical crosslinkers (α and β). (Reprinted with permission from Elsevier)[149]

The previously mentioned functionalization strategies were employed to functionalize different materials with ILs/PILs regarding several applications.

PIL-based polymer blends were prepared by mixing imidazolium-based poly(ionic liquids) with different polymers (e.g. PVDF, Pebax® 1657) to obtain solid-state polymer electrolytes[151] and gas separation membranes.[152] Crosslinked imidazolium-based polymers were prepared to obtain mechanically robust polyelectrolytes towards different applications, namely as batteries,[119] actuators,[153] CO_2 sensors[154] and capacitors.[155] Surface functionalized materials were obtained by the deposition of layer-by-layer ammonium- and imidazolium-based ILs/PILs onto the surface of poly(ether sulfone) membranes, glass substrates and stainless-steel wires to enhance its surface properties (e.g. charge density, antifouling capacity, hydrophobicity etc.) regarding several applications such as antifouling membranes,[156] superhydrophobic surfaces[157] and fibers for separation processes.[158]

Table 1.1 summarizes different IL functionalized materials reported in the literature which were obtained by IPNs, copolymerization and grafting functionalization methods, as well as their envisaged application. Notice that most of the reported functionalized materials were obtained from the polymerization of imidazolium-based ILs which highlights the versatility of this ionic liquid. Table 1.1 also indicates that few studies were conducted on the functionalization of natural-origin polymers with ILs which opens new opportunities to be explored. As can be also concluded from Table 1.1 most of IL-functionalized materials developed so far target the development of materials for electronic devices such as batteries, fuel cells and solid electrolytes. Therefore, the development of IL functionalized materials for biomedical applications is a new and challenging research field that has not been explored yet.

Table 1.1 List of IL-functionalized materials obtained from different functionalization strategies (IPNs, copolymerization, grafting) reported in the literature and corresponding envisaged applications.

Interpenetrating polymer networks (IPNs)			
Network #1	**Network #2**	**Application**	**Ref.**
Crosslinked Epoxy-amine resin	Poly(ethylene glycol) dimethacrylate sulfonimide ethylmethylimidazolium	Electrochemical devices	159
Poly(vinyl acetate)	Crosslinked poly(1-vinyl-3-octylimidazolium hexafluorophosphate)	Gas separation	160
Bacterial nanocellulose	Crosslinked poly(methacroylcholine chloride)	Fuel cells	161
Poly(*N*-isopropylacrylamide)	Crosslinked poly(tributyl-hexyl phosphonium 3-sulfopropylacrylate)	Flow control in microfluidics	162
Poly(silver acrylate)	Poly(1-(10-(acryloyloxy)decyl)-3-methylimidazolium chloride	Absorbent gel	163
Poly(*N*-isopropylacrylamide -co-spiropyran-co-acrylic acid)	Crosslinked poly(tributylhexyl phosphonium 3-sulfopropyl acrylate)	Polymer actuator	164
Glass fiber	Crosslinked poly(1-ethyl-3-vinylimidazolium bromide-co-3-aminoethyl-1-vinylimidazolium bromide hydrobromide)	Batteries	165
Crosslinked poly(ethylene glycol)	Poly(diallyldimethylammonium) bis(trifluoromethanesulfonyl)imide	Batteries	166
Poly(ethylene oxide)	Crosslinked poly(1-vinyl-3-methylimidazolium bis(trifluoromethylsulfonyl)imide)	Batteries	167

Table 1.1 Cont.

Copolymerization			
Comonomer #1	**Comonomer #2**	**Application**	**Ref.**
Ethyl acrylate	1-(2-ethoxyethyl)-3-vinylimidazolium bromide	Solid electrolytes for energy devices	168
Styrene	1-(4-vinylbenzyl)-3-methylimidazolium chloride	Photovoltaic cells	169
N-vinyl-3-ethylimidazolium bromide	*N*-vinyl-3-octylimidazolium bromide	Antimicrobial coatings and batteries	1706
4-[12-(4-butyl-4'-oxy-azobenzene)dodecyl] oxycarbonylstyrene	4-vinylbenzylhexylimidazolium bis(trifluoromethanesulfonyl)imide	Solid polymer electrolyte	171
N-isopropylacrylamide	1-ethyl-3-vinylimidazolium bromide	Ionic conductive material	172
2-hydroxyethyl methacrylate	1,4-di(vinylimidazolium)butane bisbromide	Electrochemical double-layer capacitor	122
N,*N*-dimethylacrylamide	1-butyl-3-(4-vinylbenzyl)imidazolium tetrafluoroborate	Nano-objects	173
Stryene	1-(4-vinylbenzyl)-3-methylimidazolium chloride	Not specified	174
Acrylic acid	4-vinylbenzyl-3-butylimidazolium bis(trifluoromethylsulfonyl)imide	Drug delivery system	175
Divinylbenzene	1-ethyl-3-vinylimidazolium bromide 1-butyl-3-vinylimidazolium hexafluorophosphate	Catalysis	176
N-isopropylacrylamide	3-butyl-1-vinylimidazolium bromide	Temperature sensor Electrochromic devices	177
Ethylene glycol methyl ether methacrylate	Lithium 1-[3-(methacryloyloxy)propylsulfonyl]-1-(trifluoromethylsulfonyl)imide	Solid polyelectrolytes	178

Table 1.1 Cont.

Grafting			
Host matrix/Surface	**Grafted material**	**Application**	**Ref.**
2-Hydroxyethyl cellulose	Poly(1-(11-acryloyloxyundecyl)-3-methylimidazolium bromide	Antibacterial coatings	179
Chitosan	3-(3-vinylimidazolyl)propane-1-sulfonate	Catalysis	180
Multi-walled carbon nanotubes	Poly(1-(4-vinylbenzyl)-3-methylimidazolium chloride)	Catalysis	181
Cellulose nanofibrils	Poly(1-ethyl-3-vinylimidazolium bromide)	Catalysis	182
Thiol-basalt fibers	1-dodecyl-3-vinylimidazolium bromide	Coating	183
Chitosan	4-methoxypyridinium ethoxysalicylaldehyde	Antifouling	184
Nose clips	Poly(1-vinyl-3-allylimidazolium iodide)	Antibacterial coating	185
Cellulose	1-allyl-3-vinylimidazolium bromide 1-hexyl-3-vinylimidazolium bromide 1-butyl-3-vinylimidazolium chloride	Ultrafiltration membrane	186
Poly(vinyl alcohol)	1-butydulfonate-3-vinylimidazole hydrogen sulfate	Catalysis	187
Acrylate-based copolymers	(2-(methacryloyloxy)ethyl) trimethylammonium chloride	Drug release	188
Hyaluronic acid	Poly(1-vinyl-3-hexylimidazolium bromide)	Drug delivery	189
Silica-coated iron oxide nanoparticles	dimethyl-dodecyl-4-vinylbenzyl ammonium chloride	Magnetic adsorbent	190
Carbon dots	2-methacryloyloxyethyl-*N*,*N*-dimethylbuthan-ammonium bromide	Lubricant additives	191

1.4 Relevant scientific contribution of the multi-responsive electroactive systems developed in this PhD Thesis

Reputed and well-experienced research groups in the scientific community of ionic liquids have been developing advanced IL-based/PIL-based materials for several applications, namely for batteries,[94,117,118,120,192,193] actuators,[109,111,194] capacitors,[95] gas harvesting,[115,116] sensors,[195] lubricants,[196] catalysis,[197] fragrance precursors,[198] tissue engineering scaffolds,[96] and sorbents.[199] In this context, the present doctoral work broadens the application horizon of ionic liquids towards the fabrication of multi-responsive electroactive IL-based polyelectrolytes and opens a new window for their potential application in biomedicine (e.g. tissue engineering scaffolds, drug delivery systems, hemostatic dressings etc.), in separation processes (e.g. electro-assisted wastewater treatment) and in electrochemical devices (e.g. non-leaching soft actuators). Multi-stimuli-responsive materials offer several advantages over conventional single-stimulus-responsive ones as they exhibit precise tuning of the envisaged response. This characteristic is particularly important when these materials are to be applied in complex environments (e.g. *in vivo*). In order to develop biocompatible platforms that respond to simultaneously applied-stimuli, chemically functionalized IL-based copolymers and/or IL-based semi-IPNs still represent an unexplored research field. These materials allow the development of hydrogels sensitive to different external stimulus including relative humidity, ionic strength, pH and electrical current. This PhD Thesis focused on the chemical modification of natural and/or synthetic polymers with 1-butyl-3-vinylimidazolium chloride aiming the design of innovative IL-based polycationic multi-stimuli-responsive platforms. The relevant and original scientific contribution of this PhD Thesis relies on: A) development of electro-responsive polysaccharide/IL-based semi-IPN hydrogels that present fixed charge density (independent of media's pH), ionic conductivity, response over changes in ionic strength (by swelling/shrinking) and electrical current; sustained sorption/desorption and

iontophoretic permeation/release of charged biomolecules and which are also cyto- and hemo-biocompatible; B) design of IL-based electroactive copolymers that respond to external variations of ionic strength and of electrical stimulus by presenting tunable electromechanical actuation as a function of their surface properties.

1.5 References

(1) Hoffman, A. S. Hydrogels for biomedical applications. *Advanced Drug Delivery Reviews* **2012**, 64, 18-23.

(2) Caló, E.; Khutoryanskiy, V. V. Biomedical applications of hydrogels: A Review of patents and commercial products. *European Polymer Journal* **2015**, 65, 252-267.

(3) Feksa, L. R.; Troian, E. A.; Muller, C. D.; Viegas, F.; Machado, A. B.; Rech, V. C. Hydrogels for biomedical applications. Nanostructures for the Engineering of Cells, Tissues and Organs from Design to Applications **2018**, 403-438.

(4) Derakhshanfar, S.; Mbeleck, R.; Xu, K.; Zhang, X.; Zhong, W.; Xing, M. 3D bioprinting for biomedical devices and tissue engineering: A review of recent trends and advances. *Bioactive Materials* **2018**, 3, 144-156.

(5) Gupta, A.; Kowalczuk, M.; Heaselgrave, W.; Britland, S. T.; Martin, C.; Radecka, I. The production and application of hydrogels for wound management: A review. *European Polymer Journal* **2019**, 111, 134-151.

(6) Ionov, L. Hydrogel-based actuators: possibilities and limitations. *Materials Today* **2014**, 17, 494-503.

(7) Koetting, M. C.; Peters, J. T.; Steichen, S. D.; Peppas, N. A. Stimulus-responsive hydrogels: Theory, modern advances, and applications. *Materials Science and Engineering R* **2015**, 93, 1-49.

(8) Mahinroosta, M.; Farsangi, Z. J.; Allahverdi, A.; Shakoori, Z. Hydrogels as intelligent materials: A brief review of synthesis, properties and applications. *Materials Today Chemistry* **2018**, 8, 42-55.

(9) Thakur, S.; Arotiba, O. A. Synthesis, swelling and adsorption studies of a pH-responsive sodium alginate-poly(acrylic acid) superabsorbent hydrogel. *Polymer Bulletin* **2018**, 10, 4587-4606.

(10) Aycan, D.; Alemdar, N. Development of pH-responsive chitosan-based hydrogel modified with bone ash for controlled release of amoxicillin. *Carbohydrate Polymers* **2018**, 184, 401-407.

(11) Lim, H. L.; Hwang, Y.; Kar, M.; Varghese, S. Smart hydrogels as functional biomimetic systems. *Biomaterials Science* **2014**, 2, 603-618.

(12) He, S.; Li, H.; Chen, H. Preparation of light-sensitive polymer/graphene composite via molecular recognition by β-cyclodextrin. *Journal of Materials Science* **2018**, 53, 14337-14349.

(13) Palza, H.; Zapata, P. A.; Angulo-Pineda, C. Electroactive Smart Polymers for Biomedical Applications. *Materials* **2019**, 12, 277.

(14) Balint, R.; Cassidy, N. J.; Cartmell, S. H. Conductive polymers: Towards a smart biomaterial for tissue engineering. *Acta Biomaterialia* **2014**, 10, 2341-2353.

(15) Ghasemi-Mobarakeh, L.; Prabhakaram, M. P.; Morshed, M.; Nars-Esfahani, M. H.; Baharvand, H.; Kiani, S.; Al-Deyab, S. S.; Ramakrishna, S. Application of conductive polymers, scaffolds and electrical stimulation for nerve tissue engineering. *Journal of Tissue Engineering and Regenerative Medicine* **2011**, 5, 17-35.

(16) Nezakati, T.; Seifalian, A.; Tan, A.; Seifalian, A. M. Conductive Polymers: Opportunities and Challenges in Biomedical Applications. *Chemical Reviews* **2018**, 118, 6766-6843.

(17) Alegret, N.; Dominguez-Alfaro, A.; Mecerreyes, D. 3D Scaffolds Based on Conductive Polymers for Biomedical Applications. *Biomacromolecules* **2019**, 20, 73-89.

(18) Gajendiran, M.; Choi, J.; Kim, S.-J.; Kim, K.; Shin, H.; Koo, H-J.; Kim, K. Conductive biomaterials for tissue engineering applications. *Journal of Industrial and Engineering Chemistry* **2017**, 51, 12-26.

(19) Szunerits, S.; Teodorescu, F.; Boukerroub, R. Electrochemically triggered release of drugs. *European Polymer Journal* **2016**, 83, 467-477.

(20) Maziz, A.; Simaite, A.; Bergaud, C. Ionic Electrochemical Actuators. Polymerized Ionic Liquids, Eftekhari, A. (ed.), The Royal Society of Chemistry, **2018**.

(21) Melling, D.; Martinez, J. G.; Jager, E. W. H. Conjugated Polymer Actuators and Devices: Progress and Opportunities. *Advanced Materials* **2019**, 31, 1808210.

(22) Yuk, H.; Lu, B.; Zhao, X. Hydrogel bioeletronics. *Chemical Society Reviews* **2019**, 48, 1642-1667.

(23) Aziz, S. B.; Woo, T. J.; Kadir, M. F. Z.; Ahmed, H. M. A conceptual review on polymer electrolytes and ion transport models. *Journal of Science: Advanced Materials and Devices* **2018**, 3, 1-17.

(24) Na, R.; Liu, Y.; Lu, N.; Zhang, S.; Liu, F.; Wang, G. Mechanically robust hydrophobic association hydrogel electrolyte with efficient ionic transport for flexible supercapacitors. *Chemical Engineering Journal* **2019**, 374, 738-747.

(25) Li, R.; Zhang, K.; Cai, L.; Chen, G.; he, M. Highly stretchable ionic conducting hydrogels for strain/tactile sensors. *Polymer* **2019**, 167, 154-158.

(26) Zhou, Y.; Wan, C.; Yang, Y.; Yang, H.; Wang, S.; Dai, Z.; Ji, K.; Jiang, H.; Chen, X.; Long, Y. Highly Stretchable, Elastic, and Ionic Conductive Hydrogel for Artificial Soft Electronics. *Advanced Functional Materials* **2019**, 29, 1806220.

(27) Boaretto, N.; Meabe, L.; Martinez-Ibañez, M.; Armand, M.; Zhang, H. Review – Polymer Electrolytes for Rechargeable Batteries: From Nanocomposite to Nanohybrid. *Journal of the Electrochemical Society* **2020**, 167, 070524.

(28) Rahimi, N.; Molin, D. G.; Cleij, T. J.; van Zandvoort, M. A.; Post, M. J. Electrosensitive Polyacrylic Acid/Fibrin Hydrogel Facilitates Cell Seeding and Alignment. *Biomacromolecules* **2012**, 13, 1448-1457.

(29) Dias, A. M. A.; Cortez, A. R.; Barsan, M. M.; Santos, J. B.; Brett, C. M. A.; de Sousa, H. C. Development of greener multi-responsive chitosan biomaterials doped with biocompatible ammonium ionic liquids. *ACS Sustainable Chemistry & Engineering* **2013**, 1, 1480-1492.

(30) Paradee, N.; Sirivat, A.; Niamlang, S.; Prissanaroon-Ouajai, W. Effects of crosslinking ratio, model drugs, and electric field strength on electrically controlled release for alginate-based hydrogel. *Journal of Materials Science: Materials in Medicine* **2012**, 23, 999-1010.

(31) Kim, S. J.; Kim, H. I.; Shin, S. R.; Kim, S. I. Electrical behavior of chitosan and poly(hydroxyethyl methacrylate) hydrogel in the contact system. *Journal of Applied Polymer Science* **2004**, 92, 915-919.

(32) Chen, Z.; Tan, X. A Control-Oriented and Physics-Based Model for Ionic Polymer-Metal Composites Actuators. *IEEE/ASME Transactions on Mechatronics* **2008**, 13, 519-529.

(33) Diao, W.; Wu, L.; Ma, X.; Wang, L.; Bu, X.; Ni, W.; Yang, X.; Fang, Y. Reversibly highly stretchable and self-healable zwitterion-containing polyelectrolyte hydrogel with high ionic conductivity for high-performance flexible and cold-resistance super capacitor. *Journal of Applied Polymer Science* **2020**, 137, e48995.

(34) Shin, S.-H.; Lee, W.; Kim, S.-M.; Lee, M.; Koo, J. M.; Hwang, S. Y.; Oh, D. X.; Park, J. Ion-conducting self-healing hydrogels based on interpenetrating polymer network for a multimodal sensor. *Chemical Engineering Journal* **2019**, 371, 452-460.

(35) Sénéchal, V.; Saadaoui, H.; Rodriguez-Hernandez, J.; Drummond, C. Electro-responsive polyelectrolyte-coated surfaces. *Faraday Discussions* **2017**, 199, 335-347.

(36) Lin, C.-Y.; Luo, S.-C.; Yu, J.-S.; Chen, T.-C.; Su, W.-F. Peptide-Based Polyelectrolyte Promote Directional and Long Neurite Outgrowth. *ACS Applied Bio Materials* **2019**, 2, 518-526.

(37) Paitatwachapun, S.; Paradee, N.; Sirivat, A. Controlled release of acetylsalicylic acid from polythiophene/carrageenan hydrogel via electrical stimulation. *Carbohydrate Polymers* **2016**, 137, 214-221.

(38) Pérez-Martínez, C. J.; Chávez, S. D. M.; del Castillo-Castro, T.; Ceniceros, T. E. L.; Castillo-Ortega, M. M.; Rodríguez-Félix, D. E.; Ruiz, J. C. G. Electroconductive nanocomposite hydrogel for pulsatile drug release. *Reactive and Functional Polymers* **2016**, 100, 12-17.

(39) Murdan, S. Electro-responsive drug delivery from hydrogels. *Journal of Controlled Release* **2003**, 92, 1-17.

(40) Delgado, D.; Hefter, G.; Minakshi, M. Alternative Energies, Advanced Structured Materials, Ferreira, G. (ed.). ©Springer-Verlag Berlin Heidelberg, **2013**.

(41) Guy, R. H.; Kalia, Y. N.; Delgado-Charro, M. B.; Merino, V.; López, A.; Marro, D. Iontophoresis: electrorepulsion and electroosmosis. *Journal of Controlled Release* **2000**, *64*, 129-132.

(42) Kanaan, A. F.; Barsan, M. M.; Brett, C. M. A.; Alvarez-Lorenzo, C.; Concheiro, A.; de Sousa, H. C.; Dias, A. M. A. Sustainable Electro-Responsive Semi-Interpenetrating Starch/Ionic Liquid Copolymer Networks for the Controlled Sorption/Release of Biomolecules. *ACS Sustainable Chemistry & Engineering* **2019**, 7, 10516-10532.

(43) Watanabe, M.; Imaizumi, S.; Yasuda, T.; Kokubo, H. Ion Gels for Ionic Polymer Actuator. Soft Actuators, Asaka, K.; Okuzaki, H. (eds.), Springer Japan, **2014**.

(44) Adesanya, K.; Vanderleyden, E.; Embrechts, A.; Glazer, P.; Mendes, E.; Dubruel, P. Properties of electrically responsive hydrogels as a potential dynamic tool for biomedical applications. *Journal of Applied Polymer Science* **2014**, 41195, 1-9.

(45) Kikuchi, K.; Tsuchitani, S. Ionic conductive polymers. Soft Actuators, Asaka, K.; Okuzaki, H. (eds.), Springer **2014**, 81-93.

(46) Carpi, F.; Smela, E. Biomedical Applications of Electroactive Polymer Actuator. John Wiley & Sons Ltd. **2009**.

(47) Lee, A. A.; Colby, R. H.; Kornyshev, A. A. Electroactuation with single charge carrier ionomers: the roles of electrostatic pressure and steric strain. *Soft Matter* **2013**, 9, 3767-3776.

(48) Tanaka, T.; Nishio, I.; Sun, S-.T.; Ueno-Nishio, S. Collapse of Gels in an Electric Field. *Science* **1982**, 218, 467-469.

(49) Kishi, R.; Osada, Y. Reversible Volume Change of Microparticles in an Electric Field. *Journal of the Chemical Society, Faraday Transactions* **1989**, 85, 655-662.

(50) Hirose, Y.; Giannetti, G.; Marquardt, J.; Tanaka, T. Migration of Ions and pH Gradients in Gels under Stationary Electric Fields. *Journal of The Physical Society of Japan* **1992**, 61, 4085-4097.

(51) Doi, M.; Matsumoto, M.; Hirose, Y. Deformation of Ionic Polymer Gels by Electric Fields. *Macromolecules* **1992**, 25, 5504-5511.

(52) Glazer, P. J.; van Erp, M.; Embrechts, A.; Lemay, S. G.; Mendes, E. Role of pH gradients in the actuation of electro-responsive polyelectrolyte gels. *Soft Matter* **2012**, 8, 4421-4426.

(53) Morales, D.; Palleau, E.; Dickey, M. D.; Velev, O. D. Electro-actuated hydrogel walkers with dual responsive legs. *Soft Matter* **2014**, 10, 1337-1348.

(54) Chang, L.; Liu, Y.; Yang, Q.; Yu, L.; Liu, J.; Zhu, Z.; Lu, P.; Wu, Y.; Hu, Y. Ionic Electroactive Polymers Used in Bionic Robots: A Review. *Journal of Bionic Engineering* **2018**, 15, 765-782.

(55) Jiang, H.; Fan, L.; Yan, S.; Li, F.; Li, H.; Tang, J. Tough and electro-responsive hydrogel actuators with bidirectional behavior. *Nanoscale* **2019**, 11, 2231-2237.

(56) Zolfagharian, A.; Kouzani, A. Z.; Maheepala, M.; Khoo, S. Y.; Kaynak, A. Bending control of a 3D printed polyelectrolyte soft actuator with uncertain model. *Sensors and Actuators A: Physical* **2019**, 288, 134-143.

(57) Chang, X. L.; Chee, P. S.; Lim, E. H.; Chong, W. C. Radio-frequency enable ionic polymer metal composite (IPMC) actuator for drug release application. *Smart Materials and Structures* **2019**, 28, 015024.

(58) Shi, Q.; Liu, H.; Tang, D.; Li, Y.; Li, X.; Xu, F. Bioactuators based on stimulus-responsive hydrogels and their emerging biomedical applications. *NPG Asia Materials* **2019**, 11, 64.

(59) Wilkes, J. S. A short history of ionic liquids-from molten salts to neoteric solvents. *Green Chemistry* **2002**, 4, 73-80.

(60) Wasserscheid, P.; Keim, W. Ionic Liquids – New "Solutions" for Transition Metal Catalysis. *Angewandte Chemie International Edition* **2000**, 39, 3772-3789.

(61) Earle, M. J.; Seddon, K. R. Ionic liquids: green solvents for the future in: Abraham, M. A.; Moens, L. Clean solvents. Alternative media for chemical reactions and processing. American Chemical Society, **2002**, 10-25.

(62) Plechkova, N. V.; Seddon, K. R. Applications of ionic liquids in the chemical industry. *Chemical Society Reviews* **2008**, 37, 123-50.

(63) Welton, T. Room-Temperature Ionic Liquids. Solvents for Synthesis and Catalysis. *Chemical Reviews* **1999**, 99, 2071-2083.

(64) Boruń, A. Conductance and ionic association of selected imidazolium ionic liquids in various solvents: A review. *Journal of Molecular Liquids* **2019**, 276, 214-224.

(65) Yavir, K.; Marcinkowski, Ł.; Marcinkowski, R.; Namieśnik, J.; Kloskowski, A. Analytical applications and physicochemical properties of ionic liquid-based hybrid materials: A review. *Analytica Chimica Acta* **2019**, 1054, 1-16.

(66) Ventura, S. P. M.; Gonçalves, A. M. M.; Sintra, T.; Pereira, J. L.; Gonçalves, F.; Coutinho, J. A. P. Designing ionic liquids: the chemical structure role in the toxicity. *Ecotoxicology* **2013**, 22, 1-12.

(67) Vila, J.; Varela, L. M.; Cabeza, O. Cation and anion sizes influence in the temperature dependence of the electrical conductivity in nine imidazolium based ionic liquids. *Electrochimica Acta* **2007**, 52, 7413-7417.

(68) Kulkarni, P. S.; Branco, L. C.; Crespo, J. G.; Nunes, M. C.; Raymundo, A.; Afonso, C. A. M. Comparison of Physicochemical Properties of New Ionic Liquids Based on Imidazolium, Quaternary Ammonium, and Guanidinium Cations. *Chemistry – A European Journal* **2007**, 13, 8478-8488.

(69) Pernak, J.; Chwala, P. Synthesis and anti-microbial activities of choline-like quaternary ammonium chlorides. *European Journal of Medicinal Chemistry* **2003**, 38, 1035-1042.

(70) Egorova, K. S.; Ananikov, V. P. Toxicity of Ionic Liquids: Eco(cyto)activity as Complicated, but Unavoidable Parameter for Task-Specific Optimization. *ChemSusChem* **2014**, 7, 336-360.

(71) Yanghuai, Z.; Biying, A. O.; Siwei, X.; Hosmane, N. S.; Maguire, J. A. Ionic Liquids in Catalytic Biomass Transformation in Applications of Ionic Liquids in Science and Technology, Handy, S. T. (ed.), **2011**.

(72) Amde, M.; Liu, J.-F.; Pang, L. Environmental Application, Fate, Effects, and Concerns of Ionic Liquids: A Review. *Environmental Science & Technology* **2015**, 49, 12611-12627.

(73) Costa, S. P. F.; Azevedo, A. M. O.; Pinto, P. C. A. G.; Saraiva, M. L. M. F. S. Environmental Impact of Ionic Liquids: Recent Advances in (Eco)toxicology and (Bio)degradability. *ChemSusChem* **2017**, 10, 2321-2347.

(74) Ostadjoo, S.; Berton, P.; Shamshina, J. L.; Rogers, R. D. Scaling-Up Ionic Liquid-Based Technologies: How Much Do We Care About Their Toxicity? *Prima Facie* Information on 1-Ethyl-3-Methylimidazolium Acetate. *Toxicological Sciences* **2018**, 161, 249-265.

(75) Pawłowska, B.; Telesiński, A.; Biczak, R. Phytotoxicity of ionic liquids. *Chemosphere* **2019**, 237, 124436.

(76) Armand, M.; Endres, F.; MacFarlane, D. R.; Ohno, H.; Scrosati, B. Ionic-liquid materials for the electrochemical challenges of the future. *Nature Materials* **2009**, 8, 621-629.

(77) Prasad, K.; Murakami, M.; Kaneko, Y.; Takada, A.; Nakamura, Y.; Kadokawa, J. Weak gel of chitin with ionic liquid, 1-allyl-3-methylimidazolium bromide. *International Journal of Biological Macromolecules* **2009**, 45, 221-225.

(78) Izawa, H.; Kadokawa, J. Preparation and characterizations of functional ionic liquid-gel and hydrogel materials of xanthan gum. *Journal of Materials Chemistry* **2010**, 20, 5235-5241.

(79) Prasad, K.; Mine, S.; Kaneko, Y.; Kadokawa, J. Preparation of cellulose-based ionic porous material compatibilized with polymeric ionic liquid. *Polymer Bulletin* **2010**, 64, 341-349.

(80) Taheri, N.; Abdolmaleki, A.; Fashandi, H. Pyridinium-based ionic liquid/water mixture intended for sufficient dissolution of cellulose, chitosan and chitin: The pivotal contribution of water. *Carbohydrate Polymers* **2018**, 195, 413-419.

(81) Liu, X.; Chen, X.; Xu, Y.; Chen, T.; Zeng, X. Effects of Water on Ionic liquid Electrochemical Microsensor for Oxygen Sensing. *Sensors and Actuators B: Chemical* **2019**, 285, 350-357.

(82) Berthod, A.; Ruiz-Ángel, M. J.; Carda-Broch, S. Recent advanced on ionic liquids uses in separation techniques. *Journal of Chromatography A* **2018**, 1559, 2-16.

(83) Capela, E. V.; Quental, M. V.; Domingues P.; Coutinho, J. A. P.; Freire, M. G. Effective separation of aromatic and aliphatic amino acid mixtures using ionic-liquid-based aqueous biphasic systems. *Green Chemistry* **2017**, 19, 1850-1854.

(84) Liu, H; Yu, H. Ionic liquids for electrochemical energy storage devices applications. *Journal of Materials Science & Technology* **2019**, 35, 674-686.

(85) Safna Hussan, K. P.; Thayyil, M. S.; Deshpande, S. K.; Jinitha, T. V.; Kolte J. Development of ion conducting ionic liquid-based gel polymer electrolyte membrane PMMA/BMPyr.TFSI – With improved electrical, optical, thermal, and structural properties. *Solid State Ionics* **2017**, 310, 166-175.

(86) Dias, A. M. A.; Marceneiro, S.; Johansen, H. D.; Barsan, M. M.; Brett, C.; de Sousa, H. C. Phosphonium ionic liquids as greener electrolytes for poly(vinyl chloride)-based ionic conducting polymers. *RSC Advances* **2016**, 6, 88979-88990.

(87) Liew, C-.W.; Ramesh, S.; Arof, A. K. Investigation of ionic liquid-doped ion conducting polymer electrolytes for carbon-based electric double layer capacitors (EDLCs). *Materials and Design* **2016**, 92, 829-835.

(88) Petkovic, M.; Seddon, K. R.; Rebelo, L. P. N.; Silva Pereira, C. Ionic liquids: a pathway to environmental acceptability. *Chemical Society Reviews* **2011**, 40, 1383-1403.

(89) Gundolf, T.; Rauch, B.; Kalb, R.; Rossmanith, P.; Mester, P. Influence of bacterial lipopolysaccharide modifications on the efficacy of antimicrobial ionic liquids. *Journal of Molecular Liquids* **2018**, 271, 220-227.

(90) Wilms, W.; Woźniak-Karczewska, M.; Syguda, A.; Niemczak, M.; Ławniczak, Ł.; Pernak, J.; Rogers, R. D.; Chrzanowski, L. Herbicidal ionic liquids – a promising future for

old herbicides? Review on synthesis, toxicity, biodegradation and efficacy studies. *Journal of Agricultural and Food Chemistry* **2020**, 68, 10456-10488.

(91) Marrucho, I. M.; Branco, L. C.; Rebelo, L. P. N. Ionic liquids in Pharmaceutical Applications. *Annual Review of Chemical and Biomolecular Engineering* **2014**, 5, 527-546.

(92) Egorova, K. S.; Gordeev, E. G.; Ananikov, V. P. Biological Activity of Ionic Liquids and Their Application in Pharmaceutics and Medicine. *Chemical Reviews* **2017**, 117, 7132-7189.

(93) Mejri, R.; Dias, J. C.; Besbes Hentati, S.; Martins, M. S.; Costa, C. M.; Lanceros-Mendez, S. Effect of anion type in the performance of ionic liquid/poly(vinylidene fluoride) electromechanical actuators. *Journal of Non-Crystalline Solids* **2016**, 453, 8-15.

(94) Serra, J. P.; Pinto, R. S.; Barbosa, J. C.; Correia, D. M.; Gonçalves, R.; Silva, M. M.; Lanceros-Mendez, S.; Costa, C. M. Ionic liquid based Fluropolymer solid electrolytes for Lithium-ion batteries. *Sustainable Materials and Technologies* **2020**, 25, e00176.

(95) Rana, H. H.; Park, J. H.; Ducrot, E.; Park, H.; Kota, M.; Han, T. H.; Lee, J. Y.; Kim, J.; Kim, J-H.; Howlett, P.; Forsyth, M.; MacFarlane, D.; Park, S. H. Extreme properties of double networked ionogel electrolytes for flexible and durable energy storage devices. *Energy Storage Materials* **2019**, 19, 197-205.

(96) Meira, R. M.; Correia, D. M.; Ribeiro, S.; Costa, P.; Gomes, A. C.; Gama, F. M.; Lanceros-Méndez, S.; Ribeiro, C. Ionic-Liquid-Based Elecroactive Polymer Composites for Muscle Tissue Engineering. *ACS Applied Polymer Materials* **2019**, 10, 2649-2658.

(97) Marr, P.C.; Marr, A. C. Ionic liquid gel materials: applications in green and sustainable chemistry. *Green Chemistry* **2016**, 18, 105-128.

(98) D'Angelo, A. J.; Grimes, J. J.; Panzer, M. J. Deciphering Physical versus Chemical Contributions to the Ionic Conductivity of Functionalized Poly(methacrylate)-Based Ionogel Electrolytes. *The Journal of Physical Chemistry B* **2015**, 119, 14959-14969.

(99) Terasawa, N. High-performance transparent actuator made from Poly (dimethylsiloxane)/Ionic liquid gel. *Sensors and Actuators B: Chemical* **2018**, 257, 815-819.

(100) Kataoka, T.; Ishioka, Y.; Mizuhata, M.; Minami, H.; Maruyama, T. Highly Conductive Ionic-Liquid Gels Prepared with Orthogonal Double Networks of a Low-Molecular-Weight Gelator and Cross-Linked Polymer. *ACS Applied Materials & Interfaces* **2015**, 7, 23346-23352.

(101) Leones, R.; Sentanin, F.; Nunes, S. C.; Esperança, J. M. S. S.; Gonçalves, M. C.; Pawlicka, A.; Zea Bermudez, V.; Silva, M. M. Effect of the alkyl chain length of the ionic liquid anion on polymer electrolytes properties. *Electrochimica Acta* **2015**, 184, 171-178.

(102) Kim, O.; Kim, S. Y.; Park, B.; Hwang, W.; Park, M. J. Factors Affecting Electromechanical Properties of Ionic Polymer Actuators Based on Ionic Liquid-Containing Sulfonated Block Copolymers. *Macromolecules* **2014**, 47, 4357-4368.

(103) Nevstrueva, D.; Murashko, K.; Vunder, V.; Aabloo, A.; Pihlajamäki, A.; Mänttäri, M.; Pyrhönen, J.; Koiranen, T.; Torop, J. Natural cellulose ionogels for soft artificial muscles. *Colloids and Surfaces B: Biointerfaces* **2018**, 161, 244-251.

(104) Lai, J.; Zhou, H.; Jin, Z.; Li, S.; Liu, H.; Jin, X.; Luo, C.; Ma, A.; Chen, W. Highly Stretchable, Fatigue Resistant, Electrically Conductive and Temperature Tolerant Ionogels for High-performance Flexible Sensors. *ACS Applied Materials & Interfaces* **2019**, 11, 26412-26420.

(105) Elamin, K.; Shojaatalhosseini, M.; Danyliv, O.; Martinelli, A.; Swenson, J. Conduction mechanism in polymeric membranes based on PEO or PVdF-HFP and containing a piperidinium ionic liquid. *Electrochimica Acta* **2019**, 299, 979-986.

(106) Safna Hussan, K. P.; Shahin Thayyil, M.; Jinitha, T. V.; Jayant, K. Development of an ionogel membrane PVA/[EMIN] [SCN] with enhanced thermal stability and ionic

conductivity for electrochemical application. *Journal of Molecular Liquids* **2019**, 274, 402-413.

(107) Gil-González, N.; Akyazi, T.; Castaño, E.; Benito-Lopez, F.; Morant-Miñana, M. C. Elucidating the role of the ionic liquid in the actuation behavior of thermo-responsive ionogels. *Sensors and Actuators B: Chemical* **2018**, 260, 380-387.

(108) Sinawang, G.; Kobayashi, Y.; Zheng, Y.; Takashima, Y.; Harada, A.; Yamaguchi, H. Preparation of Supramolecular Ionic Liquid Gels Based on Host-Guest Interactions and Their Swelling and Ionic Conductive Properties. *Macromolecules* **2019**, 52, 2932-2938.

(109) Mejri, R.; Dias, J. C.; Hentati, S. B.; Botelho, G.; Esperança, J. M. S. S.; Costa, C. M.; Lanceros-Mendez, S. Imidazolium-based ionic liquid type dependence of the bending response of polymer actuators. *European Polymer Journal* **2016**, 85, 445-451.

(110) Saito, S.; Katoh, Y.; Kokubo, H.; Watanabe, M.; Maruo, S. Development of a soft actuator using a photocurable ionic gel. *Journal of Micromechanics and Microengineering* **2009**, 15, 035005.

(111) Correia, D. M.; Barbosa, J. C.; Costa, C. M.; Reis, P. M.; Esperança, J. M. S. S.; de Zea Bermudez, V.; Lanceros-Méndez, S. Ionic Liquid Cation Size-Dependent Electromechanical Response of Ionic Liquid/Poly(vinylidene fluoride)-Based Soft Actuators. *The Journal of Physical Chemistry C* **2019**, 123, 12744-12752.

(112) Martins, P.; Correia, D. M.; Correia, V.; Lanceroz-Mendes, S. Polymer-based actuators: back to the future. *Physical Chemistry Chemical Physics* **2020**, 22, 15163-15182.

(113) Yuan, J.; Antonietti, M. Poly(Ionic Liquid)s as Ionic Liquid-Based Innovative Polyelectrolyte. Applications of ionic liquids in polymer science. David Mecerreyes (ed.) Springer-Verlag Berlin Heidelberg **2015**.

(114) Nulwala, H.; Mirjafari, A.; Zhou, X. Ionic liquids and poly(ionic liquid)s for 3D printing – A focused mini-review. *European Polymer Journal* **2018**, 108, 390-398.

(115) Zulfiqar, S.; Sarwar, M. I.; Mecerreyes, D. Polymeric ionic liquids for CO_2 capture and separation: potential, progress and challenges. *Polymer Chemistry* **2015**, 6, 6435-6451.

(116) Shahrom, M. S. R.; Wilfred, C. D.; MacFarlane, D. R.; Vijayraghavan, R.; Chong, F. K. Amino acid based poly(ionic liquid) materials for CO_2 capture: Effect of anion. *Journal of Molecular Liquids* **2019**, 276, 644-652.

(117) Wang, X.; Chen, F.; Girard, G. M. A.; Zhu, H.; MacFarlane, D. R.; Mecerreyes, D.; Armand, M.; Howlett, P. C.; Forsyth, M. Poly(Ionic Liquid)s-in-Salt Electrolytes with Co-coordination-Assisted Lithium-Ion Transport for Safe Batteries. *Joule* **2019**, 3, 2687-2702.

(118) Wang, X.; Zhu, H.; Girard, G. M. A.; Yunis, R.; MacFarlane, D. R.; Mecerreyes, D.; Bhattacharyya, A. J., Howlett, P. C.; Forsyth, M. Preparation and characterization of gel polymer electrolytes using poly(ionic liquids) and high lithium salt concentration ionic liquids. *Journal of Materials Chemistry A* **2017**, 5, 23844-23852.

(119) Chen, L.; Fu, J.; Lu, Q.; Shi, L.; Li, M.; Dong, L.; Xu, Y.; Jia, R. Cross-linked polymeric ionic liquids ion gel electrolytes by in situ radical polymerization. *Chemical Engineering Journal* **2019**, 378, 122245.

(120) Rao, J.; Wang, X.; Yunis, R.; Ranganathan, V.; Howlett, P. C.; MacFarlane, D. R.; Forsyth, M.; Zhu, H. A novel proton conducting ionogel electrolyte based on poly(ionic liquids) and protic ionic liquid. *Electrochimica Acta* **2020**, 346, 136224.

(121) Biswas, Y.; Banerjee, P.; Mandal, T. K. From Polymerizable Ionic Liquids to Poly(ionic liquid)s: Structure-Dependent Thermal, Crystalline, Conductivity, and Solution Thermoresponsive Behaviors. *Macromolecules* **2019**, 52, 945-958.

(122) Taghavikish, M.; Subianto, S.; Gu. Y.; Sun, X.; Zhao, X. S.; Choudhury, N. R. A Poly(ionic liquid) Gel Electrolyte for Efficient all Solid Electrochemical Double-Layer Capacitor. *Scientific Report* **2018**, 8, 10918.

(123) Kokubo, H.; Sano, R.; Murai, K.; Ishii, S.; Watanabe, M. Ionic Polymer Actuators Using Poly(ionic liquid) Electrolytes. *European Polymer Journal* **2018**, 106, 266-272.

(124) Kanaan, A. F.; Piedade, A. P.; de Sousa, H. C.; Dias, A. M. A. Effect of mold assemblies-induced interfaces in the mechanical actuation of electro-responsive ionic liquid-based polycationic hydrogels. *Applied Materials Today* **2020**, 20, 100711.

(125) Muñoz-Bonilla, A.; Fernández-García, M. Poly(ionic liquid)s as antimicrobial materials. *European Polymer Journal* **2018**, 105, 135-149.

(126) Qian, W.; Texter, J.; Yan, F. Frontiers in poly(ionic liquid)s: syntheses and applications. *Chemical Society Reviews* **2017**, 46, 1124-1159.

(127) Shaplov, A. S.; Ponkratov, D. O.; Vlasov, P. S.; Lozinskaya, E. I.; Gumileva, L. V.; Surcin, C.; Morcrette, M.; Armand, M.; Aubert, P.-H.; Vidal, F.; Vygodskii, Y. S. Ionic semi-interpenetrating networks as a new approach for highly conductive and stretchable polymer materials. *Journal of Materials Chemistry A* **2015**, 3, 2188-2198.

(128) Shaplov, A. S.; Marcilla, R.; Mecerreyes, D. Recent Advances in Innovative Polymer Electrolytes based on Poly(ionic liquid)s. *Electrochimica Acta* **2015**, 175, 18-34.

(129) Marcilla, R.; Alcaide, F.; Sardon, H.; Pomposo, J. A.; Pozo-Gonzalo, C.; Mecerreyes, D. Tailor-made polymer electrolytes based upon ionic liquids and their application in all-plastic electrochromic devices. *Electrochemistry Communications* **2006**, 8, 482-488.

(130) Shaplov, A. S.; Lozinskaya, E. I.; Ponkratov, D. O.; Malyshkina, I. A.; Vidal, F.; Aubert, P.-H.; Okatova, O. V.; Pavlov, G. M.; Komarova, L. I.; Wandrey, C.; Vygodskii, Y. S. Bis(trifluoromethylsulfonyl)amide based “polymeric ionic liquids”: Synthesis, purification and peculiarities of structure-properties relationships. *Electrochimica Acta* **2011**, 57, 74-90.

(131) De, S.; Cramer, C.; Schönhoff, M. Humidity Dependence of the Ionic Conductivity of Polyelectrolyte Complexes. *Macromolecules* **2011**, 44, 8936-8943.

(132) Choi, U. H.; Mittal, A.; Price Jr., T. L.; Gibson, H. W.; Runt, J.; Colby, R. H. Polymerizable Ionic Liquids with Enhanced Static Dielectric Constants. *Macromolecules* **2013**, 46, 1175-1186.

(133) Matsumoto, K.; Talukdar, B.; Endo, T. Methacrylate-based ionic liquid: radical polymerization/copolymerization with methyl methacrylate and evaluation of molecular weight of the obtained homopolymers. *Polymer Bulletin* **2011**, 66, 199-210.

(134) Kalia, S.; Sabaa, M. W.; Kango, S. Polymer grafting: A versatile means to modify the polysaccharides. Polysaccharide Based Graft Copolymers. Kalia, S.; Sabaa, M. W. (eds.) Springer-Verlag Berlin Heidelberg **2013**.

(135) Zoratto, N.; Matricardi, P. Semi-IPNs and IPN-based hydrogels. Polymeric Gels Characterization, Properties and Biomedical Applications, Pal, K.; Banerjee, I. (eds.), Elsevier, **2018**.

(136) Markovic, G.; Visakh, P. M. Polymer blends: sate of art. Recent Developments in Polymer Macro, Micro and Nano Blends, Visakh, P. M.; Markovic, G.; Pasquini, D. (eds.). Elsevier, **2017**.

(137) Richardson, J. J.; Cui, J.; Björnmalm, M.; Braunger, J. A.; Ejima, H.; Caruso, F. Innovation in Layer-by-Layer Assembly. *Chemical Reviews* **2016**, 116, 14828-14867.

(138) Fu, J.; Schlenoff, J. B. Driving Forces for Oppositely Charged Polyion Association in Aqueous Solutions: Enthalpic, Entropic, but Not Electrostatic. *Journal of the American Chemical Society* **2016**, 138, 980-990.

(139) Berger, J.; Reist, M.; Mayer, J. M.; Felt, O.; Peppas, N. A.; Gurny, R. Structure and interactions in covalently and ionically crosslinked chitosan hydrogels for biomedical applications. *European Journal of Pharmaceutics and Biopharmaceutics* **2004**, 57, 19-34.

(140) Hu, W.; Wang, Z.; Xiao, Y.; Zhang, S.; Wang, J. Advances in crosslinking strategies for biomedical hydrogels. *Biomaterials Science* **2019**, 7, 843-855.

(141) Odian, G. Principles of Polymerization. John Wiley & Sons, **2004**.

(142) Huang, J.; Turner, S. R. Recent advances in alternating copolymers: The synthesis, modification, and applications of precision polymers. *Polymer* **2017**, 116, 572-586.

(143) Herk, A. V. General Aspects of Copolymerization. Synthesis and Applications of Copolymers, Parthiban, A. (ed.) John Wiley & Sons, **2014**.

(144) Sabaa, M. W. Chitosan-g-copolymers: Synthesis, properties and applications. Polysaccharide Based Graft Copolymers. Kalia, S.; Sabaa, M. W. (eds.), Springer-Verlag Berlin Heidelberg, **2013**.

(145) Haroon, M.; Wang, L.; Yu, H.; Abbasi, N. M.; Zain-ul-Abdin; Saleem, M.; Khan, R. U.; Chen, Q.; Wu, J. Chemical modification of starch and its application as an absorbent material. *RSC Advances* **2016**, 6, 78264-78285.

(146) Banerjee, S.; Paira, T. K.; Mandal, T. K. Surface confined atom transfer radical polymerization: access to custom library of polymer-based hybrid materials for speciality applications. *Polymer Chemistry* **2014**, 5, 4153-4167.

(147) Jenkins, A. D.; Kratochvìl, P.; Stepto, R. F. T.; Suter, U. W. Glossary of basic terms in polymer science (IUPAC Recommendations 1996). *Pure Applied Chemistry* **1996**, 68, 2287-2311.

(148) James, J.; Thomas, G. V.; Akhina, H.; Thomas, S. Micro- and Nano-Structured Interpenetrating Polymer Netoworks: State of the Art, New Challenges and Opportunities. Micro- and Nano-structured Interpenetrating Polymer Networks: From Design to Applications, Thomas, S.; Grande, D.; Cvelbar, U.; Raju, K.V.S.N.; Narayan, R.; Thomas, S. P.; Akhina, H. (eds.) John Wiley & Sons, **2016**.

(149) Matricardi, P.; Meo, C. D.; Coviello, T.; Hennink, W. E.; Alhaique, F. Interpenetrating Polymer Networks polysaccharide hydrogels for drug delivery and tissue engineering. *Advanced Drug Delivery Reviews* **2013**, 65, 1172-1187.

(150) Lohani, A.; Singh, G.; Bhattacharya, S. S.; Verma, A. Interpenetrating polymeric networks as innovative drug delivery systems. *Journal of Drug Delivery* **2014**, 1, 11.

(151) Zhang, M.; Zuo, Q.; Wang, L.; Yu, S.; Mai, Y.; Zhou, Y. Poly(ionic liquid)-based polymer composites as high-performance solid-state electrolytes: benefits from the nanophase separation and alternating polymer structure. *Chemical Communications* **2020**, 56, 7929-7932.

(152) Mazzei, I. R.; Nikolaeva, D.; Fuoco, A.; Loïs, S.; Fantini, S.; Monteleone, M.; Esposito, E.; Ashtiani, S. J.; Lanč, M.; Vopička, O.; Friess, K.; Vankelecom, I. F. J.; Jansen, J. C. Poly[3-ethyl-1-vinyl-imidazolium] diethyl phosphate/Pebax® 1657 Composite Membranes and Their Gas Separation Membranes. *Membranes* **2020**, 10, 224.

(153) Shen, C.; Zhao, Q.; Evans, C. M. Precise Network Polymerized Ionic Liquids for Low-Voltage, Dopant-Free Soft Actuators. *Advanced Materials Technologies* **2018**, 4, 1800535.

(154) Wu, J.; Yin, M.-j.; Seefeldt, K.; Dani, A.; Guterman, R.; Yuan, J.; Zhang, A. P.; Tam, H.-Y. In situ μ-printed optical fiber-tip CO2 sensor using a photocrosslinkable poly(ionic liquid). *Sensors and Actuators B: Chemical* **2018**, 259, 833-839.

(155) Li, H.; Feng, Z.; Zhao, K.; Wang, Z.; Liu, J.; Liu, J.; Song, H. Chemically crosslinked liquid crystalline poly(ionic liquid)s/halloysite nanotubes nanocomposite ionogels with superior ionic conductivity and a high modulus. *Nanoscale* **2019**, 11, 3689-3700.

(156) Li, J. L.; Zhang, Y.; Zhang, S.; Liu, M.; Li, X.; Cai, T. Hyperbranched poly(ionic liquid) functionalized poly(ether sulfone) membranes as healable antifouling coatings for osmotic power generation. *Journal of Materials Chemistry A* **2019**, 7, 8167-8176.

(157) Genua, A.; Mecerreys, D.; Alduncín, J. A.; Mondragon, I.; Marcilla, R.; Grande, H.-J. Polymeric ionic liquids for the past preparation of superhydrophobic coatings by the simultaneous spraying of oppositely charged polyelectrolytes and nanoparticles. *Polymer Journal* **2011**, 43, 966-970.

(158) Patinha, D. J. S.; Wang, H.; Yuan, J.; Rocha, S. M.; Silvestre, A. J. D.; Marrucho, I. M. Thin Porous Poly(ionic liquid) Coatings for Enhanced Headspace Solid Phase Microextraction. *Polymers* **2020**, 12, 1909.

(159) Juger, J.; Vancaeyzeele, C.; Plesse, C.; Nguyen, G. M. T.; Braz Ribeiro, F.; Teyssié, D.; Vidal, F. Polymeric Ionic liquid based interpenetrating polymer network for all-solid self-standing polyelectrolyte material. *European Polymer Journal* **2018**, 106, 257-265.

(160) Zhang, C.; Zhang, W.; Gao, H.; Bai, Y.; Sun, Y.; Chen, Y. Synthesis and gas transport properties of poly(ionic liquid) based semi-interpenetrating polymer network membranes for CO_2/N_2 separation. *Journal of Membrane Science* **2017**, 528, 72-81.

(161) Vilela, C.; Sousa, N.; Pinto, R. J. B.; Silvestre, A. J. D.; Figueiredo, F. M. L.; Freire, C. S. R. Exploiting poly(ionic liquids) and nanocellulose for the development of bio-based anion-exchange membranes. *Biomass and Bioenergy* **2017**, 100, 116-125.

(162) Gallagher, S.; Florea, L.; Fraser, K. J.; Diamond, D. Swelling and Shrinking Properties of Thermo-Responsive Polymeric Ionic Liquid Hydrogels with Embedded Linear pNIPAAM. *International Journal of Molecular Sciences* **2014**, 15, 5337-5349.

(163) Becht, G. A.; Sofos, M.; Seifert, S.; Firestone, M. A. Formation of a Liquid-Crystalline Interpenetrating Poly(ionic liquid) Network Hydrogel. *Macromolecules* **2011**, 44, 1421-1428.

(164) Tudor, A.; Florea, L.; Gallagher, S.; Burns, J.; Diamond, D. Poly(Ionic Liquid) Semi-Interpenetrating Network Multi-Responsive Hydrogel. *Sensors* **2016**, 16, 219.

(165) Su, A.; Guo, P.; Li, J.; Kan, D.; Pang, Q.; Li, T.; Sun, J.; Chen, G.; Wei, Y. An organic-inorganic semi-interpenetrating network ionogel electrolyte for high-voltage lithium metal batteries. *Journal of Materials Chemistry A* **2020**, 8, 4775-4783.

(166) Li, X.; Zheng, Y.; Pan, Q.; Li, C. Y. Polymerized Ionic Liquid-Containing Interpenetrating Network Solid Polymer Electrolytes for All-Solid-State Lithium Metal Batteries. *ACS Applied Materials & Interfaces* **2019**, 11, 34904-34912.

(167) Li, Y.; Sun, Z.; Shi, L.; Lu, S.; Sun, Z.; Shi, Y.; Wu, H.; Zhang, Y.; Ding, S. Poly(ionic liquid)-polyehtylene oxide semi-interpenetrating polymer network solid electrolyte for safe lithium metal batteries. *Chemical Engineering Journal* **2019**, 375, 121925.

(168) Guo, P.; Zhang, H.; Liu, X.; Sun, J. Counterion-Mediated Intrinsic Healing of Poly(ionic liquid) Copolymers. *ACS Applied Materials & Interfaces* **2018**, 10, 2105-2113.

(169) Park, J. B.; Isik, M.; Park, H. J.; Jung, I. H.; Mecerreyes, D.; Hwang, D.-H. Polyestyrene-*block*-Poly(ionic liquid) Copolymers as Work Function Modifiers in Inverted Organic Photovoltaic Cells. *ACS Applied Materials & Interfaces* **2018**, 10, 4887-4894.

(170) Cordella, D.; Debuigne, A.; Jérôme, C.; Kochovski, Z.; Taton, D.; Detrembleur, C. One-Pot Synthesis of Double Poly(Ionic Liquid) Block Copolymers by Cobalt-Mediated Radical Polymerization-Induced Self-Assembly (CMR-PISA) in Water. *Macromolecular Rapid Communications* **2016**, 37, 1181-1187.

(171) Zhang, Y-.D.; Ping, J.; Wu, Q-.W.; Pan, H-.B.; Fan, X-.H.; Shen, Z.; Zhou, Q-.F. Bulk self-assembly and ionic conductivity of a block copolymer containing an azobenzene-based liquid crystalline polymer and a poly(ionic liquid). *Polymer Chemistry* **2017**, 8, 1689-1698.

(172) Nakabayashi, K.; Sato, Y.; Isawa, Y.; Lo, C-.T.; Mori, H. Ionic Conductivity and Assembled Structures of Imidazolium Salt-Based Block Copolymers with Thermoresponsive Segments. *Polymers* **2017**, 9, 616.

(173) Yang, Y.; Zheng, J.; Man, S.; Sun, X.; An, Z. Synthesis of poly(ionic liquid)-based nano-objects with morphological transition via RAFT polymerization-induced self-assembly in ethanol. *Polymer Chemistry* **2018**, 9, 824-827.

(174) Wu, B.; Zhang, W.; Gao, N.; Zhou, M.; Liang, Y.; Wang, Y.; Li, F.; Li, G. Poly (ionic liquid)-Based Breath Figure Films: A New Kind of Honeycomb Porous Films with Great Extendable Capability. *Scientific Reports* **2017**, 7, 13973.

(175) He, H.; Rahimi, K.; Zhong, M.; Mourran, A.; Leubke, D. R.; Nulwala, H. B.; Möller, M.; Matyajaszewski, K. Cubosomes from hierarchical self-assembly of poly(ionic liquid) block copolymers. *Nature Communications* **2017**, 8, 14057.

(176) Kuzmicz, D.; Coupillaud, P.; Men, Y.; Vignolle, J.; Vendraminetto, G.; Ambrogi, M.; Taton, D.; Yuan, J. Functional mesoporous poly(ionic liquid)-based copolymer monoliths: From synthesis to catalysis and microporous carbon production. *Polymer* **2014**, 55, 3423-3430.

(177) Chen, F.; Ren, Y.; Guo, J.; Yan, F. Thermo- and electro-dual responsive poly(ionic liquid) electrolyte based smart windows. *Chemical Communications* **2017**, 53, 1595-1598.

(178) Porcarelli, L.; Shaplov, A. S.; Salsamendi, M.; Nair, J. R.; Vygodskii, Y. S.; Mecerreyes, D.; Gerbaldi, C. Single-Ion Block Copoly(ionic liquid)s as Electrolytes for All-Solid State Lithium Batteries. *ACS Applied Materials & Interfaces* **2016**, 8, 10350-10359.

(179) Joubert, F.; Yeo, R. P.; Sharples, G. J.; Musa, O. M.; Hodgson, D. R. W.; Cameron, N. R. Preparation of an Antibacterial Poly(ionic liquid) Graft Copolymer of Hydroxyethyl Cellulose. *Biomacromolecules* **2015**, 16, 3970-3979.

(180) Zhang, W-.H.; Liu, S-.S.; Liu, P.; Xu, J.; Xue, B.; Wei, X-.Y.; Li, Y-.X. Chitosan grafted with a heteropolyanion-based ionic liquid as an effective and reusable catalyst for acetylation. *RSC Advances* **2016**, 6, 414104-41409.

(181) Le, C. M. Q.; Cao, X. T.; Bach, L. G.; Lee, W-.K.; Kang, I.; Lim, K. T. Direct grafting imidazolium-based poly(ionic liquid) onto multiwalled carbon nanotubes via Diels-Alder "click" reaction. *Molecular Crystals and Liquid Crystals* **2018**, 660, 143-149.

(182) Grygiel, K.; Wicklein, B.; Zhao, Q.; Eder, M.; Pettersson, T.; Bergström, L.; Antonietti, M.; Yuan, J. Omnidispersible poly(ionic liquid)-functionalized cellulose nanofibrils: surface grafting and polymer membrane reinforcement. *Chemical Communication* **2014**, 50, 12486-12489.

(183) Feng, J.; Wang, X.; Tian, Y.; Luo, C.; Sun, M. Basalt fibers grafted with a poly(ionic liquids) coating for in-tube solid-phase microextraction. *Journal of Separation Science* **2018**, 41, 3267-3274.

(184) Elshaarawy, R. F. M.; Dechnik, J.; Hassan, H. M. A.; Dietrich, D.; Betiha, M. A.; Schmidt, S.; Janiak, C. Novel high throughput mixed matrix membranes embracing poly ionic liquid-grafted biopolymer: Fabrication, characterization, permeation and antifiouling performance. *Journal of Molecular Liquids* **2018**, 266, 484-494.

(185) Zhou, C.; Song, H.; Zhang, F.; Liu, J.; Li, J.; Liu, B.; Liang, J. A facile method to fabricate an antimicrobial coating based on poly(1-vinyl-3-allylimidazolium iodide) (PAVI) and poly(ethylene glycol) dimethyl acrylate (PEGDMA). *Polymer Bulletin* **2019**, 76, 5433-5449.

(186) Tripathi, T.; Kamaz, M.; Wickramasinghe, S. R.; Sengupta, A. Designing Electric Field Responsive Ultrafiltration Membranes by Controlled Grafting of Poly(Ionic Liquid) Brush. *International Journal of Environmental Research and Public Health* **2020**, 17, 271.

(187) Li, M.; Zhang, W.; Zhou, S.; Zhao, Y. Preparation of poly(vinyl alcohol)/palygorskite-poly (ionic liquids) hybrid catalytic membranes to facilitate esterification. *Separation and Purification Technology* **2020**, 230, 115746.

(188) Bielas, R.; Mielańczyk, A.; Skonieczna, M.; Mielańczyk, Ł.; Neugebauer, D. Choline supported poly(ionic liquid) graft copolymers as novel delivery systems of anionic pharmaceuticals for anti-inflammatory and anti-coagulant therapy. *Scientific Reports* **2019**, 9, 14410.

(189) Lu, B.; Li, Y.; Wang, Z.; Wang, B.; Pan, X.; Zhao, W.; Ma, X.; Zhang, J. A dual responsive hyaluronic acid graft poly(ionic liquid) block copolymer micelle for an efficient CD44-targeted antitumor drug delivery. *New Journal of Chemistry* **2019**, 43, 12275-12282.

(190) Yang, H.; Zhang, J.; Liu, Y.; Wang, L.; Bai, L.; Yang, L.; Wei, D.; Wang, W.; Niu, Y.; Chen, H. Rapid removal of anionic dye from water by poly(ionic liquid)-modified nanoparticles. *Journal of Molecular Liquids* **2019**, 284, 383-392.

(191) Mou, Z.; Wang, B.; Lu, H.; Dai, S.; Huang, Z. Synthesis of poly(ionic liquid)s brush-grafted carbon dots for high-performance lubricant additives of polyethylene glycol). *Carbon* **2019**, 154, 301-312.

(192) Watanabe, M.; Thomas, M. L.; Zhang, S.; Ueno, K.; Yasuda, T.; Dokko, K. Application of Ionic Liquids to Energy Storage and Conversion Materials and Devices. *Chemical Reviews* **2017**, 117, 7190-7239.

(193) Mendes, T.; Zhang, X.; Wu, Y.; Howlett, P. C.; Forsyth, M.; Macfarlane, D. R. Supported Ionic Liquid Gel Membrane Electrolytes for a Safe and Flexible Sodium Metal Battery. *ACS Sustainable Chemistry & Engineering* **2019**, 7, 3722-3726.

(194) Dias, J. C.; Correia, D. M.; Costa, C. M.; Ribeiro, C.; Maceiras, A.; Vilas, J. L.; Botelho, G.; de Zea Bermudez, V.; Lanceros-Mendes, S. Improved response of ionic liquid-based bending actuators by tailored interaction with the polar fluorinated polymer matrix. *Electrochimica Acta* **2019**, 296, 598-607.

(195) Fernandes, L. C.; Correia, D. M.; Pereira, N.; Tubio, C. R.; Lanceros-Méndez, S. Highly Sensitive Humidity Sensor Based on Ionic Liquid-Polymer Composites. *ACS Applied Polymer Materials* **2019**, 1, 2723-2730.

(196) Di Lecce, S.; Kornyshev, A. A.; Urbakh, M.; Bresme, F. Electrotunable Lubrication with Ionic Liquids: the Effects of Cation Chain Length and Substrate Polarity. *ACS Applied Materials & Interfaces* **2020**, 12, 4105-4113.

(197) Coupillaud, P.; Pinaud, J.; Guidolin, N.; Vignolle, J.; Fèvre, M.; Veaudecrenne, E.; Mecerreyes, D.; Taton, D. Poly(ionic liquid)s Based on Imidazolium Hydrogen Carbonate Monomer Units as Recyclable Polymer-Supported N-Heterocyclic Carbenes: Use in

Organocatalysis. *Journal of Polymer Science, Part A: Polymer Chemistry* **2013**, 51, 4530-4540.

(198) Berton, P.; Shamshina, J. L.; Bica, K.; Rogers, R. D. Ionic Liquid as Fragrance Precursors: Smart Delivery Systems for Volatile Compounds. *Industrial & Engineering Chemistry Research* **2018**, 57, 16069-16076.

(199) Shamshina, J. L.; Zavgorodnya, O.; Berton, P.; Chhotaray, P. K.; Choudhary, H.; Rogers, R. D. An Ionic Liquid Platform for Spinning Composite Chitin-Poly(lactic acid) Fibers. *ACS Sustainable Chemistry & Engineering* **2018**, 6, 10241-10251.

Chapter 2

Sustainable electro-responsive semi-interpenetrating starch/ionic liquid copolymer networks for the controlled sorption/release of biomolecules

This chapter comprises the work published in

ACS Sustainable Chemistry & Engineering (2019) by

Akel F. Kanaan, Madalina M. Barsan, Christopher M.A. Brett, Carmen Alvarez-Lorenzo, Angel Concheiro, Hermínio C. de Sousa, Ana M. A. Dias

2.1 Abstract

The main objective of this work was the development and characterization of sustainable electro-responsive ionic liquid-based cationic copolymers. For this purpose degradable semi-interpenetrating polymer networks (s-IPNs) based on starch and on ion-conducting cationic copolymers of 2-hydroxyethyl methacrylate (HEMA) and 1-butyl-3-vinylimidazolium chloride (BVImCl), cross-linked with *N,N'*-methylenebis(acrylamide) (MBA) were synthesized by following principles of green chemistry. Cross-linked poly(HEMA-co-BVImCl) copolymers were also prepared for comparison. The resulting cationic hydrogels (copolymer and s-IPNs) were characterized in terms of their physicochemical, thermomechanical, morphological, and electrochemical properties, as well as in terms of cell viability and proliferation against fibroblast cells. Furthermore, the electro-assisted sorption/release capacity of the prepared hydrogels towards L-tryptophan (used as a model biomolecule) was also studied at different applied DC voltages (0, 2, 5 and 100 V). Results demonstrated that the properties of the synthetized hydrogels can be tuned, depending on their

relative chemical composition, presenting electronic conductivity and ionic conductivity values in the 0.1 to 5.2 S cm^{-1} range, and complex shear modulus in the 0.6 to 6.4 MPa range. The sorption/release capacity of the s-IPNs after 3 h at 25 ºC can also be modulated between 2.5 and 70 % and 4.5 and 40 %, depending on the applied DC voltage and/or sorption/release medium. Finally, none of the synthesized cationic hydrogels induced fibroblast cells lysis, although s-IPNs had a lower impact on cell proliferation than poly(HEMA-co-BVImCl) copolymers, indicating a favorable effect of starch on the biocompatibility of the synthetized s-IPNs. The designed cationic hydrogels could be useful for the development of efficient, stable, degradable and cheaper soft and multi-responsive platforms with potential applications in bio-separation processes, wastewater treatment systems (e.g. pharmaceutical), biomedical devices (e.g. sustained delivery of specific charged-biomolecules) and non-leaching electrochemical devices.

Keywords: Semi-IPN; starch; polymerizable imidazolium-based ionic liquids; L-tryptophan; electro-assisted sorption/release; electric stimuli-responsive hydrogel.

2.2 Introduction

Stimuli-responsive hydrogels, also called ‘smart’ hydrogels, are defined as hydrophilic three-dimensional cross-linked networks that are able to absorb high amounts of water and to respond to different external or internal applied stimuli (e.g. ionic strength, pH, temperature, light and electrical field) through changes in their structures (e.g. swelling, shrinking and/or bending).[1] In recent years much effort has been made to engineer smart multi-responsive hydrogels presenting improved functionalities such as fast response to the applied stimulus, high mechanical stability, biodegradability, biocompatibility and low cost.[2-4]

Biocompatible electrically responsive hydrogels represent an interesting sub-class of stimuli-responsive materials since they present narrow and precise response under fine and tunable control of the applied stimuli, e.g. intensity, orientation and duration of the applied electrical current.[5,6] These materials may find a broad range of applications in biomedicine, for instance as components of tissue engineering scaffolds, as soft electro-actuators and as controlled release/sorption systems for bioactive molecules, mostly due to their biocompatibility, soft nature and high water swelling capacity, which make them able to mimic different living tissues.[7-12]

Polyelectrolytes can endow hydrogels with electro-activity relying on ion-conduction mechanisms that result from the interactions between conductive ions and the ionized functional groups present in the polyelectrolyte backbone. In some cases, ion-conductive materials also present electric conductivity in response to an external applied electrical field due to mechanisms not yet completely understood.[13] Examples of natural- and synthetic-based ion-conducting electro-active polyelectrolytes include chitosan and poly(acrylic acid), respectively.[14-17]

Multifunctional tailor made electro-responsive polyelectrolytes can be successfully obtained through the chain-growth polymerization of vinyl-functionalized ionic liquids.[18] Poly(ionic liquid)s (PILs) combine the properties of monomeric ionic liquids (ILs), such as task-specific design, negligible vapor pressure, broad electrochemical window and high ionic conductivity[19-28] with the mechanical properties of polymers, originating a new sub-class of polyelectrolytes which may present promising electro-responsive properties.[19,29-34] Previous studies have shown that the ionic conductivity of PILs is highly influenced, for example, by the cation/anion chemical structure of the IL monomer, by the presence of spacers in PIL's molecular structure and by PIL's molecular weight, structural organization and glass transition temperature.[30,35,36]

The main advantages of using PILs as electro-active hydrogels include the fact that PILs are not pH sensitive polyelectrolytes (i.e. they may stay ionized over broad pH ranges), and they do not require the use of dopants to be electrically active since the ionic conductivity is promoted by the diffusion of the IL counter ions (anions or cations depending on the vinyl-functionalized moiety that constitutes the PIL backbone). Nevertheless, the application of PILs is hampered in low ionic strength aqueous solutions since these materials usually behave as superabsorbent hydrogels, due to their high intrinsic charge density, leading to significant loss of mechanical and structural/morphological stability. Moreover, important issues such as PILs biocompatibility and biodegradability have been almost completely neglected so far.

The development of IL-based copolymers and/or IL-based interpenetrating polymer networks (IPNs) are interesting alternative strategies that can contribute to overcome some of those issues. According to the IUPAC definition, IPNs are polymers comprising two or more networks which are at least partially interlaced on a molecular scale, but not covalently bonded to each other, and cannot be separated unless chemical bonds are broken. When the networks can be separated these materials are known as semi-interpenetrating polymer networks (s-IPNs).[37] IPNs and semi-interpenetrating polymer networks (s-IPNs) allow combining specific properties of different polymer networks (e. g. mechanical resistance, stimuli-responsiveness, biocompatibility, etc.) to obtain a different material presenting improved and/or new task-specific tailored properties.[37-39] PIL-based IPNs and s-IPNs have been recently purposed for the development of matrices for proteins encapsulation[40], stretchable electronics[41], actuators and/or electrochromic devices[42], multi-stimuli responsive sensors[43], anion-exchange membranes[44] and gas separation membranes.[45]

The main motivation of this work was the development of more stable, sustainable and cytocompatible electric stimuli-responsive IL-based hydrogels. With this in mind, poly(HEMA-co-BVImCl) copolymers, comprised by 2-hydroxyethyl methacrylate (HEMA)

and by 1-butyl-3-vinylimidazolium chloride (BVImCl) cross-linked with *N,N'*-methylenebis(acrylamide) (MBA) and s-IPNs composed by starch (St) and poly(HEMA-co-BVImCl) copolymers were synthesized and characterized. The use of poly(HEMA-co-BVImCl) instead of poly(BVImCl) aims to improve the mechanical stability of the polycationic hydrogel, while maintaining PIL characteristic properties. Moreover, the co-monomer HEMA can be regarded as a spacer that may enhance the ionic conduction of chloride anions through the copolymer matrice, and that also may lead to a decrease of the final cost of the envisaged devices (considering HEMA and BVImCl relative costs). s-IPNs were developed in order to evaluate their potential to tune the properties of the prepared poly(HEMA-co-BVImCl) copolymer by incorporating starch, at different relative compositions, in their final structures. The obtained hydrogels were characterized for their swelling capacities in different media, thermomechanical stabilities, ionic/electric conductivities, tunable capacities to remove/release a charged bio-molecule from different media, and cytocompatibility with fibroblast cells.

Finally, it is important to refer that an effort was made to synthesize the s-IPNs by following principles of green chemistry. This was accomplished by employing: i) simple one-pot synthesis procedures at mild conditions, chemically stable and low volatile reactants and water as the reaction solvent; ii) biodegradable compounds (starch) or compounds that can be degraded originating non-toxic derivatives (HEMA and BVImCl); iii) small amounts of BVImCl (the functional monomer) in comparison with other IL-based liquid-liquid extraction/separation processes; iv) small amounts of polymerization catalyst (thermal initiator); and v) starch (a biodegradable, biocompatible, readily available and cheap renewable feedstock[46-48]) as a strategy to tune the properties of the poly(HEMA-co-BVImCl) copolymer. Moreover, the proposed strategy originates hydrogels that present long-term stability in aqueous media, avoiding BVImCl leaching/leakage during usage, and consequently avoiding air/water contamination.

2.3 Materials and Methods

2.3.1 Materials

Water soluble potato starch (St); 2-hydroxyethyl methacrylate (HEMA, 99 %), *N,N'*-methylenebis(acrylamide) (MBA, 99 %); 2,2'-Azobis (2-methylpropionamidine) dihydrochloride (AIBA, 97 %); L-tryptophan (Try, ≥ 98 %) and potassium sulfate (used to create a controlled relative humidity (RH) ≥ 90 % at 25 ºC) were obtained from Sigma-Aldrich. The ionic liquid 1-butyl-3-vinylimidazolium chloride (BVImCl, 95 %) was acquired from Io-Li-Tec, Germany. For the cells assay, BALB/3T3 clone A31 cells (CCL-163^{TM}) were obtained from ATCC, Dulbecco's modified Eagle's medium (DMEM)/F12 Ham nutrient mixture and the cell proliferation reagent MTT were obtained from Sigma-Aldrich, while the cytotoxicity detection KitPlus (LDH) was obtained from Roche. Buffer solutions used for the water swelling capacity and/or electro-sorption measurements were phosphate buffered saline (PBS, pH = 7.4, I = 0.169 M) from Sigma-Aldrich, a phosphate buffer (PB, pH = 7.14, I = 0.027 M), an acetate buffer (AB, pH = 4.0, I = 0.008 M) and Trizma base buffer (TRIZ, pH = 9.9, I ≈ 0 M), which were prepared as follows (for 500 mL): i) PB, 0.31 g of monobasic sodium phosphate (NaH_2PO_4) and 0.52 g of sodium phosphate dibasic (Na_2HPO_4), both from Riedel-de Haen, dissolved in bi-distilled water; ii) AB, 0.07 g of sodium acetate 3-hydrated ($CH_3COONa.3H_2O$) from Panreac and 0.20 mL of acetic acid (CH_3COOH) from Fluka, dissolved in bi-distilled water; and iii) TRIZ, 0.5 g of Trizma base ($NH_2C(CH_2OH)_3$) from Sigma-Aldrich, dissolved in bi-distilled water. The final pH of all solutions was measured using a pH meter (Standard pH Meter, Jenway).

2.3.2 Synthesis of s-IPN hydrogels based on starch and poly(HEMA-co-BVImCl)

s-IPNs studied in this work resulted from the synthesis of cross-linked poly(HEMA-co-BVImCl) copolymers in two aqueous starch solutions (0.5 and 1 % w/v). Cross-linked

poly(HEMA-co-BVImCl) copolymers and the homopolymer poly(HEMA) were also synthesized for comparison purposes (synthesized in the same volume of water used for the starch solutions). Poly(HEMA), presents phase separation during polymerization in aqueous media, depending on the initial HEMA/water ratio.[49] In this work, the chemical composition of the prepared copolymers was chosen to fall in the phase diagram region where macroporous phase-separated hydrogels are formed, assuming that the incorporation of BVImCl into the mixture does not significantly change the typical phase separation behavior observed for poly(HEMA).

Co-monomers (HEMA/MBA/BVImCl) were dissolved under stirring for 24 h at room temperature in water to prepare poly(HEMA) and poly(HEMA-co-BVImCl), or in starch solutions to prepare s-IPNs. Starch solutions (0.5 and 1.0 wt%) were previously obtained by dissolving starch in bi-distilled water at 100 ºC for 15 min under stirring to obtain transparent and homogeneous solutions that were then cooled to room temperature. Higher starch concentrations were tested but they were not considered in this work because they originated non-homogeneous s-IPNs (phase separation visible at naked eye) that presented low mechanical stability, probably due to the higher viscosity that may hinder co-polymerization/cross-linking reactions.

Cross-linked poly(HEMA-co-BVImCl) was obtained by free radical polymerization using MBA as cross-linker agent (0.5 % on molar basis, relatively to the total number of mole of monomers in solution), and AIBA as a thermal initiator (0.2 % on molar basis, relatively to the total number of mole of monomers in solution). The above indicated solutions were sonicated for 5 min to remove oxygen and inserted in Teflon squared molds (10 × 10 cm) separated by 2 mm using a silicon spacer. The molds were placed in an oven at 50 ºC for 8 h and then at 70 ºC for 24 h to ensure complete polymerization. The obtained opaque hydrogels were washed in distilled water (2 L replaced twice a day for 3 days) to remove any unreacted monomers.

After washing, half of each sample was oven-dried at 50 ºC for 48 h and the other half was freeze-dried (using a freeze drier from Telstar, Lyoquest 85 Plus, Spain) at -80 ºC under vacuum (0.1 mPa) for 48 h. The chemical composition and the schematic structure of the cationic hydrogels prepared in this work are presented in Table 2.1 and Figure 2.1, respectively. Hydrogel samples were coded as indicated in Table 2.1 for simplicity.

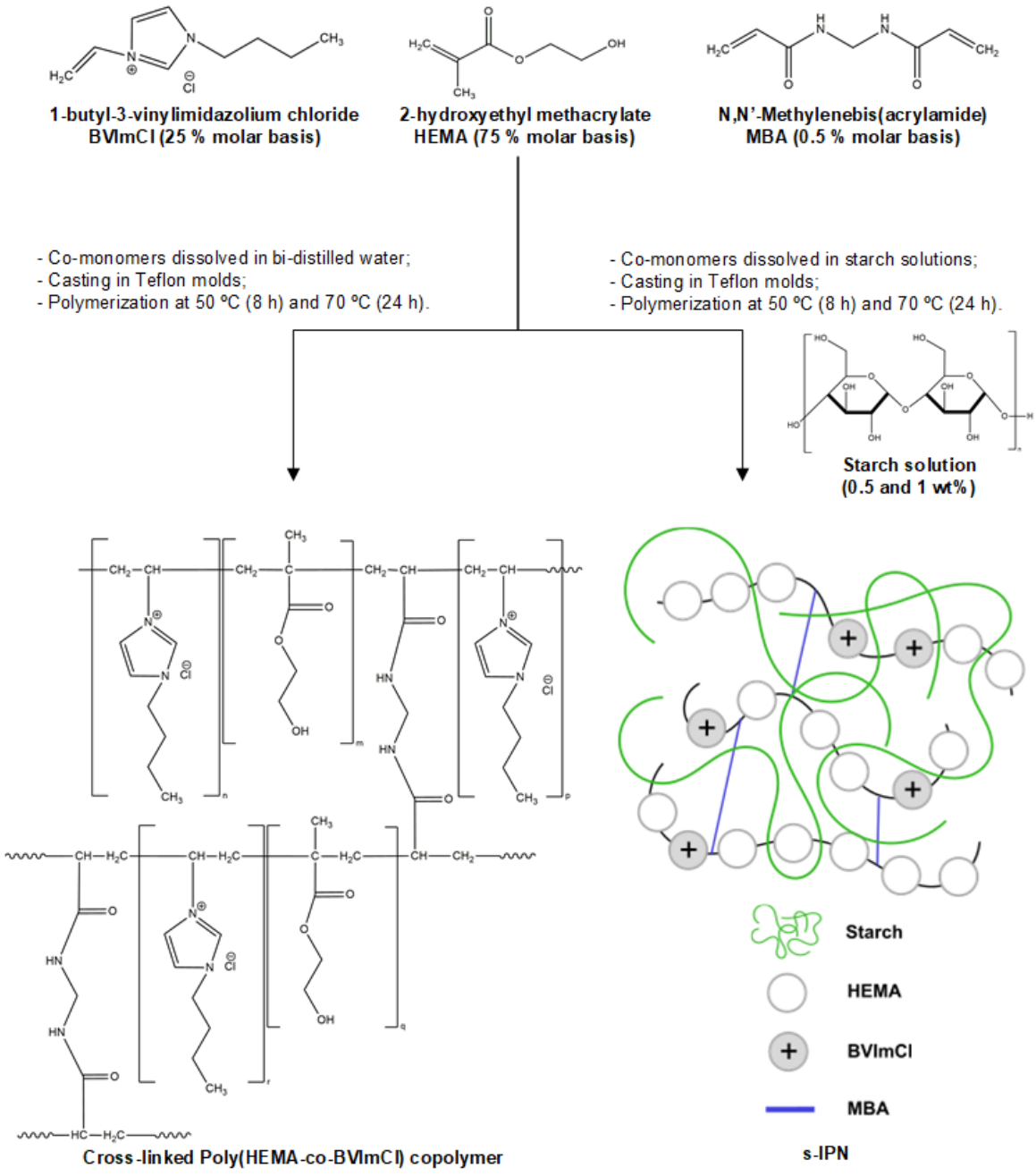

Figure 2.1 Schematic representation of the hydrogels' chemical structure.

Table 2.1 Feed compositions and elemental analyses of the hydrogels synthesized in aqueous media (6.44 mL). Fixed amounts of cross-linker, *N,N'*-methylenebis(acrylamide) (MBA) and of initiator, 2,2'-Azobis (2-methylpropionamidine) dihydrochloride (AIBA) were employed for all samples (0.0616 and 0.0247 mmol, respectively).

Hydrogels	Code	St (mg)	HEMA (mmol)	BVImCl (mmol)	$BVImCl_{theo}$ (mmol IL/g dry sample)*	$BVImCl_{exp}$ (mmol IL/g dry sample)**
Poly(HEMA)	poly(HEMA)	--	12.37	--	--	--
Poly(HEMA-co-BVImCl)	poly(HEMA-co-BVImCl)	--	9.28	3.09	1.717	0.974 ± 0.0978
sIPN_Poly(HEMA-co-BVImCl)_0.5%St	s-IPN/St0.5	32.2	9.28	3.09	1.717	0.933 ± 0.1607
sIPN_Poly(HEMA-co-BVImCl)_1.0%St	s-IPN/St1.0	64.4	9.28	3.09	1.717	1.082 ± 0.0079

* Ratio between the number of moles of BVImCl and the total weight of fed reactants (HEMA+BVImCl+MBA+AIBA);

** Calculated from elemental analysis data as detailed in supplementary material (Table S2.1, Appendix A).

2.3.3 Characterization of the hydrogels

2.3.3.1 Chemical analysis

Attenuated total reflection Fourier transform infrared (FTIR-ATR) spectra were acquired using a spectrophotometer (Perkin Elmer, Spectrum Two, U.K.) at 128 scans and 4 cm^{-1} resolution between 400 and 4000 cm^{-1}. Elemental analysis was performed to determine the chemical composition of the prepared samples after synthesis and washing procedures. The analysis was carried out in triplicate for each sample in an elemental analyzer (Fisons Instruments, model EA1108 CHNS-O) by the differential thermal conductivity method.

2.3.3.2 Morphological properties

A scanning electron microscope (Jeol, model JSM-530, Japan) coupled with energy dispersive X-ray spectroscopy analysis (Phillips, EDX Genesis, model XL 30) was used to observe the morphology (surface and cross-section) of freeze-dried hydrogels, as well as the distribution of BVImCl through the prepared hydrogel matrices (by elemental mapping). SEM-EDX micrographs were obtained at 10 KeV for gold-sputtered samples under argon atmosphere.

2.3.3.3 Thermomechanical properties

The thermal stability of freeze-dried hydrogels was measured using a thermogravimetric analyzer (TA Instruments, Q500, USA). Samples (± 10 mg) were dried at 50 ºC under vacuum for 24 h before analysis. Measurements were conducted from 25 ºC up to 600 ºC at a heating rate of 10 ºC/min, under nitrogen atmosphere with a flow rate of 40 mL/min. Samples were also analyzed by differential scanning calorimetry (DSC-Q100 equipment from TA Instruments), applying consecutive heating (from 40 up to 150 ºC), cooling (from 150 down to -80 ºC), and reheating (from -80 up to 200 ºC) runs at 10 ºC/min, under nitrogen atmosphere

(50 mL/min). Samples (± 7 mg) were dried before analysis (by freeze-drying) to remove residual water and then sealed immediately in aluminum pans.

The mechanical performance of freeze-dried hydrogels was accessed using a temperature-controlled stress rheometer (ModelRS1, Haake, Vreden, Germany), with a cylindrical sensor system Z34 DIN connected to a temperature-controlled recirculation bath (Haake Phoenix II). Rheological measurements were performed in oscillatory shear mode at a constant shear stress of 100 Pa, and at a frequency sweep of 0.1 - 100 rad/s at 25 ºC. Samples were kept in bi-distilled water for 24 h before measurements. Circular shaped water-swollen discs (2 cm diameter and ± 2 mm thickness) were placed between the rotatory and the stationary surfaces separated by a fixed gap of 1.5 mm. The complex shear modulus of the samples was calculated following a procedure previously reported in the literature.[50] Measurements were replicated for each sample (at least twice).

2.3.3.4 Swelling

The water swelling capacity (WSC) of freeze-dried hydrogels was measured at 25 ºC in three different aqueous media, having different pH and ionic strength (I) values, namely bi-distilled water; phosphate buffer (I = 0.027 M; pH = 7.0) and phosphate buffered saline (I = 0.169 M; pH = 7.4). Dried samples were weighted and then immersed into 15 mL of each medium. At predefined time intervals, swollen samples were weighed (after removing the excess of surface water using a filter paper) and immersed again into the corresponding medium. This process was repeated at pre-established time intervals of 30 min (for the first 3 h), 1 h (for the following 5 h), once a week (for two months), and again after five months. The pH of each medium was checked during measurements (using a Standard pH meter, Meter Lab). The WSC capacity was calculated as the ratio between the weight of water absorbed at time *t* and the initial weight of the film (before immersion, $t = 0$) and the results are presented in terms of $g_{water}/g_{dried\ hydrogel}$.

The water vapor sorption (WVS) capacity of freeze- and oven-dried hydrogels was measured for samples previously dried at 50 ºC for 24 h under vacuum (Vacuum oven, J.P. Selecta, s.a.). Samples were placed in Petri dishes and stored at 25 ºC in hermetic flasks containing a potassium sulfate saturated solution, to increase the relative humidity, RH of the flasks up to 90 % (at 25 ºC). Samples were weighed after 24 h and returned to the RH controlled flask and then weighted again after 48 h to guarantee that WVS equilibrium was attained. The shape and size of the samples after each measurement was monitored using a digital camera. The WVS capacity of the samples was calculated as the ratio between the weight of water absorbed at time *t* and the initial weight of the freeze- or oven-dried samples and results are presented in terms of $g_{water}/g_{dried\ hydrogel}$ (%). Both WSC and WVS measurements were performed in duplicate.

2.3.3.5 Impedance spectroscopy measurements

Electrochemical impedance spectroscopy (EIS) experiments were performed using a potentiostat/galvanostat/ZRA, (Gamry Instruments, Reference 600). A root mean square (rms) perturbation of 350 mV was applied over a frequency range between 1.0 MHz and 0.1 Hz (ten frequency values per decade), superimposed on a fixed potential difference of 0.10 V between the two electrodes. Freeze-dried and oven-dried samples were cut into a squared shape (1 cm^2) and stored at 90 % RH and room temperature for 24 h, before EIS measurements. Samples were then placed between two blocking electrodes (1 cm^2, SS316 steel) in the measurement cell in air. The spectra were fitted using appropriate electrical equivalent circuits (ZView 3.2 software, Scribner Associates Inc., U.S.A.). In this work the constant phase element (CPE) was defined as $CPE = \{(Ci\omega)^{\alpha}\}^{-1}$, where C is a constant, *i* is the square root of -1, ω is the angular frequency, and α is a parameter that varies between 0.5 (for heterogeneous/porous surfaces) and 1.0 (for homogeneous/smooth surfaces), and which reflects the non-uniformity and the

surface roughness of the material. The resistivity of the hydrogels (ρ, MΩ cm) was obtained from Z_w while the conductivity (σ, S cm^{-1}) was calculated as the inverse of the resistivity.

2.3.3.6 Electro-assisted L-tryptophan sorption and desorption experiments

Electro-assisted sorption and desorption experiments were performed using a flatbed electrophoresis unit MULTI (Carl Roth, Deutschland) at room temperature (± 22 ºC) which is comprised by a horizontal chamber with adjustable anode and cathode platinum electrodes, and which was connected to an electrophoresis power supply EPS 500/400 (Pharmacia Fine Chemicals, Sweden). Electro-assisted sorption experiments were carried out by placing the electrodes (3 cm apart) over a polystyrene Petri dish containing a fixed volume (~ 20 mL) of aqueous solutions of the amino acid L-tryptophan (Try) [50.3 mg/mL] dissolved in bi-distilled water, TRIZ and AB. Freeze-dried hydrogel samples (± 20 mg) were previously hydrated up to equilibrium in bi-distilled water (for 24 h) and placed in a midway position between the electrodes. L-tryptophan (Try) sorption experiments were conducted at different applied voltages (0, 2, 5 and 100 V) for 3 h and in each aqueous media (bi-distilled water, TRIZ and AB). The amount of Try removed from each solution by the hydrogels with and without application of an electrical potential was quantified (at 278 nm) using a previously obtained calibration curve of Try in each aqueous media: bi-distilled water ([Try] = 0.1981 × Abs, R^2 = 0.998), TRIZ ([Try] = 0.1602 × Abs, R^2 = 0.999) and AB ([Try] = 0.2057 × Abs, R^2 = 0.999). Electro-assisted Try desorption experiments were conducted at different applied voltages (0, 2, and 5 V), for 3 h, and employing the samples that were previously loaded at 2 V. The amount of Try released from the hydrogel was quantified using the calibration curves referred above. Electro-assisted sorption and desorption experiments were conducted at least in duplicate.

2.3.3.7 Cytocompatibility

Cytocompatibility studies were carried out following the direct contact test (ISO standard 10993-5:2009) using Balb/3T3 cells and by two different assays (cell viability, LDH and cell proliferation, MTT). For both assays, Balb/3T3 cells (20.000 cells/well) were cultured in 24 wells-plate during 12 h in Dulbecco's modified Eagle's medium (DMEM)/F12 Ham nutrient mixture (Sigma-Aldrich, USA), supplemented with 10 % fetal bovine serum (FBS), 1 % L-Glut 200 mM and 1 % penicillin (10.000 UI/mL)/streptomycin (10.000 µg/mL) solution, and kept in a humidified atmosphere with 5 % CO_2, 90 % RH at 37 °C. Freeze-dried hydrogels were cut into pieces of approximately 16 mm^2 and pre-incubated in culture medium for 24 h. Samples were then sterilized for 30 min with UV radiation (at both sides) and incubated on the cell monolayer for 24 h. The LDH assay was performed by mixing aliquots (100 µL) of the cell culture medium with the reaction medium (100 µL). The positive control (100 µL of medium of lysated cells with Triton X-100) and the negative control (100 µL of medium with no lysozyme cell content) were also mixed with the reaction medium (100 µL). Plates were incubated for 15 min at 15-25 ºC, protected from light, and the absorbance at 490 nm was immediately measured in (UV Bio-Rad Model 680 microplate reader, USA). The cell viability was calculated using equation (1):

$$\text{Cell viability}(\%) = \frac{\text{Abs}_{\text{exp}} - \text{Abs}_{\text{negative control}}}{\text{Abs}_{\text{positive control}} - \text{Abs}_{\text{negative control}}} \quad (1)$$

Cell proliferation was measured following the protocol of the Cell Proliferation Kit I (MTT). Briefly, culture medium and samples were removed from wells, and the wells replenished with DMEM/F12 supplemented (250 µL). MTT labelling reagent (25 µL) was added and the plate was maintained at 37 ºC, 95 % RH and 5 % CO_2 for 4 hours. The solubilization solution (250 µL) was then added and kept at 35 ºC, 95 % RH and 5 % CO_2 overnight. Finally, the absorbance

was recorded at 550 nm (UV Bio-Rad Model 850 microplate reader, USA). Cell proliferation (%) was calculated using equation (2):

$$\text{Cell proliferation}(\%) = \frac{\text{Abs}_{\text{exp}}}{\text{Abs}_{\text{control}}} \text{x}100 \quad (2)$$

2.3.3.8 Statistical analysis

The statistical analysis of the data obtained was performed by the One-way ANOVA test. Statistical significance was considered for *p*-values < 0.05.

2.4 Results and discussion

2.4.1 Structural and morphological characterization

The chemical composition of the obtained hydrogels was evaluated by elemental analysis (Table 2.1) and FTIR-ATR (Figure 2.2). The presence of the IL (BVImCl) in poly(HEMA-co-BVImCl) and s-IPN samples was confirmed by the increase (> 2.5 wt %) in the amount of elemental nitrogen (from the imidazolium cation) measured for these samples when compared to poly(HEMA). The small amount of elemental nitrogen measured for poly(HEMA) samples was attributed to the cross-linking agent (MBA) and to the initiator (AIBA). The IL content in all samples (with or without starch) was not statistically different to within 5 % and it corresponds to an effective incorporation of BVImCl in the hydrogels of ~ 0.58 ± 0.045 % of the theoretical value (Table 2.1), as calculated from elemental analysis results (Table S2.1, Appendix A). This result may be due to a low reactivity of the IL vinyl monomer, when compared to HEMA (which was not evaluated in this work), and/or IL loss while washing the hydrogels.

The infrared spectra of all samples showed the characteristic peak of HEMA, namely the C=O ester bond at 1707 cm^{-1} (Figure 2.2A), CH_2 bending, C-O stretching and CH_3 wagging at 1456,

1251 and 1156 cm^{-1}, respectively (Figure 2.2B) and the C-H stretching vibrations at 2871 and 2945 cm^{-1} [51-53] (Figure 2.2C).

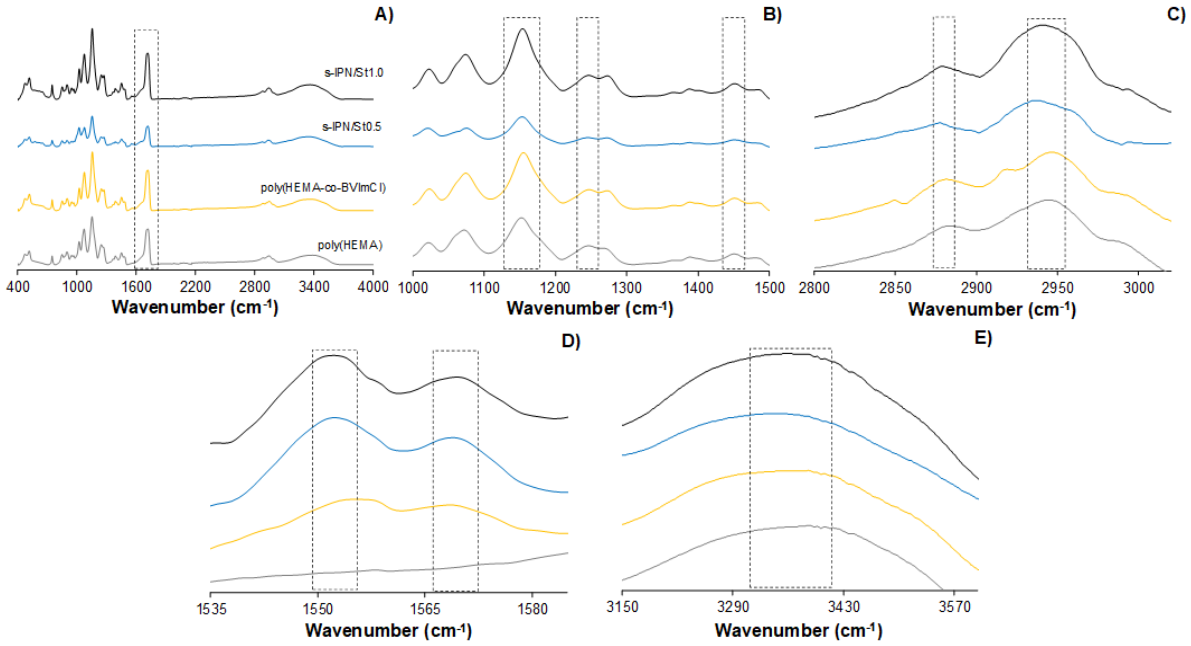

Figure 2.2 FTIR-ATR spectra of the synthesized hydrogels. Samples are coded as: poly(HEMA) (—), poly(HEMA-co-BVImCl) (—), s-IPN/St0.5 (—) and s-IPN/St1.0 (—).

The characteristic peaks of BVImCl in the 1569-1552 cm^{-1} range, assigned to the C=C imidazolium ring vibration[54,55], were observed in poly(HEMA-co-BVImCl) and s-IPN hydrogels (Figure 2.2D). Additionally, poly(HEMA-co-BVImCl) also presented a band at 2918 cm^{-1} which can be assigned to C-H aliphatic stretching of BVImCl.[54] This band was not distinguished for s-IPN because overlapping with the broad bands observed at 2936 and 2944 cm^{-1} due to the C-H stretching of starch[56,57] (Figure 2.2C). Finally, and when compared to poly(HEMA), a significant shift of 11 cm^{-1} for poly(HEMA-co-BVImCl) and of 24.5 cm^{-1} for s-IPNs were observed in the O-H stretch vibration region (3000–3600 cm^{-1}) which may be justified by the higher hygroscopic nature of these samples resulting from their higher hydrophilicity as it will be discussed later (Figure 2.2E). Finally, bands assigned to vinyl

vibration of HEMA and BVImCl monomers (1620-1680 cm^{-1})[53,58,59] were not detected in any of the spectra confirming that polymerization has occurred and/or that unreacted monomers were successfully removed from the hydrogels during washing.

The morphology of freeze-dried hydrogels and the elemental mapping of nitrogen and chlorine distribution through the hydrogel structures were analyzed by scanning electron microscopy (SEM) and energy dispersive X-ray spectroscopy (EDX), respectively (Figure S2.1, Appendix A). Oven-dried samples were also analyzed by SEM but all of them revealed compact structures, with no relevant differences among them (data not shown). Hydrogels containing IL, namely for poly(HEMA-co-BVImCl) and s-IPNs, presented a macroporous structure with large interconnecting cavities, being clearly different from the globular dense structure of poly(HEMA). As previously discussed in the literature, the observed globular structure of poly(HEMA) results from phase separation that occurs as the water soluble monomer HEMA is being converted into non-soluble poly(HEMA).[49] The presence of the IL in the copolymer backbone decreased the original hydrophobicity of poly(HEMA), thus avoiding phase separation. The cationic nature of the hydrogels induced high water sorption capacities that led to the formation of macroporous structures after removing water by freeze-drying. Compared to poly(HEMA-co-BVImCl), s-IPNs exhibited denser structures due to the entrapment of starch within the macro cavities of the copolymer structures. EDX results measured for the s-IPN/St1.0 showed a homogeneous distribution of chlorine and nitrogen atoms (from BVImCl) through the hydrogel structure.

2.4.2 Swelling

The water swelling capacity (WSC) of the synthesized freeze-dried hydrogels was evaluated in different media (bi-distilled water; phosphate buffer (PB) and phosphate buffer saline (PBS)) at 25 ºC; the swelling profiles are depicted in Figure 2.3. The WSC of the hydrogels after 24 h

of immersion in different media is also presented in Figure 2.3D for comparison. In general terms, the WSC of the hydrogels increased in the order PBS (I = 0.169 M) < PB (I = 0.027 M) < bi-distilled water (I ≈ 0 M). Water sorption equilibria (plateau in WSC profiles) were promptly attained for all the hydrogels (< 1 h), which maintained their structural integrity (in all the tested media and for at least 5 months).

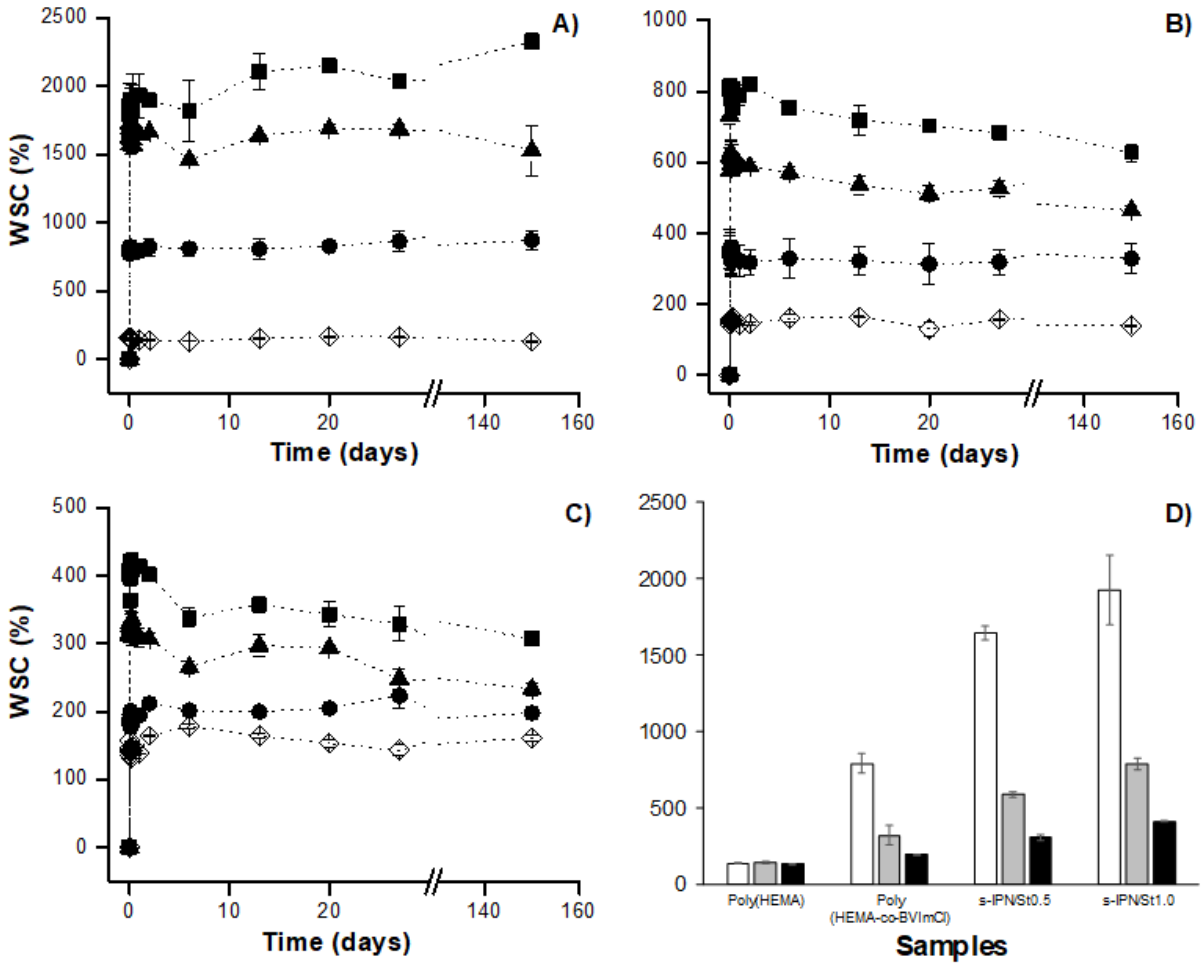

Figure 2.3 Water sorption capacity (WSC) profiles of the synthetized hydrogels at 25 ºC in different aqueous media: A) Bi-distilled water; B) PB and C) PBS. Symbols represent: poly(HEMA) (◊), poly(HEMA-co-BVImCl) (●), s-IPN/St0.5 (▲) and s-IPN/St1.0 (■). D) Equilibrium water sorption capacity data measured for the hydrogels at 25 ºC after 24 h of immersion in different aqueous media: Bi-distilled water (□); PB (■) and PBS (■).

The WSC of all polycationic hydrogels in bi-distilled water (Figure 2.3A) was much higher than that of neutral poly(HEMA). This effect is a result of two mechanisms, namely the ionic pressure that is established between the cationic hydrogel and water (which presents negligible ionic strength) and the electrostatic repulsion between positively charged monomers present in the copolymer backbone. In the first case, water molecules diffuse into the copolymer network to dilute the higher amount of charges existing inside the hydrogel, up to a certain limit (equilibrium) that is mainly defined by the mechanical elastic response of the hydrogel. This means that the hydrogels swell, up to a certain limit which highly depends on its cross-linking degree. In the second case, electrostatic repulsion lead to an increase in the free volume in-between copolymer chains which favor water molecules to diffuse inside the hydrogel network up to a certain swelling limit as mentioned above. The effect of the ionic strength of the medium over the WSC of the hydrogels can be seen in Figures 2.3B-2.3D. The WSC of the hydrogels in saline media followed a similar trend to that observed in water (poly(HEMA) < poly(HEMA-co-BVImCl) < s-IPNs), however, and as expected, the presence of salts in PB and in PBS led to a significant decrease in the WSC of the cationic hydrogels (~ 46 % in PB and 63 % in PBS) when compared to WSC measured in pure water, and consequently to a lower mechanical response of the hydrogels when immersed in saline media. This result is justified by the higher ionic strengths of the saline media (0.027 M in PB and 0.169 M in PBS) when compared to water, which led to a decrease in the ionic pressure that is established between the hydrogel network and the external media (in this case both the hydrogel and the media have charges). As a consequence, the amount of water that diffuses inside the hydrogel decreases because the difference between the number of charges inside and outside the hydrogel network is lower and therefore equilibrium (or charge dilution) is attained at lower WSC. Moreover the anions present in the buffer saline solutions may also induce a charge screening effect around the cationic groups of the hydrogel decreasing the electrostatic cation-cation repulsions between

positively charged monomers also leading to a decrease in the ionic pressure difference between the polymer network and the external solution.[60,61] The WSC of s-IPNs were significantly higher than that of poly(HEMA-co-BVImCl) (× 2 and × 2.4 for s-IPN containing 0.5 and 1.0 wt % of starch, respectively) due to starch hydrophilic nature which favors hydrogel-water interactions.[62] The physicochemical and functional properties of starch depend on the raw material source (e. g. wheat, cassava, rice, maize, potato) and potato starch (that was used in this work) has one the highest water swelling capacities.[63] The WSC of starch-based s-IPNs in PBS (~ 360 %) is significantly higher than that observed for other starch-based IPN systems, synthetized using acrylate-based monomers.[64,65]

The water vapor sorption (WVS) capacity of freeze- and oven-dried hydrogels is given in Figure 2.4. The equilibrium was attained in 48 h and there was no significant influence of the employed drying method on the WVS capacity of the hydrogels at 25 ºC and RH ≥ 90 % (no statistical difference at *p*-value > 0.05). The WVS capacity of the hydrogels ranked similarly as for the WSC: poly(HEMA) < poly(HEMA-co-BVImCl) < s-IPN/St0.5 < s-IPN/St1.0. The WVS capacity of s-IPNs was twice that measured for poly(HEMA) which again confirms that the hydrophilic and hygroscopic character of starch and BVImCl.[66]

Interestingly, and as can be seen in Figure S2.2 (Appendix A), the volume of the polycationic freeze-dried hydrogels was significantly reduced (samples shrank down to one third their original area) after 24 h of exposure to high RH, at constant temperature revealing an effective mechanical response of these hydrogels during WVS experiments and when exposed to high RHs. It is hypothesized that water vapor molecules become strongly adsorbed to the hydrogels internal pore walls, due to strong BVImCl-water and starch-water interactions, leading to condensation above a certain water vapor concentration, that ultimately lead to the collapse of the macroporous structure of the hydrogels due to hydrogen-bonding interaction among water molecules condensed within the pores.[67,68]

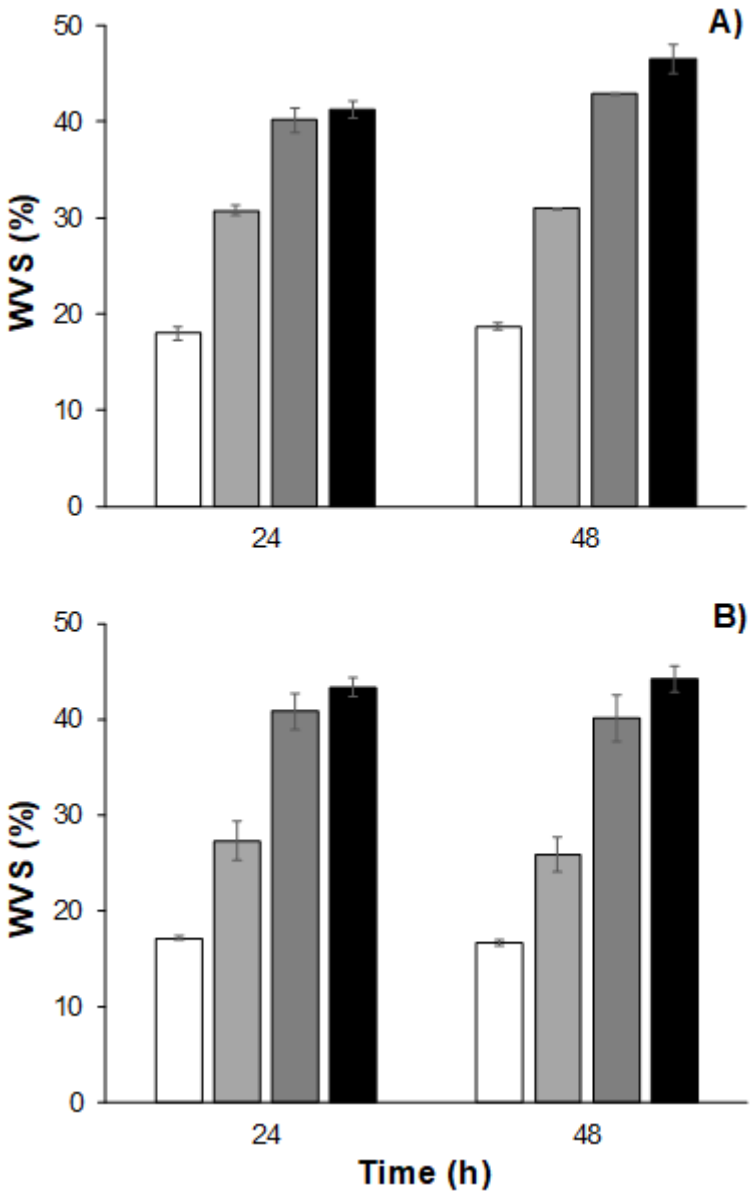

Figure 2.4 Water vapor sorption (WVS) capacity of the oven-dried hydrogels (A) and freeze-dried hydrogels (B) measured at RH ≥ 90% and 25 ºC for poly(HEMA) (□), poly(HEMA-co-BVImCl) (■), s-IPN/St0.5 (■) and s-IPN/St1.0 (■).

2.4.3 Thermomechanical properties

The thermogravimetric profiles of poly(HEMA) and starch presented a one-step degradation profile (with maximum degradation peak (T_{peak}) of 385 ºC and 306 ºC, respectively) in agreement with data previously reported in the literature.[69,70] Differently, poly(HEMA-co-BVImCl)and s-IPNs hydrogels presented three degradation steps with maximum T_{peak} values

between 255-289 ºC, 322-329 ºC and 409-417 ºC, respectively (Figure S2.3, Appendix A and Table 2.2). These events may result from the thermal degradation of BVImCl, HEMA-co-BVImCl and HEMA rich domains, respectively that may be present along the polycationic structure. Moreover, TGA results also indicated that the thermal stabilities of the polycationic hydrogels are similar and lower than that of the neat poly(HEMA) (Table 2.2). Polycationic hydrogels also present higher weight losses ~ at 150 ºC (up to 4.5 wt %), which can be attributed to residual water evaporation and which confirms that the presence of the IL increased the hydrophilicity of the hydrogels (when compared to poly(HEMA)).

The effect of IL-functionalization over poly(HEMA) chain mobility was indirectly accessed by comparing the glass transition temperatures (T_g) of the prepared hydrogels (determined from DSC analysis). The T_g of the poly(HEMA) homopolymer measured was determined as 117.3 ± 1.2 ºC (Table 2.2 and Figure S2.3, Appendix A) which is in reasonable agreement with the value of ~ 115 ºC previously reported in the literature.[71] The T_g value measured for s-IPN/St1.0 (121.1 ± 1.8 ºC) is also in agreement with that previously reported for poly(HEMA)-starch composites, (~ 120 ºC).[72] No statistically significant difference (p-value > 0.05) was observed for T_g values of poly(HEMA) and of polycationic samples (poly(HEMA-co-BVImCl) and s-IPNs), which indicates that the thermomechanical properties of poly(HEMA) are mostly maintained after functionalization, probably due to the relative low amount of IL incorporated in the copolymer backbone.

The viscoelastic properties of water-swollen hydrogels (at equilibrium) were measured by oscillatory frequency sweeps at 25 ºC, and the results are presented as the change of the storage modulus (G') and of the loss modulus (G'') as a function of the angular frequency of tested hydrogels (Figure 2.5A). The complex shear modulus (G^*) was calculated from G' and G'' data and as previously described in the literature[50] and the results are presented in Table 2.2 and in Figure 2.5B. With the exception of s-IPN/St1.0, all hydrogels presented a typical

frequency dependent gel-like behavior (G' > G'' and tan δ < 1, over the frequency range analyzed), converging to a plateau (Figure 2.5A).

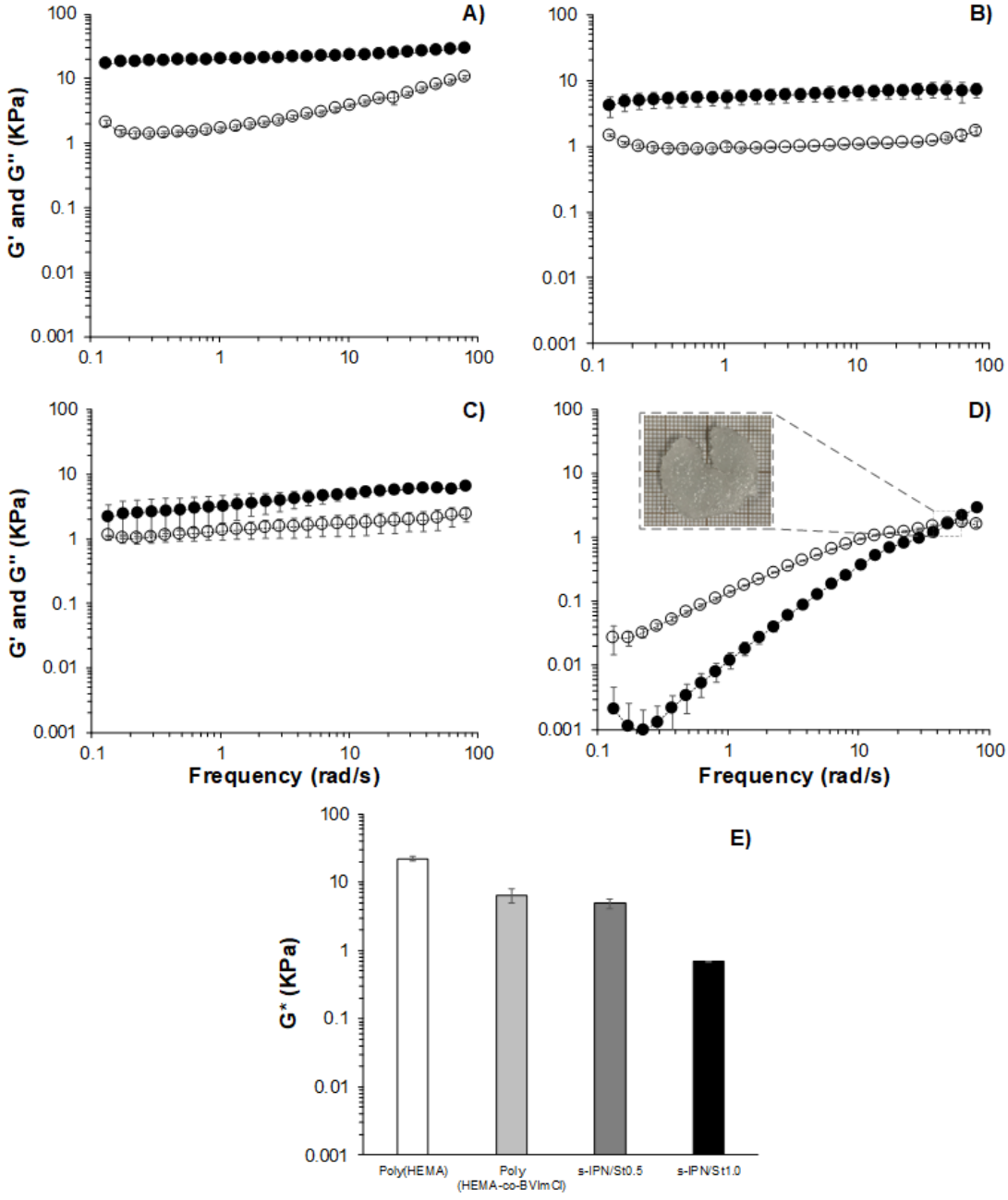

Figure 2.5 Rheological measurements of hydrogels hydrated in bi-distilled water at 25 ºC (at equilibrium): A) Poly(HEMA); B) Poly(HEMA-co-BVImCl); C) s-IPN/St0.5; D) s-IPN/St1.0. The viscoelastic properties are represented as shear/storage modulus (G', ●), loss modulus (G'', ○) and loss factor (tan δ, ■) as a function of oscillatory frequency. E) Complex shear modulus (G*) calculated for a frequency of 1 Hz.

Table 2.2 Thermomechanical data measured for the prepared hydrogels. Parameters $Wt_{150ºC}$ (%), $T_{5\%}$ (ºC), T_{onset} (ºC) and T_{peak} (ºC) were measured by TGA; glass transition temperatures (T_g) were measured by DSC; and complex shear modulus (G*) and loss factor (tan δ) at 1 Hz were measured by rheology.

Hydrogels	$Wt_{150ºC}$ (%)[a]	$T_{5\%}$ (ºC)[b]	T_{onset} (ºC)[c]	T_{peak1} (ºC)[d]	T_{peak2} (ºC)[d]	T_{peak3} (ºC)[d]	T_g (ºC)[e]	G* (MPa)[f]	tan δ (-)[f]
Poly(HEMA)	2.3	332.5	349.2	-	-	385.1	117.3 ± 1.2	22.0 ± 1.2	0.14 ± 0.1
Poly(HEMA-co-BVImCl)	3.9	208.2	253.3	285.5	322.1	416.9	120.7 ± 0.9	6.4 ± 1.1	0.16 ± 0.1
s-IPN/St0.5	3.6	205.5	254.8	286.3	322.8	413.3	119.6 ± 0.2	4.9 ± 0.5	0.38 ± 0.2
s-IPN/St1.0	4.5	206.9	259.3	288.5	322.3	413.2	121.1 ± 1.8	0.6 ± 0.0	3.52 ± 0.3

[a] Weight loss (%) at 150 ºC;

[b] Temperature where the weight loss is 5% (wt);

[c] Temperature which thermal degradation starts to occur;

[d] Maximum degradation temperature from DTG curves (obtained from first derivative of weight loss vs temperature curve);

[e] Obtained from the integration of a "step" of heat flow vs temperature curve;

[f] According to literature.[52]

A similar gel-like behavior was previously reported for poly(HEMA) hydrogels cross-linked with diethylene glycol dimethacrylate at 25 ºC.[73] For the frequency range analyzed, G', G'' and G* values measured for poly(HEMA-co-BVImCl) and s-IPN samples were lower (up to 10 × lower) than those measured for poly(HEMA) according to the sequence poly(HEMA) > poly(HEMA-co-BVImCl) > s-IPN/St0.5 > s-IPN/St1.0, meaning that poly(HEMA-co-BVImCl) and s-IPN samples present a lower capacity to store mechanical perturbation in the form of elastic deformation (Table 2.2). This sequence follows the inverse trend observed for the water swelling capacity of the samples (Figure 2.3). Therefore, these results indicate that the water content of the hydrogels plays a major role in their viscoelastic properties[74] by enhancing hydrogel chain mobility (by disrupting interchain hydrogen bonding) thus softening its network and increasing its flexibility. The rheological properties of s-IPN/St1.0 were strongly dependent on the applied frequency, presenting a viscous-like behavior (G' < G'' and

tan δ > 1) at frequencies below 50 rad/s and a crossover point at ~ 50 rad/s, which resulted from an overload of the applied mechanical perturbation over the intermolecular forces of the s-IPN/St1.0 structure that led to the rupture of the hydrogel (image in Figure 2.5A).

Finally, and as can be observed in Table 2.2, the tan δ value measured for poly(HEMA-co-BVImCl) was similar to that of poly(HEMA) while higher tan δ values were obtained for s-IPN samples, and they increased with the amount of starch in the s-IPN structure. Higher loss factors (tan δ > 0.1) are typical of biological gels and soft tissues.[75]

2.4.4 Electrochemical properties

The effect of IL and starch contents on the electrical resistivity of prepared polycationic hydrogels was evaluated by electrochemical impedance spectroscopy. A symmetrical cell with two steel electrodes was used and hydrogels were placed in between the two electrodes. Additionally, the effect of hydrogel porosity on its electrical resistivity was also assessed by analyzing both dense and porous samples which were obtained by conventional drying (in an oven at 50 ºC) and by freeze-drying, respectively. Since the electrical resistivity of hydrogels is greatly affected by their water contents[76], all samples were maintained in controlled relative humidity (RH ≥ 90 %), at 25 ºC, and overnight before analysis. The impedance spectra of the polycationic hydrogels are shown in Figure 2.6A and 2.6B, for freeze-dried and oven-dried samples, respectively. The spectrum of poly(HEMA) is not represented due to the high resistivity of this sample, which behaves as an insulator under the employed conditions. Therefore, and as a first conclusion, these results show that IL-functionalization induces an increase in the electrical conductivity of the poly(HEMA)-based hydrogels. As can be seen in Figure 2.6A and 2.6B, all spectra presented a semicircle at higher to intermediate frequencies (due to charge transfer reactions, and to a non-ideal double layer capacitance at the film/electrode interface), diffusive lines at intermediate/low frequencies (due to ion diffusion

through the hydrogel), followed by capacitive lines at lower frequencies (due to charge separation processes in the bulk of the hydrogel).

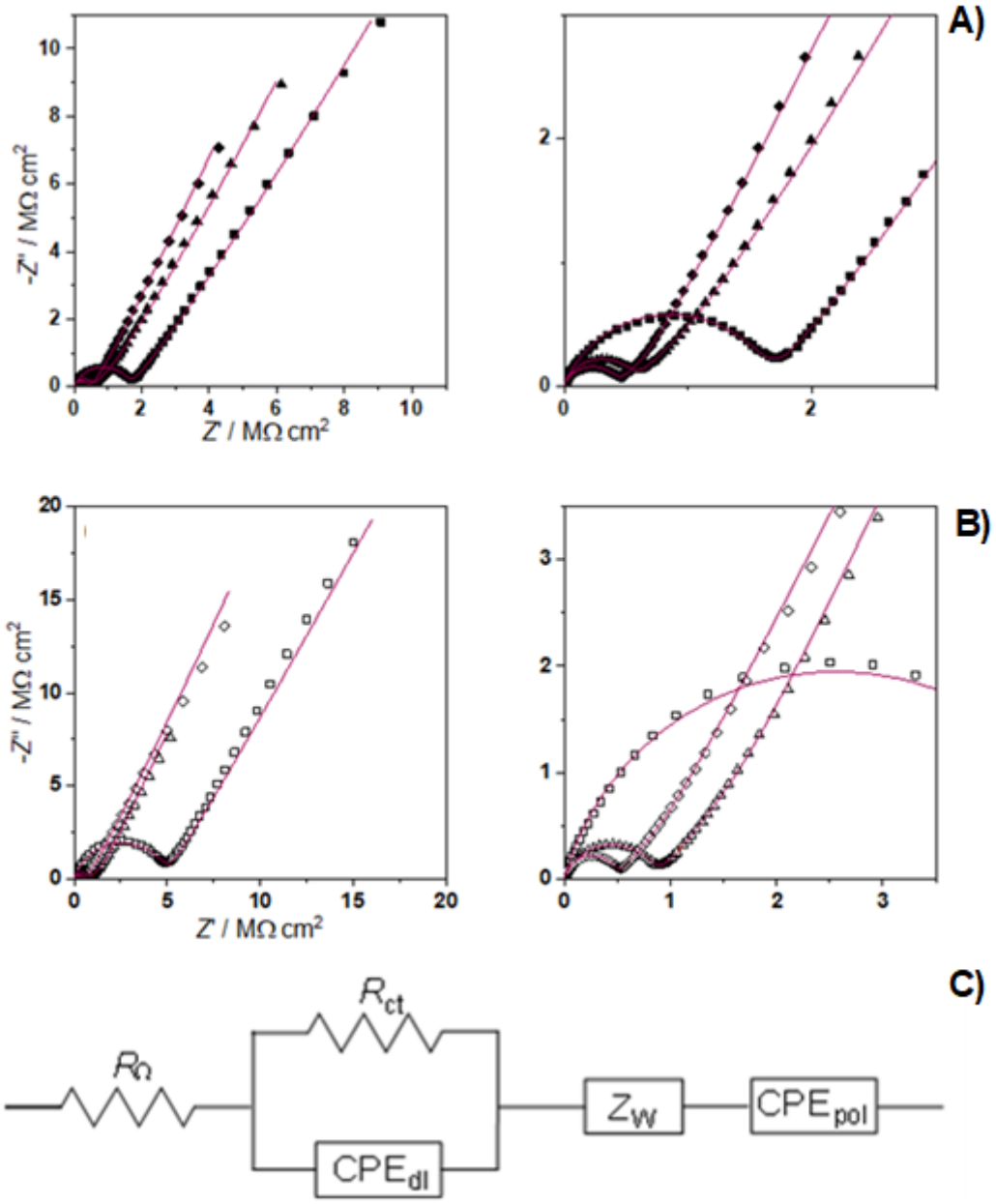

Figure 2.6 Complex plane plots obtained for prepared hydrogels: poly(HEMA-co-BVImCl) (■, □), s-IPN/St0.5 (▲, Δ) and s-IPN/St1.0 (♦, ◊) where filled and open symbols represent freeze-dried (A) and oven-dried (B) hydrogels, respectively. The equivalent circuit used to fit the impedance spectra is represented in Figure 2.6C.

The values of the resistive and capacitive elements were estimated by fitting the impedance spectra to the equivalent circuit model (Figure 2.6C) and are presented in Table 2.3. According to the equivalent circuit model (Figure 2.6C), all fitted spectra present a cell resistance (R_{Ω}) that comprises the resistance intrinsic to the equipment (electrical contacts, wires and steel electrodes). The obtained value of R_{Ω} (5.0 ± 2.8 kΩ) is not presented in Table 3 since the cell resistance R_{Ω} is not related to the sample electrical characteristics. The equivalent circuit is further described by a parallel combination of a charge-transfer resistance (R_{ct}) with a non-ideal double layer capacitance (CPE_{dl}), in series with a Warburg diffusional resistance (Z_w), followed by a polarization capacitance (CPE_{pol}).

As observed, when comparing the equivalent circuit values from Table 2.3 for oven- and freeze-dried polycationic hydrogels (poly(HEMA-co-BVImCl) and s-IPNs), it can be seen that freeze-drying leads to a decrease in R_{ct} and Z_w values, and to an increase in the CPE_{pol} values. This confirms that the morphology of the hydrogels has a major influence on the ion conductivity through their physical structure. Since the drying process influences hydrogels porosity, the freeze-dried samples are more porous and therefore less resistive when compared to the oven-dried ones. Porous structures enhance the diffusivity of ions through the swollen network channels (working as 'shortcuts') and resulting in higher conductivity[77,78], although being also dependent on geometric properties such as pore interconnectivity, size, shape and tortuosity.[78-80]

Nevertheless, data presented in Table 2.3 show that the amount of starch significantly influences all the equivalent circuit elements: the increase in starch content led to a decrease in the R_{ct} and Z_w values, and to an increase in the CPE_{pol} values. The ionic conductivities of freeze-dried hydrogels increase according to the sequence poly(HEMA-co-BVImCl) < s-IPN/St0.5 < s-IPN/St1.0, which may be explained in terms of the water vapor content of each hydrogel, which increases with the amount of starch (Figure 2.4).

Table 2.3 Equivalent circuit element values obtained from fitting EIS spectra shown in Figure 2.6, for oven-dried and for freeze-dried hydrogels.

Hydrogels	R_{ct} kΩ cm^2	CPE_{dl} pF s$^{\alpha-1}$cm^{-2}	a_1	$^*Z_W$ kΩ s$^{\alpha-1}$cm^2	$^*\rho$/ MΩ cm	$^*\sigma$/ S cm^{-1}	τ/ ms	a_w	$^*CPE_{pol}$ nF s$^{\alpha-1}$ cm^{-1}	a_2
Oven-dried hydrogels										
Poly(HEMA-co-BVImCl)	4870	140	0.83	1230	16.4	0.1	760	0.50	3.1	0.66
s-IPN/St0.5	841	132	0.80	1350	22.5	0.2	300	0.41	7.0	0.68
s-IPN/St1.0	471	41	0.92	595	7.4	2.0	41	0.42	6.6	0.62
Freeze-dried hydrogels										
Poly(HEMA-co-BVImCl)	1650	192	0.77	163	1.6	0.7	142	0.48	11.4	0.59
s-IPN/St0.5	530	135	0.84	480	4.0	3.2	38	0.41	15.8	0.60
s-IPN/St1.0	413	188	0.81	345	2.5	5.2	27	0.40	28.6	0.59

* values normalized by sample thickness.

Higher water contents are known to enhance free chloride anions diffusivity through the hydrogel network, and consequently to increase the ionic conductivity of polyelectrolyte-based materials.[76]

Recent studies on the electrochemical properties of several materials functionalized with different ionic liquids have reported ionic conductivities ranging between 10^{-6} - 10^{-2} S cm^{-1} at room temperature (~ 25 ºC).[29,30,77,81,82] The ionic conductivity values obtained in the present work for prepared polycationic hydrogels were significantly higher than those reported so far, which is most probably due to the high water contents (> 40 %wt) of these samples and to the homogeneous distribution of BVImCl through the hydrogel network that was achieved in these samples (as confirmed by SEM-EDX). Nevertheless, it is important to refer that conductivity measurements of IL-functionalized materials are very much dependent on a large number of variables, including the chemical composition and morphology of the studied material (IL types and compositions, charge densities and charge distributions, presence of spacers, purities, etc.),

as well as on the experimental measuring conditions (set-up, temperature, relative humidity, etc.) which clearly hamper fair/clear comparisons between different works.

Finally, another interesting feature of the prepared cationic hydrogels is that they both present ionic and electronic conductivities. As illustrated in Figure 2.7, s-IPN/St1.0 mediates electron transfer onto a LED under a DC current of 1 V at room temperature (~ 25 ºC). It is hypothesized that this hydrogel behaves as a single-ion conducting material where the transport of electrons, and consequently the electrical conductivity, resulted from oxidation of Cl^- ions at the anode. This allows the generation of small electrical currents (269 μA, measured with a multimeter) through the hydrogel, which reveals some potential for the application of these materials as electrochemical devices such as fuel cells, batteries, etc.

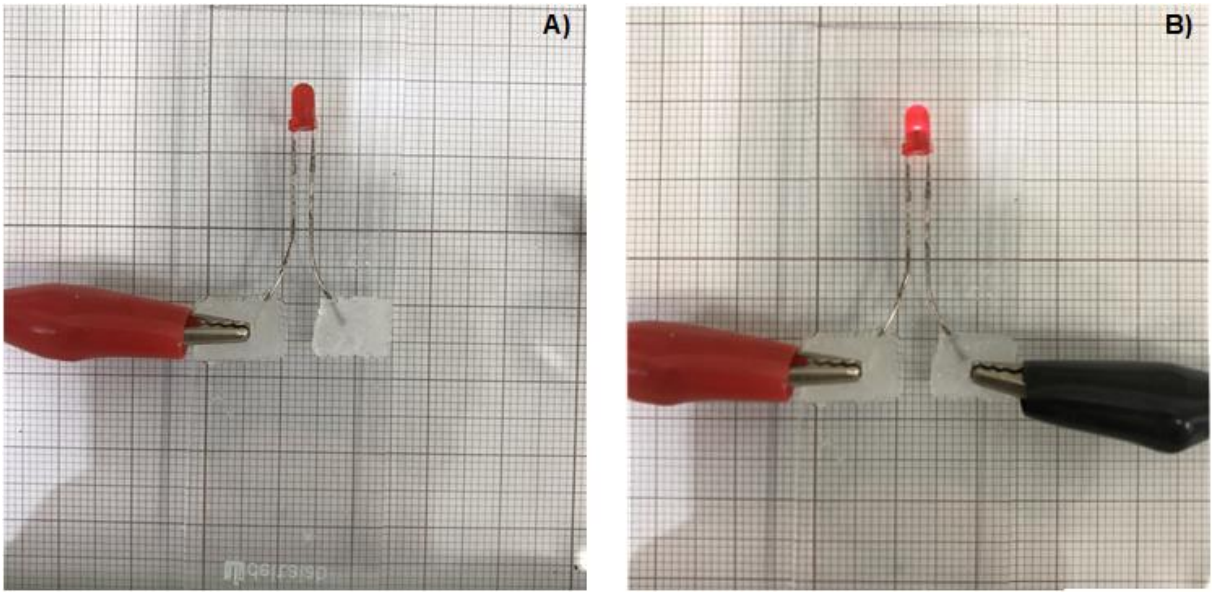

Figure 2.7 Schematic representation of electronic conductivity response of s-IPN/St1.0 hydrogel (in water equilibrium) before (A) and after (B) the application of a potential difference of 1 V at room temperature (~ 25 ºC).

2.4.5 Electro-assisted sorption/desorption of L-tryptophan

The sorption/desorption capacity of the prepared polycationic hydrogels towards L-tryptophan (Try) (used as a model charged biomolecule) was evaluated for samples immersed in different

aqueous media and submitted to different applied electrical stimuli. The capacity to control the removal/release of charged biomolecules from aqueous media is advantageous to optimize (bio)separation processes and for the development of controlled release devices in general and for potential Try-based therapeutic applications in particular (such as anxiety and depression).[83] Electro-assisted sorption (at an applied voltage of 2 and 100 V) and desorption (at an applied voltage of 2 and 5 V) experiments were carried out at room temperature (~ 25 ºC) and the results are presented in Figure 2.8 and Figure 2.9, respectively.

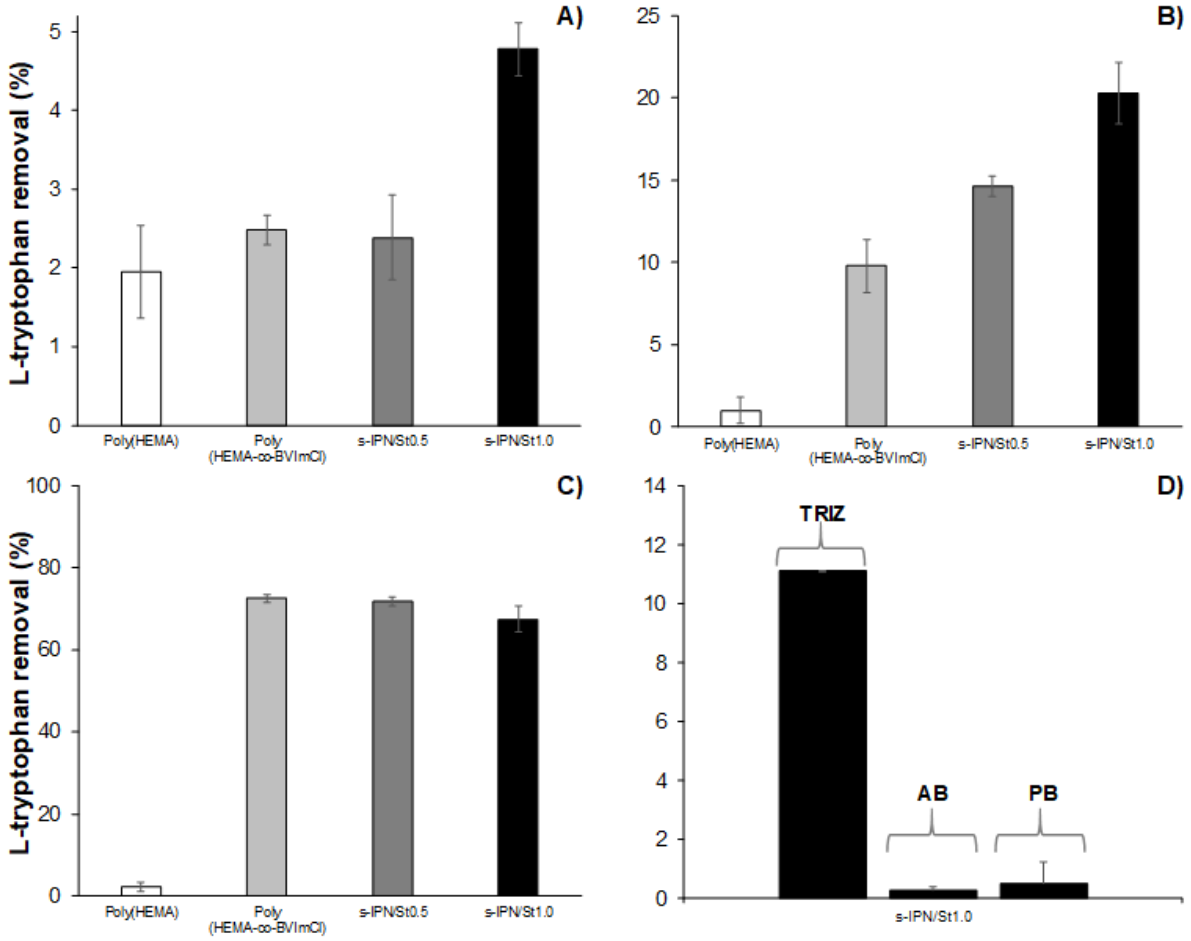

Figure 2.8 Electro-assisted sorption of L-tryptophan [50.3 mg/L] in bi-distilled water at 0 V (A), 2 V (B) and 100 V (C) and in different aqueous media: Trizma base buffer (TRIZ), acetate buffer (AB) and phosphate buffer (PB) at 2 V (D) at room temperature (~ 25 ºC).

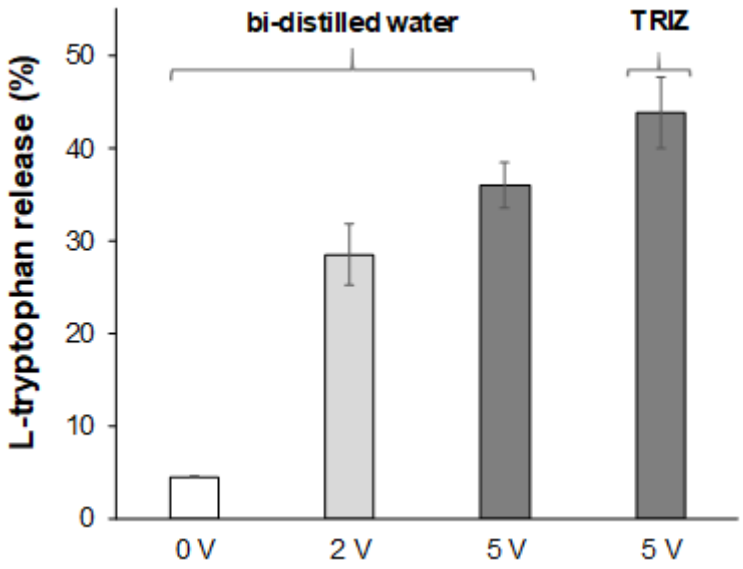

Figure 2.9 Electro-assisted desorption of L-tryptophan [50.3 mg/L] for s-IPN/St1.0 in different media, namely bi-distilled water and Trizma base buffer (TRIZ), at different applied voltages (0, 2 and 5 V) at room temperature (~ 25 ºC). The distance between the electrodes was 3 cm and the experiments were carried out in a constant volume (18 mL) of amino acid solution.

Conventional sorption/desorption experiments (passive sorption with no applied voltage) were also performed for comparison purposes. The total number of moles of Try in solution (4.4 μmol, in 18 mL of a solution with a concentration of 50.3 mg/L) was confirmed to be lower than the estimated number of moles of ionic liquid (~ 21.4 μmol) present in ~ 20 mg of the s-IPN/St1.0 hydrogel (as calculated from data given in Table 2.1).

As can be seen in Figure 2.8A, when no electrical potential is applied, the amino acid sorption capacity of the hydrogels, poly(HEMA-co-BVImCl), and s-IPN/St0.5 was similar (*p*-value > 0.05) to that of poly(HEMA) while the sorption capacity of s-IPN/St1.0 is almost twice the value that of the other hydrogels. This indicates that, under these experimental conditions (25 ºC and 0 V), the Try sorption capacity of poly(HEMA-co-BVImCl) and s-IPN/St0.5 is mainly governed by amino acid diffusion into the hydrogel matrix rather than by IL-amino acid electrostatic interactions (since the water sorption capacity was found to be more dependent on hydrogels WSC than on their IL content). The higher passive-sorption capacity observed for s-

IPN/St1.0 may result from the slightly higher IL content in this sample (Table 2.1) which may promote enhanced hydrogel/Try electrostatic interactions, and higher WSC (Figure 2.3), which will improve Try diffusion into the hydrogel matrix.

The effect of an applied voltage on Try sorption capacity is presented in Figure 2.8B and 2.8C, for samples submitted to DC voltages of 2 and 100 V, respectively. Results show that the Try sorption capacity was significantly improved, compared to passive sorption, even at the lowest applied potential. Moreover, it was interesting to notice that at the lowest applied voltage (Figure 2.8B) it is possible to modulate the Try sorption capacity of the hydrogels.

During the electro-assisted sorption experiments of polycationic hydrogels (poly(HEMA-co-BVImCl) and s-IPNs) it was observed that the pH of the employed media decreased to ~ 4.5. This happens because when the electrical stimulus is applied, free chloride anions (from BVImCl) move towards the positively charged electrode (anode), while positively charged imidazolium cations cannot move (to the cathode) since they are covalently attached to the hydrogel network. At the anode, oxidative reactions take place leading to the formation of hydrochloric and hypochlorous acids in aqueous media[84] which justifies the observed decrease in the pH of the amino acid solution. Notice that at a pH of 4.5, the concentration of positively charged amino acid molecules ([NH_3^+–R–COOH]) increases, since this pH is lower than the isoelectric point of L-tryptophan, which is equal to 5.89[85,86] and therefore, electrostatic interactions between Try and the polycationic hydrogels are not favored. Nevertheless, the electro-assisted sorption increased up to 20 % at 2 V and up to 70 % at 100 V, when compared to results obtained from passive sorption (0 V). The average amount of Try absorbed/adsorbed by passive sorption after 10 days was 14.6 ± 6.1 % which is lower than that obtained by electro-assisted sorption at 2 V for s-IPN/St1.0, and for all polycationic hydrogels at 100 V, only after 3 h. When an electrical potential is applied, the concentration of positively charged Try species ([NH_3^+–R–COOH]) increases in the vicinity of the anode, while the concentration of negatively

charged species ([NH_2–R–COO^-]) increases at the cathode as a result of water hydrolysis, which induces the formation of hydronium ions (acidic pH) at the anode and hydroxide ions (alkaline pH) at the cathode. As their concentration increases, protonated species are attracted to the cathode while deprotonated species are attracted to the anode. This migration between electrodes, induced by the applied voltage, promotes interactions between [NH_2–R–COO^-] and the polycationic hydrogel and consequently its adsorption from the medium. Such an effect was more evident at higher applied potential (100 V, Figure 2.8C) because the driving force that enhances charged Try diffusion increases, leading to higher Try sorption capacity (> 65 % compared to poly(HEMA)).[87] Moreover, no significant difference (*p*-value > 0.05) was observed for the sorption capacity of all tested polycationic hydrogels at 100 V suggesting that the total amount of Try absorbed/adsorbed was mainly governed by the amount of cationic functional groups available to establish electrostatic interactions in each hydrogel, which are similar for all samples (Table 2.1).

It is important to refer that, during the experiments performed at 100 V, a brownish foam was formed near both electrodes probably resulting from the hypochlorous acid-mediated oxidation of Try molecules.[88] The amount of Try oxidized in the electrodes was quantified (after careful removal of the foam adhered to the electrodes) leading to ~ 4.4 ± 0.17 % of the initial amount of Try in solution. The side of hydrogel facing the cathode also showed a brown-colored layer; however the bulk solution did not present any evidence of Try oxidation, and as was confirmed by the comparison of the UV spectra of the Try solution before and after the electro-assisted experiment (at 100 V for 3 h) (Figure S2.4, Appendix A). Overall, these findings indicate that it is possible to modulate Try, or even other amino acid, removal from aqueous media by controlling the intensity of the applied DC current. Moreover, and although the electro-sorption experiments carried out at 100 V led to some degree of oxidation of Try, these results indicate potential applications of these cationic hydrogels in processes for which the integrity of the

molecules is not a relevant requisite (e. g. wastewater treatment; (bio)remediation); or for the removal/separation of molecules less sensitive to degradation under electrical potential stimulus.

The effect of the nature of the medium and of pH on the electro-assisted sorption was also evaluated for s-IPN/St1.0 hydrogels, since they presented the highest electro-assisted Try sorption yield in water (Figure 2.8D**)**. The quantification of Try removed/release in bi-distilled water, and in TRIZ and AB buffers, was performed according to previously constructed calibration curves at 25 ºC. The spectra of Try after electro-assisted desorption experiments at 5 V was confirmed by UV spectrophotometry (Figure S2.4, Appendix A). Preliminary electro-assisted sorption experiments were also performed in PBS buffer, however the oxidation of Try was evident even at lower applied voltage.

The Try sorption capacity of the hydrogels immersed in Trizma base buffer, used to avoid pH changes during the experiments, decreased to ~ 11.1 ± 0.02 %. During these experiments, only a slight decrease of pH was observed from 9.9 to 9.3, indicating that Try molecules were mostly negatively charged ([NH_2–R–COO^-]). These results suggest that the hydrogel sorption capacity depends on the electrophoretic flow of Try charged molecules between electrodes. When an electrical potential is applied in the Trizma base buffer medium, a unidirectional migration of negatively charged Try molecules is stablished from the cathode to anode, restraining ionic interactions with the s-IPN/St1.0 hydrogel.

Negligible Try removal (≤ 0.1 %) was observed for hydrogels immersed in acidic and neutral buffer media as shown in Figure 2.8D. At low pH (below the isoelectric point of L-tryptophan), ionic interactions between positively charged Try species and the polycationic hydrogel are not favored. When s-IPN/St1.0 samples were immersed in the neutral phosphate buffer medium, significant gel shrinkage was observed what may have hampered Try diffusion into the hydrogel network and further interactions with the cationic hydrogel. Gel shrinkage was

hypothesized to be due to the divalent phosphate anions (HPO_4^{2-}) present in the buffer that may have worked as ionic cross-linkers of the polycationic hydrogel chains thus decreasing the number of cationic groups that were available to adsorb Try. This behavior was not observed in any of the other tested monovalent-based aqueous solutions. Moreover, when hydrogels previously soaked in the phosphate buffer were immersed in bi-distilled water at room temperature, they remained shrunken confirming the presence of relatively strong ionic cross-linking.

Desorption/release experiments of Try from the hydrogel s-IPN/St1.0 were carried out at low applied voltages (0, 2 and 5 V), to avoid Try oxidation, with samples previously exposed to the same sorption conditions (at 25 ºC and 2 V, for 3 h in bi-distilled water). The results presented in Figure 2.9 show that Try desorption into water under an applied voltage of 2 V is 24 % higher than for passive desorption (0 V). The delivery of charged species from an electrically-responsive hydrogel may depend on three main mechanisms, namely electrically-induced swelling/deswelling (which alters pore sizes leading to different diffusion kinetics), electrically-induced erosion of hydrogel (release of charged species due to network degradation), and electrophoresis (migration of charged molecules through the hydrogel induced by an electrical field).[89] In this work, since no induced swelling/deswelling and/or erosion of the hydrogel s-IPN/St1.0 was observed during electro-assisted experiments, it was assumed that Try desorption/release occurs mainly by electrophoresis, and considering that passive desorption is governed only by Try diffusion from the hydrogel to the medium due to gradient concentrations. A further increase in the applied potential (5 V) led to an increase in the amount of amino acid released to the medium (~ 7.5 %) when compared to results obtained at 2 V. Recent studies on the effect of the applied electrical stimulus on the release of acetyl salicylic acid from a polysaccharide-based hydrogel also showed an increase of ~ 30 % after an increase of the applied electrical stimulus from 0 up to 5 V.[90]

The electro-assisted desorption of L-tryptophan into TRIZ was also carried out at 5 V. Figure 2.9 shows that the release of Try was higher in TRIZ (~ 7.8 %) than in bi-distilled water, during 3 h of measurements at 5 V. This might be explained in terms of the different amounts of amino acid that were previously adsorbed in each sample. It was expected that, for a lower quantity of adsorbed amino acid, a higher desorption percentage would be obtained during 3 h of measurements. However, and due to the fact that the amount of adsorbed amino acid in bi-distilled water and TRIZ differ significantly, it is not possible to perform a direct comparison between the amounts of L-tryptophan desorbed in these two situations. Any evidence of Try degradation was observed as confirmed from the UV spectra of Try molecules after electro-assisted desorption/release experiments at 2 and 5 V (Figure S2.4, Appendix A).

Different IL-based liquid-liquid extraction systems were previously tested for the separation of Try from aqueous media.[91-93] The highest Try removal capacity (96 %) reported in those works was observed when using the water/potassium phosphate/1-butyl-3-methylimidazolium methylsulfonate ABS system, after 24 h of contact.[91] To the best of our knowledge there are no previous studies on the separation/removal of Try from aqueous environments using electro-responsive hydrogels based on ILs. Therefore, this work presents innovative research on the development of IL-based materials for the controlled and selective removal/separation and/or release of biomolecules, depending on the charge of the target molecule, on the chemical composition of the hydrogels, on the medium and on the applied electric stimulus.

2.4.6 Cytocompatibility

The cytocompatibility of the freeze-dried hydrogels was evaluated for Balb/3T3 fibroblasts by cell viability (LDH) and the cell proliferation (MTT) assays (Figure 2.10A and 2.10B). As can be seen in Figure 2.10A, and after 48 h of direct contact, LDH results clearly showed high cell viabilities (~ 100 %) for all hydrogels, meaning that tested samples did not induce cell wall

lysis. It has been reported that the toxicity of ILs depends on many structural variables such as cation/anion alkyl chain length, cation/anion type, presence of specific functional groups but also on external factors such as the nature of cell line tested.[22,94]

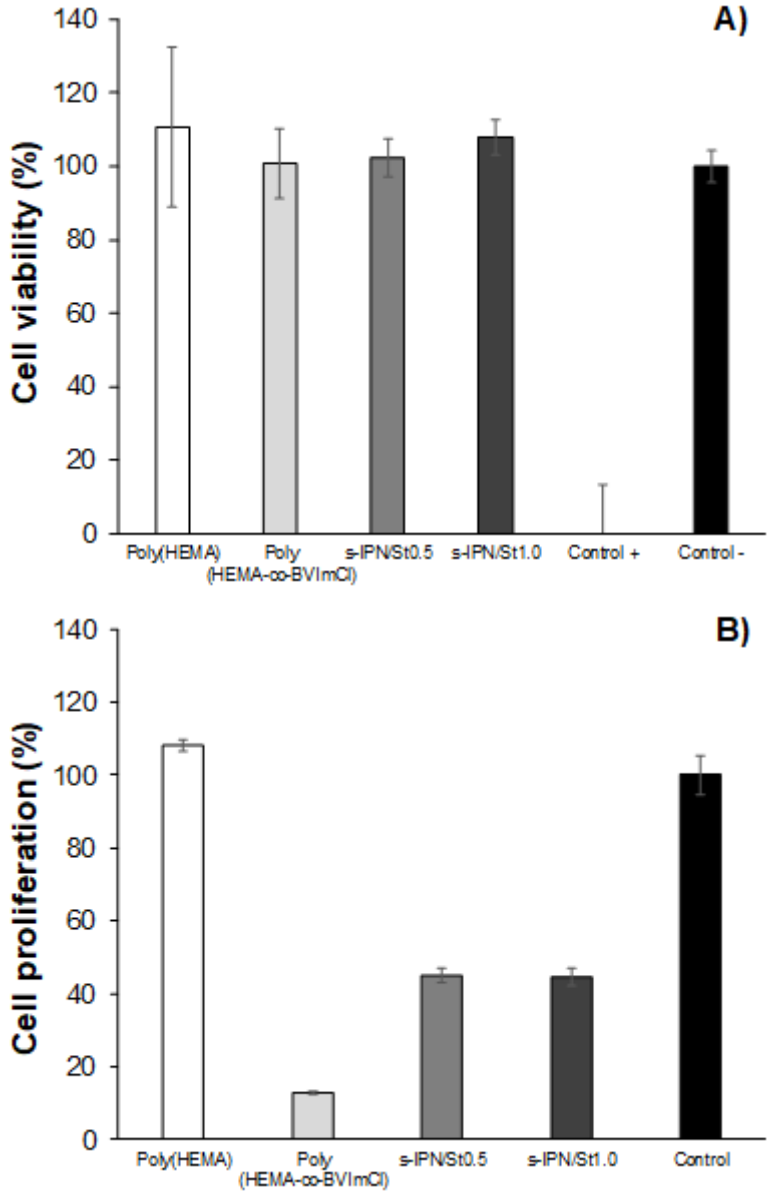

Figure 2.10 *In vitro* cytocompatibility of the prepared hydrogels tested against fibroblasts measured by the cell viability, LDH (A) and the cell proliferation, MTT (B) assays.

For example, ILs bearing short alkyl chain lengths (number of carbons lower than six), and chloride counter ions, tend to be less toxic.[95,96] Moreover, the polymerization of IL-based

monomers is known to further decrease their cytotoxicities.[97] However, and as can be seen in Figure 2.10B, the presence of the IL in the poly(HEMA-co-BVImCl) hydrogel seems to affect fibroblast metabolic activity, mostly if compared with poly(HEMA) (which is well known for its relative good biocompatibility).[98] In a previous study, the cytotoxicity of several imidazolium-based ionic liquids against normal fetal lung fibroblasts by using the MTT assay was also reported. In particular, 1-butyl-3-methylimidazolium salicylate presented high cytotoxicity, even at low concentrations, and when compared to other imidazolium-based ionic liquids containing the same anion but longer alkyl chains.[99] These results seem to indicate that the mechanism by which ILs affect cell metabolic activity, as measured by the MTT assay, does not depend only on the IL alkyl chain. The cationic nature of vinylpyridinium-based PILs has been previously reported as the main responsible for cell growth inhibition (against mouse fibroblasts and hamster ovary cells) due to electrostatic complexation of the polycation with negatively-charged biomolecules present in cell membranes (such as proteins or phospholipids).[100] However the capacity to inhibit cell proliferation, as observed for poly(HEMA-co-BVImCl), is interesting for other applications such as the development of antifouling materials, thus avoiding materials biodegradation and consequent loss of function during usage in aqueous media.

An increase of 30 % in cell proliferation was observed for the prepared s-IPNs, independently of the employed starch composition (p-value > 0.05), when compared to poly(HEMA-co-BVImCl) samples (Figure 2.10B). This result can be explained by the natural biocompatibility of starch[46,47,101] which may have balanced poly(HEMA-co-BVImCl) inherent cytotoxicity. Previous studies on the influence of starch concentration over cell viability of chitosan-starch microparticles (measured by MTS assay against osteoblast cell line Saos-2) showed a significant increase of 20 % in cell viability with starch concentration, which is in agreement with data herein reported.[102] Therefore, and contrary to poly(HEMA-co-BVImCl), s-IPNs have

the potential to be further optimized for the development of biomaterials with improved biocompatibility and biodegradability envisaged for biomedical/pharmaceutical applications such as controlled drug delivery devices and/or scaffolds for tissue engineering.

2.5 Conclusions

This work evidenced the potential of semi-interpenetrating polymer networks (s-IPNs) as an efficient strategy to develop multi stimuli-responsive IL-based cationic hydrogels for the electro-assisted removal/separation/release of charged molecules. The employed strategy makes use of starch, as a biocompatible, biodegradable and low-cost biopolymer obtained from renewable sources, to tune the physicochemical, rheological, electrical and biological properties of IL-based copolymers. Another major feature of this approach is that it uses relatively low IL amounts and originates hydrogels presenting long-term stability and functionality in aqueous media avoiding IL loss/contamination during usage.

The obtained hydrogels were responsive to changes in relative humidity, ionic strength and electrical current. Compared to the copolymer poly(HEMA-co-BVImCl), freeze dried s-IPNs exhibited higher water sorption capacity, ionic/electrical conductivity (5.2 S cm^{-1}), fibroblast proliferation capacity and loss factors which are typical of biological gels and soft tissues. These materials can find applications in electro-membrane extraction processes (e. g. bio-separation processes, wastewater treatment processes, (bio)remediation, etc.). In this work the electro-assisted sorption/release capacity of L-tryptophan from the prepared hydrogels was studied as a proof of concept. Results showed that the sorption/release capacity of this charged molecule can be easily tuned by modifying the intensity of the applied potential, the medium and the chemical composition of the hydrogel. It can be theorized that sorption/desorption of L-tryptophan resulted from a combined mechanism of electrophoretic flow and electrostatic interactions of the L-tryptophan with the cationic hydrogel. Moreover, and considering that the

controlled sorption/release of molecules by/from electro-responsive systems depends on a large number of other variables including duration of the electrical stimulus, intrinsic properties of the electro-responsive material (degree of cross-linking and swelling/de-swelling/shrinking behavior), and relative position of the samples and electrodes it is possible to assume that the systems developed in this work can be further optimized.

2.6 Acknowledgements

This work was financially supported by Fundação para a Ciência e Tecnologia (FCT-MEC) Portugal under contract UID/EQU/00102/2013, and MINECO (SAF2017-83118-R) Spain, Agencia Estatal de Investigación (AEI) Spain, and FEDER. A. M. A. Dias acknowledges FCT-MEC for a contract under the program Investigador FCT IF/00455/2013. A. F. Kanaan acknowledges CNPq, Brazil, for the scholarship with reference 200808/2014-1. Authors also acknowledge Dr. Fernando Augusto Pinto Garcia for providing the electrophoresis power supply EPS 500/400 (Pharmacia Fine Chemicals, Sweden).

2.7 References

(1) Ferreira, N. N.; Ferreira, L. M. B.; Cardoso, V. M. O.; Boni, F. I., Souza, A. L. R., Gremião, M. P. D. Recent advances in smart hydrogels for biomedical applications: From self-assembly to functional properties. *European Polymer Journal* **2018**, 99, 117-133.

(2) Mahinroosta, M.; Farsangi, Z. J.; Allahverdi, A.; Shakoori, Z. Hydrogels as intelligent materials: A brief review of synthesis, properties and applications. *Materials Today Chemistry* **2018**, 8, 42-55.

(3) Ferreira, N. N.; Ferreira, L. M. B.; Cardoso, V. M. O.; Boni, F. I.; Souza, A. L. R.; Gremião, M. P. D. Recent advances in smart hydrogels for biomedical applications: From self-assembly to functional approaches. *European Polymer Journal* **2018**, 99, 117-133.

(4) Li, X.; Su, X. Multifunctional smart hydrogels: potential in tissue engineering and cancer therapy. *Journal of Materials Chemistry B* **2018**, 6, 4714-4730.

(5) Adesanya, K.; Vanderleyden, E.; Embrechts, A.; Glazer, P.; Mendes, E.; Dubruel, P. Properties of electrically responsive hydrogels as a potential dynamic tool for biomedical applications. *Journal of Applied Polymer Science* **2014**, 41195, 1-9.

(6) Pairatwachapun, S.; Paradee, N.; Sirivat, A. Controlled release of acetylsalicylic acid from polythiophene/carrageenan hydrogel via electrical stimulation. *Carbohydrate Polymer* **2016**, 137, 214-221.

(7) Yuk, H.; Lu, B.; Zhao, X. Hydrogel bioelectronics. *Chemical Society Reviews* **2019**, 48, 1642-1667.

(8) Schmidt, D. J.; Moskowitz, J. S.; Hammond, P. T. Electrically Triggered Release of a Small Molecule Drug from a Polyelectrolyte Multilayer Coating. *Chemistry of Materials* **2010**, 22, 6416-6425.

(9) Hoffman, A. S. Hydrogels for biomedical applications. *Advanced Drug Delivery Reviews* **2012**, 64, 18-23.

(10) Caló, E.; Khutoryanskiy, V. V. Biomedical applications of hydrogels: A review of patents and commercial products. *European Polymer Journal* **2015**, 65, 252-267.

(11) Lorenzo, R. A.; Carro, A. M.; Concheiro, A.; Alvarez-Lorenzo, C. Stimuli-responsive materials in analytical separation. *Analytical and Bioanalytical Chemistry* **2015**, 407, 4927-4948.

(12) Szunerits, S.; Teodorescu, F.; Boukherroub, R. Electrochemically triggered release of drugs. *European Polymer Journal* **2016**, 83, 467-477.

(13) Vidinha, P.; Lourenço, N. M. T.; Pinheiro, C.; Brás, A. R.; Carvalho, T.; Santos-Silva, T.; Mukhopadhay, A.; Romão, M. J.; Parola, J.; Dionisio, M.; Cabral, J. M. S.; Afonso, C. A. M.;

Barreiros, S. Ion jelly: a tailor-made conducting material for smart electrochemical devices. *Chemical Communication* **2008**, 5842-5844.

(14) Borisova, O. V.; Billon, L.; Richter, R. P.; Reimhult, E.; Borisov, O. V. pH- and Electro-Responsive Properties of Poly(acrylic acid) and Poly(acrylic acid)-*block*-poly(acrylic acid-*grad*-styrene) Brushes Studied by Quartz Crystal Microbalance with Dissipation Monitoring. *Langmuir* **2015**, 31, 7684-7694.

(15) Dias, A. M. A.; Cortez, A. R.; Barsan, M. M.; Santos, J. B.; Brett, C. M. A.; de Sousa, H. C. Development of Greener Multi-Responsive Chitosan Biomaterials Doped with Biocompatible Ammonium Ionic Liquids. *ACS Sustainable Chemistry & Engineering* **2013**, 1, 1480-1492.

(16) Chen, J.; Gao, L-. x.; Han, X.; Chen, T.; Luo, J.; Liu, K.; Gao, Z.; Zhang, W. Preparation and electro-response of chitosan-*g*-poly(acrylic acid) hydrogel elastomers with interpenetrating network. *Materials Chemistry and Physics* **2016**, 169, 105-112.

(17) Jayaramudu, T.; Ko, H-. U.; Kim, H. C.; Kim, J. W.; Li, Y.; Kim; J. Transparent and semi-interpenetrating network P(vinyl alcohol)- P(Acrylic acid) hydrogels: pH responsive and electroactive application. *International Journal of Smart and Nano Mater*ials **2017**, 8, 80-94.

(18) Li, Y.; Zhang, C.; Zhou, Y.; Dong, Y.; Chen, W. Novel multi-responsive polymer materials: When ionic liquids step in. *European Polymer Journal* **2015**, 69, 441-448.

(19) Mecerreyes, D. Polymeric ionic liquids: Broadening the properties and applications of polyelectrolytes. *Progress in Polymer Science* **2011**, 36, 1629-1648.

(20) Huber, B.; Rossrucker, L.; Sundermeyer, J.; Roling, B. Ion transport properties of ionic liquid-based polyelectrolytes. *Solid State Ionics* **2013**, 247-248, 15-21.

(21) Leones, R.; Sabadini, R. C.; Esperança, J. M. S. S.; Pawlicka, A.; Silva, M. M. Playing with ionic liquids to uncover novel polyelectrolytes. *Solid State Ionics* **2017**, 300; 46-52.

(22) Egorova, K. S.; Gordeev, E. G.; Ananikov, V. P. Biological Activity of Ionic Liquids and Their Application in Pharmaceutics and Medicine. *Chemical Reviews* **2017**, 117, 7132-7189.

(23) Chen, J.; Xie, F.; Li, X.; Chen, L.; Ionic liquids for the preparation of biopolymer materials for drug/gene delivery: a review. *Green Chemistry* **2018**, 20, 4169-4200.

(24) Fatima, J.; Ullah, F.; Zakaria, M. R.; Akil, H. Md. An approach to classification and hi-tech applications of room-temperature ionic liquids (RTILs): A review. *Journal of Molecular Liquids* **2018**, 271, 403-420.

(25) Berthod, A.; Ruiz-Ángel, M. J.; Carda-Broch, S. Recent advances on ionic liquid uses in separation techniques. *Journal of Chromatography A* **2018**, 1559, 2-16.

(26) Liu H.; Yu H. Ionic liquids for electrochemical energy storage devices applications. *Journal of Material Science & Technology* **2019**, 35, 674-686.

(27) Zhao, Q.; Chu, H.; Zhao, B.; Liang, Z.; Zhang, L.; Zhang, Y. Advances of ionic liquids-based methods for protein analysis. *TrAC Trends in Analytical Chemistry* **2018**, 108, 239-246.

(28) Sasikumar, B.; Arthanareeswaran, G.; Ismail, A. F. Recent progress in ionic liquid membranes for gas separation. *Journal of Molecular Liquids* **2018**, 266, 330-341.

(29) Shaplov, A. S.; Marcilla, R.; Mecerreyes, D. Recent Advances in Innovative Polymer Electrolytes based on Poly(ionic liquid)s. *Electrochimica Acta* **2015**, 175, 18-34.

(30) Qian, W.; Texter, J.; Yan, F. Frontiers in poly(ionic liquid)s: syntheses and applications. *Chemical Society Reviews* **2017**, 46, 1124-1159.

(31) Muñoz-Bonilla, A.; Fernández-Gracía, M. Poly(ionic liquid)s as antimicrobial materials. *European Polymer Journal* **2018**, 105, 135-149.

(32) Chen, M.; White, B. T.; Kasprzak C. R.; Long, T. E. Advances in phosphonium-based ionic liquids and poly(ionic liquid)s as conductive materials. *European Polymer Journal* **2018**, 108, 28-37.

(33) Nulwala, H.; Mirjafari, A.; Zhou, X. Ionic liquids and poly(ionic liquid)s for 3D printing - A focused mini-review. *European Polymer Journal* **2018**, 108, 390-398.

(34) Lee, C-. P.; Ho, K-. C. Poly(ionic liquid)s for dye-synthesized solar cells: A mini-review. *European Polymer Journal* **2018**, 108, 420-428.

(35) Delhorbe, V.; Bresser, D.; Mendil-Jakani, H.; Rannou, P.; Bernard, L.; Gutel, T.; Lyonnard, S.; Picard, L. Unveiling the Ion Conduction Mechanism is Imidazolium-Based Poly(ionic liquids): A Comprehensive investigation of the Structure-to-Transport Interplay. *Macromolecules* **2017**, 50, 4309-4321.

(36) Salas-de la Cruz, D.; Green, M. D.; Ye, Y.; Elabd, Y. A.; T. E. Long, T. E.; Winey, K. I. Correlating backbone-to-backbone distance to ionic conductivity in amorphous polymerized ionic liquids. *Journal of Polymer Science, Part B: Polymer Physics* **2012**, 50, 338-346.

(37) Jones, R. G. Definition of terms relating to the structure and processing of sols, gels, networks, and inorganic-organic hybrid materials (IUPAC Recommendations 2007). *Pure and Applied Chem*istry **2007**, 79, 1801-1829.

(38) Lohani, A.; Singh, G.; Bhattacharya, S. S.; Verma, A. Interpenetrating Polymer Networks as Innovative Drug Delivery Systems. *Journal of Drug Delivery* **2014**, 583612, 1-11.

(39) Dragan, E. S. Design and applications of interpenetrating polymer network hydrogels. A review. *Chemical Engineering Journal* **2014**, 243, 572-590.

(40) Becht, G. A.; Sofos, M.; Seifert, S.; Firestone, M. A. Formation of a Liquid-Crystalline Interpenetrating Poly(Ionic liquid) Network Hydrogel. *Macromolecules* **2011**, 44, 1421-1428.

(41) Shaplov, A. S.; Ponkratov, D. O.; Vlasov, P. S.; Lozinskaya, E. I.; Gumileva, L. V.; Surcin, C.; Morcrette, M.; Armand, M.; Aubert, P-. H.; Vidal, F.; Vygodskii, Y. S. Ionic semi-interpenetrating networks as a new approach for highly conductive and stretchable polymer materials. *Journal of Materials Chemistry A* **2015**, 3, 2188-2198.

(42) Juger, J.; Vancaeyzeele, C.; Plesse, C.; Nguyen, G. M. T.; Braz Ribeiro, F.; Teyssié, D.; Vidal, F. Polymeric Ionic liquid based interpenetrating polymer network for all-solid self-standing polyelectrolyte material. *European Polymer Journal* **2018**, 106, 257-265.

(43) Tudor, A.; Florea, L.; Gallagher, S.; Burns, J.; Diamond, D. Poly(Ionic Liquid) Semi-Interpenetrating Network Multi-Responsive Hydrogel. *Sensors* **2016**, 16, 219.

(44) Vilela, C.; Sousa, N.; Pinto, R. J. B.; Silvestre, A. J. D.; Figueiredo, F. M. L.; Freire, C. S. R. Exploiting poly(ionic liquids) and nanocellulose for the development of bio-based anion-exchange membranes. *Biomass Bioenergy* **2017**, 100, 116-125.

(45) Zhang, C.; Zhang, W.; Gao, H.; Bai, Y.; Sun, Y.; Chen, Y. Synthesis and gas transport properties of poly(ionic liquid) based semi-interpenetrating polymer network membranes for CO_2/N_2 separation. *Journal of Membrane Science* **2017**, 528, 72-81.

(46) Elvira, C.; Mano, J. F.; San Román, J.; Reis, R. L. Starch-based biodegradable hydrogels with potential biomedical applications as drug delivery systems. *Biomaterials* **2002**, 23, 1955-1966.

(47) Salgado, A. J.; Coutinho, O. P.; Reis, R. L. Novel starch-based scaffolds for bone tissue engineering: Cytotoxicity, cell culture and protein expression. *Tissue Engineering* **2004**, 10, 465-474.

(48) Li, Y.; Tan, Y.; Xu, K.; Lu, C.; Wang, P. A biodegradable starch hydrogel synthesized via thiol-ene click chemistry. *Polymer Degradation and Stability* **2017**, 137, 75-82.

(49) Dalton, P. D.; Shoichet, M. S. Creating porous tubes by centrifugal forces for soft tissue application. *Biomaterials* **2001**, 22, 2661-2669.

(50) Willems, N.; Yang, H.-y.; Langelaan, M. L. P.; Tellegen, A. R.; Grinwis, G. C. M.; Kranenburg, H.-J. C.; Riemers, F. M.; Plomp, S. G. M.; Craenmehr, E. G. M.; Dhert, W. J. A.; Papen-Botterhuis, N. E.; Meij, B. P.; Creemers, L. B.; Tryfonidou, M. A. Biocompatibility and intradiscal application of a thermoreversible celecoxib-loaded poly-N-isopropylacrylamide

MgFe-layered double hydroxide hydrogel in a canine model. *Arthritis Research & Therapy* **2015**, 17, 1-16.

(51) Sinha, M.; Gupte, T. Design and evaluation of artificial cornea with core-skirt design using polyhydroxyehtyl methacrylate and graphite. *International Ophthalmology* **2018**, 38, 1225-1233.

(52) Hernandez-Martínez, A. R.; Lujan-Montelongo, J. A.; Silva-Cuevas, C.; Mota-Morales, J. D.; Cortez-Valadez, M.; Ruíz-Baltazar, A. J.; Cruz, M.; Herrera-Ordonez, J. Swelling and methylene blue adsorption of poly(*N*,*N*-dimethacrylamide-*co*-2-hydroxyethyl methacrylate) hydrogel. *Reactive and Functional Polymers* **2018**, 122, 75-84.

(53) Salmieri, S.; Khan, R. A.; Safrany, A.; Lacroix, M. Gamma rays-induced 2-hydroxyehtyl methacrylate graft copolymerization on methylcellulose-based films: Structure analysis and physicochemical properties. *Industrial Crops and Products* **2015**, 70, 64-71.

(54) Al-Mohammed, N. N.; Alias, Y.; Abdullah, Z. Bis-imidazolium and benzimidazolium based gemini-type ionic liquid structure: synthesis and antibacterial evaluation. *RSC Advances* **2015**, 5, 92602-92617.

(55) Cavoue, T.; Abassi, H. B.; Vayssade, M.; Nhien, A. N. V.; Kang, I. -K.; Kwon, G. -W.; Porceau, G.; Dubot, P.; Andaloussi, S. A.; Versace, D. -L. Imidazolium-based titanium substrates against bacterial colonization. *Biomaterials Science* **2017**, 5, 561-569.

(56) Kizil, R.; Irudayaraj, J.; Seetharaman, K. Characterization of Irradiated Starches by Using FT-Raman and FTIR Spectroscopy. *Journal of Agricultural and Food Chemistry* **2002**, 50, 3912-3918.

(57) Worzakowska, M. Starch-g-poly(benzyl methacrylate) copolymers. *Journal of Thermal Analysis and Calorimetry* **2016**, 124, 1309-1318.

(58) Talu, M.; Demiroğlu, E. U.; Yurdakul, Ş.; Badoğlu, S. FTIR, Raman and NMR spectroscopy and DTF theoretical studies on poly(N-vinylimidazole). *Spectrochimica Acta Part A: Molecular and Biomolecular Spectroscopy* **2015**, 134, 267-275.

(59) Hsueh, Y-. H.; Liaw, W-. C.; Kuo, J-. M.; Deng, C-. S.; Wu, C-. H. Hydrogel Film-Immobilized *Lactobacillus brevis* RK03 for γ-Aminobutyric Acid Production. *International Journal of Molecular Sciences* **2017**, 18, 2324-2337.

(60) Drozdov A.D.; Christiansen, J. deC. Swelling of pH-sensitive hydrogels. *Physical Review E* **2015**, 91, 022305, 1-15.

(61) Dodoo, S.; Steitz, R.; Laschewsky, A.; von Klitzing, R. Effect of ionic strength and type of ions on the structure of water swollen polyelectrolyte multilayers. *Physical Chemistry Chemical Physics* **2011**, 13, 10318-10325.

(62) Ganguly, S.; Maity, T.; Mondal, S.; Das, P.; Das, N. C. Starch functionalized biodegradable semi-IPN as a pH-tunable controlled release platform for memantine. *International Journal of Biological Macromolecules* **2017**, 95, 185-198.

(63) Kaur, L.; Singha, J.; Liu, Q. Starch - A potential biomaterial for biomedical applications, in: *Nanomaterials and Nanosystems for Biomedical Applications*, Mozafari, M. R. (ed.) Springer, Netherlands, **2007**, 83-98.

(64) Dragan, E. S.; Apopei, D. F. Multiresponsive macroporous semi-IPN composite hydrogels based on native or anionically modified potato starch. *Carbohydrate Polymers* **2013**, 92, 23-32.

(65) Dragan, E. S.; Loghin, D. F. A.; Cocarta, A. -I.; Doroftei, M. Multi-stimuli-responsive semi-IPN cryogels with native and anionic potato starch entrapped in poly (N,N-dimethylaminoethyl methacrylate) matrix and their potential in drug delivery. *Reactive and Functional Polymers* **2016**, 105, 66-77.

(66) Restolho, J.; Mata, J. L.; Colaço, R.; Saramago, B. Moisture Absorption in Ionic Liquid Films. *The Journal of Physical Chemistry C* **2013**, 117, 10454-10463.

(67) Brovchenko, I.; Oleinikova, A. Effect of Pore Size on the Condensation/Evaporation Transition of Confined Water in Equilibrium with Saturated Bulk Water. *The Journal of Physical Chemistry B* **2011**, 115, 9990-10000.

(68) Czepirski, L.; Komorowska-Czepirska, E.; Szymońska, J. Fitting of different models for water vapour sorption on potato starch granules. *Applied Surface Science* **2002**, 196, 150-153.

(69) Worthley, C. H.; Constantopoulos, K. T.; Ginic-Markovic, M.; Pillar, R. J.; Matisons, J. G.; Clarke, S. Surface modification of commercial cellulose acetate membranes using surface-initiated polymerization of 2-hydroxylehtyl methacrylate to improve membrane surface biofouling resistance. *Journal of Membrane Science* **2011**, 385-386, 30-39.

(70) Pineda-Gómez, P.; Angel-Gil, N.; Valencia-Muñoz, C.; Rosales-Rivera, A.; Rodríguez-García, M. E. Thermal degradation of starch sources: Green banana, potato, cassava and corn - kinetic study by non-isothermal procedures. *Starch* **2014**, 66, 691-699.

(71) Khoonsap, S.; Narkkun, T.; Ratphonsan, P.; Klinsrisuk, S.; Amnuaypanich, S. Enhancing the grafting of poly(2-hydroxyehtyl methacrylate) on silica nanoparticles (SiO_2-*g*-PHEMA) by the sequential UV-induced graft polymerization with a multiple-UV irradiation. *Advanced Powder Technology* **2014**, 25, 1304-1310.

(72) Ulu, A.; Koytepe, S.; Ates, B. Synthesis and characterization of biodegradable pHEMA-starch composites for immobilization of L-asparaginse. *Polymer Bulletin* **2016**, 73, 1891-1907.

(73) Karpushkin, E.; Dušková-Smrčková, M.; Šlouf, M.; Dušek, K. Rheology and porosity control of poly(2-hydroxyehtyl methacrylate) hydrogels. *Polymer* **2013**, 54, 661-672.

(74) Meakin, J. R.; Hukins, D. W. L.; Aspden, R. M.; Imrie, C. T. Rheological properties of poly(2-hydroxyethyl methacrylate) (pHEMA) as a function of water content and deformation frequency. *Journal of Material Science: Materials in Medicine* **2003**, 14, 783-787.

(75) Barbucci, R. Hydrogels Biological Properties and Applications, Springer-Verlag Mailand, Italy, **2009**.

(76) Khan, M.; Schuster, S.; Zharnikov, M. Effect of Humidity on Electrical Conductivity of Pristine and Nanoparticle-Loaded Hydrogel Nanomembranes. *The Journal of Physical Chemistry C* **2015**, 119, 14427-14433.

(77) Ye, Y-. S.; Rick, J.; Hwang, B-. J. Ionic liquid polymer electrolytes. *Journal of Materials Chemistry A* **2013**, 1, 2719-2743.

(78) Dias, A. M. A.; Marceneiro, S.; Johansen, H. D.; Barsan, M. M.; Brett, C. M. A.; de Sousa, H. C. Phosphonium ionic liquids as greener electrolytes for poly(vinyl chloride)-based ionic conducting polymers. *RSC Advances* **2016**, 6, 88979-88990.

(79) Cai, J.; Wei, W.; Hu, X.; Wood, D. A. Electrical conductivity models in saturated porous media: A review. *Earth-Science Reviews* **2017**, 171, 419-433.

(80) Kim, O.; Kim, S. Y.; Lee, J.; Park, M. J.; Building Less Tortuous Ion-Conduction Pathways Using Block Copolymers Electrolytes with a Well-Defined Cubic Symmetry. *Chemistry of Materials* **2016**, 28, 318-325.

(81) Eftekhari, A.; Saito, T. Synthesis and properties of polymerized ionic liquids. *European Polymer Journal* **2017**, 90, 245-272.

(82) Soares, B. G. Ionic liquid: A smart approach for developing conducting polymer composites. *Journal of Molecular Liquids* **2018**, 262, 8-18.

(83) Haleem, J. D. Improving therapeutics in anorexia nervosa with tryptophan. *Life Sciences* **2017**, 178, 87-93.

(84) Kishimoto, N.; Katayama, Y.; Kato, M.; Otsu, H. Technical feasibility of UV/electro-chlorine advanced oxidation process and pH response. *Chemical Engineering Journal* **2018**, 334, 2363-2372.

(85) Yang, X.; Bing, T.; Mei, H.; Fang, C.; Cao, Z.; Shangguan, D. Characterization and application of a DNA aptamer binding to L-tryptophan. *Analyst* **2011**, 136, 577-585.

(86) Xie, Y.; Jing, K. -J.; Lu, Y. Kinetics, equilibrium and thermodynamic studies of L-tryptophan adsorption using a cation exchange resin. *Chemical Engineering Journal* **2011**, 171, 1227-1233.

(87) Pérez-Martínez, C. J.; Chávez, S. D. M.; Castillo-Castro, T.; Ceniceros, T. E. L.; Castillo-Ortega, M. M.; Rodríguez-Félix, D. E.; Ruiz, J. C. G. Electroconductive nanocomposite hydrogel for pulsatile drug release. *Reactive and Functional Polymers* **2016**, 100, 12-17.

(88) Kerkaert, B.; Mestdagh, F.; Cucu, T.; Aedo, P. R.; Ling, S. Y.; De Meulenaer, B. Hypochlorous and peracetic acid induced oxidation of dairy proteins. *Journal of Agricultural and Food Chemistry* **2011**, 59, 907-914.

(89) Palza, H.; Zapata, P. A.; Angulo-Pineda, C. Electroactive Smart Polymers for Biomedical Applications. *Materials* **2019**, 12, 277.

(90) Pairatwachapun, S.; Paradee, N.; Sirivat, A. Controlled release of acetylsalicylic acid from polythiophene/carrageenan hydrogel via electrical stimulation. *Carbohydrate Polymers* **2016**, 137, 214-221.

(91) Patinha, D. J. S.; Alves, F.; Rebelo, L. P. N.; Marrucho, I. M. Ionic liquid aqueous biphasic systems: Effect of the alkyl chains in the cation versus the anion. *The Journal of Chemical Thermodynamics* **2013**, 65, 106-112.

(92) Tomé, L. I. N.; Catambas, V. R.; Teles, A. R. R.; Freire, M. G.; Marrucho, I. M.; Coutinho, J. A. P. Tryptophan extraction using hydrophobic ionic liquids. *Separation and Purification Technology* **2010**, 72, 167-173.

(93) Capela, E. V.; Quental, M. V.; Domingues, P.; Coutinho, J. A. P.; Freire, M. G. Effective separation of aromatic and aliphatic amino acid mixtures using ionic-liquid-based aqueous biphasic systems. *Green Chemistry* **2017**, 19, 1850-1854.

(94) Amde, M.; Liu, J.-F.; Pang, L. Environmental Application, Fate, Effects, and Concerns of Ionic Liquids: A Review. *Environmental Science & Technology* **2015**, 49, 12611-12627.

(95) Xia, Y.; Liu, D.; Dong, Y.; Chen, J.; Liu, H. Effect of ionic liquids with different cations and anions on photosystem and cell structure of *Scenedesmus obliquus*. *Chemosphere* **2018**, 195, 437-447.

(96) Liu, H.; Zhang, X.; Chen, C.; Du, S.; Dong, Y. Effects of imidazolium chloride ionic liquids and their toxicity to *Scenedesmus obliquus*. *Ecotoxicology Environmental Safety* **2015**, 122, 83-90.

(97) Bacon, L. S.; Ross, R. J.; Daugulis, A. J.; Parent, J. S. Imidazolium-based polyionic liquid absorbents for bioproduct recovery. *Green Chemistry* **2017**, 19, 5203-5213.

(98) Filipović, V. V.; Nedeljković, B. Đ. B.; Vukomanović, M.; Tomić, S. Lj. Biocompatible and degradable scaffolds based on 2-hydroxyehtyl methacrylate, gelatin and poly(beta amino ester) crosslinkers. *Polymer Testing* **2018**, 68, 270-278.

(99) Vraneš, M.; Tot, A.; Javonović-Šanta, S.; Karaman, M.; Dožić, S.; Tešanović, K.; Kojić, V.; Gadžurić, S. Toxicity reduction of imidazolium-based ionic liquids by the oxygenation of the alkyl substituent. *RSC Advances* **2016**, 6, 96289-96295.

(100) Täuber, K.; Lepenies, B.; Yuan, J. Polyvinylpyridinium-type gradient porous membranes: synthesis, actuation and intrinsic cell growth inhibition. *Polymer Chemistry* **2015**, 6, 4855-4858.

(101) Marques, A. P.; Pirraco, R. P.; Reis, R. L. Biocompatibility of starch-based polymers, in: Natural-Based Polymers for Biomedical Applications. Reis, R. L.; Neves, N. M.; Mano, J. F.; Gomes, M. E.; Marques, A. P.; Azevedo, H. S. (eds.) Woodhead Publishing Series in Biomaterials, **2008**, 738-760.

(102) Balmayor, E. R.; Baran, T. E.; Unger, M.; Marques, A. P.; Azevedo, H. S.; Reis, R. L. Presence of starch enhances *in vitro* biodegradation and biocompatibility of a gentamicin

delivery formulation. *Journal of Biomedical Materials Research, Part B: Applied Biomaterials* **2015**, 103, 1610-1620.

Chapter 3

Effect of mold assemblies-induced interfaces in the mechanical actuation of electro-responsive ionic liquid-based polycationic hydrogels

This chapter comprises the work published in Applied Materials Today (2020) by

Akel F. Kanaan, Ana P. Piedade, Hermínio C. de Sousa, Ana M. A. Dias

3.1 Abstract

This work aims the development of electro-active polycationic soft-actuators based on copolymers of 2-hydroxyethyl methacrylate (HEMA) and 1-butyl-3-vinylimidazolium chloride (BVImCl), cross-linked with *N,N'*-methylene bis(acrylamide), and reinforced with mesoporous silica nanoparticles. Polycationic hydrogels were obtained by free radical polymerization in aqueous solution and using mold assemblies presenting different surface properties (e.g. Teflon® and glass). Obtained results demonstrated that a mold assembly-induced effect, at the mold/polymerization solution interface, originates "surface-to-bulk" heterogeneous copolymer concentration gradients when using Teflon®-Teflon® and Teflon®-glass mold assemblies, while homogeneous hydrogel networks were obtained when using only glass mold assemblies. Results were compared with those obtained from cross-linked poly(2-hydroxyethyl methacrylate) hydrogels to prove that the observed surface-induced polymerization effect occurs only in the presence of the ionic liquid co-monomer. Hydrogels synthesized in Teflon®-Teflon® molds presented the highest mechanical response under external electric stimulus and in different aqueous media of different pH and ionic strength. On the contrary, hydrogels synthesized in glass-glass mold assemblies presented limited

mechanical actuation and only when immersed in saline aqueous media. The mechanical actuation of hydrogels synthesized in Teflon®-glass molds was shown to depend on the orientation of the applied electric current. The electro-actuation response of the synthesized electro-active polycationic hydrogels was discussed based on the ion enrichment/depletion mechanism. All prepared cationic hydrogels were also able to generate small electrical currents. Overall, these results show that mold assemblies presenting different surface properties can be employed to tune the electro-actuation responsiveness of ionic liquid-based soft actuators and lead to the development of engineering devices with a broad range of applications, including artificial muscles and tissue engineering scaffolds.

Keywords: surface-induced heterogeneous copolymer concentration gradients; stimuli-responsive polymers; polycationic hydrogels; ionic liquid-based copolymers; electromechanical actuation.

3.2 Introduction

Soft actuators are materials able to convert external stimulus (e.g. magnetic field, pH, electrical current, ionic strength, temperature, etc.) into a mechanical perturbation. They have been explored as platforms for the development of distinct materials, biomaterials and devices for diverse applications including artificial muscles and scaffolds for cell growth and differentiation.[1-3]

Electroactive polymers (EAP) are materials that respond mechanically under electrical stimulus by bending, swelling or shrinking.[4] This class of "smart" materials can be classified as dielectric or ionic EAPs, depending on their actuation mechanisms.[5] The actuating mechanism of the former is driven by Coulomb interactions between two compliant electrodes placed in both sides of a polymer (often elastomers such as silicones and polyurethanes). Under

application of high voltages (> 1 kV), the polymer squeezes, due to attractive electrostatic interactions that take place between the electrodes, which results in material deformation.[4,6,7] Despite this class of responsive materials can operate in dry conditions, the demand of high electric fields to induce actuation hampers their broad usage for many applications (including biomedical).[7,8] On the contrary, the actuation mechanism of ionic EAPs typically involves the diffusion of ions through swollen polymer matrices and from/to the electrodes under low electrical voltage (e.g. < 5 V) and in open-air conditions.[4] Nevertheless, the electro-actuation responses of ionic EAPs in aqueous environments having low ionic strengths require the application of high electrical current intensities to induce effective mechanical actuation.[9]

Ionic polymers such as methacrylic acid modified Pluronic (P127)[10,11], acrylic acid-acrylamide copolymer[12,13], Nafion®[14], Flemion®[15], carboxylate functionalized polyacrylamide[9] and chitosan[16] have been employed for the development of electro-active ionic actuators. More recently, ionic liquids (ILs) are being proposed as interesting electrolytes for the development of ionic EAP mainly due to their electrochemical properties, chemical stability, and negligible vapor pressure.[17] In this framework, different ILs have been employed as electrolytes immobilized within hydrogel matrices for the development of ionogels.[17-23] However, and depending on the envisaged final application, polyelectrolytes obtained from polymerizable ILs, also known as poly(ionic liquids) (PILs), may have some advantages over ionogels as they prevent electrolyte leaching during usage (e.g. in aqueous media) which, consequently, enhances the long term activity and performance of the IL-based ionic actuators.[24] Moreover, PILs do not require the use of additional ionic dopants/additives, since the counter-ion of the polymerizable IL (cation or anion) is free to diffuse under electrical stimulus. The performance of PIL-based ionic EAPs depends on several variables including: the chemical structure of the employed IL cation/anion, amount of employed IL, IL distribution through the polymer network, presence of spacers (other monomers than polymerizable ILs), 3D structure of the

formed PIL network, and also on the external conditions, namely the employed actuation media/set-up (air/solution, temperature, relative humidity, presence/concentration /type of salts, etc.).[19,20,22,24-30]

The procedures employed for the synthesis/processing of PIL-based EAPs may also have a major influence on the materials' properties, although they are often neglected in the literature. In particular, the relative hydrophilicities/hydrophobicities of employed monomers, co-monomers, cross-linkers, and vessels/recipients/mold materials employed during polymerization reactions may have a major influence on the final chemical and physical properties of the synthesized polymer networks. Previous studies on the free radical solution polymerization in aqueous media of several hydrophilic vinyl monomers in Teflon® mold assemblies reported the formation of a mold assembly-induced interface that originates hydrogel networks presenting surface-to-bulk gradient concentrations. This polymer concentration heterogeneity affects the overall and final network structure after polymerization, mainly in terms of polymer density and polymer free-volume, which ultimately affect the physicochemical and biological properties of the synthetized hydrogels.[31-37]

The main motivation for this work was to explore this already reported surface-induced phenomenon, which leads to surface-to-bulk polymer concentration heterogeneity, as an extra variable to better control and tune the electromechanical responsiveness of IL-based polycationic hydrogels under electrical stimulus. For that purpose, copolymers of 2-hydroxyethyl methacrylate (HEMA) and 1-butyl-3-vinylimidazolium chloride (BVImCl), poly(HEMA-co-BVImCl) copolymers, cross-linked with *N,N'*-methylenebis(acrylamide) (MBA), and reinforced with mesoporous silica nanoparticles (MCM-41) were synthesized by free radical polymerization in aqueous media. Polymerization reactions were carried out in different mold assemblies, namely Teflon®-Teflon®, Teflon®-glass and glass-glass.

Synthesized hydrogels were characterized for their physicochemical, surface and mechanical properties; for their mechanical responsiveness in different aqueous media; and for their electro-active capacity under different electric stimulus (0, 50, 100 and 200 V) and when immersed in different aqueous media of different pHs (5.0, 6.0 and 9.0) and ionic strengths (~ 0 and 10 mM).

3.3 Materials and Methods

3.3.1 Materials

Ammonium persulfate (APS, 99 %), 2-hydroxyethyl methacrylate (HEMA, 99 %), N,N'-methylenebis(acrylamide) (MBA, 99 %) and MCM-41 mesoporous silica nanoparticles (hexagonal; pore volume: 0.98 cm^3/g; pore sizes: 2.3-2.7 nm; surface area: 1000 m^2/g; bulk density: 0.34 g/cm^3), phosphate buffered saline (PBS) and sodium chloride (NaCl) were obtained from Sigma-Aldrich. The ionic liquid 1-butyl-3-vinylimidazolium chloride (BVImCl, 95 %) was obtained from Io-Li-Tec, Germany. Hydrochloric acid (HCl, 37 % w/w) and sodium hydroxide (NaOH) were obtained from Panreac Quimica SA and AkzoNobel, respectively.

3.3.2 Preparation of poly(HEMA-co-BVImCl) hydrogels reinforced with mesoporous silica nanoparticles

Cross-linked poly(HEMA-co-BVImCl) cationic copolymers, reinforced with mesoporous silica nanoparticles (MCM-41), were obtained by free radical polymerization in aqueous solution following a procedure previously described in the literature[38] with some modifications: 1.12 mL of HEMA (9.27 mmol), 0.57 g of BVImCl (3.10 mmol), 9.50 mg of MBA (as cross-linker, 0.5 % on a molar basis, relatively to the total number of moles of monomers in solution) and 8.00 mg of MCM-41 silica nanoparticles (0.4 % w/w, relatively to the total weight of monomers in solution) were mixed in a flask containing 6.44 mL of

deionized water and stirred (at 1500 rpm) overnight. The mixture was then sonicated (5 min) to remove dissolved oxygen and nitrogen, and after the addition of 5.64 mg of APS (0.2 % on a molar basis, relatively to the total number of moles of co-monomers in solution), was further stirred (at 1500 rpm) for 1 h. The final solution was transferred into different mold-assemblies (assembled square plaques separated by 1 mm using a silicone spacer) made with Teflon® and/or glass square plaques presenting distinct surface properties (Figure S3.1, Appendix B). Mold assemblies containing the polymerization solution were then placed in an oven at 50 ºC (for 8 h) and then at 70 ºC (for 24 h) to guarantee complete polymerization. The obtained cationic cross-linked hydrogels were washed in 2 L of deionized water which was replaced three times a day, for 2 days, to remove unreacted monomers and initiator. The complete leaching of unreacted substances was confirmed by UV-spectroscopy, using a spectrophotometer Jasco, model V530, Japan. After complete washing, samples were maintained immersed in deionized water at room temperature (~ 22 ºC). Samples were coded according to the materials used to prepare the mold assemblies where the polymerization took place: molds prepared using the same material (Teflon® and glass) on both sides of the mold assembly were coded as (T-T) and (G-G) samples, respectively while mold assemblies prepared using a combination of those materials were coded as (T-G) samples.

Cross-linked poly(2-hydroxyethyl methacrylate) hydrogels (poly(HEMA)) were also prepared for comparison purposes, following the same procedure and the same monomer/cross-linker/initiator/MCM-41 molar ratios (12.36 mmol of HEMA, corresponding to the total number of moles of HEMA and BVImCl comonomers; 9.50 mg of MBA; 5.64 mg of APS; 8.00 mg of MCM-41 silica nanoparticles and 6.44 mL of deionized water). Cross-linked poly(HEMA) samples were coded as T-T* and G-G* according to the mold assemblies employed for their synthesis (Teflon®-Teflon® and glass-glass, respectively).

3.3.3 Characterization of the prepared cationic hydrogels

3.3.3.1 Physicochemical characterization

Elemental analysis was carried out using an elemental analyzer (Fissons Instruments, model EA1108 CHNS-O) to determine the real BVImCl/HEMA ratio of all the prepared hydrogels (T-T, G-G, T-G T-T* and G-G*) after synthesis and washing procedures. Analyses were performed in triplicate.

The wettability of the surfaces of water swollen cationic hydrogels (T-T, G-G, T-G, T-T* and G-G*) was determined by water contact angle (WCA) measurements using an OCA20 contact angle apparatus (Dataphysics Instruments GmbH, Germany) and the sessile drop method (10 μL) at room temperature (~ 22 ºC). Measurements were performed in triplicate and the results were fitted using the Laplace-Young model.

Surface zeta potential measurements were performed to determine the surface charge of the water swollen cationic hydrogels using an electrokinetic analyzer for solid surfaces (SurPASS from Anton Paar, GmbH). Experiments were carried out using the adjustable gap cell, for G-G, T-T* and G-G* samples, and the cylindrical cell, for T-T samples. For the adjustable gap measurements, the gap height between samples was adjusted to 100 μm. Measurements were performed using a KCl solution ([1.0 mM] and pH = 7.4) at room temperature (~ 22 ºC). All experiments were performed in duplicate (8 measurements in each evaluation) under pressure flow of 200 mbar.

Energy dispersive X-ray spectroscopy analysis was performed using a scanning electron microscope (Jeol, model JSM-530, Japan) coupled with energy dispersive X-ray spectroscopy analysis (Phillips, EDX Genesis, model XL 30). SEM-EDX experiments were carried out in order to analyze the distribution of BVImCl (by elemental mapping of nitrogen and chlorine) on each surface side of oven-dried (50 ºC for 24 h) hydrogels, synthesized in different mold

assemblies (T-T, G-G and T-G). Micrographs were obtained at 5 kV for gold-sputtered samples (300 Å) under argon atmosphere.

3.3.3.2 Rheological measurements

The rheological properties of the prepared cationic hydrogels were measured at 25 ºC in oscillatory stress mode at a constant frequency (1 Hz) and stress sweeps between 0.1-200 Pa. Experiments were performed in a temperature-controlled rheometer (ModelRS1, Haake, Vreden, Germany) with a cylindrical sensor system (Z34 DIN) connected to a temperature-controlled recirculation bath (Haake Phoenix II). Hydrogels (T-T, G-G and T-G) were previously swollen in deionized water, and then cut in circular discs (2 cm diameter) and placed between the rotatory plates separated by a fixed gap of 1.0 mm. Measurements were performed, at least, in duplicate.

3.3.3.3 Water swelling capacity and mechanical deformation at different aqueous media

The water swelling capacity (WSC) of the prepared cationic hydrogels (T-T, G-G, and T-G) was measured at room temperature (~ 22 ºC), by the sequential immersion in deionized water and in PBS (ionic strengths of ~ 0 and 0.17 M, respectively). Water swollen samples (at sorption equilibrium) were weighed (after removing the excess of water from the surface of the hydrogels); immersed in PBS (15 mL) and weighed again after 24 h (again removing the excess of water from the surface of the hydrogels); and then immersed again in deionized water (15 mL) and re-weighed after 24 h. This process was initially repeated over 5 days and later once a week by immersing the samples in fresh solutions. The WSC of the hydrogels was calculated as the ratio between the weight of water absorbed at time t and the initial weight of the dried hydrogel (obtained after oven-drying the samples at 50 ºC for 24 h). Measurements were performed in duplicate and the results are presented in terms of $g_{water}/g_{dried\ hydrogel}$.

3.3.3.4 Mechanical actuation of the hydrogels under electrical stimulus

Electro-actuation measurements were performed using a flatbed electrophoresis unit MULTI (Carl Roth, Deutschland) at room temperature (~ 22 ºC). The unit is comprised by a horizontal chamber with adjustable anode and cathode platinum electrodes placed over a movable frame. The distance between the electrodes was set to 5 cm. The chamber was filled with a fixed volume (400 mL) of each aqueous medium, namely: deionized water, NaCl aqueous solution (NaCl, [10.2 mM], pH ≈ 6.0, I = 10 mM), acidic solution (HCl, [0.01 mM], pH = 5.0, I = 0.01 mM) and alkaline solution (NaOH, [0.01 mM], pH = 9.0, I = 0.01 mM). The final pH of each solution was measured using a pH meter (Standard pH Meter, Meter Lab). Hydrogels (T-T, G-G and T-G) previously swollen in each media were cut in a rectangular shape (0.5 × 4.0 cm), supported by two glass spheres positioned in the middle of each sample, and placed midway between the electrodes. Electro-actuation experiments were performed at different voltages (50, 100 and 200 V) using an electrophoresis power supply EPS 500/400 (Pharmacia Fine Chemicals, Sweden). The mechanical response (bending) of the electrically stimulated samples was recorded using a digital camera and quantified by measuring the arctangent of the bending angle (θ^{o}) of the hydrogels (measured using a millimeter paper grid placed under the chamber). Electro-actuation experiments were performed in duplicate.

3.3.3.5 Preliminary electronic conductivity experiments

The electronic conductivity of the prepared hydrogels (T-T, G-G, T-G, T-T* and G-G*) was assessed by mediating electron transfer onto a LED under a DC current of 1 V (supplied by an electrophoresis power supply EPS 500/400 from Pharmacia Fine Chemicals, Sweden). Two separated squared samples (~ 1 × 1 cm) of water swollen hydrogels (in sorption equilibrium) were employed to close the electrical circuit comprising a LED and the electrophoresis power supply. One sample was placed in direct contact with the cathodes of the LED and of the

electrophoresis power supply while the other was placed in direct contact with the anodes of the LED and of the electrophoresis power supply allowing the electrical current to flow through the hydrogels towards the LED. Experiments were carried in duplicate at room temperature (~ 22 ºC).

3.3.3.6 Statistical analysis

Experimental data was analyzed by the one-way ANOVA test and statistical significance was considered for *p*-values < 0.05.

3.4 Results and discussion

Previous studies demonstrated that the surface properties of hydrogels comprised by different hydrophilic monomers/co-monomers such as acrylic acid, acrylamide and *N,N'*-dimethyl acrylamide are strongly dependent on the nature of the materials that are employed as substrates on which those hydrogels are synthetized.[31-37] The presence of residual trapped oxygen (from air) near hydrophobic mold plaque materials (e.g. Teflon®) and/or the affinity of the hydrophilic monomer solution towards the mold plaque material were reported as the variables that mostly contribute to the formation of "surface-to-bulk" heterogeneous hydrogel networks.[31,32] According to these studies, the free radical polymerization in aqueous media is slowed/hampered near hydrophobic surfaces, when compared to the bulk, due to monomer/co-monomer/initiator concentration gradients between surface and the bulk. This results in the formation of heterogeneous polymer concentration distributions, having a less cross-linked and/or entangled network at the surface of the hydrogel that was in contact with highly hydrophobic mold plaque materials, and a denser network (having a high cross-linked/entangled copolymer concentration) at the bulk of the hydrogel.[31,33,34]

In the present work, and based on this knowledge, we took advantage of the distinct surface properties of Teflon® and/or glass to prepare IL-based cationic hydrogels having distinct surface properties, depending on the nature of the materials that were employed for their synthesis. Moreover, and for the first time, we reported the effect of the obtained "surface-to-bulk" heterogeneous networks on the electromechanical actuation capacity of the obtained polycationic hydrogels.

3.4.1 Effect of mold assemblies on the physicochemical properties of IL-based cationic hydrogels

In what follows, we evaluated if the employed mold plaque assemblies (Teflon®-Teflon®, Teflon®-glass, glass-glass) were able to induce the formation of "surface-to-bulk" hydrogel concentration gradients on the HEMA/BVImCl/MBA system studied in this work. As previously discussed, and as a pre-requisite for this effect to occur[31,33,34], the co-monomers in solution should have different affinities for the materials employed as mold assemblies. In the present work, this pre-requisite was satisfied since the contact angles of aqueous solutions of HEMA/BVImCl/MBA monomers (at the same molar composition that was used for the polymerization reactions) on Teflon® and glass were ~ 71 º and ~ 27 º, respectively meaning that the co-monomer solution has higher affinity (wettability) for the later (Figure S3.1, Appendix B).

Evident morphological differences were observed for hydrogels synthesized in Teflon® and/or glass mold assemblies when immersed in deionized water (Figure 3.1). As can be observed, hydrogels synthesized in Teflon® mold assemblies (T-T) present a whitish layer in the bulk and soft transparent surface layers (~ 1.5 mm thickness), characteristic of low cross-linked hydrogels. On the contrary, hydrogels synthesized in glass mold assemblies (G-G) present a whitish and homogeneous cross-section. Hydrogels synthesized in T-G mold assemblies

present two distinct surfaces, namely a transparent soft and jelly layer (~ 1.0 mm thickness), at the surface in contact with the Teflon®, and a whitish smooth and denser surface, at the surface in contact with glass. These surfaces are similar (at a macroscopic level) to those observed for hydrogels synthesized in T-T and G-G mold assemblies, respectively. Therefore, they are in accordance with the hypothesis that by employing different mold plaque materials it is possible to induce the formation of heterogeneous hydrogel networks having gradient surface-to-bulk HEMA-IL copolymer concentrations. Finally, it is interesting to notice that poly(HEMA) hydrogels present homogeneous macroscopic aspect, independently of the mold plaque material employed for its synthesis. This result means that the above referred mold plaque material induced effect is very much dependent on the nature of the co-monomers employed to synthesize the hydrogels. Moreover, this observation makes clear that the physicochemical properties of the BVImCl monomer have a major contribution to potentiate the mold plaque material effect.

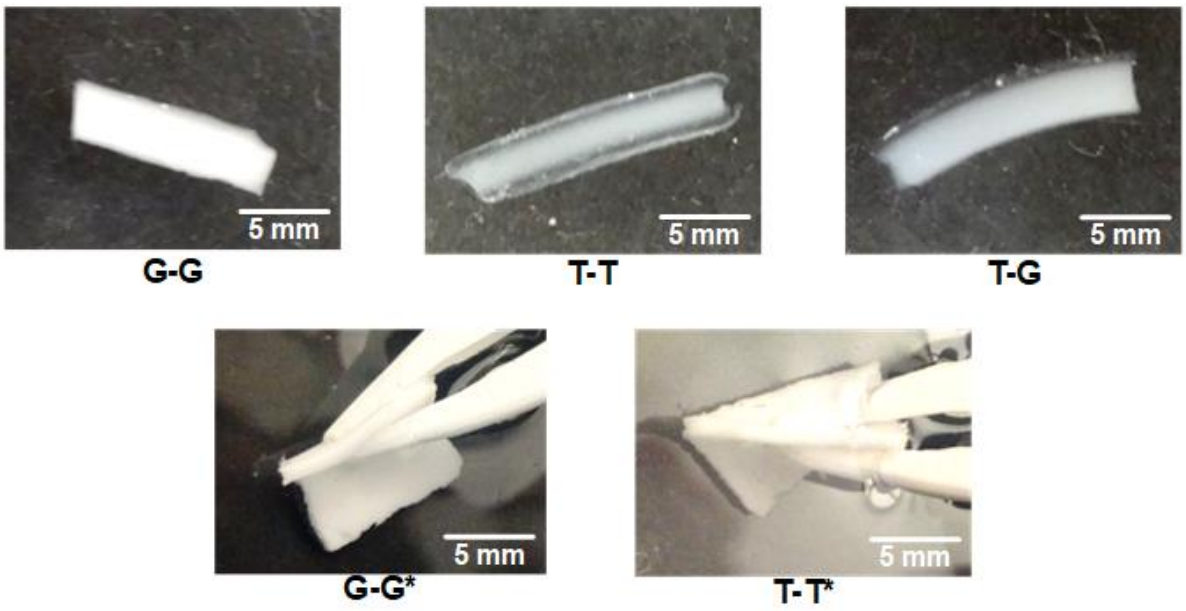

Figure 3.1 Macroscopic differences observed for poly(HEMA-co-BVImCl) hydrogels synthesized in different mold assemblies (T-T, G-G and T-G) and for poly(HEMA), used as control, synthesized in glass and Teflon® mold plaques (G-G* and T-T*, respectively).

The relative composition/distribution of the IL monomer, BVImCl, through the hydrogel networks was evaluated by energy dispersive X-ray spectroscopy, elemental analysis, surface zeta potential and water contact angle analysis. Elemental mapping analysis shows a homogeneous distribution of the IL monomer (homogeneous distribution of nitrogen and chlorine atoms) and of silica nanoparticles (homogeneous distribution of silicon atoms) on the surfaces of all hydrogels prepared in different mold assemblies (Figure S3.2, Appendix B). As can be seen in Table S3.1 (Appendix B), the final amount of IL quantified for hydrogel samples synthesized in different mold assemblies follows the sequence T-T < G-G < T-G. This result shows that the hydrogels synthesized in Teflon® molds (T-T) present a lower IL content per weight of sample (and consequently, lower charge density) than hydrogels synthesized in G-G and T-G mold assemblies. This result also indicates that the free radical polymerization of cross-linked HEMA/BVImCl co-monomers may have been hampered/slowed when using Teflon® mold assemblies, leading to the formation of a less cross-linked and/or entangled network at the hydrogel's surfaces, as previously reported in the literature. At this point we are not able to explain why samples synthetized in G-G mold assemblies do not present the highest amount of $IL/g_{dry\ hydrogel}$, as would be expected, based on our previous discussion.

Surface zeta potential values measured for water swollen poly(HEMA-co-BVImCl) samples were +23.6 ± 2.4 mV and +69.6 ± 5.5 mV for hydrogels synthetized in T-T and G-G mold assemblies, respectively. As a comparison, surface zeta potential values measured for poly(HEMA) presented negative values of -40.1 ± 4.9 mV and -92.7 ± 14.5 mV for T-T* and G-G*, respectively due to the presence of hydroxyl groups, from HEMA and, eventually, also from silanol groups, from silica MCM-41 nanoparticles. The positive charges measured for poly(HEMA-co-BVImCl) clearly confirm the presence of BVImCl in the copolymer structure. The lower value measured for copolymers synthetized in T-T mold assemblies reflects the lower IL content (lower charge density) of these samples in agreement with elemental analysis

data, as discussed above. It is interesting to mention that the charge density of poly(HEMA) synthetized in T-T* mold assemblies is lower than in G-G* ones, what indicates that the free radical polymerization of the homopolymer is also is also affected by Teflon® mold plaques.

The wettability of water swollen hydrogel surfaces was assessed by water contact angle (WCA) measurements. As can be seen in Table S3.1 (Apendix B), lower WCA (at least ~ 3 × lower), and consequently higher wettability, was observed for hydrogel surfaces that were in contact with Teflon® mold plaques, if compared to those that were in contact with glass. This result again confirms the looser/less-crosslinked network of copolymers formed near Teflon® mold plaques which originates highly hydrated (Figure 3.1), and consequently, more hydrophilic surfaces. On the contrary, the denser network of copolymers formed near glass mold plaques is less hydrated, having a more hydrophobic nature. This happens most probably due to the self-molecular organization of the hydrophobic moieties of HEMA (the methyl group) and BVImCl (the butyl chain of the imidazolium cation) at the air/liquid interface towards air, during WCA measurements.[39,40] The WCA of poly(HEMA) hydrogels synthesized in Teflon® (T-T*, 10.1 ± 0.1 º) and glass (G-G*, 9.1 ± 0.6 º) mold plaques were statistically similar (*p*-value > 0.05). This result confirms the important contribution of the co-monomer BVImCl to the mold plaques induced effect over the free radical polymerization of the copolymer poly(HEMA-co-BVImCl). This contribution may result from a lower reactivity of the co-monomer BVImCl, which may be particularly affected by the presence of residual entrapped oxygen from air near Teflon® mold plaques; and/or from its higher affinity for the glass mold plaque, due to its intrinsic hydrophilic nature, which favors its diffusion/concentration towards/near the more hydrophilic mold. Both hypotheses favor the existence of copolymer concentration gradients, depending on the mold plaque assemblies employed, which are responsible for the different surface properties observed for the synthetized IL-based cationic hydrogels.

The presence of a looser vs denser hydrogel network structure formed near Teflon® and glass mold plaques, respectively was also supported by rheological data measured for the synthetized hydrogels (Figure 3.2).

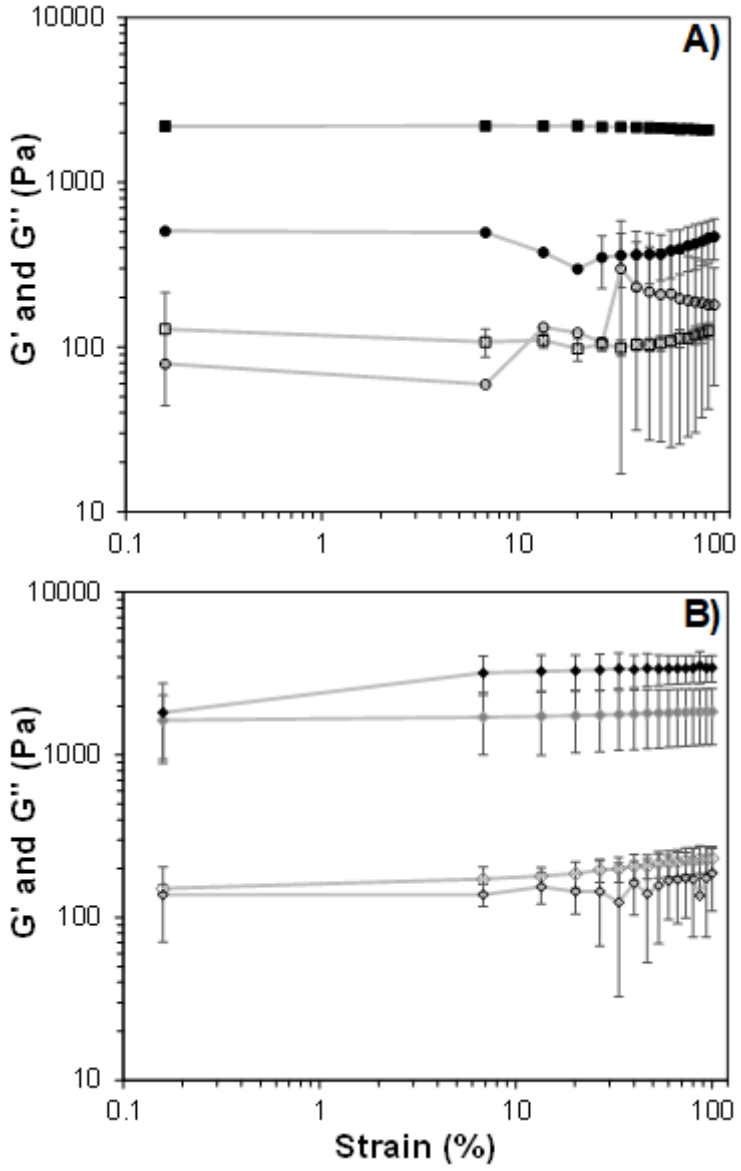

Figure 3.2 Rheological properties of poly(HEMA-co-BVImCl) hydrogels as a function of oscillatory strain sweeps (at 1 Hz) measured at 25 ºC. Storage modulus (G') and loss modulus (G'') are represented as filled and open symbols, respectively. Symbols represent hydrogels that were synthesized in T-T and G-G mold assemblies (A) and in T-G- mold assemblies (B), namely: G-G (■), T-T (●), T-G (◆) and T-G (◆). Underlined letters represent the hydrogel's surface that was in contact with Teflon® (T) and glass (G) for T-G mold assemblies.

Results show that all the hydrogels presented a linear viscoelastic zone where the storage modulus does not depend on the applied stress, indicating that the three-dimensional structure of the hydrogels in not significantly affected up to the point at which the yield stress is achieved. This yield stress, defined as the shear stress at which G' crossovers G'' and/or at which G' profiles are no longer linear, indicating the onset of irreversible plastic deformation, was attained at ~ 27 Pa (which corresponds to 14 % of the applied strain in Figure 3.2) for hydrogels synthesized in Teflon® mold assemblies. On the contrary, hydrogels synthesized in glass mold assemblies maintained their mechanical stability in the entire stress range tested (Figure 3.2A). The lower copolymer/cross-linking concentration at both surfaces, which leads to highly hydrated hydrogel structures, justifies the lower mechanical resilience of hydrogels synthetized in Teflon® mold assemblies. Hydrogels synthesized in Teflon®/glass mold assemblies (T-G) presented linear viscoelastic profiles, for both measured surfaces, and for shear stresses at least up to 200 Pa (Figure 3.2B) as well as G' values that are higher than those measured for hydrogels synthesized in Teflon® mold plaques (T-T). Nevertheless, and as expected, G' values measured at the surfaces that were in contact with Teflon® were significantly lower (p-value < 0.05) than those measured at the surfaces that were in contact with glass, confirming the less dense/cross-linked structure of the former.

3.4.2 Effect of mold assemblies on the water swelling capacity of IL-based cationic hydrogels

The effect of the different mold assemblies on the water swelling capacities (WSC) of the prepared cationic poly(HEMA-co-BVImCl) hydrogels in aqueous media, at two different ionic strengths (I), was measured at room temperature (~ 22 ºC) for samples immersed in deionized water (I ≈ 0 M) and PBS (I ≈ 0.17 M). All samples achieved water swelling equilibrium after 24 h (data not shown). Results presented in Figure 3.3 show that the highest WSC (at least 1.5 × higher) was observed for hydrogels synthesized in Teflon® mold assemblies (T-T) followed

by those synthesized in T-G and G-G mold plaques. Interestingly, hydrogels presenting the highest charge density (those prepared in glass mold assemblies) do not present the highest WSC.

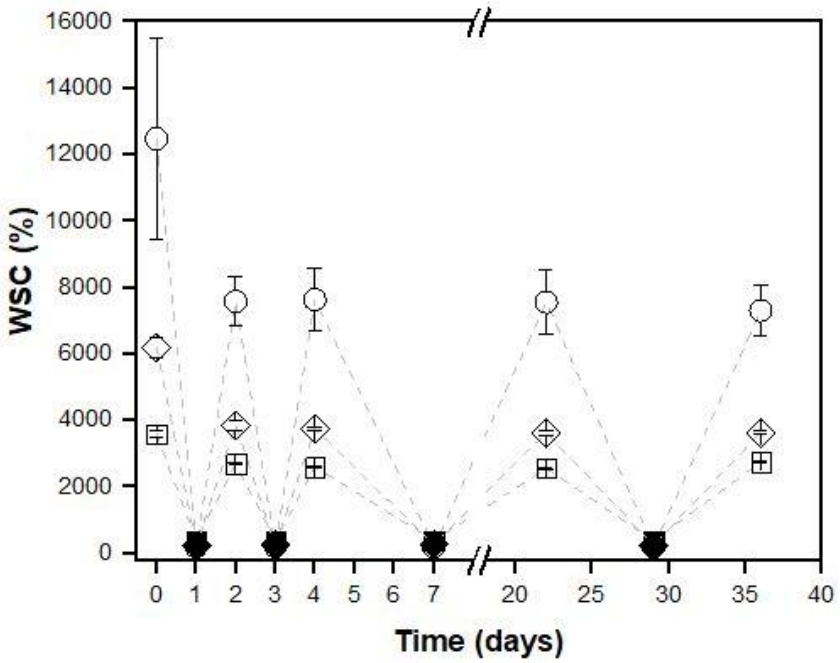

Figure 3.3 Reversible water swelling capacity (WSC) of poly(HEMA-co-BVImCl) hydrogels synthesized in different mold substrates when immersed in deionized water and in PBS (I ≈ 0.17 M) represented by open and filled symbols, respectively. Symbols represent hydrogels that were synthesized in T-T (○), G-G (□) and T-G (◇) mold assemblies.

When hydrogels synthesized in T-G mold assemblies were immersed in deionized water it was observed that they spontaneously curve always in the same direction, with the surface that was in contact with the Teflon® outside the curvature (Figure S3.3, Appendix B). This observation may be justified by the higher wettability of this surface (as confirmed by water contact angles data, Table S3.1, Appendix B) which results from the less dense and less cross-linked structure of this surface layer, as discussed above.

The effect of the ionic strength of the medium on the WSC of the hydrogels is also reported in Figure 3.3. The water swelling equilibrium in PBS media was attained in ~ 3 min at room temperature (~ 22 ºC) (Movie S3.1, Appendix B). Results clearly show that all hydrogels are responsive to changes in the ionic strength of the media, independently of the mold assemblies that were employed during their synthesis. As expected, the presence of salts in PBS led to a decrease in the WSC of all cationic poly(HEMA-co-BVImCl) hydrogels (~ 92 %), since their presence decreases the osmotic pressure gradient between the cationic hydrogel and the medium. The total molar amount of net charges in PBS (15 mL) was estimated to be at least ~ 560 × higher than that of IL cations present in each hydrogel, leading to the shrinking or squeezing-out effect observed when water swollen samples (at equilibrium) are immersed in PBS. As can be also seen in Figure 3.3, after the first immersion in PBS the WSC of the hydrogels decreases when they are immersed in deionized water. This happens because the cationic poly(HEMA-co-BVImCl) hydrogels were further cross-linked by disodium phosphate anions that are present in PBS which decreases the free volume in-between the copolymer chains, and therefore the WSC of the hydrogels. After the 1st immersion in PBS the hydrogels present a new WSC equilibrium which is maintained for all subsequent immersions in water. Finally, all hydrogels maintained their mechanical stability and responsiveness to changes in the ionic strength of the medium during the entire monitoring period (up to 35 days).

3.4.3 Effect of mold assemblies on the electromechanical properties of IL-based cationic hydrogels in different media

The mechanical deformation of polyelectrolytes under an electric field has been previously reported in the literature[9,41-46] however most studies focused on pH dependent polyanionic systems. Moreover, different mechanisms have been proposed to explain/model the electro-actuation response of ionic hydrogels, including the Coulomb, electro-osmosis,

electrochemical and enrichment/depletion mechanisms.[41,44,47,48] However, and up till now, there is no consensus about which is/are the most accurate mechanism(s) to fully describe the phenomena. This happens mostly due to the complexity of systems studied so far and also due to the variability of the experimental procedures used to study those electro-actuation mechanisms (e.g. due to differences in experimental setups, relative position of the actuator towards the electrodes, properties of the actuator, osmotic gradient between the actuator and the external media, etc.).[9,49]

In this work, and to our knowledge, we report for the first time the electromechanical properties of pH independent IL-based cationic hydrogels under an external electrical stimulus and when immersed in different media, and we expect to contribute for a deeper comprehension of the electro actuation mechanisms involved in these particular polyelectrolyte systems. The mechanical response of the prepared hydrogels under electrical stimulus was quantified as the maximum displacement amplitude of each hydrogel from its equilibrium position (vertical in-between electrodes) towards the electrodes. For the hydrogels synthesized in T-G mold assemblies, the surface that was in contact with Teflon® during polymerization was facing the cathode. The observed mechanical displacement (bending) of IL-based polycationic hydrogels synthetized in T-T and T-G mold assemblies was towards the anode (Figure 3.4A and Movie S3.2, Appendix B). Bending results observed for hydrogels synthesized in T-T and T-G mold assemblies immersed in deionized water are presented in Figure 3.4. As can be seen in Figure 3.4B hydrogels synthesized in T-T mold assemblies presented the highest bending angle towards the anode when compared to those synthesized in T-G mold assemblies (at least 1.5 × higher).

Interestingly hydrogels synthesized in T-T mold plaques are the ones that presented the lowest IL content (lowest charge density) for a fixed hydrogel area/volume. This result indicates that the electro-actuation response of these hydrogels is mainly governed by their morphological

and physicochemical properties (e.g. lower cross-linking density and higher WSC) rather than on their charge density. The combination of these variables enhances the diffusion of mobile chlorine counter-anions through the hydrogel network towards the anode when the hydrogel is under an electrical stimulus. Consequently, a continuous migration of anions takes place from the side of the hydrogel facing the cathode to the side facing the anode.

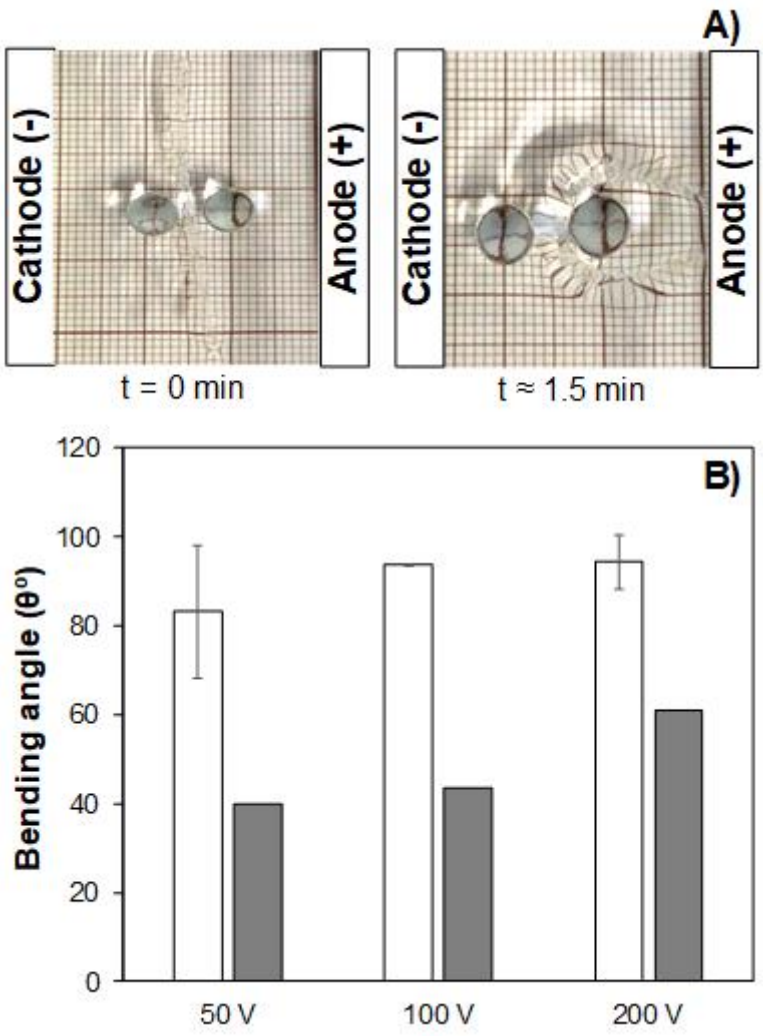

Figure 3.4 Illustration of the electro-actuation response of hydrogels synthesized in T-T mold assemblies under an applied voltage of 100 V (A) and Bending angles of hydrogels synthesized in different mold assemblies under applied electric stimulus for copolymer (HEMA-co-BVImCl) hydrogels synthesized in T-T (□) and T-G (■) mold assemblies (B). Experiments were carried out with samples immersed in deionized water at room temperature (~ 22 ºC).

This results in the formation of an electric double layer at the hydrogel surface facing the anode (which induces an extra screening of the polycationic network by the chlorine counter-anions), and on a depletion of anions on the cathode side, originating a non-neutral positively charged surface that expands by swelling, leading the hydrogel to bend towards the anode.[50-52] The observed bending of the hydrogel towards the anode is in agreement with the enrichment/depletion mechanism, which takes into account the asymmetric transport of cations/anions through the hydrogel network leading to ionic strength gradients in the boundaries between the hydrogel and the surrounding media.[41]

The electro-mechanical actuation response of the hydrogels synthesized in T-T mold assemblies was consistently maintained during at least 24 h. It was also observed that the time required for hydrogels synthesized in T-T mold plaques to achieve maximum displacement equilibrium decreased with the applied voltage: ~ 2.5 min (at 50 V), ~ 1.6 min (at 100 V) and ~ 0.8 min (at 200 V), since ion diffusion is enhanced at higher applied voltages leading to faster actuation responses.[19] Moreover, by inverting the direction of the electrical current, hydrogels synthesized in Teflon® mold assemblies quickly and fully bend backwards, due to the fast migration of chlorine counter-anions towards the "new" anode (Movie S3.3, Appendix B). On the contrary, for hydrogels synthesized in T-G mold assemblies, the diffusion of chlorine ions through the hydrogel network is hampered by the higher density of the copolymer network on the surface that was in contact with glass during polymerization, as discussed above, which leads to lower bending angles (Figure 3.4B). Moreover, and as shown in Figure 3.5, when the direction of the electric current is changed (the surface of the hydrogel that was in contact with glass facing the cathode), these hydrogels are not able to completely invert their movement, as previously observed for hydrogels synthesized in Teflon® mold assemblies.

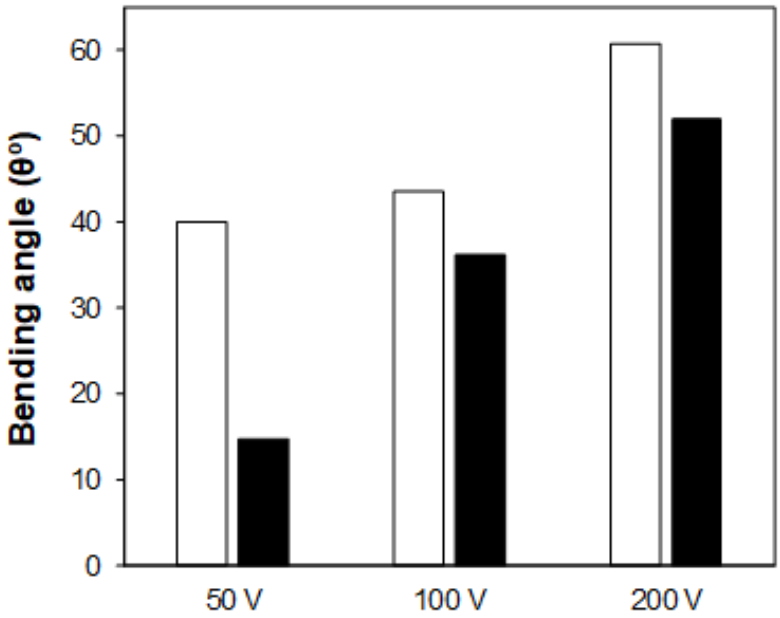

Figure 3.5 Bending angles of hydrogels synthesized in T-G mold assemblies under different applied voltages by placing the surface of the hydrogel that was in contact with Teflon® during polymerization facing the cathode (□), and after reversing the direction of the electric current (■). Experiments were carried out with samples immersed in deionized water at room temperature (~ 22 ºC).

Finally, any mechanical response was observed (at a macroscopic level), at any tested applied voltages, for hydrogels synthesized in G-G mold assemblies (G-G) immersed in deionized water. This result indicates that the mechanical response of the hydrogels was highly dependent on the surface-to-bulk concentration heterogeneity of the hydrogels that results from the copolymer gradient density induced by the mold plaque materials employed to synthesize the hydrogels, as previously discussed. Additionally, and despite their higher surface charge density, it is hypothesized that their denser copolymer network, and consequently their lower WSC, may hinder the diffusion of the IL counter-ions up to the hydrogel surface facing the anode. Therefore, an insufficient accumulation of IL counter anions occurs at the hydrogel surface facing the anode which hampers the formation of the charge gradient that ultimately results in the mechanical response of the hydrogel. This hypothesis agrees with previous works

which reported the major influence of the WSC of electro-active materials on their electromechanical response.[53]

3.4.4 Effect of the pH of the medium on the electromechanical properties of IL-based cationic hydrogels

Conventional ionic actuators are based on polyelectrolytes bearing ionizable groups which are protonated/deprotonated depending on the pH of the medium. Therefore, the mechanical actuation of these materials depends on the pH conditions in which they will be employed.[48] On the contrary, IL-based electro-active materials are expected to be less sensitive to pH changes since they contain ionized groups which are not pH dependent (they are permanent polyelectrolytes).

In this work, the effect of pH on the electro-actuation capacity of poly(HEMA-co-BVImCl) hydrogels was evaluated only for hydrogels synthesized in T-T mold plaques since those were the ones that presented higher mechanical response. Any noticeable morphological change (swelling/shrinking) was observed when the hydrogels were immersed in acid/alkaline aqueous media during measurements. As can be seen in Figure S3.4 (Appendix B) the pH of the medium does not significantly affect (p-value > 0.05) the electro-actuation capacity of the hydrogels for any of the applied voltages. As before, the average times required to achieve maximum bending angles varied according to the intensity of the applied voltage, and they were very similar to those measured when the hydrogels were immersed in deionized water (~3 min at 50 V, ~2.3 min at 100 V and ~1 min at 200 V). Moreover, hydrogels also presented equivalent inverse bending when the direction of the electric current is inverted (Movie S3.4, Appendix B). These results allow to infer that bending in acid/alkaline media can be also explained by the enrichment/depletion mechanism.

3.4.5 Influence of the ionic strength of the medium on the electromechanical properties of IL-based cationic hydrogels

In order to evaluate the effect of the ionic strength of the medium on the bending capacity of IL-based electro-active hydrogels, electro-actuation measurements were performed having the hydrogels immersed in a saline solution (NaCl, I = 10 mM). This study was performed for the hydrogels that presented the highest and the lowest bending when immersed in deionized water (hydrogels synthesized in T-T and G-G mold assemblies, respectively). Hydrogels were immersed in the saline solution for 24 h before measurements to ensure osmotic equilibrium. After this period, hydrogels shrunk to different extents due to their responsiveness to changes in the ionic strength of the media (as previously observed when samples were immersed in PBS, Figure 3.3). Water swollen hydrogels synthesized in T-T and G-G mold assemblies decreased their volumes by 5.6 and 1.6 times, respectively when immersed in the saline solution. The ionic strength of the saline solution was guaranteed to be significantly higher than that of the hydrogel matrices, based on elemental analysis results. At these conditions, both hydrogels presented reversed mechanical actuation, depending on the direction of the applied electrical current (Movie S3.5, Appendix B). The bending angles measured for hydrogels synthesized in T-T and G-G mold assemblies were 32.3 ± 4.6 º and 16.0 ± 1.0 º, respectively. These results show that the electro-actuation capacity of hydrogels synthesized in Teflon® mold assemblies decreases with the ionic strength of the media, most probably due to the observed extensive hydrogel shrinkage that may have hampered the diffusion of chlorine counter-anions through the hydrogel matrices. On the contrary, the saline solution seams to enhance the electro-actuation capacity of hydrogels synthesized in G-G mold assemblies, which did not present any mechanical actuation response when immersed in deionized water. Consistent bending displacement was observed during at least 24 h for hydrogels synthesized in G-G mold assemblies when immersed in saline solution. It is hypothesized that the observed mechanical

actuation may result from an increase in the concentration of mobile ions inside the hydrogel matrix, after its previous immersion in the saline solution (for 24 h), in order to achieve Donnan equilibrium.[51] This higher amount of mobile ions favors the formation of an electric double layer at the anode side (and a depleted layer at the cathode side) which ultimately leads to bending, as previously discussed. Although a similar effect was expected to occur for the hydrogels synthesized in Teflon® mold assemblies, it is supposed that the formation of the electric double layer may not have been enough to overlap the volume contraction observed for this sample, which may have compromised its actuation capacity.

3.4.6 Preliminary experiments on the electronic conductivity of IL-based cationic hydrogels

Preliminary experiments were performed to evaluate if the synthesized IL-based cationic hydrogels also present electronic conductivity, besides the ionic conductivity discussed above. As can be seen in Figure 3.6 all the prepared poly(HEMA-co-BVImCl) hydrogels were able to mediate electron transfer onto a LED under a DC current of 1 V at room temperature (~ 22 ºC), and to generate small electrical currents through the hydrogel for at least two hours.

The intensity of the light emitted from the LED was not visually affected by the hydrogel structure. On the contrary, poly(HEMA) hydrogels were not able to light on the LED (Figure S3.5, Appendix B), confirming that the observed electronic conductivity is promoted by the presence of the IL in the hydrogel network. It is hypothesized that the electronic conductivity observed for poly(HEMA-co-BVImCl) hydrogels may result from the transport of electrons that are produced by the oxidation of chlorine counter-anions at the anode. Nevertheless, more studies must be performed to better understand the mechanism behind the observed phenomena.

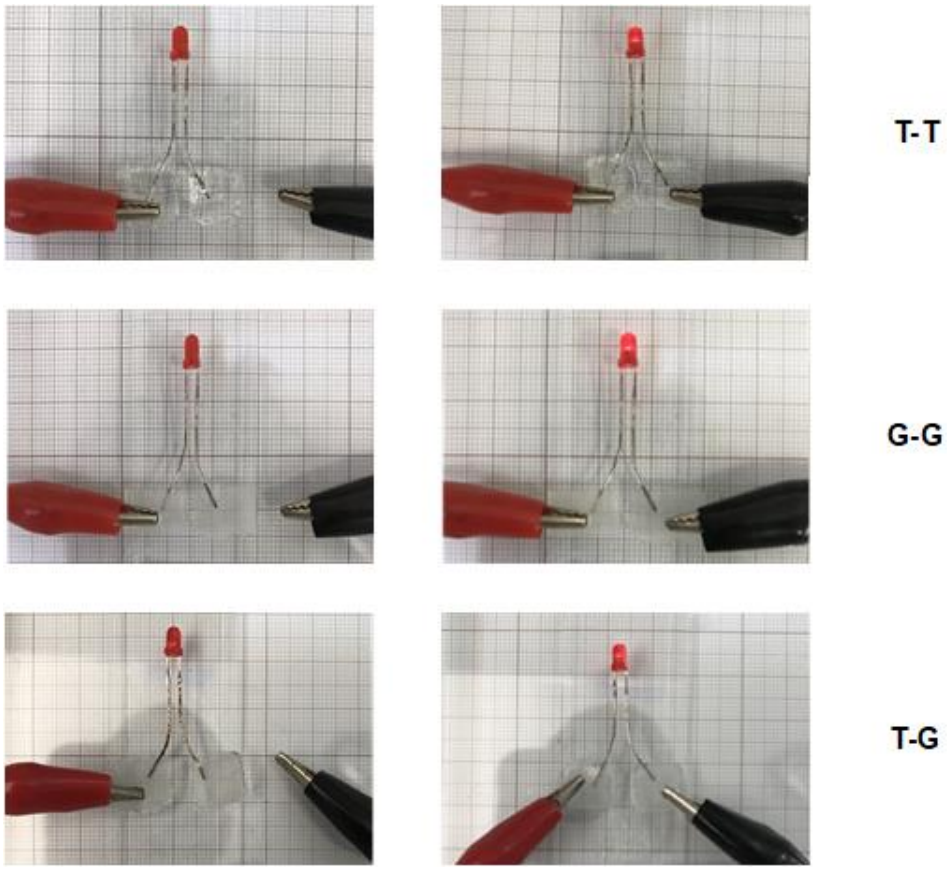

Figure 3.6 Test of the electronic conductivity of water swollen poly(HEMA-co-BVImCl) hydrogels synthesized in different mold assemblies before (left column) and after (right column) the application of a potential difference of 1 V at room temperature (~ 22 ºC).

3.5 Conclusions

This work clearly shows, for the first time, that it is possible to tune the physicochemical, mechanical, and electromechanical properties of IL-based polycationic hydrogels by employing different mold plaque materials during the free radical polymerization of those hydrogels in aqueous media. This evidence results from a surface phenomenon that occurs at the mold/solution interface and which induces the formation of hydrogel networks presenting different surface-to-bulk concentration gradients depending on the hydrophobicity of the mold assemblies employed.

Obtained results showed that hydrogels synthesized in more hydrophobic Teflon® mold assemblies present evident surface-to-bulk copolymer concentration heterogeneity, while those synthesized in glass mold assemblies were homogeneous. Hydrogels, having distinct surface properties, can be obtained by combining different mold plaque materials (having different surface properties). The electromechanical responsiveness of the prepared poly(HEMA-co-BVImCl) hydrogels was highly dependent on the surface properties of the hydrogels. Hydrogels synthesized in Teflon® mold assemblies presented the highest electro-actuation capacity in aqueous media and independently of the pH of the media. The electro-actuation capacity of these hydrogels was explained based on the ion enrichment/depletion mechanism, and it was mostly dependent on the physicochemical and morphological structure of the hydrogel, rather than on its ionic charge density. These results permit to infer about the importance of chlorine counter -anions diffusion through the loser/less-crosslinked hydrogel structure (observed for hydrogels synthesized in Teflon® mold assemblies) on the electro-actuation capacity of the prepared hydrogels. Denser hydrogel structures obtained when using hydrophilic glass mold plaque materials, hamper chlorine diffusion and consequently the mechanical actuation of the hydrogels. Nevertheless, the electro-actuation of these hydrogels can be stimulated in saline solutions after loading the hydrogel with an amount of mobile ions high enough to induce actuation. Finally, it was also possible to obtain hydrogels for which the electromechanical response depends on the direction of the applied electric current, just by employing different mold plaque materials during the polymerization reaction.

This work presents an efficient and simple strategy to tune the electromechanical responsiveness of IL-based polycationic hydrogels which can be further explored for the development of target specific soft ionic electro-actuators. Moreover, all the prepared hydrogels also presented electric conductivity which may also be further explored for the development of electrochemical devices (e.g. fuel cells and batteries).

3.6 Acknowledgements

This work was financially supported by Fundação para a Ciência e Tecnologia (FCT-MEC) under contracts UID/EQU/00102/2019 and UID/EMS/00285/2020. A. M. A. Dias acknowledges FCT-MEC for a contract under the program Investigador FCT IF/00455/2013 and under the program Stimulus of Scientific Employment - Individual Support, CEECIND/01248/2017. A. F. Kanaan acknowledges CNPq, Brazil, for the scholarship with reference 200808/2014-1. The authors also acknowledge Dr. F. A. P. Garcia for providing the electrophoresis power supply EPS 500/400 (Pharmacia Fine Chemicals, Sweden).

3.7 References

(1) Rus, D.; Tolley, M. T. Design, fabrication and control of robots. *Nature* **2015**, 521, 467–475.

(2) Strauβ, S.; Dudziak, S.; Hagemann, R.; Barcikowski, S.; Fliess, M.; Israelowtiz, M.; Kracht, D.; Kuhbier, J. W.; Radtke, C.; Reimers, K.; Vogt, P. M. Induction of Osteogenic Differentiation of Adipose Derived Stem Cells by Microstructured Nitinol Actuator-Mediated Mechanical Stress. *PLoS One* **2012**, 7, e51264.

(3) Asaka, K.; Okuzaki, H. Soft Actuators: Materials, Modeling, Applications, and Future Perspectives, Springer, Japan, **2014**.

(4) Watanabe, M.; Imaizumi, S.; Yasuda, T.; Kobuko, H. Ion Gels for Ionic Polymer Actuators, in: Asaka, K.; Okuzaki, H. (Eds.), Soft Actuators: Materials, Modeling, Applications, and Future Perspectives, Springer, Japan, **2014**, pp. 141-156.

(5) Bar-Cohen, Y.; Zhang, Q. Electroactive Polymer Actuators and Sensors. *MRS Bulletin* **2008**, 33, 173–181.

(6) Kim, O.; Kim, S. J.; Park, M. J. Low-voltage-driven soft actuators. *Chemical Communications* **2018**, 54, 4895–4904.

(7) Maziz, A.; Simaite, A.; Bergaud, C. Ionic Electrochemical Actuators, in: Eftekhari, A. (Ed.), Polymerized Ionic Liquids, The Royal Society of Chemistry, United Kingdom, **2018**, pp. 456-488.

(8) Mirfakhrai, T.; Madden, J. D. W.; Baughman, R. H. Polymer artificial muscles. *Materials Today* **2007**, 10, 30–38.

(9) Glazer, P. J.; van Erp, M.; Embrechts, A.; Lemay, S. G.; Mendes, E. Role of pH gradients in the actuation of electro-responsive polyelectrolyte gels. *Soft Matter* **2012**, 8, 4421–4426.

(10) Glazer, P. J.; Verbrugghe, P.; Adesanya, K.; Herijgers, P.; Dubruel, P.; Mendes, E. Electro-actuation of biocompatible Pluronic/methacrylic acid hydrogel in blood plasma an in blood-mimicking buffers. *RSC Advances* **2014**, 4, 1890–1894.

(11) Adesanya, K.; Vanderleyden, E.; Embrechts, A.; Glazer, P.; Mendes, E.; Dubruel, P. Properties of Electrically Responsive Hydrogels as a Potential Dynamic Tool for Biomedical Applications. *Journal of Applied Polymer Science* **2014**, 131, 41195–41204.

(12) Shiga, T.; Kurauchi, T. Deformation of Polyelectrolyte Gels under the Influence of Electric Field. *Journal of Applied Polymer Science* **1990**, 39, 2305–2320.

(13) Browe, D. P.; Wood, C.; Sze, M. T.; White, K. A.; Scott, T.; Olabisi, R. M.; Freeman, J. W. Characterization and optimization of actuating poly[ethylene glycol] diacrylate/acrylic acid hydrogels as artificial muscles. *Polymer 2017*, 117, 331–341.

(14) Aabloo, A.; De Luca, V.; Di Pasquale, G.; Graziani, S.; Cugliuzzo, C.; Johanson, U.; Marino, C.; Pollicino, A.; Puglisi, R. A new class of ionic electroactive polymers based on green synthesis. *Sensors and Actuators A: Physical* **2016**, 249, 32–44.

(15) Park, I.; Jung, K.; Kim, D.; Kim, S.; Kim, K. J. Physical Principles of Ionic Polymer-Metal Composites as Electroactive Actuators and Sensors. *MRS Bulletin* **2008**, 33, 190–195.

(16) Dias, A. M. A.; Cortez, A. R.; Barsan, M. M.; Santos, J. B.; Brett, C. M. A.; de Sousa, H. C. Development of Greener Multi-Responsive Chitosan Biomaterials Doped with

Biocompatible Ammonium Ionic Liquids. *ACS Sustainable Chemistry & Engineering* **2013**, 1, 1480–1492.

(17) Mejri, R.; Dias, J. C.; Hentati, S. B.; Martins, M. S.; Costa, C. M.; Lanceros-Mendez, S. Effect of anion type in the performance of ionic liquid/poly[vinylidene fluoride] electromechanical actuators. *Journal of Non-Crystalline Solids* **2016**, 453, 8–15.

(18) Wang, Z.; He, B.; Wang, Q.; Yin, Y. Electromechanical bending behavior study of soft photocurable ionogel actuator using a new finite element method. *Smart Materials and Structures* **2016**, 25, 095018.

(19) Mejri, R.; Dias, J. C.; Hentati, S. B.; Botelho, G.; Esperança, J. M. S. S.; Costa, C. M.; Lanceros-Mendez, S. Imidazolium-based ionic liquid type dependence of the bending response of polymer actuator. *European Polymer Journal* **2016**, 85, 445–451.

(20) Dias, J. C.; Lopes, A. C.; Magalhães, B.; Botelho, G.; Silva, M. M.; Esperança, J. M.S. S.; Lanceros-Mendez, S. High performance electromechanical actuators based on ionic liquid/poly[vinylidene fluoride]. *Polymer Testing* **2015**, 48, 199–205.

(21) Okuzaki, H.; Takagi, S.; Hishiki, F.; Tanigawa, R. Ionic liquid/polyurethane/PEDOT:PSS composites for electro-active polymer actuators. *Sensors and Actuators B: Chemical* **2014**, 194, 59–63.

(22) Kim, O.; Kim, H.; Choi, U. H.; Park, M. J. One-volt-driven superfast polymer actuators based on single-ion conductors. *Nature Communications* **2016**, 7, 13576.

(23) Imaizumi, S.; Kato, Y.; Kokubo, H.; Watanabe, M. Driving Mechanisms of Ionic Polymer Actuators Having Electric Double Layer Capacitor Structures. *The Journal of Physical Chemistry B* **2012**, 116, 5080–5089.

(24) Kokubo, H.; Sano, R.; Murai, K.; Ishii, S.; Watanabe, W. Ionic Polymer Actuators Using Poly(ionic liquid) Electrolytes. *European Polymer Journal* **2018**, 106, 266–272.

(25) Mahadeva, S. K.; Kim, J. An electro-active paper actuator made with cellulose-polypyrrole-ionic liquid nanocomposite: influence of ionic liquid concentration, type of anion and humidity. *Smart Materials and Structures* **2010**, 19, 105014.

(26) Kim, O.; Kim, S. Y.; Park, B.; Hwang, W.; Park, M. J. Factors Affecting Electromechanical Properties of Ionic Polymer Actuators Based on Ionic Liquid-Containing Sulfonated Block Copolymers. *Macromolecules* **2014**, 47, 4357–4368.

(27) Liu, Y.; Lu, C.; Twigg, S.; Lin, J.; Hatipoglu, G.; Liu, S.; Winograd, N.; Zhang, Q. M. Ion distribution in ionic electroactive polymer actuators. *Electroactive Polymer Actuators and Devices [EAPAD]* **2011**, SPIE.

(28) Shaplov, A. S.; Marcilla, R.; Mecerreyes, D. Recent Advances in Innovative Polymer Electrolytes based on Poly(ionic liquid)s. *Electrochimica Acta* **2015**, 175, 18–34.

(29) Eftekhari, A.; Saito, T. Synthesis and properties of polymerized ionic liquids. E*uropean Polymer Journal* **2017**, 90, 245–272.

(30) Qian, W.; Texter, J.; Yan, F. Frontiers in poly(ionic liquid)s: syntheses and applications. *Chemical Society Reviews* **2017**, 46, 1124–1159.

(31) Gong, J. P.; Kii, A.; Xu, J.; Hattori, Y.; Osada, Y. A Possible Mechanism for the Substrate Effect on Hydrogel Formation. *The Journal of Physical Chemistry B* **2001**, 105, 4572–4576.

(32) Peng, M.; Kurokawa, T.; Gong, J. P.; Osada, Y.; Zheng, Q. Effect of Surface Roughness of Hydrophobic Substrate on Heterogeneous Polymerization of Hydrogels. *The Journal of Physical Chemistry B* **2002**, 106, 3073–30814.

(33) Narita, T.; Hirai, A.; Xu, J.; Gong, J. P.; Osada, Y. Substrate Effects of Gel Surfaces on Cell Adhesion and Disruption. *Biomacromolecules* **2000**, 1, 162–167.

(34) Kii, A.; Xu, J.; Gong, J. P.; Osada, Y.; Zhang, X. Heterogeneous Polymerization of Hydrogels on Hydrophobic Substrate. *The Journal of Physical Chemistry B* **2001**, 105, 4565–4571.

(35) Zhang, X.; Xu, J.; Okawa, K.; Katsyuama, Y.; Gong, J. P.; Osada, Y. *In Situ* Monitoring of Hydrogel Polymerization Using Speckle Interferometry. *The Journal of Physical Chemistry B* **1999**, 103, 2888–2891.

(36) Narita, T.; Knaebel, A.; Munch, P.; Candau, S. J.; Gong, J. P.; Osada, Y. Microrheological Investigation of Substrate-Induced Gradient Structure in Hydrogels. *Macromolecules* **2001**, 34, 5725–5726.

(37) Peng, M.; Gong, J. P.; Osada, Y.; Zhang, X.; Zheng, Q. Real-Time Laser Sheet Refraction To Monitor in Situ the Heterogeneity of Polymerization Processes on Teflon Surface. *Macromolecules* **2001**, 34, 7829–7835.

(38) Kanaan, A. F.; Barsan, M. M.; Brett, C. M. A.; Alvarez-Lorenzo, C.; Concheiro, A.; de Sousa, H. C.; Dias, A. M. A. Sustainable Electro-Responsive Semi-Interpenetrating Starch/Ionic Liquid Copolymer Networks for the Controlled Sorption/Release of Biomolecules. *ACS Sustainable Chemistry & Engineering* **2019**, 7, 10516–10532.

(39) Shimizu, K.; Tariq, M.; Freitas, A. A.; Pádua, A. A. H.; Lopes, J. N. C. Self-Organization in Ionic Liquids: From Bulk to Interfaces and Films. *Journal of the Brazilian Chemical Society* **2016**, 27, 349–362.

(40) Lovelock, K. R. J. Influence of the ionic liquid/gas surface on ionic liquid chemistry. *Physical Chemistry Chemical Physics* **2012**, 14, 5071–5089.

(41) Doi, M.; Matsumoto, M.; Hirose, Y. Deformation of Ionic Polymer Gels by Electric Fields. *Macromolecules* **1992**, 25, 5504–5511.

(42) Zolfagharian, A.; Kaynak, A.; Khoo, S. Y.; Zhang, J.; Nahavandi, S.; Kouzani, S. Control-Oriented Modelling of a 3D-Printed Soft Actuator. *Materials* **2019**, 12, 71.

(43) Zolfagharian, A.; Kaynak, A.; Khoo, S. Y.; Kouzani, A. Z. Polyelectrolyte Soft Actuators: 3D Printed Chitosan and Cast Gelatin. *3D Printing and Additive Manufacturing* **2018**, 5, 138–150.

(44) Tanaka, T.; Nishio, I.; Sun, S.; Ueno-Nishio, S. Collapse of Gels in an Electric Field. *Science* **1982**, 218, 467–469.

(45) Shiga, T.; Hirose, Y.; Okada, A.; Kurauchi, T. Deformation of ionic polymer gel film in electric fields. *Journal of Material Science* **1994**, 29, 5715–5718.

(46) Li, Y.; Sun, Y.; Xiao, Y.; Gao, G.; Liu, S.; Zhang, J.; Fu, J. Electric Field Actuation of Tough Electroactive Hydrogels Cross-Linked by Functional Triblock Copolymer Micelles. *ACS Applied Materials & Interfaces* **2016**, 8, 26326–26331.

(47) Kishi, R.; Osada, Y. Reversible Volume Change of Microparticles in an Electric Field. *Journal of the Chemical Society, Faraday Transactions 1: Physical Chemistry in Condensed Phases* **1989**, 85, 655–662.

(48) Hirose, Y.; Giannetti, G.; Marquardt, J.; Tanaka, T. Migration of Ions and pH Gradients in Gels under Stationary Electric Fields. *Journal of Physical Society of Japan* **1992**, 61, 4085–4097.

(49) Osada, Y.; Okuzaki, H.; Hori, H. A polymer gel with electrically driven motility. *Nature* **1992**, 355, 242–244.

(50) Mahinroosta, M.; Farsangi, Z. J.; Allahverdi, A.; Shakoori, Z. Hydrogels as intelligent materials: A brief review of synthesis, properties and applications. *Materials Today Chemistry* **2018**, 8, 42–55.

(51) Morales, D.; Palleau, E.; Dickey, M. D.; Velev, O. D. Electro-actuated hydrogel walkers with dual responsive legs. *Soft Matter* **2014**, 10, 1337–1348.

(52) Lim, H. L.; Chuang, J. C.; Tran, T.; Aung, A.; Arya, G.; Varghese, S. Dynamic Electromechanical Hydrogel Matrices for Stem Cell Culture. *Advanced Functional Materials* **2011**, 21, 55–63.

(53) Jeong, H. M.; Kim, H. S.; La, H. S. The Effect of Cross-Linking on the Actuation of an Electroactive IPMC Prepared with a Fluorinated Acrylic Copolymer. *Journal of Macromolecular Science, Part B: Physics* **2006**, 45, 119–130.

Chapter 4

Semi-interpenetrating chitosan/ionic liquid polymer networks as electro-responsive biomaterials for potential wound dressings and iontophoretic applications

This chapter comprises the work submitted to Materials Science and Engineering: C (2020) by **Akel F. Kanaan**, Ana P. Piedade, Hermínio C. de Sousa, Ana M. A. Dias

4.1 Abstract

The goal of this work was to enhance and to tune the physicochemical, mechanical, electro-responsive and biological properties of chitosan-based biomaterials to obtain biocompatible, mechanically stable, and multi-stimuli responsive hemostatic wound dressings, having modulated iontophoretic permeation and controlled release of positively charged biomolecules. To accomplish this objective, polycationic semi-interpenetrating co-polymer networks (semi-IPN) were prepared by combining chitosan (CS) and ionic liquid-based polymers and co-polymers, namely poly(1-butyl-3-vinylimidazolium chloride) (poly(BVImCl)) and poly(2-hydroxymethyl methacrylate-co-1-butyl-3-vinylimidazolium chloride) (poly(HEMA-co-BVImCl)). Results show that prepared semi-IPNs presented high mechanical stability and were positively charged over a broad pH range, including basic pH. Semi-IPNs also presented faster permeation and release rates of lidocaine hydrochloride (LH), under external electrical stimulus (0.56 mA/cm^2) in aqueous media at 32 ºC. The kinetic release constants and the LH diffusion coefficients measured under electrical stimulus were ~ 1.5 and > 2.7 times higher for those measured for passive release. Finally, both semi-IPNs were non-hemolytic (hemolytic index ≤ 0.2 %) and showed strong hemostatic activity (blood clotting index of ~ 12 ± 1 %). All together,

these results show that the prepared polycationic semi-IPN hydrogels presented advantageous mechanical, responsive and biological properties that enable them to be potentially employed for the design of new, safer and advanced stimuli-responsive biomaterials for several biomedical applications such as hemostatic and wound healing dressings and iontophoretic patches.

Keywords: chitosan; ionic liquid based semi-IPNs; electro-responsive hydrogels; hemostatic wound dressings; iontophoresis.

4.2 Introduction

Transdermal drug delivery represents an efficient and advantageous alternative over conventional systemic oral drug administration routes, as it avoids drug first-pass liver metabolism and drug degradation thus allowing a better control/modulation of drug delivery.[1] Several transdermal drug delivery strategies have focused on the permeation enhancement of different drugs through the skin. Those strategies can be classified as chemical strategies, when they are based on the use of chemical permeation enhancers (e.g. alcohols, glycols and ionic liquids);[2-5] and physical strategies, when techniques such as sonophoresis, magnetophoresis, microneedles, electroporation, microwaves, photoacoustic waves and iontophoresis are employed.[6-12]

Iontophoresis is a non-invasive therapeutic drug delivery procedure based on the application of low current densities (≤ 0.5 mA/cm^2) to improve the transport of drugs across a biological barrier. The two main mechanisms involved in iontophoretic transport include electro-migration and electro-osmosis. Electro-migration, also known as electro-repulsion, is defined as the ordered movement of ionic species in the presence of an electrical field, from the electrode side having the same polarity of the ionic species towards the oppositely charged

electrode (cationic molecules migrate towards cathode and vice-versa).[13] Electro-osmosis is defined as the convective solvent flow induced by an electrical field across a charged membrane. The direction of the electro-osmotic flow depends on the charge (zeta potential) of the membrane. When an electrical field is applied, the free counter ions of the charged membrane migrate towards the oppositely charged electrode, carrying water molecules in the process, which results in a solvent flow (the electro-osmotic flow across a cationic membrane is from the cathode to the anode).[14-16]

Iontophoresis has been employed in several clinical areas (e.g. dermatology, dentistry, ophthalmology and otorhinolaryngology) for the transport/delivery of different therapeutic molecules such as local anesthetics, antibiotics as well as anti-inflammatory, anticancer and antibacterial drugs.[17] Iontophoretic systems were also previously employed to enhance drug permeation through the skin;[13,18-28] bladder;[13,29] eyes;[30-33] oral cavity;[34-37] and nails.[38-40]

Iontophoresis can be regarded as a tunable drug delivery process since there are several variables that can be changed in order to control drug transport as, for example, the intensity and the duration of the applied electrical stimulus, the type and mode of the applied electrical stimulus (alternating current (AC) vs direct current (DC), and continuous vs pulsed electrical current), the drug concentration and the drug molecular weight, the pH and the ionic strength of the drug solution, etc.[15,17,18,41-43] Moreover, the electrical stimulus may be applied over aqueous drug solutions or over solid/semi-solid matrices containing the drug. The later can play an additional role to tune drug permeation profiles, depending on the chemical nature of the matrix, drug/matrix ratio, etc. Different synthetic- and natural-based polymeric matrices (e.g. poly(acrylic acid) and Pluronic®, silk fibroin and chitosan in the form of particles, gels/viscous ointments, hydrogels, and films) were already employed as vehicles to design iontophoretic systems.[44-51] Efforts have been made to employ natural-based materials for a broad range of biomedical applications, including iontophoretic applications, due to their

intrinsic biodegradability, availability, biocompatibility and low cost. However, these materials often present low mechanical stability and pH dependent charge density which limits its broader usage.

Chitosan (CS), obtained from the deacetylation of chitin which is a natural-based polymer found for example in the exoskeletons of arthropods and cell walls in fungi, has been previously employed as solid/semi-solid vehicle for the development of iontophoretic devices, in the form of CS-coated nanoparticles,[47,48] gels[49,50] and hydrogels.[51] Chitosan is a pH dependent polycationic biopolymer that presents remarkable properties for pharmaceutical and biomedical applications such as biodegradability, biocompatibility, bioadhesion and antimicrobial activity, low-cost and large availability.[52-54] However, and since chitosan-based hydrogels are pH sensitive, they present low mechanical resilience in biological fluids. To overcome this issue, several strategies have been reported in the literature aiming to improve chitosan properties and/or to design chitosan-based task-specific materials for diverse applications (including interpenetrating polymer networks (IPNs); grafting co-polymerization, chemically crosslinked blends, etc.[55-61]

Ionic liquids (ILs) are usually considered to be organic salts that are liquid at temperatures below 100 ºC and that present unique properties such as negligible vapor pressure, high chemical stability, and ionic conductivity.[62] ILs are also known as task-specific compounds since it is possible to tune their properties through the proper selection of their cation/anion pairs. ILs' cations and/or anions can be functionalized with polymerizable chemical groups (such as vinyl groups) and further polymerized and co-polymerized to obtain poly(ionic liquid)s (PILs) or IL-based co-polymers. These have been successfully employed in the development of distinct applications such as conductive electronic devices,[63] catalysts,[64] gas separation membranes,[65] antibacterial dressings[66] and multi-stimuli responsive hydrogels.[67-70] Over the last years different ILs have also been employed to functionalize chitosan aiming to

improve some of its properties and/or to obtain advanced multifunctional chitosan-based materials presenting improved thermal stability; catalytic activity; conductivity as well as improved antimicrobial and adsorption capacities.[71-76]

Semi-interpenetrating polymer networks (s-IPNs) can be employed as an advantageous approach to improve/alter the properties of a given polymer, while avoiding the chemical modification of its pristine structure.[61,67,77-81] Briefly, s-IPNs are polymers comprising two or more networks which are at least partially interlaced on a molecular scale, but not covalently bonded to each other, and that can, in principle, be separated from the constituent polymer network(s) without breaking any chemical bonds.[82] The major advantage of this approach is that each individual network retains a great part of their individual properties while synergistic improvements are expected to occur in the physicochemical, thermomechanical, responsive, and/or biological properties of the generated s-IPN.

This work involves the preparation of multi-responsive semi-interpenetrating chitosan/ionic liquid-based hydrogels presenting improved mechanical stability and higher charge density over a broader pH range. The ultimate goal of this work is to take advantage of the useful and well-known properties of chitosan as a biomaterial and of the high chemical stability and pH independent electro-responsive properties of IL-based polymers/co-polymers in the preparation of novel biomaterials that can be employed for the development of iontophoretic and/or hemostatic biomedical devices. In order to accomplish this objective, biocompatible and electro-responsive polycationic s-IPNs based on chitosan (CS) and on cross-linked IL-based homopolymers and co-polymers were synthetized by solution free radical co-polymerization of 1-butyl-3-vinylimidazolium chloride (BVImCl) and 2-hydroxyethyl methacrylate (HEMA), cross-linked with *N*,*N*-methylenebis(acrylamide) (MBA), in aqueous CS solutions. Obtained s-IPN hydrogels were extensively characterized in terms of their physicochemical and functional properties (elemental analysis, zeta potential, solid-state nuclear magnetic

resonance-^{13}C-NMR, water swelling capacity in different aqueous media having different pH and ionic strengths and adsorption capacity towards anionic molecules (employing methyl orange and bromocresol green as model molecules); morphological properties (helium pycnometry and scanning electron microscopy-SEM); thermomechanical properties (rheology, thermogravimetry and differential scanning calorimetry); electro-assisted drug delivery properties (in vitro electro-assisted iontophoresis permeation/release experiments using lidocaine hydrochloride as a model drug) and biological properties (blood compatibility and blood clotting experiments). Results were compared with those obtained for CS hydrogels, which were previously partially deprotonated (pre-treated with a basic solution) to allow their manipulation in aqueous media.

4.3 Materials and Methods

4.3.1 Materials

Low molecular weight chitosan (CS, Mw between 50 and 190 kDa and DDA ≥ 75 %, according to supplier's information); 2-hydroxyethyl methacrylate (HEMA, 99 %), 2,2'-Azobis (2-methylpropionamidine) dihydrochloride (AIBA, 97 %) and lidocaine hydrochloride monohydrate (LH) were obtained from Sigma-Aldrich. *N,N'*-methylenebis(acrylamide) (MBA, 96 %) was obtained from Acros Organics. Acetic acid (AAc, 99 %) was obtained from Fluka. The ionic liquid 1-butyl-3-vinylimidazolium chloride (BVImCl, 95 %) was acquired from Io-Li-Tec, Germany. Methyl orange (MO) and bromocresol green (BG) were obtained from Estabelecimentos Barral, Portugal. The chemical structure of MO, BG, and LH, are presented in Figure S4.1 (Appendix C).

Nitric acid (HNO_3, 60 % w/v) and sodium hydroxide (NaOH, 99 %) were supplied by José M. Vaz Pereira, S.A., Portugal and AkzoNobel (Netherlands), respectively. Regenerated cellulose

dialysis membrane (molecular weight cutoff of 6000 - 8000 kDa) was obtained from Spectra/Por® 1 Dialysis (United Sates of America).

Buffer solutions employed for water swelling capacity and adsorption experiments were phosphate buffered saline (PBS, pH = 7.4, I = 0.17 M) acquired from Sigma-Aldrich; bicarbonate buffer (BB, pH = 9.3, I = 0.17 M) and acetate buffer (AB, pH = 4.3, I = 0.17 M). Bicarbonate (BB) and acetate buffers (AB) were prepared as follows (for 500 mL of distilled water): BB - 0.23 g of sodium bicarbonate ($NaHCO_3$), 0.07 g of sodium carbonate (Na_2CO_3) and 2.67 g of sodium chloride (NaCl), all obtained from Sigma-Aldrich; AB - 0.196 g of sodium acetate 3-hydrated ($CH_3COONa.3H_2O$) from Panreac, 0.146 mL of acetic acid (CH_3COOH, 99 %) from Fluka, and 4.71 g of NaCl. The pH of buffer solutions was measured using a pH meter (Standard pH meter, Meter Lab).

The following reactants were employed for blood compatibility experiments: rabbit blood was acquired from healthy rabbits by intracardiac puncture at Agrarian School of Coimbra; a citrate-dextrose solution (ACD) from Sigma-Aldrich was employed as a blood anticoagulant agent and was mixed with whole blood (ACD:blood at ratio of 1:9 v/v). Drabkin's and hemoglobin (Hb) solutions were prepared as follows: Drabkin's solution: 50 mg of potassium cyanide (KCN, 96 %), 140 mg of potassium phosphate monobasic (KH_2PO_4, 99 %), 200 mg of potassium hexacyanoferrate (III) ($K_3Fe(CN)_6$, 99 %) and 1 mL of 4-(1,1,3,3-Tetramethylbutyl)phenyl-polyethylene glycol (Triton® X-100), all obtained from Sigma-Aldrich, dissolved in bi-distilled water (1 L); Hb solution: 0.3 g of lyophilized red blood cells (hemoglobin from bovine blood) obtained from Sigma-Aldrich, dissolved in 75 mL of PBS buffer solution. Calcium chloride dihydrate ($CaCl_2.2H_2O$, 99 %) acquired from Sigma-Aldrich, glutaraldehyde solution (25 % wt) acquired from Fluka, and ethanol (EtOH, 96 %) acquired from José Manuel Gomes do Santos, were employed for blood clotting studies.

4.3.2 Synthesis of s-IPN Hydrogels

s-IPN hydrogels were synthesized as follows: CS [1 % w/v] was dissolved in an acid aqueous solution (50 mL of a [0.5 % v/v] acetic acid solution) in a 2-neck bottom-round glass reaction vessel. The CS solution was stirred (1500 rpm) for 24 h at room temperature (~ 23 ºC) to obtain a homogeneous viscous mixture (pH ~ 4.3). Afterwards 1 g of the monomer BVImCl and 16.51 mg of the cross-linker MBA (corresponding to 2 % on a molar basis of the total number of mols in 1 g of BVImCl) were added to the CS solution and stirred (1500 rpm) for 1 h at room temperature. The resulting homogeneous solution was sonicated for 30 min to remove any trapped air. The reaction vessel was connected to a condenser (- 0.1 ºC) and immersed in a thermostatic bath at 70 ºC under stirring (1500 rpm). The initiator, AIBA, was then added to the solution (3.0 mg corresponding to 0.2 % on a molar basis of the total number of mols in 1 g of BVImCl) which was further degassed bubbling nitrogen (for 1 min). The polymerization reaction was carried out for 8 h under nitrogen atmosphere. The resulting solution was cooled down by immersion in ice for 10 min, and poured into cylindrical molds (5 mL, 1.6 cm height × 2.2 cm diameter). Samples were then frozen at ~ - 20 ºC for 24 h and freeze-dried (Telstar, Lyoquest 85 plus, Spain) at - 80 ºC under vacuum (0.1 mPa) for 36 h. The resulting materials were washed in bi-distilled water (~ 2 L of fresh water replaced twice a day for 3 days) and further frozen and freeze-dried as described before.

The effect of a co-monomer on the final properties of the prepared s-IPN hydrogels was also addressed by following the same experimental procedure but now adding more 0.162 mL of the co-monomer HEMA (corresponding to 25 % on a molar basis of the total number of mols of BVImCl) to the CS + BVImCl solution. The amount of MBA and AIBA employed was maintained at 2 and 0.2 % in a molar basis, respectively but referring to the total number of mols of the co-monomers present in the reaction vessel (BVImCl+HEMA).

Additionally, s-IPN hydrogels comprised only by CS and poly(HEMA) (without BVImCl) were also synthesized by following the same experimental procedure. Briefly, 0.65 mL of the monomer HEMA (equivalent to the same number of mols in 1 g of BVImCl) was added to the previously prepared CS solution [1 % w/v] followed by the addition of MBA and AIBA (2 % and 0.2 % in a molar basis relatively to the total amount of mols of HEMA).

Hydrogel samples only comprised by CS were also obtained for comparison purposes. Briefly, CS [1 % w/v] was dissolved in the acetic acid solution (50 mL of a [0.5 % v/v] of acetic acid solution) by stirring (1500 rpm) for 24 h at room temperature and poured into cylindrical molds. As before, the samples were frozen at ~ - 20 ºC for 24 h and freeze-dried for 36 h. The resulting materials were deprotonated in a NaOH solution [1 M] for 1 h and then washed in bi-distilled water (~ 2 L of fresh water replaced twice a day for 3 days) and later frozen and freeze-dried as described before. For some analysis, the CS chains present in the s-IPN samples were also deprotonated following the same experimental procedure.

Resulting hydrogel samples were coded as: pristine chitosan deprotonated with NaOH as DCS; s-IPNs based on chitosan and poly(BVImCl) as s-IPN/CS/PIL; s-IPNs based on chitosan and poly(HEMA-co-BVImCl) as s-IPN/CS/Co-PIL and s-IPNs based on chitosan and poly(HEMA) as s-IPN/CS/poly(HEMA). s-IPNs whose CS chains were deprotonated were coded as s-IPN/DCS/PIL and s-IPN/DCS/Co-PIL.

4.3.3 Characterization of the prepared s-IPN hydrogels

4.3.3.1 Physicochemical properties

The chemical composition of the hydrogels was analyzed by elemental analysis based on the differential thermal conductivity method (Fisons Instruments, model EA1108 CHNS-O).

Solid-state ^{13}C nuclear magnetic resonance (NMR) spectra of the prepared hydrogels were obtained using a Bruker BioSpin GmbH spectrometer (188.5 Hz) at 0 ºC, 19541 scans and

high-powered decoupling (hpdec) pulse sequence with a pulse width of 1.575 μs. Acquisition time and relaxation delay were set as 0.05 and 2.5 s, respectively. Before ^{13}C-NMR measurements the freeze-dried samples were frozen in liquid nitrogen and milled with a pestle in a mortar to obtain a powder.

The charge density of all the prepared water swollen deprotonated hydrogels was assessed by zeta potential measurements in the cylindrical cell mode using an electrokinetic analyzer for solid materials (SurPASS from Anton Paar, GmbH). Measurements were performed using a KCl solution ([1.0 mM] and pH = 7.4) at room temperature (~ 23 ºC). All the experiments were performed in duplicate (8 measurements in each evaluation) under a pressure flow of 100 mbar. The charge density of the prepared hydrogels was also indirectly accessed by adsorption experiments of an anionic model molecule (methyl orange, MO, Mw = 327.33 g/mol) adsorption experiments. Freeze-dried hydrogels (~ 10 mg) were immersed in 10 mL of MO aqueous solution [1 M] and left in contact at room temperature (~ 23 ºC) for one week (168 h) in order to ensure that adsorption equilibrium was achieved. The molar concentration of MO present in the solution is in far excess when compared to the total number of cationic sites present in the polycationic hydrogels (based on elemental analysis results). The amount of MO removed by the hydrogels from the solution was quantified using a previously obtained calibration curve of MO in bi-distilled water ([MO] = 0.5402 × Abs, R^2 = 0.999). The pH of each solution was measured during sorption experiments (using a Standard pH meter, Meter Lab), since MO is pH sensitive. The experiments were performed in duplicate and the results were expressed in terms of $mmol_{sorbed\ MO}/mg_{freeze\text{-}dried\ hydrogel}$.

4.3.3.2 Thermomechanical properties

Hydrogels were frozen at - 20 ºC for 24 h and further freeze-dried at - 80 ºC under vacuum (0.1 mPa) for 36 h to reduce their residual water content. The thermal stability of all the

prepared hydrogels (~ 10 mg) was measured using a thermogravimetric analyzer (TGA Instruments, Q500, USA). Measurements were conducted from 25 ºC up to 600 ºC, at a heating rate of 10 ºC/min, under dry nitrogen atmosphere (40 mL/min). Differential scanning calorimetry (DSC) experiments were performed using a DSC-Q100 equipment from TA Instruments. After being freeze-dried samples (~ 7 mg) were immediately sealed in aluminum pans. Samples were heated (from 40 up to 150 ºC), cooled (from 150 down to - 80 ºC) and reheated (from - 80 up to 200 ºC) at 10 ºC/min under dry nitrogen atmosphere (50 mL/min) to remove their thermal history. Data was treated using TA Instruments Universal Analysis 2000 software (Version 4.2E) and the thermal events were identified based on the thermograms measured during the second heating run.

Rheological measurements were carried out using a temperature-controlled stress rheometer (ModelRS1, Haake, Vreden, Germany) with a cylindrical sensor system Z34 DIN connected to a temperature-controlled recirculation bath (Haake Phoenix II). Oscillatory shear mode experiments were performed at a constant shear stress of 100 Pa and frequency sweeps of 0.1 - 100 rad/s at 25 ºC. Before measurements, cylindrical samples (2 cm diameter and ~ 7 mm high) were swollen in bi-distilled water for 24 h. Water swollen samples were placed between the rotatory and the stationary surfaces separated by a fixed gap of 6 mm. Measurements were repeated at least twice for each sample.

4.3.3.3 Water sorption capacity of the s-IPN hydrogels in different aqueous media

The water sorption capacity (WSC) of all the prepared hydrogels was measured at 25 ºC in different aqueous media, presenting different pH and ionic strengths (I), namely in bi-distilled water; acetate buffer (pH = 4.3; I = 0.17 M), phosphate buffer saline (pH = 7.4; I = 0.17 M) and bicarbonate buffer (pH = 9.3; I = 0.17 M). Freeze-dried samples (~ 10 mg) were weighed and then immersed into 15 mL of each medium. At predefined time intervals, water swollen

samples were weighed (after removing the excess of surface water using a filter paper) and immersed again into the corresponding medium. This process was repeated at time intervals of 2 h (during the first 8 h), every 24 h (for the following 96 h) and every two weeks (for two months). The pH of each medium was checked during measurements (using a Standard pH meter, Meter Lab). The WSC capacity of the samples was calculated as the ratio between the weight of water absorbed at time *t* and the initial weight of the dried hydrogels (before immersion) and the results are presented in terms of $g_{water}/g_{freeze\text{-}dried\ hydrogel}$. Measurements were performed in duplicate.

4.3.3.4 adsorption capacity of the s-IPN hydrogels in different aqueous media

The capacity of the synthetized hydrogels to adsorb anionic molecules was accessed by employing bromocresol green (BG, Mw = 698.02 g/mol) as a model molecule. Freeze-dried samples (~ 10 mg) were immersed in 10 mL of BG aqueous solutions (15.8 g/L in bi-distilled water, PBS, and BB) and stored at room temperature (~ 23 ºC). Measurements were carried out after 24, 48 and 144 h of immersion and the results are expressed in terms of $g_{BG\ removed}/g_{freeze\text{-}dried\ hydrogel}$. The amount of BG removed from each solution by the polycationic hydrogels was quantified using a previously obtained calibration curve of BG in bi-distilled water ([BG] = 29.21 × Abs, R^2 = 0.998); in PBS ([BG] = 27.99 × Abs, R^2 = 0.997) and in BB ([BG] = 29.36 × Abs, R^2 = 0.998). Experiments were replicated twice.

4.3.3.5 Electro-assisted *in vitro* iontophoretic permeation/release kinetics of lidocaine hydrochloride

Electro-assisted permeation kinetics experiments were performed *in vitro* employing a thermostatized vertical Franz diffusion cell (SES GmbH - Analysesysteme, Germany) and Ag/AgCl electrodes which were prepared as follows: two Ag wires (12 cm length and 1 mm

thickness) were previously washed in a HNO_3 solution [0.1 M] and further immersed in a KCl solution [3 M]. An electrical tension of 10 V was applied during 4 h at room temperature (~ 23 ºC) using an electrophoresis power supply EPS 500/400 (Pharmacia Fine Chemicals, Sweden). After that period, the silver wire connected to the anode (positively charged electrode) presented a greyish color, resulting from the formation of an AgCl coating, while the silver wire connected to the cathode (negatively charged electrode) maintained its initial color (Ag electrode). Both Ag and AgCl electrodes were washed again in HNO_3 solution [0.1 M] and rinsed with bi-distilled water.

Before the experiments, freeze-dried hydrogels (~ 22 mg) were cut into disks (~ 1.6 cm diameter and ~ 2 mm thickness) and immersed in bi-distilled water for 24 h to guarantee water sorption equilibrium. Water swollen samples were placed in the donor compartment at the Franz cell and on the top of a dialysis membrane (non-charged regenerated cellulose membrane with molecular weight cutoff of 6000 - 8000 kDa), that was used as a support in between donor and receptor compartments. Permeation experiments employing only the dialysis membrane (without the hydrogels) were also performed as control. The effective diffusional surface area of the swollen samples was 1.76 cm^2. The receptor and the donor compartments of the Franz cell were then filled with 12 mL of bi-distilled water and 2.5 mL of a lidocaine hydrochloride (LH) solution (0.44 mg/mL corresponding to 5 % $wt_{LH}/wt_{freeze\text{-}dried\ hydrogel}$), respectively. The Ag electrode, connected to the anode of the electrophoresis power supply, was immersed in the donor compartment (1 cm above the sample) while the AgCl electrode, connected to the cathode of the electrophoresis power supply, was placed in the receptor compartment (Figure S4.2, Appendix C). Experiments were performed at 32 ºC (usually employed to simulate the temperature of the skin) and under constant stirring (300 rpm) of the receptor compartment. The donor compartment was sealed with parafilm to prevent solvent evaporation during the experiments. A constant electrical density of 0.56 mA/cm^2 was then applied over the

electrophoretic system and aliquots (0.5 mL) were withdrawn from the receptor compartment at time intervals of 5, 10, 15, 30, 60, 120 and 180 min for further LH quantification. The volume of the receptor compartment was maintained during the entire experiment by replacing each removed aliquot by fresh bi-distilled water (0.5 mL). The cumulative amount of permeated drug was analyzed by UV spectrometry (at 262 nm) and quantified using a previously obtained calibration curve of LH in bi-distilled water ([LH] = 0.7469 × Abs, R^2 = 0.999).

Electro-assisted LH release kinetics experiments were performed following a similar experimental procedure and experimental conditions however with some modifications. For these experiments freeze-dried hydrogels (~ 22 mg) were previously hydrated in 0.4 mL of a LH solution (2.75 mg/mL corresponding to 5 % $wt_{LH}/wt_{freeze\text{-}dried\ hydrogel}$) and the Ag electrode was placed in direct contact on top of the samples in the donor compartment. The volume of the LH solution that was employed was determined based on the water sorption capacity of the DCS hydrogels (which presented the lowest WSC among the synthesized hydrogels) and in order to guarantee that the LH solution is totally absorbed by all freeze-dried samples.

Passive LH permeation and release kinetic experiments were carried out following the same experimental procedure but without the application of the electrical stimulus. Both passive and electro-assisted permeation and release kinetic experiments were replicated at least twice.

4.3.3.6 Calculation of the release kinetic coefficients

LH release kinetic coefficients were calculated by the fitting experimental release curves using the Korsmeyer-Peppas equation:

$$\frac{M_t}{M_\infty} = kt^n \quad (1)$$

where M_t and M_∞ are the absolute cumulative amount of LH released from the hydrogels at time *t* and at infinite release time, respectively; *k* is the kinetic constant; and *n* is the release

exponent (which gives information on the involved released mechanisms).[83] This equation was applied for M_t/M_∞ values ranging from 10 up to 60 %.

When the drug is molecularly dispersed in the matrix, the Fick's second law of diffusion can be solved, allowing modeling the short-time (Eq. 2) and the long-time (Eq. 3) LH release periods:[83]

$$\frac{M_t}{M_\infty} = 4\left(\frac{tD_1}{l^2\pi}\right)^{1/2} \quad (2)$$

$$\frac{M_t}{M_\infty} = 4 - \frac{8}{\pi^2} exp\left(-\frac{t\pi D_2}{l^2}\right) \quad (3)$$

In these equations, *l* is the thickness of the sample and D_1 and D_2 are the short-time and the late-time diffusion coefficients, respectively, for each of the considered release periods, and which are assumed to be constant.[84,85] Equations 2 and 3 were applied for M_t/M_∞ values ranging from 10-60 % and 40-100 %, respectively.

4.3.3.7 Blood compatibility assays

Hemocompatibility experiments (*in vitro*) were carried out according to the International Standard Organization (ISO 10993-4) and as described in the American Society for Testing and Materials (ASTM) standard.[86] Samples with a surface area of 21 cm^2 were previously immersed in PBS for 24 h (to guarantee water sorption equilibrium). Water swollen samples were placed in falcon tubes and immersed in 7 mL of rabbit blood solution (1 mL of rabbit blood previously treated with ACD diluted in PBS at $[Hb]_{blood}$ = 10 ± 1 mg/mL). Negative and positive controls were obtained by adding the same amount of rabbit blood to 7 mL of PBS and bi-distilled water, respectively, without any sample. The tubes were incubated at 37 ºC for 3 h and carefully stirred manually twice every 60 min in order to assure the contact of the blood solution with the samples. The blood solution was then transferred to falcon tubes and centrifuged at 2200 rpm for 15 min using a centrifuge Z-366 HERMLE Labortechnik GmbH.

Later, 1 mL of the supernatant was removed and diluted in 1 mL of Drabkin's solution. The quantification of hemoglobin (Hb) released from red blood cells by hemolysis was determined from a previously obtained calibration curve of Hb in PBS ([Hb] = 1.4518 × Abs, R^2 = 1) at 540 nm using a UV-vis spectrophotometer (Jasco, model V-650, Japan). Hemolysis (in %) was calculated as follows:

$$Hemolysis\ (\%) = \frac{[Hb]_{sample} - [Hb]_{negative\ control}}{[Hb]_{positive\ control} - [Hb]_{negative\ control}} \quad (4)$$

According to the ASTM F756-00 2000 standard, materials are classified as non-hemolytic, slightly hemolytic, or hemolytic when the hemolysis index ranges between 0 - 2 %, 2 - 5 % and > 5 %, respectively. Hemocompatibility experiments were triplicated.

4.3.3.8 Blood clotting assays

Blood clotting experiments (*in vitro*) were carried out following previously reported methods[87,88] with some modifications. Briefly, freeze-dried samples were cut into squares (1 cm^2) and placed into 50 mL falcon tubes. Then, 200 μL of blood (previously treated with ACD) were carefully dropped onto the surface of the samples followed by the addition of 20 μL of $CaCl_2$ solution [0.2 M] to initiate the blood clotting process. Samples were incubated at 37 ºC for 10 min and then bi-distilled water (25 mL) was slowly poured into testing tubes to stop the coagulation process, while avoiding the destruction of the formed clots. The tubes were incubated in a thermoshaker (Laboshake Gerhardt) at 37 ºC and 30 rpm for 10 min. After contact with water, the Hb released from hemolyzed red blood cells that were not incorporated into the formed clots was measured at 540 nm (Abs_{sample}) in a UV-vis spectrophotometer (Jasco, model V-650, Japan).

The absorbance of ACD treated blood (200 μL) in 25 mL of bi-distilled water was used as control ($Abs_{control}$). The blood clotting index (BCI) of the studied samples was calculated as follows:

$$BCI\ (\%) = \frac{Abs_{sample}}{Abs_{control}} \times 100 \quad (5)$$

meaning that samples presenting higher hemostatic potential will have lower BCI values. Blood clotting experiments were triplicated.

The morphology of the formed clots was evaluated by scanning electron microscopy (SEM) analysis using a SEM microscope (Jeol, model JSM-530, Japan) at room temperature (25 ºC) and at 5 keV for gold-sputtered samples under argon atmosphere. Before analysis samples containing the clots were immersed in glutaraldehyde solution [5 % v/v] during 10 min for clots immobilization. These samples were then dehydrated by sequential immersion for 10 min in ethanol:bi-distilled water solutions at 25:75, 50:50, 75:25 and 100:0 ratios (v/v). Finally, the samples were dried overnight at room temperature (~ 23 ºC) to allow ethanol to evaporate. Samples without clots were processed following the same procedure and were used as controls for comparison purposes.

4.3.3.9 Statistical analysis

One-way ANOVA test was applied for the statistical analysis of data obtained in this work. Statistical significance was considered for *p*-values < 0.05.

4.4 Results and discussion

4.4.1 Physicochemical properties

IL-based s-IPNs (s-IPN/CS/PIL and s-IPN/CS/Co-PIL) obtained after synthesis and washing procedures were mechanically stable in water without any further treatment with NaOH. On the contrary, and as expected, CS-based hydrogels were stable only after being deprotonated in NaOH [1 M] for 1 h. Interestingly, s-IPN/CS/poly(HEMA) hydrogels disintegrate when immersed in water suggesting that the ionic vinylic monomer, BVImCl, has an important role

on the formation of a stable 3D cross-linked network of the synthetized materials (Movie S4.1, Appendix C).

The presence of BVImCl on the prepared s-IPNs was confirmed by the observed increase in the nitrogen content (~ 15 %) of these samples determined from elemental analysis when compared to pristine CS (Table S4.1, Appendix C), assuming that the same amount of CS (corresponding to an average nitrogen content of ~ 6.15 ± 0.09 %) was maintained in all samples. Zeta potential measurements were performed for s-IPNs treated with NaOH in order to permit a fair comparison with neat chitosan, which is only stable in aqueous media after NaOH treatment, as mentioned before. Obtained results show an increase in the charge density of the s-IPNs, when compared to deprotonated CS (DCS), according to the following sequence: + 5.79 ± 0.71 mV for s-IPN/DCS/Co-PIL; + 5.27 ± 0.81 mV for s-IPN/DCS/PIL and + 4.36 ± 1.28 mV for DCS (p-value < 0.05). The positive charges that were measured for DCS indicates that the deprotonation performed with NaOH was not complete. No statistical difference (p-value > 0.05) was observed between s-IPN/DCS/PIL and s-IPN/DCS/Co-PIL samples, however, the observed increase in the charge density of s-IPNs (20 – 30 %) clearly confirms the presence of the ionic liquid co-monomer on these samples and its effect on sample's charge. The presence of BVImCl and HEMA on s-IPN/DCS/Co-PIL was also confirmed by solid state ^{13}C-NMR measurements (Figure S4.3, Appendix C). The characteristic peaks of CS assigned to aliphatic carbons namely, C-2 (57.36 ppm), C-6 (60.88 ppm), C-5/C-3 (74.91 ppm), C-4 (83.16 ppm) and C-1 (108.89 ppm) are identified in Figure S4.3 (Appendix C) and they are in good agreement with previously published data.[89,90] Signals attributed to C-7 and C-8 were not detected due to the high deacetylation degree of the employed chitosan.[91] On the ^{13}C-NMR spectra of s-IPN/CS/Co-PIL the appearance of three new peaks were assigned to the methyl and carbonyl groups of HEMA (at 13.62 and 180.14 ppm, respectively)[92,93] and to the methylene groups of the butyl chain of BVImCl (at 23.57 ppm).[94,95]

Adsorption capacity assays towards a monovalent anionic molecule (methyl orange, MO) were also performed to indirectly confirm the higher charge density of the prepared s-IPNs. These assays were performed for deprotonated samples (previously treated with NaOH) in order to assure that the adsorption capacity of the s-IPNs would be essentially due to the cationic groups from the IL co-monomer (since the positively charged amine groups from CS present in the s-IPNs are suposed to be deprotonated after the NaOH treatment). Therefore, a comparison was done with deprotonated CS samples. Results show that the adsorption capacity of MO by the s-IPN hydrogels follows the trend: 0.76 ± 0.01 for s-IPN/DCS/PIL; 0.61 ± 0.07 for s-IPN/DCS/Co-PIL and 0.20 ± 0.02 $mmol_{adsorbed\ MO}/mg_{freeze\text{-}dried\ hydrogel}$ for DCS. These results confirm that the adsorption capacity of the NaOH treated s-IPN hydrogels is, at least, 3.0 × higher than that measured for deprotonated CS, and that this should result from the ionic interactions between the positively charged imidazolium ring and the negatively charged sulfonic group of MO. These results are even more impressive since we have found that DCS was in fact not completely deprotonated (as seen by zeta potential measurements). No statistical difference (p-value > 0.05) was observed between the adsorption capacity of s-IPN/DCS/PIL and s-IPN/DCS/Co-PIL hydrogels, which is in agreement with zeta potential results discussed above.

4.4.2 Water sorption capacity of the s-IPN hydrogels in different aqueous media

The water sorption capacity (WSC) of the s-IPNs (s-IPN/CS/PIL and s-IPN/CS/Co-PIL) was measured in different aqueous media (having different pH and ionic strengths) and the results were compared to those measured for deprotonated chitosan (DCS) (Figure 4.1). Samples immersed in bi-distilled water (pH = 6.5 and I ~ 0 M), in PBS (pH = 7.4 and I = 0.17 M) and in bicarbonate buffer (BB, pH = 9.3 and I = 0.17 M) attained water sorption equilibrium in ~ 2 h and presented structural stability in aqueous media for a period of at least one month (Movie

S4.2, Appendix C). As can be seen in Figure 4.1A, the WSC of s-IPNs when immersed in bi-distilled water is much higher than that measured for deprotonated CS. No significant difference (*p*-value > 0.05) was observed between s-IPN/CS/PIL and s-IPN/CS/Co-PIL samples. This result is most probably justified by the higher charge density of s-IPNs, as previously discussed in zeta potential measurements, which leads to an increase in the osmotic gradient between the polycationic hydrogel and the aqueous medium, as well as to an increase in electrostatic repulsions among equally charged groups present at the hydrogels structures (which also increases the free volume between chains). Both effects lead to an increase in the WSC of the polycationic hydrogels up to a certain limit (water sorption equilibrium) which also depends on the mechanical elastic response and on the cross-linking degree of the hydrogels.[67,96,97]

When hydrogels are immersed in PBS, the observed WSC values present the same trends observed for imersion in bi-distilled water although the sorption capacity values are now slightly lower. This happens because of the lower osmotic gradients between hydrogel networks and the aqueous medium, which leads the water diffusion into the hydrogel structures; and also due to charge screening effects induced by anions present in the buffer saline solutions which decrease the electrostatic cation-cation repulsions and decrease the ionic pressure gradient between the hydrogel and the medium.[96,97] At basic pH, the higher WSC measured for s-IPNs (almost twice that of deprotonated CS) should be just due to the above referred osmotic gradient effect originated by IL positive charges (which are pH independent).

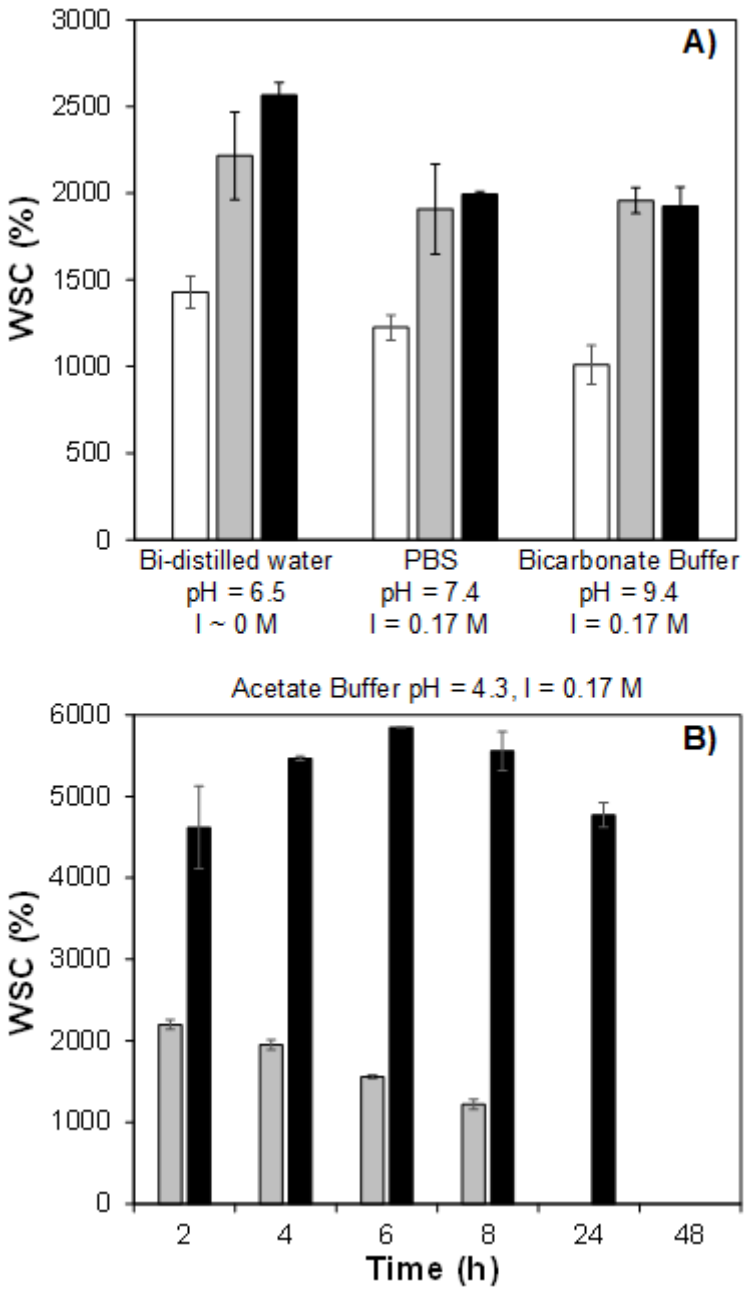

Figure 4.1 Water sorption capacity (WSC) of synthesized hydrogels at 25 ºC in different aqueous media: (A) Equilibrium water uptake capacity after 48 h of immersion in bi-distilled water (pH = 6.5, I ~ 0 M), PBS (pH = 7.4, I = 0.17 M) and Bicarbonate Buffer (pH = 9.4, I = 0.17 M); (B) Kinetic profile of the water sorption capacity of the hydrogels in Acetate Buffer (pH = 4.3, I = 0.17 M). Samples were coded as: DCS (□), s-IPN/CS/PIL (■) and s-IPN/CS/Co-PIL (■).

The WSC of the hydrogels when immersed in acidic medium (acetate buffer, pH = 3) is presented in Figure 4.1B. At low pH, DCS is not mechanically stable and it starts to dissolve immediately after immersion. This occurs due to the protonation of amino groups in acidic medium (below chitosan's pK_a), which increases the number of charges in hydrogel samples and the electrostatic repulsion between CS chains, leading to the expansion of the polymeric network beyond its elastic mechanical response, and ultimatly to CS dissolution. Similar behaviour was also observed for s-IPN/CS/PIL samples which started to lose weight after 2 h of immersion in acetate buffer. On the contrary, s-IPN/CS/Co-PIL hydrogels presented higher mechanical stability even at low pH. This happens, most probably, due to the existence of physical interactions (hydrogen bonding) between hydroxyl/amino groups from CS and hydroxyl groups from HEMA, which increase the physical cross-linking density between CS and the co-polymer chains, and consequently the mechanical stability of the s-IPN structure. Nevertheless, these samples started to lose mass after 6 – 8 h and presented complete dissolution in acidic aqueous medium between 24 – 48 h. It was also observed taht the WSC of s-IPN/CS/Co-PIL hydrogels in acidic medium was higher than that measured in bi-distilled water (~ 2 × higher). This happens because at low pH (below chitosan's pK_a), the charge density of the hydrogel increases (more amino groups from CS chains become protonated) which favors the water inflow into the hydrogels as discussed above.

4.4.3 Adsorption capacity of the s-IPN hydrogels in different aqueous media

The adsorption capacity of the prepared s-IPN hydrogels towards anionic molecules was studied in different pH and ionic strength conditions using bromocresol green (BG) as a negatively charged model molecule. Results presented in Figure S4.4 (Appendix C) clearly show that s-IPNs presented much higher BG adsorption capacity in all tested aqueous media when compared to deprotonated CS. No significant difference (p-value > 0.05) was observed

between the BG adsorption capacity of s-IPN/CS/PIL and s-IPN/CS/Co-PIL, which is in agreement with previously discussed zeta potential data. In bi-distilled water the BG adorption capacity of the s-IPNs was mainly governed by ionic interactions between cationic groups from the s-IPNs (NH_3^+ from CS and imidazolium cation from the IL monomer) and anionic groups from BG (which is di-anionic at pH higher than 4.7).[98] On the contrary, in the case of DCS, the BG adsorption capacity is only a function of the protonation/deprotonation mechanism of amine groups (which is merely a pH dependent process).

As pH increases, the protonated amino groups still present in DCS become deprotonated and therefore unable to interact ionically with BG. However, the BG adsorption capacity of the s-IPNs is still significant due to the pH independent cationic groups from poly(BVImCl) and poly(HEMA-co-BVImCl) present in their structure. Therefore, and despite a slight decrease in the BG adsorption capacity of the s-IPNs at higher pH values, it is still clearly higher than that observed for deprotonated CS.

4.4.4 Thermomechanical properties

The thermomechanical properties of the prepared s-IPNs were analyzed based on thermogravimetric, calorimetric, and rheological data (Table 4.1). The thermogravimetric profiles of the prepared hydrogels are presented in Figure S4.5 (Appendix C).

Table 4.1 Thermomechanical data measured for the prepared hydrogel samples.[a]

Samples	$Wt_{150\ ^oC}$ (%)[b]	$T_{5\%}$ (ºC)[c]	T_{onset} (ºC)[d]	T_{max} (ºC)[e]	G^* (Pa)[f]	tan δ
DCS	10.10 ± 0.42	57.27 ± 0.37	278.86 ± 0.11	298.35 ± 0.52	190.60 ± 30.55	0.80 ± 0.12
s-IPN/CS/PIL	9.34 ± 0.76	54.45 ± 0.49	239.76 ± 0.83	266.70 ± 1.27	1386.80 ± 49.57	0.19 ± 0.10
s-IPN/CS/Co-PIL	9.56 ± 0.06	57.25 ± 2.76	247.65 ± 2.19	281.45 ± 5.02	2366.00 ± 26.87	0.10 ± 0.01

[a]Parameters $Wt_{150\ ^oC}$ (%), $T_{5\%}$ (ºC), T_{onset} (ºC) and T_{max} (ºC) were measured by TGA; and complex shear modulus (G*) and loss factor (tan δ) were measured by rheology at 1 Hz;
[b]Weight loss (%) at 150 ºC;
[c]Temperature at which hydrogels's weight loss is 5 % (wt);
[d]Temperature at which hydrogels's thermal degradation initiates;
[e]Maximum degradation temperature obtained by DTG profiles obtained from the first derivative of the weight loss vs temperature profile (Figure S4.5, Appendix C);
[f]Calculated according to the literature.[99]

Results shows that all the samples present an initial weight loss (~ 9.6 %) up to 100 ºC, which was attributed to the evaporation of bounded water, and a second degradation step in the range 250 - 300 ºC, which can be attributed to chitosan's thermal degradation.[100,101] Moreover, it was observed that the thermal degradation temperature of s-IPNs (in terms of T_{onset} and T_{max}) was lower (p-value < 0.05) than that measured for deprotonated CS (Table 4.1). This result suggests that the presence of the co-polymer structure between CS chains may somehow affect inter-chain interactions characteristic of pristine CS, and consequently decrease its thermal stability.[100,101] From the calorimetric profiles (Figure S4.5, Appendix C) it is possible to observe that only s-IPNs present glass transition temperatures (T_g) at 31.5 ± 0.6 ºC for s-IPN/CS/PIL and 43.9 ± 4.1 ºC for s-IPN/CS/Co-PIL samples, which were atributed to the poly(BVImCl) and poly(HEMA-co-BVImCl) networks, respectively.

The mechanical stability of the prepared hydrogels was accessed based on the viscoelastic properties of the swollen hydrogels (Figure 4.2). Based on stress sweep measurements (left column in Figure 4.2) it is possible to observe that the critical strain measured for s-IPNs (when the storage modulus, G', crossovers the loss modulus, G'', indicating that the 3D structure of s-IPNs is irreversible deformed) is higher than that measured for deprotonated CS. These results clearly show that s-IPNs present higher mechanical stability (support higher mechanical loads) than deprotonated CS. In fact, s-IPN/CS/Co-PIL is mechanically stable over the entire applied range. Oscillatory frequency sweep tests were performed within the linear viscoelastic region of the hydrogels, at 100 Pa (value defined based on deprotonated CS results, corresponding to ~ 50 % strain). Obtained results (right column in Figure 4.2) show that all the hydrogels present typical frequency dependent gel-like behavior where G' > G'' and tan δ < 1 converging to a plateau. The crossover point measured for s-IPNs is attained at frequencies that are almost twice (10.4 rad/s) to that measured for deprotonated CS (4.8 rad/s).

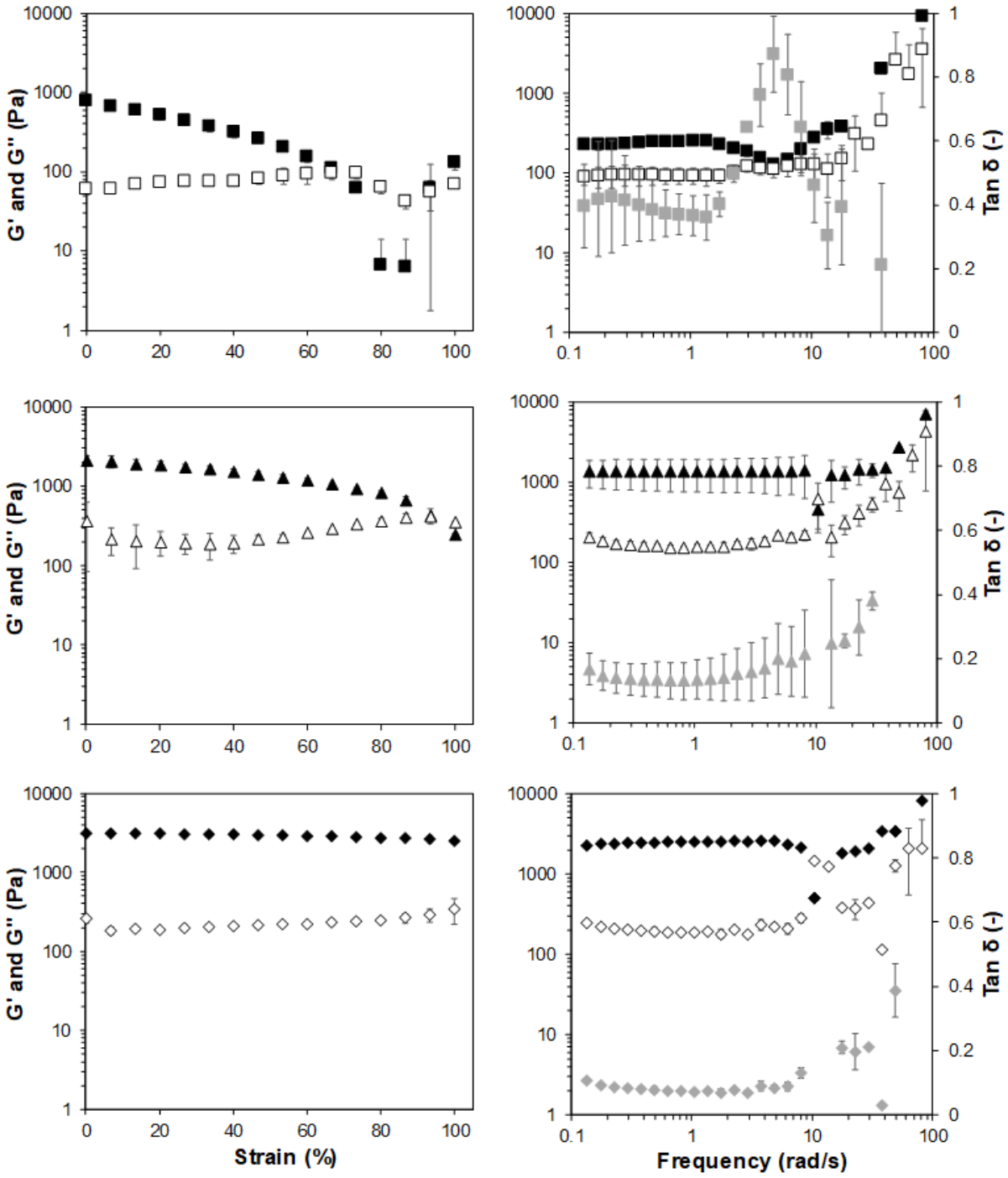

Figure 4.2 Viscoelastic properties of water swollen hydrogels (at equilibrium) measured at 25 ºC. Stress and frequency sweep measurements are represented in left and right columns, respectively. Samples were coded as: DCS (squares), s-IPN/CS/PIL (triangles) and s-IPN/CS/Co-PIL (diamonds). Storage modulus (G'), loss modulus (G'') and loss factor (tan δ) are represented as filled, open and grey symbols, respectively.

Moreover, and based on storage and loss modulus values, s-IPNs and deprotonated CS can be classified as strong hydrogels (G''/G' ratios closer to 0.1) and weak hydrogels (G''/G' ratios significantly greater than 0.1), respectively.[102] The complex shear modulus (G*) and loss factor or loss tangent (tan δ) were also evaluated at 1 Hz and the results are presented in Table 4.1. The higher G* values obtained for s-IPNs again confirm the higher resistance to plastic deformation in response to a mechanical loading of these samples when compared to deprotonated CS. Moreover, the G* determined for s-IPN/CS/Co-PIL is significantly higher than that of s-IPN/CS/PIL. This means that the presence of the comonomer HEMA enhances the mechanical resistance of the s-IPN/CS/Co-PIL when subjected to a mechanical load, most probably due to the existance of physical interactions between hydroxyl groups from HEMA, as previously discussed.

4.4.5 Electro-assisted *in vitro* iontophoretic permeation/release kinetics of lidocaine hydrochloride

The electro-assisted iontophoretic permeation/release kinetics of lidocaine hydrochloride (LH) were measured at 32 ºC. LH is a positively charged model drug at the employed experimental conditions (pK_a = 7.16)[103] which is commonly used as an anesthetic.[104] Results were compared with those obtained without the electrical stimulus (passive permeation/release kinetic studies). The effect of the electrical stimulus onto LH permeation kinetics through the cationic hydrogels is shown in Figure 4.3A. Results clearly show that LH permeation rates are significantly higher when the electrical stimulus is applied. It is hypothesized that for passive experiments, the main mechanism governing LH permeation is diffusion, resulting from drug concentration gradients between the donor and the receptor compartments of the Franz cell. On the contrary, for electro-assisted experiments, LH permeation is mainly governed by the electro-repulsion mechanism that favors LH diffusion from the positively charged electrode, in the donor compartment, to

the negatively charged electrode in the receptor compartment of the Franz cell. Moreover, under electrical stimulus, the LH permeated amounts clearly depend on the employed hydrogel, while similar permeation rates were observed for all hydrogels under passive permeation. This result indicates that in addition to LH/electrode repulsion, LH/hydrogel repulsions are also affecting drug permeation through the hydrogel matrices. When comparing LH permeation results obtained for the positively charged hydrogels and for the non-charged dialysis membrane used as control, it is possible to further confirm the effect of LH/cationic hydrogel repulsions over LH permeation rates (Figure 4.3A). This result is also in agreement with previously reported literature stating that the permeation of ionic species through charged membranes in aqueous environments depends of their charge density. Membranes having higher charge densities tend to strongly repel alike charged ions via electrostatically interactions.[105]

The effect of the hydrogel charge density over LH permeation kinetics was most noticed for the s-IPN/CS/PIL sample, meaning that high charge density of this sample hinders the diffusion of cationic LH through its network, via electrostactic repulsions, leading to slower LH permeation rates under electrical stimulus. More studies have to be performed to understand the higher LH permeation rates observed for s-IPN/CS/Co-PIL, when compared to s-IPN/CS/PIL and after 1 h, since the LH permeation rates of both hydrogels were expected to be similar considering that they have similar charge densities (based on zeta potential data). At present it is hypothesized that the presence of the co-monomer HEMA, employed as a spacer, may somehow attenuate (dilute) the frequency of the LH/hydrogel electrostatic interactions, which ultimately results in a faster LH permeation through the s-IPN/CS/Co-PIL network.

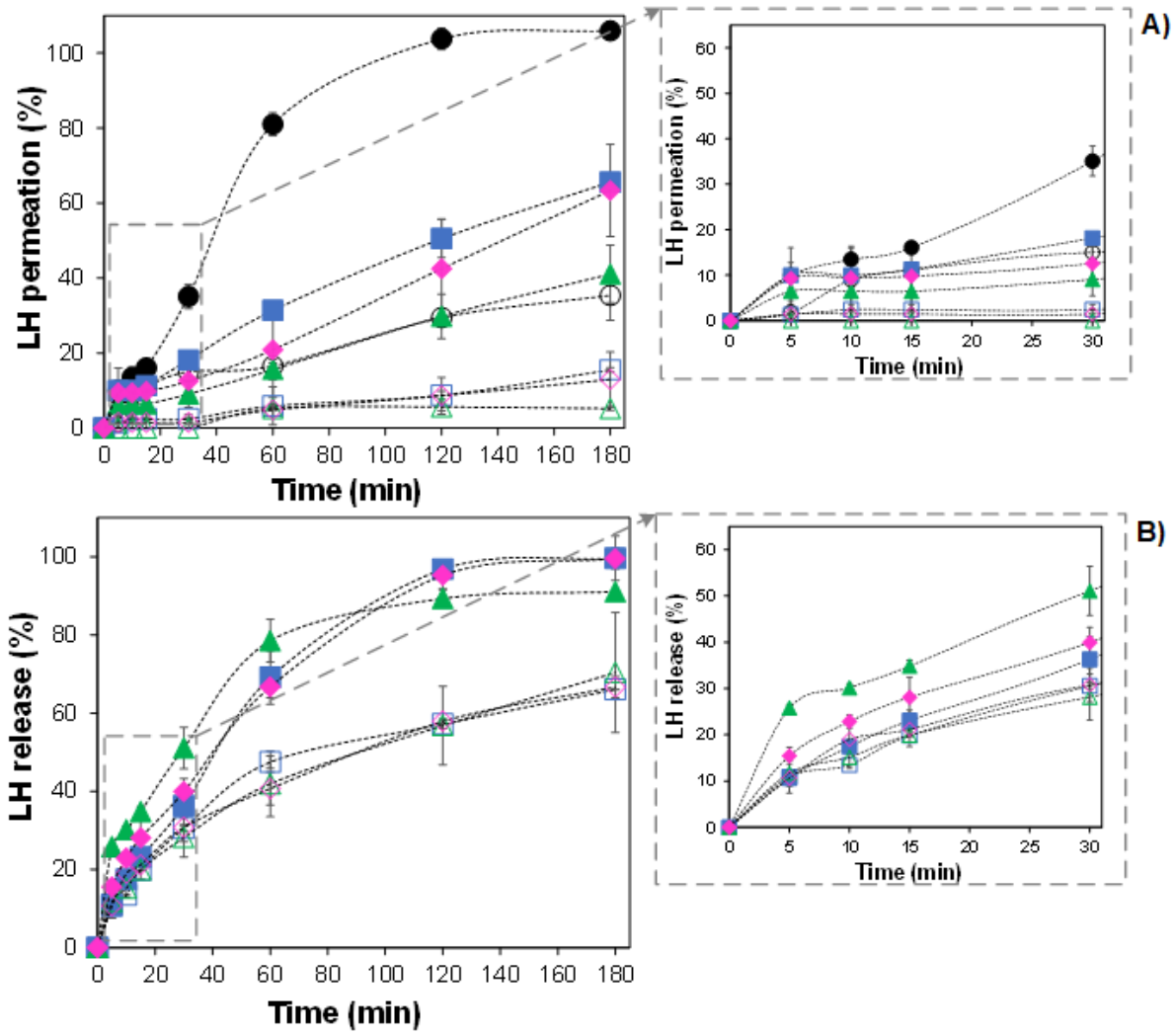

Figure 4.3 Iontophoretic lidocaine hydrochloride permeation (A) and release (B) kinetic studies in bi-distilled water at 32 ºC. Samples were coded as: Dialysis membrane (●), deprotonated CS (■), s-IPN/CS/PIL (▲) and s-IPN/CS/Co-PIL (◆). Passive (0 mA/cm^2) and anodal electro-assisted (0.56 mA/cm^2) experiments are represented as open and filled symbols, respectively.

The effect of the electrical stimulus on the LH release kinetics from the prepared hydrogels is shown in Figure 4.3B. Results again clearly show that under electrical stimulus (0.56 mA/cm^2), the release rates and the amounts of LH released from the prepared s-IPN hydrogels are significantly higher than that observed under passive release (0 mA/cm^2). This result might be explained again by the electrostatic repulsions that are established between the positively

charged hydrogel network and the charged drug which ultimately results in higher LH released amounts (for the same releasing period). Similar results were previously reported for the electro-assisted release of cationic drugs (including lidocaine hydrochloride) from different chitosan gel formulations.[106-108] Authors suggested that chitosan gel formulations having higher deacetylation degrees (thus presenting higher charge density) led to higher drug release rates due to higher matrix-drug electrostatic repulsions.[106]

The LH release kinetics were fitted to Eq.s 1, 2 and 3 and the results are presented in Table 4.2. Obtained results confirm that significantly higher release rate constant (k) and short-time (D_1) and long-time (D_2) difusion coefficients were observed when hydrogels were subjected to external electrical stimulus. When considering fitting results obtained from Eq. 1 it can be obversed that similar k values were observed for all the hydrogels when subjected to passive ($k \sim 0.41\ h^{-n}$) and electro-assisted ($k \sim 0.64\ h^{-n}$) LH release experiments.

Table 4.2 Release kinetic parameters (*n* and *k*) and diffusion coefficients (D_1 and D_2) correlated from Eq.s 1and 2-3, respectively, for passive (0 mA/cm^2) and electro-assisted (0.56 mA/cm^2) iontophoretic release of LH from the prepared hydrogels.

Stimulus	**Hydrogels**	**Kinetic parameters**			**Diffusion coefficients (cm^2/h)**			
		n	$k\ (h^{-n})^{-1}$	R^2	$D_1 \times 10^{-4}$	R^2	$D_2 \times 10^{-4}$	R^2
0 mA/cm^2	DCS	0.54 ± 0.06	0.41 ± 0.01	0.97	7.11 ± 0.30	0.98	4.97 ± 0.37	0.99
	s-IPN/CS/PIL	0.51 ± 0.05	0.40 ± 0.07	0.99	7.41 ± 3.06	0.99	6.82 ± 2.24	0.99
	s-IPN/CS/Co-PIL	0.49 ± 0.02	0.41 ± 0.03	0.98	6.71 ± 0.02	0.99	6.58 ± 0.15	0.97
0.56 mA/cm^2	DCS	0.74 ± 0.08	0.65 ± 0.04	0.99	19.0 ± 0.93	0.96	35.1 ± 5.11	0.98
	s-IPN/CS/PIL	0.38 ± 0.07	0.63 ± 0.09	0.95	25.6 ± 4.60	0.99	16.3 ± 1.94	0.99
	s-IPN/CS/Co-PIL	0.58 ± 0.06	0.63 ± 0.04	0.98	19.1 ± 0.49	0.98	30.6 ± 3.90	0.99

Moreover, and based on *n* values fitted from Eq. 1, it is possible to conclude that, for passive release experiments, LH release is mainly governed by Fickian diffusion ($n \sim 0.5$), while anomolous (non-Fickian) diffusion mechanisms ($0.5 < n < 1.0$) seems to govern the LH release from DCS and s-IPN/CS/Co-PIL hydrogels, under electrical stimulus.[83] It is important to refer that the LH release kinetis measured for the s-IPN/CS/PIL hydrogel is not acuratly fitted by Eq. 1 ($R^2 = 0.95$ and $n < 0.5$). This result indicates that, besides the electrical stimulus, the s-IPN/CS/PIL network (its chemical composition, charge distribution, morphological structure, etc.) may also have an important impact on the LH release kinetics. This hypothesis is in agreement with previously discussed LH permeation data and it is also supported by the fitting results obtained from Eq.s 2 and 3 (Table 4.2). These results show the the release kinetics measured for the s-IPN/CS/PIL sample presents a faster short-time LH release period (up to 60 % of the LH released, $t < 40$ min) and a slower long-time LH release period when compared to the other hydrogel samples (DCS and s-IPN/CS/Co-PIL).

Finally, it is important to refer that LH permeation and release kinetic experiments were performed using aqueous solutions of the drug in order to better understand the mechanisms involved in each process. Nevertheless, in the presence of saline and/or more acidic/basic solutions, s-IPNs will have a clear additional advantage over deprotonated CS, mainly in terms of mechanical stability, as discussed before.

4.4.6 Blood compatibility

Before discussing blood compatibility results, it is important to refer that the cytocompatibility of copolymers based on HEMA and BVImCl was already reported in the literature.[67] Obtained results showed that these materials present high cell viabilities (~100%) against Balb/3T3 fibroblasts. It is also already known that ionic liquids bearing short alkyl chain lengths (carbon number lower than six) and chloride counter ions, as is the case of the BVImCl, tend to be less

toxic.[109,110] Moreover, the polymerization of IL-based monomers is known to further decrease their cytotoxicity.[111] There are other recent works reported in the literature stating the low toxicity of IL-based polymers[112-114] and which support their potential to be employed for biomedical applications, for instance as wound dressings. In another hand chitosan has been extensively studied and employed for different biomedical and pharmaceutical applications, including as wound dressing materials, due to its inherent biocompatibility, antibacterial, hemostatic, and healing properties.[115-117] Having this in mind, it is reasonable to assume that the prepared semi-IPNs also present low cytotoxicity.

In vitro blood compatibility assays were employed to evaluate the hemolytic capacity of the prepared s-IPNs. Results in Figure 4.4A show that s-IPNs are non-hemolytic and present excellent blood compatibility since they present hemolytic indexes lower than 0.2 %, which is far below the hemolytic limit (2 - 5 %).

These results show that neither poly(BVImCl) nor poly(HEMA-co-BVImCl), at the employed relative chemical compositions, seem to affect the blood compatibility of the synthetized s-IPNs, which was similar to that usually observed for CS-based biomaterials such as chitosan-coated diatoms[118] and chitosan/heparin polyelectrolyte scaffolds.[119]

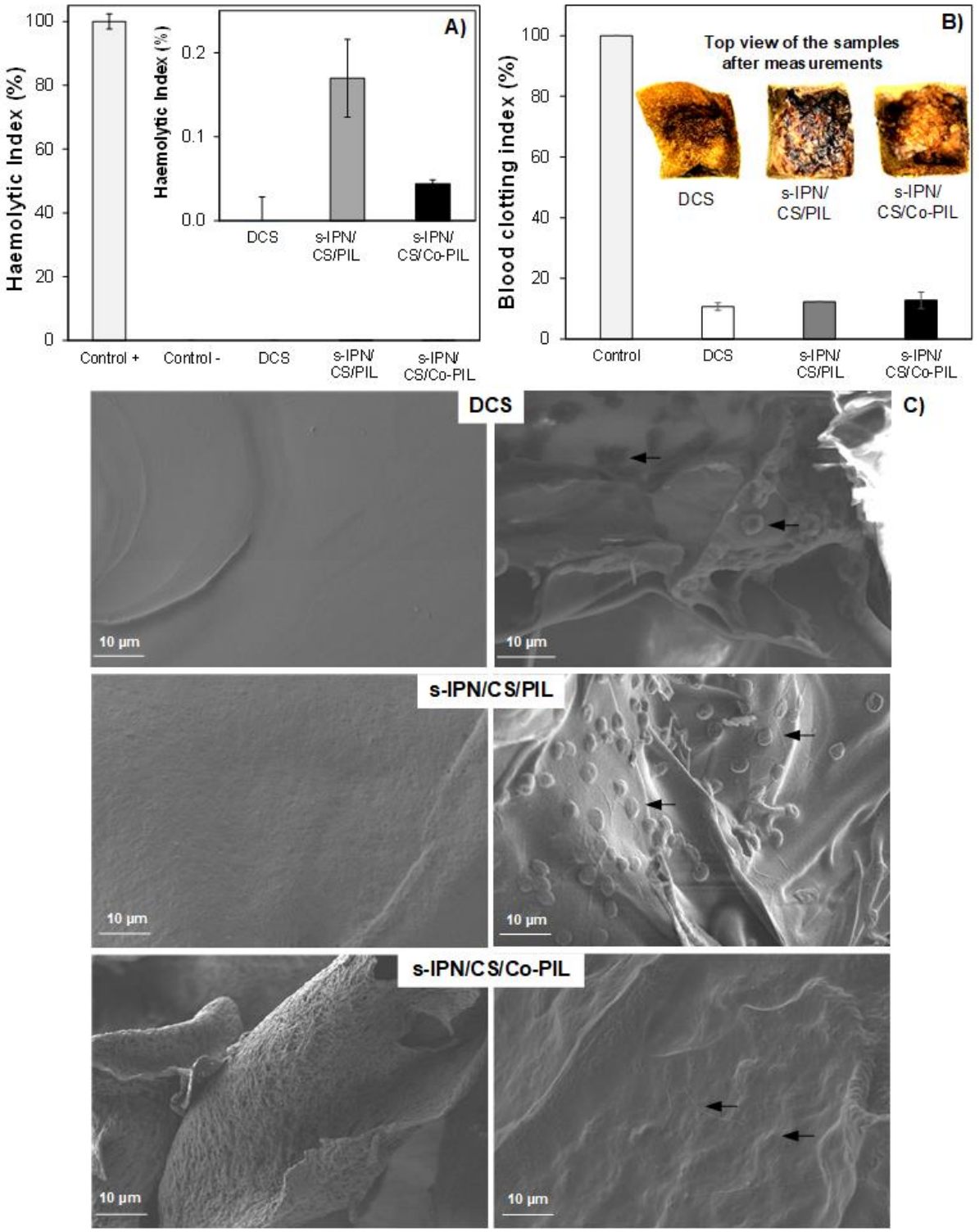

Figure 4.4 Hemolytic indexes (A) and blood clotting indexes (B) of the prepared hydrogels and SEM micrographs at the cross-section of pristine hydrogels (left column) and of hydrogels containing coagulated red blood cells (right column) (C).

The hemostatic capacity of the s-IPNs was also evaluated by whole blood clotting experiments and the results are presented in Figure 4.4B. Strong hemostatic potential (BCI ~ 12 ± 1 %) were observed for all tested hydrogels. This result indicates that the hydrogels were able to efficiently bind red blood cells, preventing them to be leached out into bi-distilled water, which would result in cell membrane rupture (lyse). Moreover, the blood clotting indexes observed in the present work were significantly lower than other previously measured for other CS-based hemostatic systems[87,120] which may addicionally indicate that the synthesized s-IPNs present promissing biomedical applications as biocompatible hemostatic wound patches/dressings. In addition, and despite similar BCI values were obtained for s-IPNs and for deprotonated CS samples, SEM micrographs permitted to identify some fibrin residues only at s-IPN samples, which may indicate that the blood clotting process was more efficient on these samples. Finally, in Figure 4.4C it is possible to observe that red blood cells attached to the s-IPN/CS/PIL hydrogel maintained their typical oval biconcave shape, which is an indication that these cells were not affected by the presence of the monomer BVImCl in the s-IPN network.

4.5 Conclusions

This work shows that IL-based s-IPNs can be used to change and tune several properties of chitosan-based hydrogels, including their thermomechanical properties, water swelling capacity and stability in different aqueous media, responsiveness to electrical stimulus, electronic conductivity and thrombogenic activity. The prepared s-IPNs presented high structural stability, without any further neutralization step, in aqueous media in the pH range between 6.5 and 9.4 and ionic strengths up to 0.17 M. The s-IPN/CS/Co-PIL was even stable in acidic medium (pH = 4.3) for at least 6 h. These results show that the prepared s-IPNs can be employed in different biological media for different pharmaceutical and biomedical applications. Rheological measurements allowed to conclude that the presence of the

comonomer HEMA on the s-IPN structure improved the mechanical stability of the s-IPN/CS/Co-PIL, which was able to support stress loads of, at least, 100 Pa. The observed increase in the charge density of the s-IPNs, even at basic pH, improved their capacity to remove anionic molecules from different aqueous media having different pH and ionic strengths. All the prepared hydrogels were sensitive to external electrical stimulus, at the tested experimental conditions, and therefore they presented higher electro-assisted permeation and release rates and amounts of lidocaine hydrochloride (used as a cationic model drug) and when compared with passive permeation/release experiments. Obtained results also showed that electro-assisted LH permeation and release rates/amounts were not only affected by the applied elecrical stimulus but also by the employed hydrogel. Among the tested samples, s-IPN/CS/PIL presented more sustained LH permeation and long-time release rates, when compared to the other tested hydrogels. Finally, the prepared s-IPNs were non-hemolytic and present strong hemostatic capacity. All together the results obtained in this work permit to conclude that the prepared s-IPNs, which combine chitosan and IL-based homopolymers and/or IL/HEMA-based co-polymers, present promising electrochemical, physicochemical, mechanical and biological properties which may be advantageous for the design and development of several pharmaceutical and biomedical apllications, namelly iontophoretic patches, wound healing dressings and/or hemostatic devices.

4.6 Acknowledgements

This work was financially supported by Fundação para a Ciência e Tecnologia (FCT-MEC) under contracts UID/EQU/00102/2019 and UIDB/00285/2020. A.M.A. Dias acknowledges FCT-MEC for a contract under the program Investigador FCT IF/00455/2013 and under the program Stimulus of Scientific Employment - Individual Support, CEECIND/01248/2017. A. F. Kanaan acknowledges CNPq, Brazil, for the scholarship with reference 200808/2014-1. The

authors also acknowledge Dr. Fernando Augusto Pinto Garcia for providing the electrophoresis power supply EPS 500/400 (Pharmacia Fine Chemicals, Sweden) and Dr. Rui Ferreira for providing fresh rabbit blood at Coimbra College of Agriculture (Escola Superior Agrária de Coimbra, ESAC-IPC).

4.7 References

(1) Benson, H. A. E. Skin Structure, Function, and Permeation in *Topical and Transdermal Drug Delivery: Principles and Practice*, (Eds: Benson, H. A. E.; Watkinson, A. C.), John Wiley & Sons, Inc., Hoboken, United States, Ch. 1, **2012**.

(2) Lane, M. E.; Santos, P.; Watkinson, A. C.; Hadgraft, J. Passive Skin Permeation Enhancement in *Topical and Transdermal Drug Delivery: Principles and Practice*, (Eds: Benson, H, A. E.; Watkinson, A. C.), John Wiley & Sons, Inc., Hoboken, United States, Ch. 2, **2012**.

(3) Dobler, D.; Schmidts, T.; Klingenhöfer, I.; Runkel, F. Ionic liquids as ingredients in topical delivery systems. *International Journal of Pharmaceutics* **2013**, *441*, 620-627.

(4) Monti, D.; Egiziano, E.; Burgalassi, S.; Chetoni, P.; Chiappe, C.; Sanzone, A.; Tampucci, S. Ionic liquids as potential enhancers for transdermal drug delivery. *International Journal of Pharmaceutics* **2017**, *516*, 45-51.

(5) Tanner, E. E. L.; Ibsen, K. N.; Mitragotri, S. Transdermal insulin delivery using choline-based ionic liquids (CAGE). *Journal of Controlled Release* **2018**, *286*, 137-144.

(6) Seah, B. C. -Q.; Teo, B. M. Recent advances in ultrasound-based transdermal drug delivery. *International Journal of Nanomedicine* **2018**, *13*, 7749-7763.

(7) Murthy, S. N.; Sammeta, S. M.; Bowers, C. Magnetophoresis for enhancing transdermal drug delivery: Mechanistic studies and patch design. *Journal of Controlled Release* **2010**, *148*, 197-203.

(8) Waghule, T.; Singhvi, G.; Dubey, S. K.; Pandey, M. M.; Gupta, G.; Singh, M.; Dua, K. Microneedles: A smart approach and increasing potential for transdermal drug delivery system. *Biomedicine & Pharmacotherapy* **2019**, *109*, 1249-1258.

(9) Shi, J.; Ma, Y.; Zhu, J.; Chen, Y.; Sun, Y.; Yao, Y.; Yang, Z.; Xie, J. A Review on Electroporation-Based Intracellular Delivery. *Molecules* **2018**, *23*, 3044.

(10) Moghimi, H. R.; Alinaghi, A. Microwaves as a Skin Permeation Enhancement Method in *Percutaneous Penetration Enhancers, Physical Methods in Penetration Enhancement*, (Eds: Dragicevic, N.; Maibach, H. I.), Springer-Verlag, Berlin, Germany, Ch. 10, **2017**.

(11) Sá, G. F. F.; Serpa, C.; Arnaut, L. G. Photoacoustic Waves as Skin Permeation Enhancement Method in *Percutaneous Penetration Enhancers, Physical Methods in Penetration Enhancement*, (Eds: Dragicevic, N.; Maibach, H. I.), Springer-Verlag, Berlin, Germany, Ch. 11, **2017**.

(12) Gratieri, T.; Kalia, Y. N. Iontophoresis: Basic Principles Method in *Percutaneous Penetration Enhancers, Physical Methods in Penetration Enhancement*, (Eds: Dragicevic, N.; Maibach, H. I.), Springer-Verlag, Berlin, Germany, Ch. 4**, 2017**.

(13) Byrne, J. D.; Yeh, J. J.; DeSimone, J. M. Use of iontophoresis for the treatment of cancer. *Journal of Controlled Release* **2018**, *284*, 144-151.

(14) Grice, J. E.; Prow, T. W.; Kendall, M. A. F.; Roberts, M. S. Electrical and Physical Methods of Skin Penetration Enhancement in *Topical and Transdermal Drug Delivery: Principles and Practice*, (Eds: Benson, H. A. E.; Watkinson, A. C.), John Wiley & Sons, Inc., Hoboken, United States, Ch. 3, **2012**.

(15) Kalia, Y. N.; Naik, A.; Garrison, J.; Guy, R. H. Iontophoretic drug delivery. *Advanced Drug Delivery Reviews* **2004**, *56*, 619-658.

(16) Guy, R. H.; Kalia, Y. N.; Delgado-Charro, M. B.; Merino, V.; López, A.; Marro, D. Iontophoresis: electrorepulsion and electroosmosis. *Journal of Controlled Release* **2000**, *64*, 129-132.

(17) Karpiński, T. M. Selected Medicines Used in Iontophoresis. *Pharmaceutics* **2018**, *10*, 204.

(18) Roustit, M.; Blaise, S.; Cracowski, J.-L. Trials and tribulations of skin iontophoresis in therapeutics. *British Journal of Clinical Pharmacology* **2013**, *77*, 63-71.

(19) Petrilli, R.; Lopez, R. F. V. Physical methods for topical skin drug delivery: concepts and applications. *Brazilian Journal of Pharmaceutical Sciences* **2018**, *54*, e01008.

(20) Zhang, Y.; Yu, J.; Kahkoska, A. R.; Wang, J.; Buse, J. B.; Gu, Z. Advances in Transdermal Insulin Delivery. *Advanced Drug Delivery Reviews* **2019**, *139*, 51-70.

(21) Iqbal, B.; Ali, J.; Baboota, S. Recent advances and development in epidermal and dermal drug deposition enhancement technology. *International Journal of Dermatology* **2018**, *57*, 646-660.

(22) Münch, S.; Wohlrab, J.; Neubert, R. H. H. Dermal and transdermal delivery of pharmaceutically relevant macromolecules. *European Journal of Pharmaceutics and Biopharmaceutics* **2017**, *119*, 235-242.

(23) Ita, K. Transdermal iontophoretic drug delivery: advances and challenges. *Journal of Drug Targeting* **2015**, *24*, 386-391.

(24) Marwah, H.; Garg, T.; Goyal, A. K.; Rath, G. Permeation enhancer strategies in transdermal drug delivery. *Drug Delivery* **2016**, *23*, 564-578.

(25) Wong, T. W. Electrical, magnetic, photomechanical and cavitational waves to overcome skin barrier for transdermal drug delivery. *Journal of Controlled Release* **2014**, *193*, 257-269.

(26) Schoellhammer, C. M.; Blankschtein, D.; Langer, R. Skin Permeabilization for Transdermal Drug Delivery: Recent Advances and Future Prospects. *Expert Opinion on Drug Delivery* **2014**, *11*, 393-407.

(27) Hao, J. Topical iontophoresis for local therapeutic effects. *Journal of Drug Delivery Science and Technology* **2014**, 24, 255-258.

(28) Pandey, P. C.; Shukla, S.; Skoog, S. A.; Boehm, R. D.; Narayan, R. J. Current Advancements in Transdermal Biosensing and Target Drug Delivery. *Sensors* **2019**, 19, 1028.

(29) Pazin, C.; Mitidieri, A. M. S.; Silva, A. P. M.; Gurian, M. B. F.; Poli-Neto, O. B.; Rosa-e-Silva, J. C. Treatment of bladder pain syndrome and interstitial cystitis: a systematic review. *International Urogynecology Journal* **2016**, 27, 697-708.

(30) Gratieri, T.; Santer, V.; Kalia, Y. N. Basic principles and current status of transcorneal and transscleral iontophoresis. *Expert Opinion on Drug Delivery* **2017**, 14, 1091-1102.

(31) Gote, V.; Sikder, S.; Sicotte, J.; Pal, D. Ocular Drug Delivery: Present Innovations and Future Challenges. *Journal of Pharmacology and Experimental Therapeutics* **2019**, 370, 602-624.

(32) Jung, J. H.; Chae, J. J.; Prausnitz, M. R. Targeting drug delivery within the suprachoroidal space. *Drug Discovery Today* **2019**, 24, 1654-1659.

(33) Madni, A.; Rahem, M. A.; Tahir, N.; Sarfraz, M.; Jabar, A.; Rehman, M.; Kashif, P. M.; Badshah, S. F.; Khan, K. U.; Santos, H. A. Non-invasive strategies for targeting the posterior segment of eye. *International Journal of Pharmaceutics* **2017**, 530, 326-345.

(34) Wanasathop, A.; Li, S. K. Iontophoretic Drug Delivery in the Oral Cavity. *Pharmaceutics* **2018**, 10, 121.

(35) Gianolla, L. I.; Sutera, F. M.; De Caro, V. Physical methods to promote drug delivery on mucosal tissues of the oral cavity. *Expert Opinion on Drug Delivery* **2013**, 10, 1449-1462.

(36) Şenel, S.; Rathbone, M. J.; Cansiz, M.; Pather, I. Recent developments in buccal and sublingual delivery systems. *Expert Opinion on Drug Delivery* **2012**, 9, 615-628.

(37) Franz-Montan, M.; Ribeiro, L. N. M.; Volpato, M. C.; Cereda, C. M. S.; Groppo, F. C.; Tofoli, G. R.; de Araújo, D. R.; Santi, P.; Padula, C.; de Paula, E. Recent advances and perspectives in topical oral anesthesia. *Expert Opinion on Drug Delivery* **2017**, 14, 673-684.

(38) Shanbhag, P. P.; Jani, U. Drug delivery through nails: Present and Future. *New Horizons in Translational Medicine* **2017**, 3, 252-263.

(39) Saner, M. V.; Kulkarni, A. D.; Pardeshi, C. V. Insights into drug delivery across the nail plate barrier. *Journal of Drug Targeting* **2014**, 22, 769-789.

(40) Shivakumar, H. N.; Juluri, A.; Desai, B. G.; Murthy, S. N. Ungual and Transungual drug delivery. *Drug Development and Industrial Pharmacy* **2012**, 38, 901-911.

(41) Rawat, S.; Vengurlekar, S.; Rakesh, B.; Jain, S.; Srikarti, G. Transdermal Delivery by Iontophoresis. *Indian Journal of Pharmaceutical Sciences* **2008**, 70, 5-10.

(42) Zhu, H.; Li, S. K.; Peck, K. D.; Miller, D. J.; Higuchi, W. I. Improvement on conventional constant current DC iontophoresis: a study using constant conductance AC iontophoresis. *Journal of Controlled Release* **2002**, 82, 249-261.

(43) Bhatia, G.; Banga, A. K. Effect of Modulated Alternating and Direct Current Iontophoresis on Transdermal Delivery of Lidocaine Hydrochloride. *BioMed Research International* **2014**, 537941, 1-6.

(44) Chansai, P.; Sirivat, A.; Niamlang, S.; Chotpattananont, D.; Viravaidya-Pasuwat, K. Controlled transdermal iontophoresis of sulfosalicylic acid from polypyrrole/poly(acrylic acid) hydrogel. *International Journal of Pharmaceutics* **2009**, 381, 25-33.

(45) Djabri, A.; Guy, R. H.; Delgado-Charro, M. B. Transdermal iontophoresis of ranitidine: An opportunity in paediatric drug therapy. *International Journal of Pharmaceutics* **2012**, 435, 27-32.

(46) Lemos, C. N.; Cubayachi, C.; Dias, K.; Mendonça, J. N.; Lopes, N. P.; Furtado, N. A. J. C.; Lopez, R. F. V. Iontophoresis-stimulated silk fibroin films as a peptide delivery system for

wound healing. *European Journal of Pharmaceutics and Biopharmaceutics* **2018**, 128, 147-155.

(47) Labala, S.; Jose, A.; Venuganti, V. V. K. Transcutaneous iontophoretic delivery of STAT3 siRNA using layer-by-layer chitosan coated gold nanoparticles to treat melanoma. *Colloids and Surfaces B: Biointerfaces* **2016**, 146, 188-197.

(48) Takeuchi, I.; Takeshita, T.; Suzuki, T.; Makino, K. Iontophoretic transdermal delivery using chitosan-coated PLGA nanoparticles for positively charged drugs. *Colloids and Surfaces B: Biointerfaces* **2017**, 160, 520-526.

(49) Taveira, S. F.; Nomizo, A.; Lopez, R. F. V. Effect of the iontophoresis of a chitosan gel on doxorubicin skin penetration and cytotoxicity. *Journal of Controlled Release* **2009**, 134, 35-40.

(50) Şenyiğit, T.; Padula, C.; Özer, Ö.; Santi, P. Different approaches for improving skin accumulation of topical corticosteroids. *International Journal of Pharmaceutics* **2009**, 380, 155-160.

(51) Fang, J.-Y.; Sung, K. C.; Wang, J.-J.; Chu, C.-C.; Chen, K.-T. The effects of iontophoresis and electroporation on transdermal delivery of buprenorphine from solutions and hydrogels. *Journal of Pharmacy and Pharmacology* **2002**, 54, 1329-1337.

(52) Kumaraswamy, R. V.; Kumari, S.; Choudhary, R. C.; Pal, A.; Raliya, R.; Biswas, P.; Saharan, V. Engineered chitosan based nanomaterials: Bioactivities, mechanisms and perspectives in plant protection and growth. *International Journal of Biological Macromolecules* **2018**, 113, 494-506.

(53) Wang, H.; Qian, J.; Ding, F. Recent advances in engineered chitosan-based nanogels for biomedical applications. *Journal of Materials Chemistry B* **2017**, 5, 6986-7007.

(54) Shariatinia, Z. Pharmaceutical applications of chitosan. *Advances in Colloid and Interface Science* **2019**, 263, 131-194.

(55) Thakur, V. K.; Thakur, M. K. Recent advances in Graft Copolymerization and Applications of Chitosan: A Review. *ACS Sustainable Chemistry & Engineering* **2014**, 2, 2637-2652.

(56) Kirschning, A.; Dibbert, N.; Dräger, G. Chemical Functionalization of Polysaccharides–Towards Biocompatible Hydrogels for Biomedical Applications. *Chemistry-A European Journal* **2018**, 24, 1231-1240.

(57) Alves, N. M.; Mano, J. F. Chitosan derivatives obtained by chemical modifications for biomedical and environmental applications. *International Journal of Biological Macromolecules* **2008**, 43, 401-414.

(58) Prabaharan, M.; Reis, R. L.; Mano, J. F. Carboxymethyl chitosan-*graft*-phosphatidylethanolamine: Amphiphilic matrices for controlled drug delivery. *Reactive and Functional Polymers* **2007**, 67, 43-52.

(59) Jana, S.; Gandhi, A.; Sen, K. K. Chitosan-Based Interpenetrating Polymer Networks: Drug Delivery Applications in *Functional Chitosan* (Eds: Jana, S.; Jana, S.), Springer Nature Singapore Pte Ltd., Singapore, Singapore, Ch. 9, **2019**.

(60) Cui, L.; Xiong, Z.; Guo, Y.;Liu, Y.; Zhao, J.; Zhang, C.; Zhu, P. Fabrication of interpenetrating polymer network chitosan/gelatin porous materials and study on dye adsorption properties. *Carbohydrate Polymers* **2015**, 132, 330-337.

(61) Suo, H.; Zhang, D.; Yin, J.; Qian, J.; Wu, Z. L.; Fu, J. Interpenetrating polymer network hydrogels composed of chitosan and photocrosslinkable gelatin with enhanced mechanical properties for tissue engineering. *Materials Science and Engineering: C* **2018**, 92, 612-620.

(62) Singh, S. K.; Savoy, A. W. Ionic liquids synthesis and applications: An overview. *Journal of Molecular Liquids* **2020**, 297, 112038.

(63) Li, H.; Feng, Z.; Zhao, K.; Wang, Z.; Liu, J.; Liu, J.; Song, H. Chemically crosslinked liquid crystalline poly(ionic liquid)s/halloysite nanotubes nanocomposite ionogels with

superior ionic conductivity, high anisotropic conductivity and a high modulus. *Nanoscale* **2019**, 11, 3689-3700.

(64) Rodrigues, D. M.; Hunter, L. G.; Bernard, F. L.; Rojas, M. F.; Vecchia, F. D.; Einloft, S. Harnessing CO2 into Carbonates Using Heterogeneous Waste Derivative Cellulose-Based Poly(ionic liquids) as Catalysts. *Catalysis Letter* **2019**, 149, 733-743.

(65) Bernard, F. L.; Santos, L. M.; Schwab, M. B.; Polesso, B. B.; Nascimento, J. F.; Einloft, S. Polyurethane-based poly (ionic liquid)s for CO_2 removal from natural gas. *Journal of Applied Polymer Science* **2019**, 136, 47536.

(66) Fang, H.; Wang, J.; Li, L.; Xu, L.; Wu, Y.; Wang, Y.; Fei, X.; Tian; J.; Li, Y. A novel high-strength poly(ionic liquid)/PVA hydrogel dressing for antibacterial applications. *Chemical Engineering Journal* **2019**, 365, 153-164.

(67) Kanaan, A. F.; Barsan, M. M.; Brett, C. M. A.; Alvarez-Lorenzo, C.; Concheiro, A.; de Sousa, H. C.; Dias, A. M. A. Sustainable Electro-Responsive Semi-Interpenetrating Starch/Ionic Liquid Copolymer Networks for the Controlled Sorption/Release of Biomolecules. *ACS Sustainable Chemistry & Engineering* **2019**, 7, 10516-10532.

(68) Kanaan, A. F.; Piedade, A. P.; de Sousa, H. C.; Dias, A. M. A. Effect of mold assemblies-induced interfaces in the mechanical actuation of electro-responsive ionic liquid-based polycationic hydrogels. *Applied Materials Today* **2020**, 20, 100711.

(69) Biswas, Y.; Maji, T.; Dule, M.; Mandal, T. K. Tunable doubly responsive UCST-type phosphonium poly(ionic liquid): a thermosensitive dispersant for carbon nanotubes. *Polymer Chemistry* **2016**, 7, 867-877.

(70) Liu, Z.; Wang, Y.; Ren, Y.; Jin, G.; Zhang, C.; Chen, W.; Yan, F. Poly(ionic liquid) hydrogel-based anti-freezing ionic skin for a soft robotic gripper. *Materials Horizons* **2020**, 7, 919-927.

(71) Cunha, B. S.; Bataglioli, R. A.; Taketa, T. B.; Lopes, L. M.; Beppu, M. M. Ionic liquid functionalization of chitosan beads for improving thermal stability and copper ions uptake from aqueous solution. *Journal of Environmental Chemical Engineering* **2019**, 7, 103181.

(72) Elshaarawy, R. F. M.; Refaee, A. A.; El-Sawi, E. A. Pharmacological performance of novel poly(ionic liquid)-grafted chitosan-*N*-salicylidene Schiff bases and their complexes. *Carbohydrate Polymers* **2016**, 146, 376-387.

(73) Li, P.-Y.; Cheng, K.-Y.; Zheng, X.-C.; Liu, P.; Xu, X.-J. Facile synthesis of water-soluble graphene-based composite: Non-covalently functionalized with chitosan-ionic liquid conjugation. *Functional Materials Letter* **2016**, 9, 1650045.

(74) Sun, J.; Wang, J.; Cheng, W.; Zhang, J.; Li, X.; Zhang, S.; She, Y. Chitosan functionalized ionic liquid as a recyclable biopolymer-supported catalyst for cycloaddition of CO2. *Green Chemistry* **2012**, 14, 654-660.

(75) Ren, H.; Li, B.; Neckenig, M.; Wu, D.; Li, Y.; Ma, Y.; Li, X.; Zhang, N. Efficient lead ion removal from water by novel chitosan gel-based sorbent modified with glutamic acid ionic liquid. *Carbohydrate Polymer* **2019**, 207, 737-746.

(76) Dias, A. M. A.; Cortez, A. R.; Barsan, M. M.; Santos, J. B.; Brett, C. M. A.; de Sousa, H. C. Development of Greener Multi-Responsive Chitosan Biomaterials Doped with Biocompatible Ammonium Ionic Liquids. *ACS Sustainable Chemistry & Engineering* **2013**, 1, 1480-1492.

(77) Matricardi, P.; Meo, C. D.; Coviello, T.; Hennink, W. E.; Alhaique, F. Interpenetrating Polymer Networks polysaccharide hydrogels for drug delivery and tissue engineering. *Advanced Drug Delivery Reviews* **2013**, 65, 1172-1187.

(78) Dragan, E. S. Design and applications of interpenetrating polymer network hydrogels. A review. *Chemical Engineering Journal* **2014**, 243, 572-590.

(79) Jimenez-Rosales, A.; Flores-Merino, M. V. A Brief Review of the Pathophysiology of Non-melanoma Skin Cancer and Applications of Interpenetrating and Semi-interpenetrating Polymer Networks in Its Treatment. *Regenerative Engineering and Translational Medicine* **2018**, 4, 187-205.

(80) Aminabhavi, T. M.; Nadagouda, M. N.; More, U. A.; Joshi, S. D.; Kulkarni, V. H.; Noolvi, M. N.; Kulkarni, P. V. Controlled release of therapeutics using interpenetrating polymer networks. *Expert Opinion On Drug Delivery* **2015**, 12, 669-688.

(81) Raina, N.; Rani, R.; Khan, A.; Nagpal, K.; Gupta, M. Interpenetrating polymer network as a pioneer drug delivery system: a review. *Polymer Bulletin* **2019**, 77, 5027-5050.

(82) Alemán, J.; Chadwick, A. V.; He, J.; Mess, M.; Horie, K.; Jones, R. G.; Kratochvíl, P.; Meisel, I.; Mita, I.; Moad, G.; Penczek, S.; Stepto, R. F. T. DEFINITIONS OF TERMS RELATING TO THE STRUCTURE AND PROCESSING OF SOLS, GELS, NETWORKS, AND INORGANIC-ORGANIC HYBRID MATERIALS (IUPAC Recommendations 2007). *Pure and Applied Chemistry* **2007**, 79, 1801-1829.

(83) Korsmeyer, R.. W.; Gurny, R.; Doelker, E.; Buri, P.; Peppas, N. A. Mechanisms of solute release from porous hydrophylic polymers. *International Journal of Pharmaceutics* **1983**, 15, 25-35.

(84) Higuchi, T. Rate of release of medicaments from ointments based containing drugs in suspension. *Journal of Pharmaceutical Sciences* **1961**, 50, 874-875.

(85) Paul, D. R.; McSpadden, S. K. Diffusional release of a solute from a polymer matrix. *Journal of Membrane Science* **1976**, 1, 33-48.

(86) ASTM F756-00, Standard Practice for Assessment of Hemolytic Properties of Materials, ASTM International, West Conshohocken, PA, **2000**.

(87) Lan, G.; Lu, B.; Wang, T.; Wang, L.; Chen, J.; Yu, K.; Liu, J.; Dai, F.; Wu, D. Chitosan/gelatin composite sponge is an absorbable surgical hemostatic agent. *Colloids and Surfaces B: Biointerfaces* **2015**, 136, 1026-1034.

(88) Gu, B. K.; Park, S. J.; Kim, M. S.; Kang, C. M.; Kim, J.-I.; Kim, C.-H. Fabrication of sonicated chitosan nanofiber mat with enlarged porosity for use as hemostatic materials. *Carbohydrate Polymers* **2013**, 97, 65-73.

(89) Zhang, W.-H.; Liu, S.-S.; Liu, P.; Xu, J.; Xue, B.; Wei, X.-Y.; Li, Y.-X. Chitosan grafted with a heteropolyanion-based ionic liquid as an effective and reusable catalyst for acetylation. *RSC Advances* **2016**, 6, 41404-41409.

(90) Saito, H.; Tabeta, R.; Ogawa, K. High-resolution solid-state carbon-13 NMR study of chitosan and its salts with acids: conformational characterization of polymorphs and helical structures as viewed from the conformation-dependent carbon-13 chemical shifts. *Macromolecules* **1987**, 10, 2424-2430.

(91) Kasaai, M. R. Determination of the degree of *N*-acetylation for chitin and chitosan by various NMR spectroscopy techniques: A review. *Carbohydrate Polymer* **2010**, 79, 801-810.

(92) Myashita, Y.; Kobayashi, R.; Kimura, N.; Suzuki, H.; Nishio, Y. Transition behavior and phase structure of chitin/ poly(2-hydroxyehtyl methacrylate) composites synthesized by a solution coagulation/bulk polymerization method. *Carbohydrate Polymers* **1997**, 34, 221-228.

(93) Mochizuki, A.; Miwa, Y.; Miyoshi, R.; Namiki, T. Relationship between water structure and properties of poly(methyl methacrylate-*b*-2-hydroxyethyl methacrylate) by solid-state NMR. *Journal of Biomaterials Science, Polymer Edition* **2017**, 28, 1199-1214.

(94) Bandomir, J.; Schulz, A.; Taguchi, S.; Schmitt, L.; Ohno, H.; Sternberg, K.; Schmitz, K.-P.; Kragl, U. Synthesis and Characterization of Polymerized Ionic Liquids: Mechanical and Thermal Properties of a Nobel Type of Hydrogels. *Macromolecular Chemistry and Physics* **2014**, 215, 716-724.

(95) Thangaraj, V.; Bhaskarapillai, A.; Velmurugan, S. Synthesis of a crosslinked poly(ionic liquid) and evaluation of its antimony binding properties. *Journal of Hazardous Materials* **2020**, 384, 121481.

(96) Drozdov, A. D.; deClaville Christiansen, J. Swelling of pH sensitive hydrogels. *Physical Review E* **2015**, 91, 1-15.

(97) Dodoo, S.; Steitz, R.; Laschewsky, A.; von Klitzing, R. Effect of ionic strength and type of ions on the structure of water swollen polyelectrolyte multilayers. *Physical Chemistry Chemical Physics* **2011**, 13, 10318-10325.

(98) Skoog, D. A.; West, D. M.; Holler, F. J.; Crouch, S. R. *Fundamentals of Analytical Chemistry*, Brooks/Cole, Belmont, United States of America **2014**.

(99) Willems, N.; Yang, H.-y.; Langelaan, M. L. P.; Tellegen, A. R.; Grinwis, G. C. M.; Kranenburg, H.-J. C.; Riemers, F. M.; Plomp, S. G. M.; Craenmehr, E. G. M.; Dhert, W. J. A.; Papen-Botterhuis, N. E.; Meij, B. P.; Creemers, L. B.; Tryfonidou, M. A. Biocompatibility and intradiscal application of a thermoreversible celecoxib-loaded poly-N-isopropylacrylamide MgFe-layered double hydroxide hydrogel in a canine model. *Arthritis Research & Therapy* **2015**, 17, 1-16.

(100) Bigucci, F.; Abruzzo, A.; Saladini, B.; Gallucci, M. C.; Cerchiara, T.; Luppi, B. Development and characterization of chitosan/hyaluronan film for transdermal delivery of thiocolchicoside. *Carbohydrate Polymers* **2015**, 130, 32-40.

(101) Gámiz-González, M. A.; Vidaurre, A.; Ribelles, J. L. G. Biodegradable chitosan-poly(ε-caprolactone) dialdehyde copolymer networks for soft tissue engineering. *Polymer Degradation and Stability* **2017**, 138, 47-54.

(102) Borzacchiello, A.; Ambrosio, L. Structure-Property Relationships in Hydrogels. *Hydrogels, Biological Properties and Applications* (Ed: Barbucci, R.), Springer-Verlag, Mlian, Italy, **2009**.

(103) Sjöberg, H.; Karami, K.; Beronius, P.; Sundelöf, L.-O. Ionization conditions for iontophoretic drug delivery. A revised pK_a of lidocaine hydrochloride in aqueous solution at 25ºC established by precision conductometry. *International Journal of Pharmaceutics* **1996**, 141, 63-70.

(104) Todd, K. H. A Review of Current and Emerging Approaches to Pain Management in the Emergency Department. *Pain and Therapy* **2017**, 6, 193-202.

(105) Zhang, M.; Guan, K.; Ji, Y.; Liu, G.; Jin, W.; Xu, N. Controllable ion transport by surface-charged graphene oxide membrane. *Nature Communications* **2019**, 10, 1253.

(106) Ramanathan, S.; Block, L. H. The use of chitosan gels as matrices for electrically-modulated drug delivery. *Journal of Controlled Release* **2001**, 70, 109-123.

(107) Varshosaz, J.; Jaffari, F.; Karimzadeh, S. Development of bioadhesive chitosan gels for topical delivery of lidocaine. *Scientia Pharmaceutica* **2006**, 74, 209-223.

(108) Li, L.; Zhang, Y.; Han, S.; Qu, Z.; Zhao, J.; Chen, Y.; Chen, Z.; Duan, J.; Pan, Y.; Tang, X. Penetration Enhancement of Lidocaine Hydrochlorid by a Novel Chitosan Coated Elastic Liposome for Transdermal Drug Delivery. *Journal of Biomedical Nanotechnology* **2011**, 7, 704-713.

(109) Bernot, R. J.; Brueseke, M. A.; Evans-White, M. A.; Lamberti, G. A. Acute and chronic toxicity of imidazolium-based ionic liquids on Daphnia magna. *Environmental Toxicology and Chemistry* **2005**, 24, 87-92.

(110) Liu, H.; Zhang, X.; Chen, C.; Du, S.; Dong, Y. Effects of imidazolium chloride ionic liquids and their toxicity to Scenedesmus obliquus. *Ecotoxicology and Environmental Safety* **2015**, 122, 83-90.

(111) Bacon, S. L.; Ross, R. J.; Daugulis, A. J.; Parent, J. S. Imidazolium-based polyionic liquid absorbents for bioproduct recovery. *Green Chemistry* **2017**, 19, 5203-5213.

(112) Zhang, Y.; Yuan, B.; Zhang, Y.; Cao, Q.; Yang, C.; Li, Y.; Zhou, J. Biomimetic lignin/poly(ionic liquids) composite hydrogel dressing with excellent mechanical strength, self-healing properties, and reusability. *Chemical Engineering Journal* **2020**, 400, 125984.

(113) Xu, Q.; Zheng, Z.; Wang, B.; Mao, H.; Yan, F. Zinc Ion Coordinated Poly(Ionic Liquid) Antimicrobial Membranes for Wound Healing. *ACS Applied Materials & Interfaces* **2017**, 9, 14656-14664.

(114) Bains, D.; Singh, G.; Kaur, N.; Singh, N. Development of Biological Self-Cleaning Wound-Dressing Gauze for the Treatment of Bacterial Infection. *ACS Sustainable Chemistry & Engineering* **2019**, 7, 969-978.

(115) Miguel, S. P.; Moreira, A. F.; Correia, I. J. Chitosan based-asymmetric membranes for wound healing: A review. *International Journal of Biological Macromolecules* **2019**, 127, 460-475.

(116) Hamedi, H.; Moradi, S.; Hudson, S. M.; Tonelli, A. E. Chitosan based hydrogels and their applications for drug delivery in wound dressings: A review. *Carbohydrate Polymers* **2018**, 199, 445-460.

(117) Kean, T.; Thanou, M. Biodegradation, biodistribution and toxicity of chitosan. *Advanced Drug Delivery Reviews* **2010**, 62, 3-11.

(118) Feng, C.; Li, J.; Wu, G. S.; Mu, Y. Z.; Kong, M.; Jiang, C. Q.; Cheng, X. J.; Liu, Y.; Chen, X. G. Chitosan-Coated Diatom Silica as Hemostatic Agent for Hemorrhage Control. *ACS Applied Materials & Interfaces* **2016**, 8, 34234-34243.

(119) Zhang, J.; Wang, D.; Jiang, X.; He, L.; Fu, L.; Zhao, Y.; Wang, Y.; Mo, H.; Shen, J. Multistructured vascular patches constructed via layer-by-layer self-assembly of heparin and chitosan for vascular tissue engineering applications. *Chemical Engineering Journal* **2019**, 370, 1057-1067.

(120) Wang, Y.; Zhou, P.; Xiao, D.; Zhu, Y.; Zhong, Y.; Zhang, J.; Sui, X.; Feng, X.; Xu, H.; Mao, Z. Chitosan-bound carboxymethylated cotton fabric and its application as wound dressing. *Carbohydrate Polymers* **2019**, 221, 202-208.

Chapter 5

Conclusions

And suggested future work

The development of novel, biocompatible and multi stimuli-responsive electroactive systems based on ionic liquid functionalized polysaccharides and/or synthetic polymers, envisaging biomedical applications, was the main motivation of this PhD thesis. The envisaged response is more precisely tuned by employing multi stimuli-responsive materials instead of conventional single-stimulus-responsive ones. This is particularly important when the materials are to be applied in complex environments (e.g. *in vivo*). Moreover, "smart" hydrogels based on natural/synthetic polymers functionalized with ILs represent a novel strategy to design advanced electro-active platforms which are suitable to be employed in environments comprising a wide range of pH. This is due to the presence of non-ionizable groups from IL-based polyelectrolytes which allows a precisely tuned electrical response (e.g. mechanical actuation (bending) and sorption/delivery of charged molecules) in response to an applied electrical stimulus. The development of biocompatible, safe, and low cost multi stimuli-responsive materials has been a scientific challenge. Within this thesis different novel electroactive stimuli-responsive cationic materials based on synthetic and/or natural polymers functionalized with the ionic liquid 1-butyl-3-vinylimidazolium chloride (BVImCl) were obtained. The components of the prepared hydrogels were carefully selected. Poly(ionic liquids) and/or ionic liquid-based copolymers were selected to endow the ionic strength and electrical current responsiveness while the polysaccharides were selected to improve the hydrogels biocompatibility, biodegradability and/or their responsiveness to other stimuli (e.g. pH responsiveness). The results reported in Chapters 2, 3 and 4 showed that several multi

stimuli-responsive materials were successfully prepared via different chemical functionalization approaches following the principles of green chemistry. The physicochemical, biological, and thermomechanical properties of these materials were extensively characterized.

In Chapters 2, 3 and 4 the ionic strength responsiveness of IL-functionalized materials was evidenced by swelling experiments. The obtained cationic polyelectrolytes presented fixed charged density which induced the ionic strength responsiveness of the hydrogels due to osmotic pressure gradients that are stablished between the hydrogel and the aqueous media. The functionalization of synthetic and/or natural polymers with BVImCl allowed the final hybrid materials to respond (via swelling or deswelling processes) to different ionic strength values as a function of the BVImCl content, polysaccharide amount and type of substrate employed during polymerization. Moreover, and as shown in Chapter 4, the development of semi-IPNs of chitosan with poly(BVImCl) and/or poly(HEMA-co-BVImCl) allowed the pH responsiveness to be tuned in different aqueous media as concluded from fluid handling and dye sorption experiments. In this case the pH response capability was provided by chitosan (from the amine groups) and it was not affected during the synthesis of the hybrid hydrogels.

All the prepared IL-functionalized materials were responsive under an applied electrical stimulus. The incorporation of the ionic liquid into natural/synthetic matrices endowed the synthesized hydrogels to respond to different electrical stimuli, in different aqueous solutions, due to the diffusion of free chloride counter-anions. Their response was dependent on the amount of ionic liquid (Chapters 2 and 4), polysaccharide content (Chapter 2) and type of mold substrate utilized during the preparation of these materials (Chapter 3). IL-based copolymers presented in Chapter 3 presented mechanical actuation (bending) in response to external electrical stimulus. Electro-active IL-based cationic polyelectrolytes

behaved as single-ions carriers allowing the diffusion of free chloride counter-anions towards the positively charged electrode. This leads to an increase in the density of positive (unprotected) charges within the hydrogel matrix and consequently to an increase in the amount of water that diffuses into the hydrogel due to osmotic gradients that are stablished, which ultimately leads to the bending of the hydrogel. It was also demonstrated that the electro-actuation responsiveness of synthesized hydrogels was highly dependent on the in-depth gradient promoted by the mold substrates employed during the polymerization reaction and on the intensity of applied electrical stimulus. Ionic liquid-functionalized hydrogels synthesized in more hydrophobic surfaces (e.g. Teflon® molds) presented the highest and fastest electro-actuation capacity towards the anode in aqueous media and independently of the pH of the media. The electro-actuation capacity of these hydrogels was majorly governed by the ion enrichment/depletion mechanism. Additionally, the observed mechanical actuation was mostly dependent on the physicochemical and morphological structure of the hydrogel rather than on its ionic charge density. Ionic liquid-functionalized hydrogels synthesized in more hydrophilic substrates (e.g. glass molds) resulted in denser structures which hindered the diffusion of chloride counter-anions within the hydrogel and consequently, lowered the electro-actuation responsiveness. Hydrogels synthesized in a combination of hydrophobic and hydrophilic mold substrates presented electro-actuation responsiveness as a function of the position of each hydrogel's surface in relation to the anode (positively charged electrode). These results show that the mechanical response of these "soft" electro-actuators can be modulated according to the type of substrate utilized during polymerization reactions. The s-IPNs developed in Chapters 2 and 4 did not present mechanical actuation (at a macroscopic scale) in response to the applied electrical stimulus. This observation could be attributed to the higher polymer density of these materials due to the presence of the polysaccharide within the copolymer's networks, which may have hindered the diffusion of counter-anions, and

consequently, the mechanical actuation of the hydrogels. In fact, in Chapter 2 it was possible to conclude that the employed drying method also affected the ionic conductivity of the prepared s-IPNs as it affects their porosity. The interconnected cavities of the freeze-dried hydrogels worked as preferential paths enhancing the diffusion of counter-anions within the swollen network channels resulting in higher electro-conductivity, when compared to that measured for compact hydrogels obtained by oven-drying. Finally, and besides ionic conductivity, IL-functionalized materials also presented electric conductivity, resulting from oxidative reactions at the anode, independently of the amount of ionic liquid, of spacer (HEMA) and of polysaccharide employed to prepare the hydrogels.

The electro-responsiveness of the IL-functionalized hydrogels was used to explore the capacity of these materials to modulate the sorption/release/permeation of charged molecules. The results obtained for the passive and electro-assisted sorption/desorption of L-tryptophan by starch based s-IPNs were presented in Chapter 2. The amino acid sorption/desorption profiles were dependent on the composition of the sorption/release media, intensity of electrical stimulus and nature of the hydrogel. Electro-assisted experiments revealed that L-tryptophan sorption/desorption profiles were governed by electrostatic interactions due to electrophoretic flow induced by the applied electrical stimulus, while passive experiments demonstrated that L-tryptophan sorption/desorption behavior was mainly governed by diffusion processes. Similar conclusions were taken in Chapter 4 for the passive and electro-assisted permeation/release of lidocaine hydrochloride into/from chitosan based s-IPNs. Passive measurements revealed that the drug permeation was highly dependent on the charge density of each hydrogel and mainly governed by diffusion mechanisms. Polycationic hydrogels behaved as polyelectrolyte barriers preventing drug diffusion, while, interconnected macroporous network of the hydrogels allowed drug permeation for higher time periods. The application of low intensity electrical stimulus (0.56 mA/cm^2) significantly

enhanced the drug permeation/release profile of lidocaine hydrochloride through/from polycationic hydrogels. Electro-assisted permeation/release results revealed a time dependent behavior. The rate of drug permeation/release was governed by anodal iontophoretic flow and electro repulsion mechanism. The presence of the co-monomer HEMA allowed tuning the electro-assisted release profile of lidocaine hydrochloride.

In what respects the influence of the IL-functionalization over the biological properties of the synthesized hybrid materials, it was possible to conclude that it did not induce cell wall lysis against fibroblasts, however, it did affect their metabolic activities (Chapter 2). The presence of starch in s-IPNs significantly enhanced the biocompatibility of the prepared hydrogels. Moreover, and as shown in Chapter 4, semi-IPNs of chitosan and poly(BVImCl) and/or poly(HEMA-co-BVImCl) were non-hemolytic when tested against rabbit red blood cells and presented potential blood clotting capacity.

To sum up, the electroactive and "smart" IL-based copolymers and semi-IPNs developed throughout this doctoral work presented as advantages their multi-stimuli responsiveness, modulated response over fine tune of electrical current, fixed charge density independent of media's pH and adjustability of the material's final properties by varying the feed compositions. Nevertheless, they also still present some disadvantages such as: restricted applications in aqueous environments; mechanical stability dependent of the employed IL amount; limited response over external stimuli under high ionic strength conditions; strong ionic interactions between developed polycationic materials with anionic molecules that hamper delivery/desorption capacity. Therefore, further studies should be made to overcome these issues and to further explore the potential of the IL-based hydrogels developed within this PhD Thesis. In the near future it would be interesting to:

i) evaluate the cell attachment and differentiation behavior (evaluated by fluorescence spectroscopy and *in vitro* reprogramming factors experiments, respectively) on each surface

of the electro-actuators presented in Chapter 3 in order to analyze the effect of their mechanical actuation and surface properties on the metabolic activities of cells (e.g. fibroblasts, bone marrow stem cells, neurons etc.);

ii) perform *in vitro* biodegradation studies on IL-functionalized polysaccharide materials (Chapters 2 and 4) via enzymatic degradation (using aqueous solutions containing proteins such as lysozyme and amylase) in order to evaluate the degradability of the synthesized hybrid hydrogels;

iii) evaluate the effect of the exchange of chloride counter-anions by different anions (e.g. bis(trifluoromethane)sulfonimide, ibuprofenate and salicylate) in the physicochemical, electrochemical and toxicological properties of the hydrogels;

iv) study s-IPNs based on different anionic polysaccharides (hyaluronic acid, alginate) and/or synthetic polymers (poly(acrylic acid), poly(acrylamide sodium salt)) functionalized with poly(BVImCl) and/or other IL-based copolymers as an interesting approach to obtain advanced amphoteric stimuli-responsive materials with broader application as antimicrobial dressings, culture cell scaffolds, membranes for bio-separation, etc.

Appendix A

Supporting information of Chapter 2

SEM micrographs of the cross-sections of freeze-dried hydrogels and elemental mapping of nitrogen and chlorine distribution through the hydrogel s-IPN/St1.0, analyzed by *energy dispersive X-ray spectroscopy* (*EDX*); Mechanical response of oven- and freeze-dried hydrogels during WVS measurements at RH ≥ 90% and 25 ºC; thermogravimetric profiles and DSC thermograms of the prepared hydrogels; UV-Visible spectra of L-tryptophan solutions in different media after electro-assisted sorption experiments; elemental analysis results.

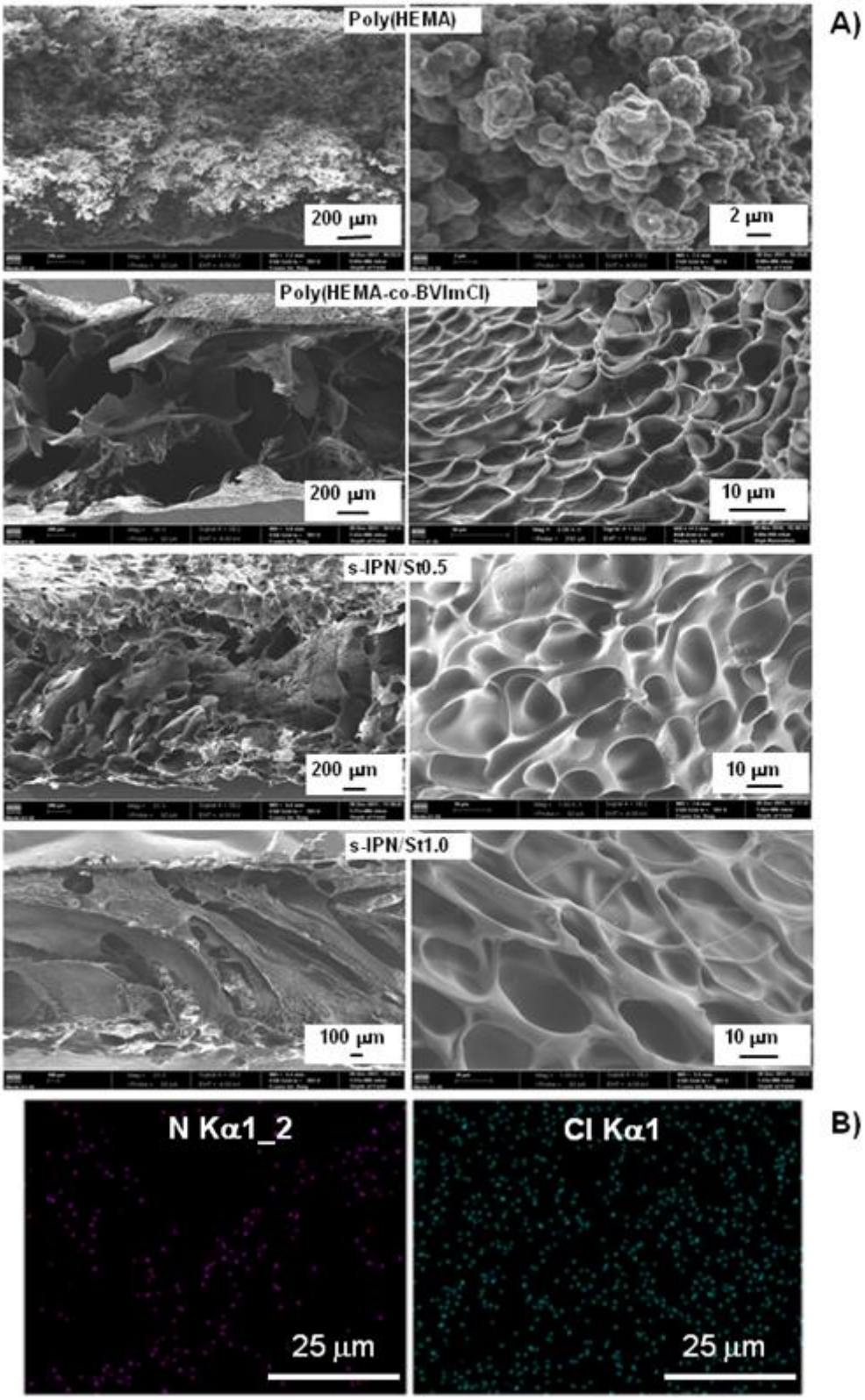

Figure S2.1 Cross-section SEM micrographs of freeze-dried hydrogels (A) and elemental mapping of nitrogen and chlorine distribution through the hydrogel s-IPN/St1.0, analyzed by energy dispersive X-ray spectroscopy (EDX) (B). Similar EDX results were obtained for hydrogels poly(HEMA-co-BVImCl) and s-IPN/St0.5.

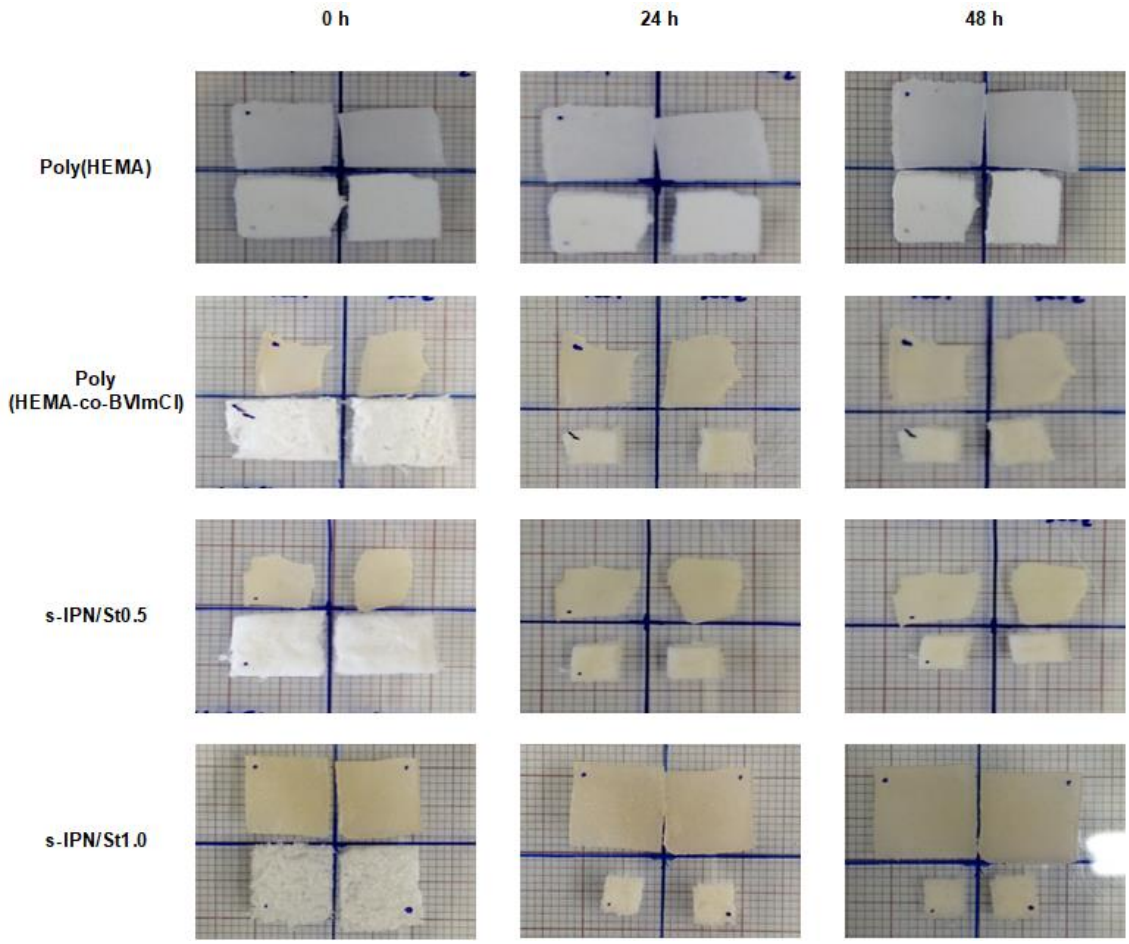

Figure S2.2 Mechanical response of oven- and freeze-dried hydrogels (upper and lower samples in each figure, respectively) during WVS measurements at RH ≥ 90% and 25 ºC.

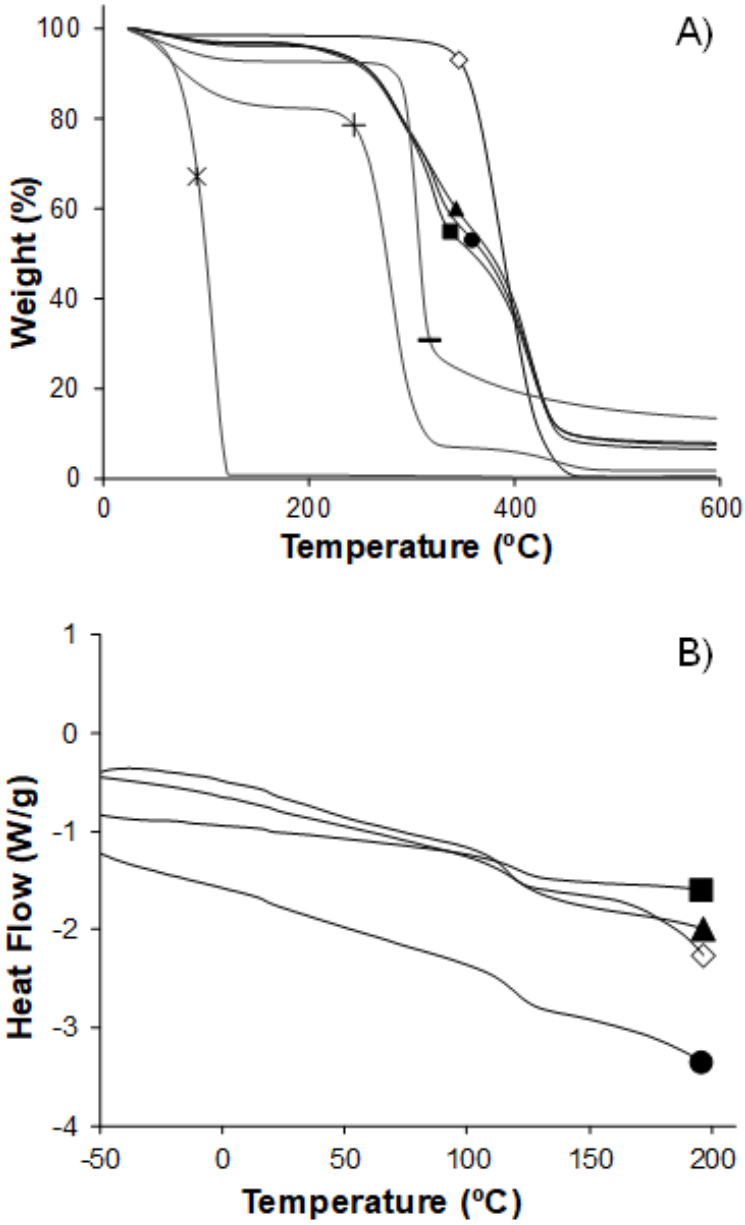

Figure S2.3 Thermogravimetric profiles (A) and DSC thermograms (B) of the hydrogels (Exothermal events oriented up). The symbols represent: poly(HEMA) (◊), poly(HEMA-co-BVImCl) (●), s-IPN/St0.5 (▲), s-IPN/St1.0 (■). The thermogravimetric profiles of pure HEMA (✳), BVImCl (+) and starch (—) are also shown for comparison.

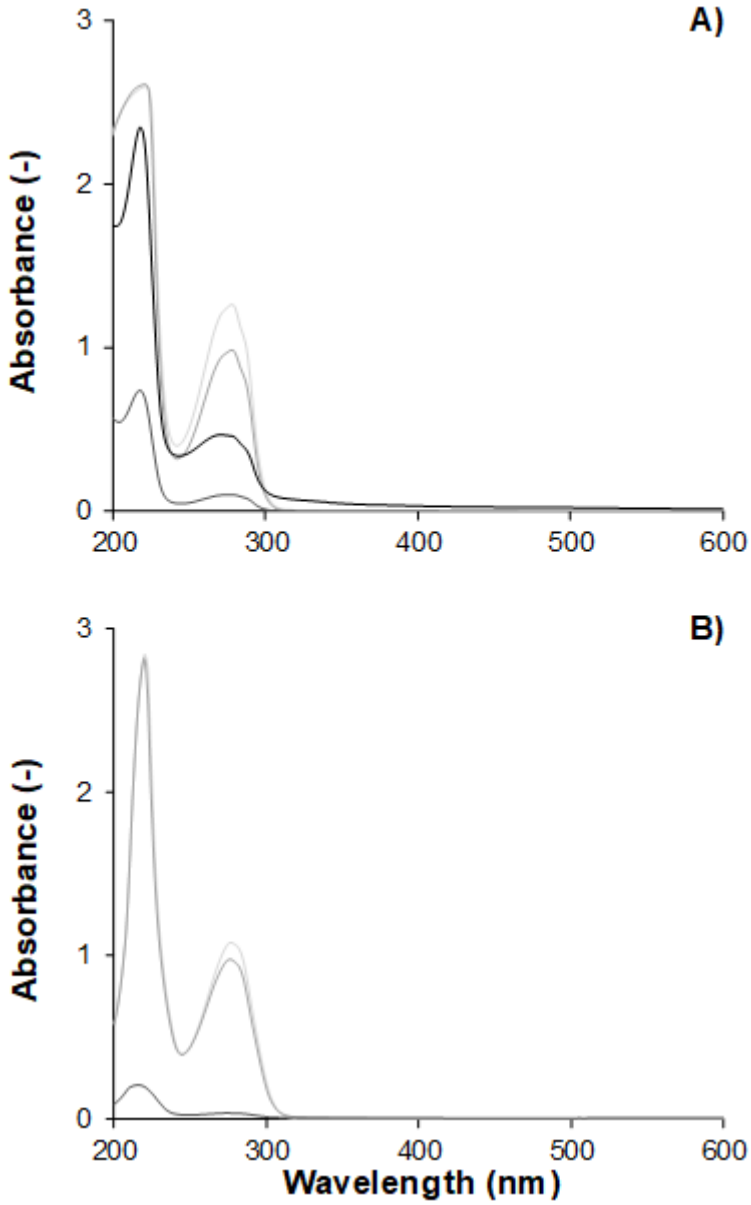

Figure S2.4 Spectra of L-tryptophan solutions in bi-distilled water (A) and in Trizma base buffer (B) after electro-assisted sorption experiments at 0 V (—), 2 V (—), 5 V (—) and 100 V (—) at room temperature (~ 25 ºC).

Table S2.1 Average values (% w/w) of nitrogen, carbon, hydrogen, and sulfur content of prepared hydrogels obtained from elemental analysis (after washing the hydrogels).

	N % (w/w)	C % (w/w)	H % (w/w)	S % (w/w)
Poly(HEMA)	0.07 ± 0.02	53.14 ± 0.15	8.08 ± 0.03	≤ 100 ppm
Poly(HEMA-co-BVImCl)	2.73 ± 0.27	53.14 ± 0.15	8.07 ± 0.07	≤ 100 ppm
s-IPN/St0.5	2.61 ± 0.45	53.18 ± 0.03	8.11 ± 0.10	≤ 100 ppm
s-IPN/St1.0	3.03 ± 0.02	52.70 ± 0.40	8.04 ± 0.03	≤ 100 ppm

Note: the experimental amount of BVImCl per weight of dry sample was calculated as follows (using the sample s-IPN/St1.0 as an example):

Basis: 100 g of s-IPN/St1.0 sample has an average of 3.03 g of nitrogen atoms (N) which correspond to 0.2164 mol of N.

1) Each molecule of BVImCl has 2 N atoms in their chemical structure (in the cation). Therefore, the number of moles of BVImCl is half that of the N atoms: 0.108 mol of BVImCl (per 100 g of dried sample).

2) The experimental amount of BVImCl per weight of dry sample was expressed in Table 2.1 as:

$$\frac{\text{BVImCl (mmol)}}{\text{100 g of dried sample s}-\text{IPN/St1.0}} = 1.082 \text{ mmol BVImCl/g of dried sample.}$$

Appendix B

Supporting information of Chapter 3

Elemental mapping of nitrogen and chlorine distribution through the hydrogels analyzed by *energy dispersive X-ray spectroscopy* (*EDX*); Quantification of the amount of BVImCl present in the cationic hydrogels synthesized in different mold assemblies (T-T, G-G and T-G) obtained by elemental analysis measurements; Water contact angles of hydrogel's surfaces; Contact angles of each mold plaques employed in the synthesis of cationic poly(HEMA-co-BVImCl) hydrogels; Mechanical response of hydrogels synthesized in different mold assemblies when immersed in deionized water; Effect of the pH on the bending angles of poly(HEMA-co-BVImCl) hydrogels synthesized in T-T mold assemblies; Electronic conductivity of poly(HEMA) hydrogels synthesized in glass and Teflon® mold assemblies; Movies of electromechanical actuation response of synthesized hydrogels.

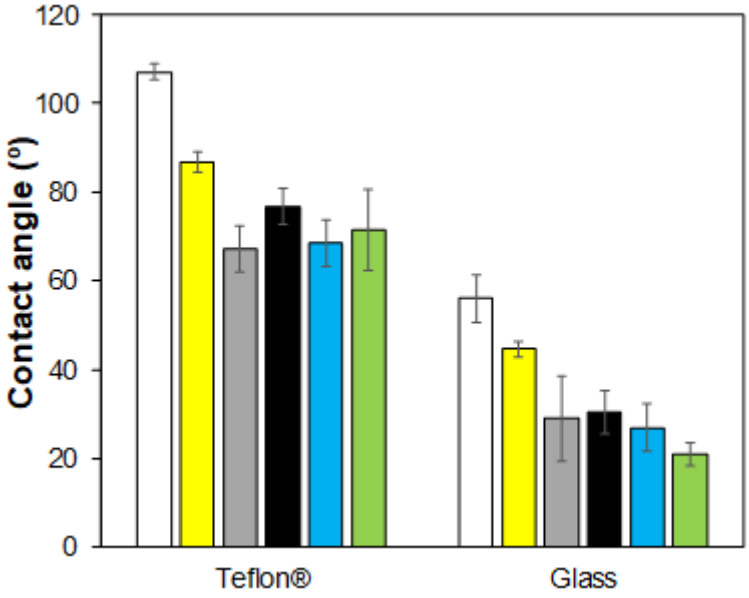

Figure S3.1 Contact angles of different aqueous solutions in the mold plaques employed in the synthesis of poly(HEMA-co-BVImCl) hydrogels, measured by the sessile drop method at room temperature (~ 22 ºC). Tested solutions were coded as: deionized water (□), deionized water + IL (■), deionized water + HEMA (■), deionized water + HEMA + IL (■), deionized water + HEMA + MBA (■) and deionized water + HEMA + IL + MBA (■).

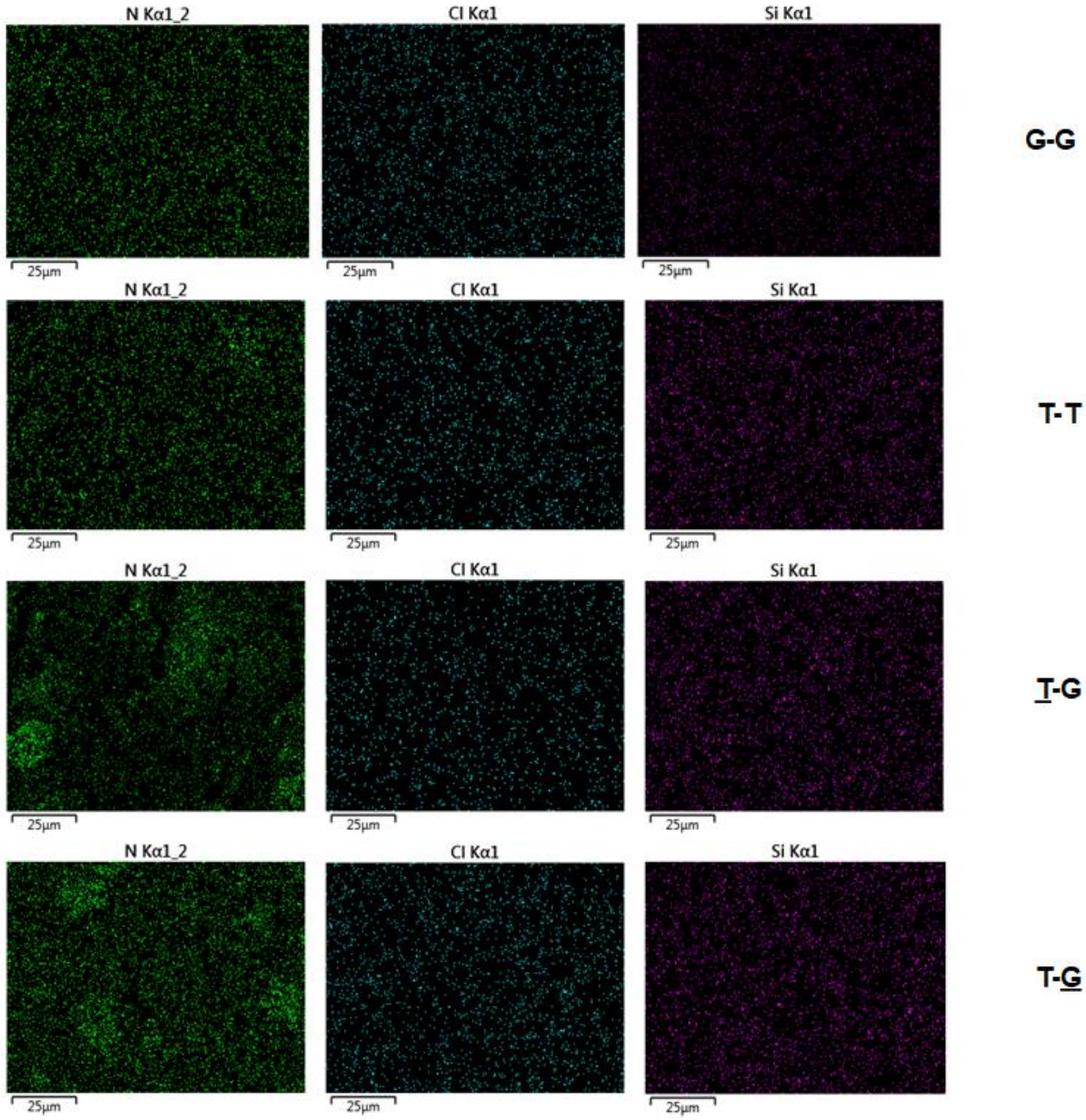

Figure S3.2 Elemental mapping of poly(HEMA-co-BVImCl) hydrogels synthesized in different mold assemblies (T-T, G-G, T-G and T-G) measured by energy dispersive X-ray spectroscopy analysis. Underlined letters represent the hydrogel surface that was in contact with Teflon® (T), and glass (G) for T-G mold assemblies.

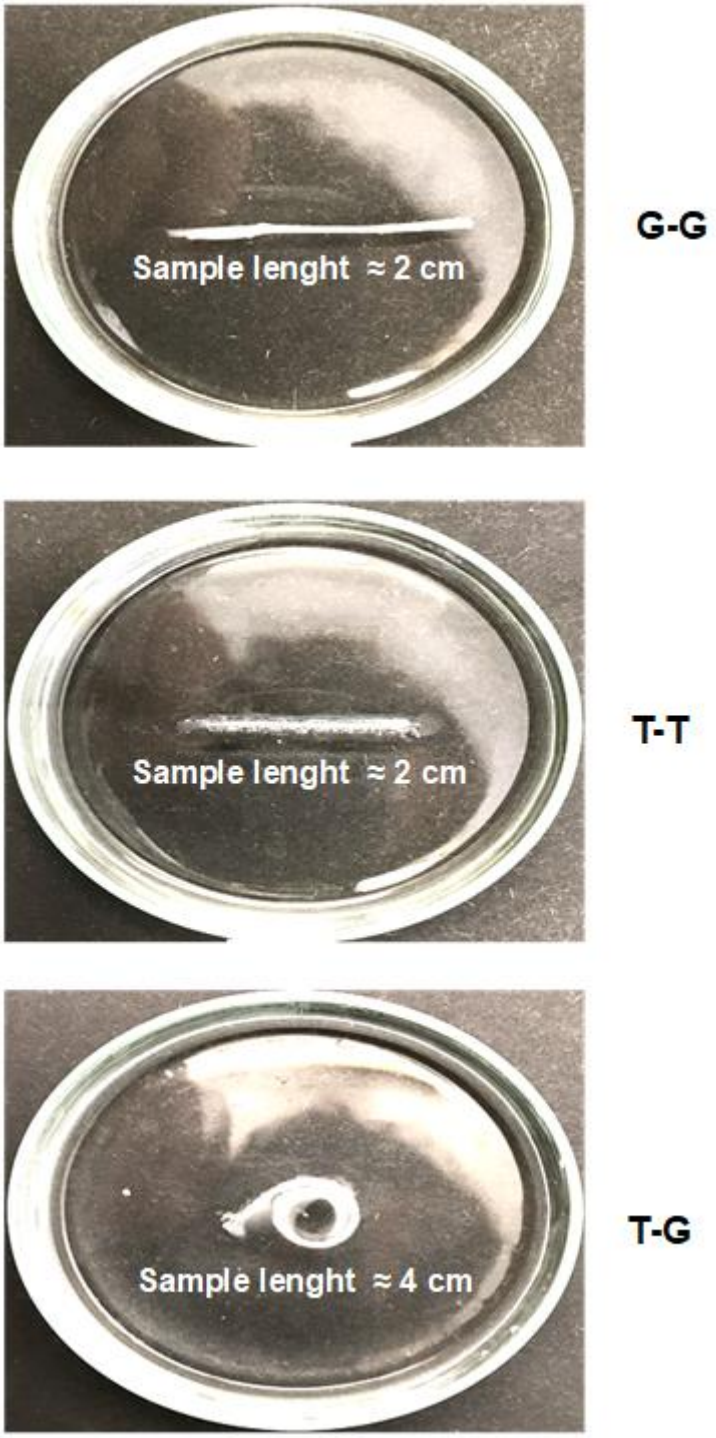

Figure S3.3 Mechanical response of poly(HEMA-co-BVImCl) hydrogels synthesized in different mold assemblies (T-T, G-G and T-G) when immersed in deionized water (at ~ 22 ºC).

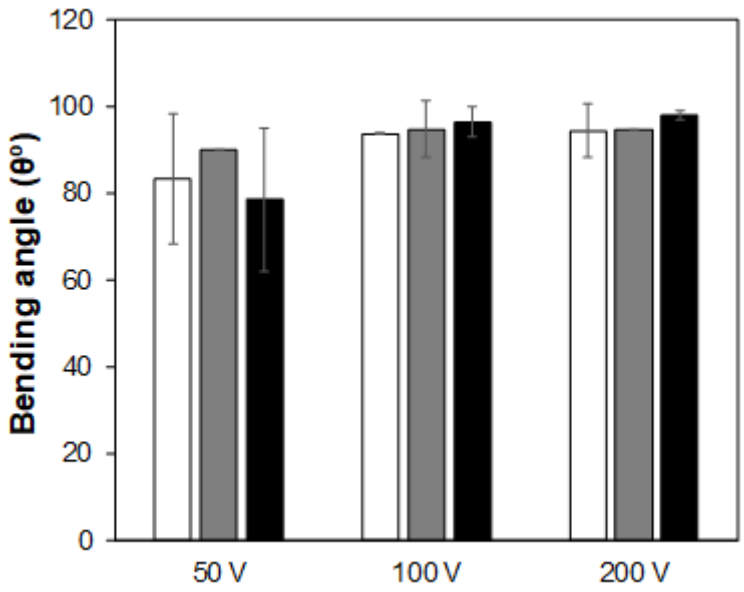

Figure S3.4 Effect of the pH on the bending angles of poly(HEMA-co-BVImCl) hydrogels synthesized in T-T mold assemblies under different applied voltages. Experiments were carried out at room temperature (~ 22 ºC) for hydrogels immersed in different aqueous media: deionized water (□), acid solution (pH = 5.0, I ≈ 0.01 mM) (■) and alkaline solution (pH = 9.0, I ≈ 0.01 mM) (■).

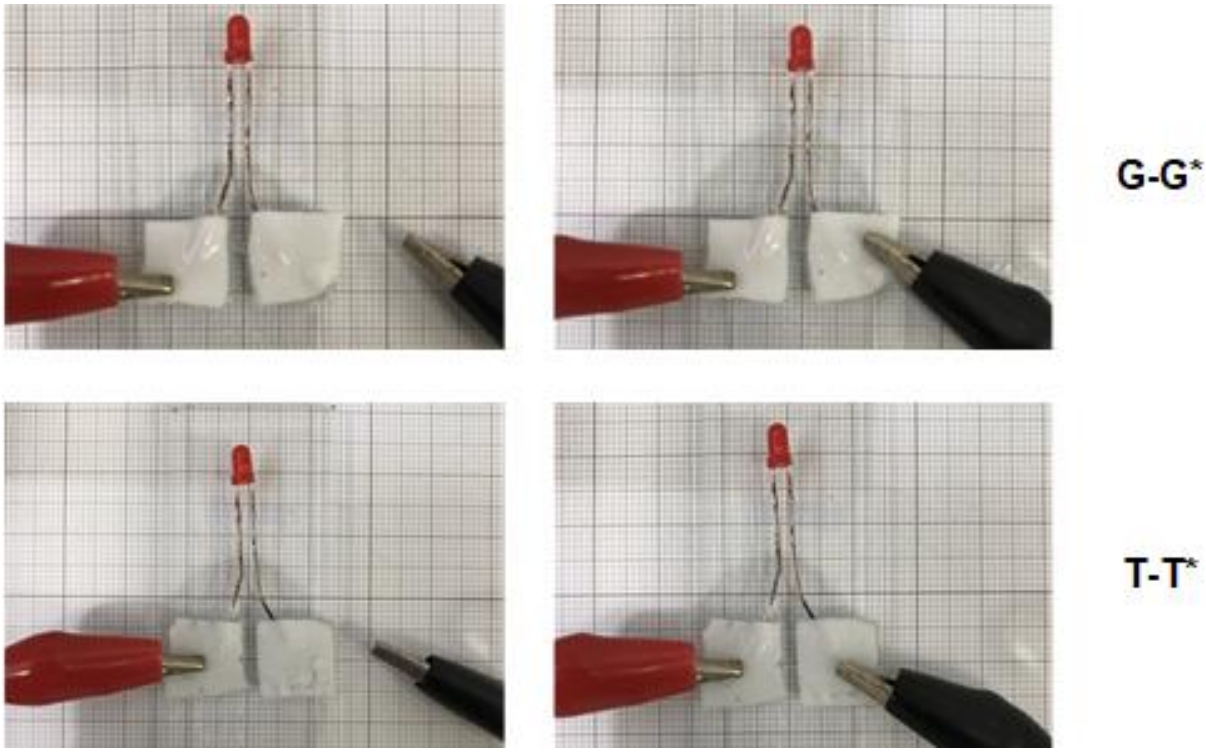

Figure S3.5 Test of the electronic conductivity of water swollen poly(HEMA) hydrogels synthesized in glass (G-G*) and Teflon® (T-T*) mold assemblies before (left column) and after (right column) the application of a potential difference of 1 V at room temperature (~ 22 ºC).

Table S3.1 Quantification of the amount of BVImCl present in the poly(HEMA-co-BVImCl) cationic hydrogels synthesized in different mold assemblies (T-T, G-G and T-G) based on elemental analysis data and water contact angles of hydrogel's surfaces measured by the sessile drop method at room temperature (~ 22 ºC).

Samples	% N (w/w)	% C (w/w)	% H (w/w)	BVImCl (mmol IL/$g_{dry\ sample}$)	Water contact angle (º)
T-T	1.20 ± 0.15	53.23 ± 0.26	7.98 ± 0.04	0.43 ± 0.05	30.30 ± 2.47
G-G	1.48 ± 0.02	53.45 ± 0.15	7.98 ± 0.04	0.53 ± 0.01	92.40 ± 2.68
T-G[a]	1.90 ± 0.12	51.59 ± 1.05	7.65 ± 0.32	0.68 ± 0.05	13.90 ± 4.17
T-G[a]					74.70 ± 5.09
T-T*[b]	0.36 ± 0.06	55.25 ± 0.20	8.77 ± 0.10	-	10.10 ± 0.10
G-G*[b]					9.10 ± 0.60

[a]Underlined letters represent the hydrogel surface that was in contact with Teflon® (T) and glass (G) for T-G mold assemblies;

[b]Poly(HEMA) hydrogels synthesized in Teflon®-Teflon® (T-T*) and glass-glass (G-G*) mold assemblies for comparison purposes.

Movie S3.1 Ionic strength response of T-T, G-G and T-G hydrogels. (https://www.sciencedirect.com/science/article/pii/S2352940720301554?dgcid=coauthor#sec0022)

Movie S3.2 Single directional bending profile of T-T hydrogel in deionized water. (https://www.sciencedirect.com/science/article/pii/S2352940720301554?dgcid=coauthor#sec0022)

Movie S3.3 Bi-directional bending profile of T-T hydrogel in deionized water. (https://www.sciencedirect.com/science/article/pii/S2352940720301554?dgcid=coauthor#sec0022)

Movie S3.4 Bi-directional bending profile of T-T hydrogel in acidic and alkaline media. (https://www.sciencedirect.com/science/article/pii/S2352940720301554?dgcid=coauthor#sec0022)

Movie S3.5 Bending angle profiles of T-T and G-G hydrogels loaded with NaCl ions . (https://www.sciencedirect.com/science/article/pii/S2352940720301554?dgcid=coauthor#sec0022)

Appendix C

Supporting information of Chapter 4

Structural illustration of methyl orange (MO), bromocresol green (BG) and lidocaine hydrochloride (LH) molecules utilized in charge density and dye adsorption measurements, and *in vitro* iontophoretic permeation/release experiments, respectively; Scheme of vertical Franz cell utilized for passive (0 mA/cm^2) and electro-assisted (0.56 mA/cm^2) permeation of LH measurements; Characteristic peaks of chitosan and s-IPNs obtained ^{13}C-NMR measurements; Bromocresol green adsorption capacity profiles of the s-IPN hydrogels in different aqueous media, namely bi-distilled water (pH = 6.5, I ~ 0 M), PBS (pH = 7.4, I = 0.17 M) and phosphate buffer (pH = 9.4, I = 0.17 M) at room temperature (~ 23 ºC); Thermogravimetric profiles of the prepared hydrogels obtained by DSC and TGA measurements; Elemental analysis of synthesized hydrogels; Movies of mechanical stability in bi-distilled water and fast swelling/deswelling response of different prepared hydrogels.

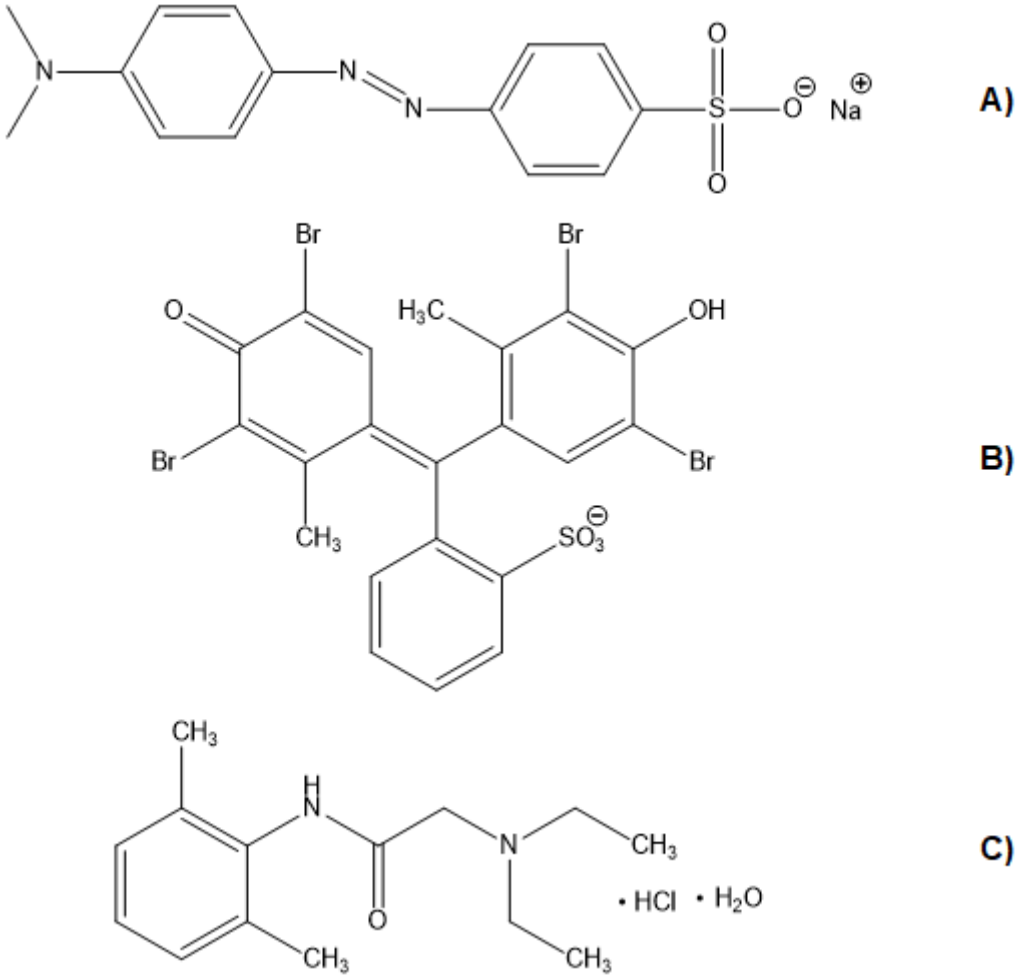

Figure S4.1 Chemical structure representation of ionic model molecules employed in this work: methyl orange, (MO) (A) bromocresol green (BG) (B), and lidocaine hydrochloride (LH) (C).

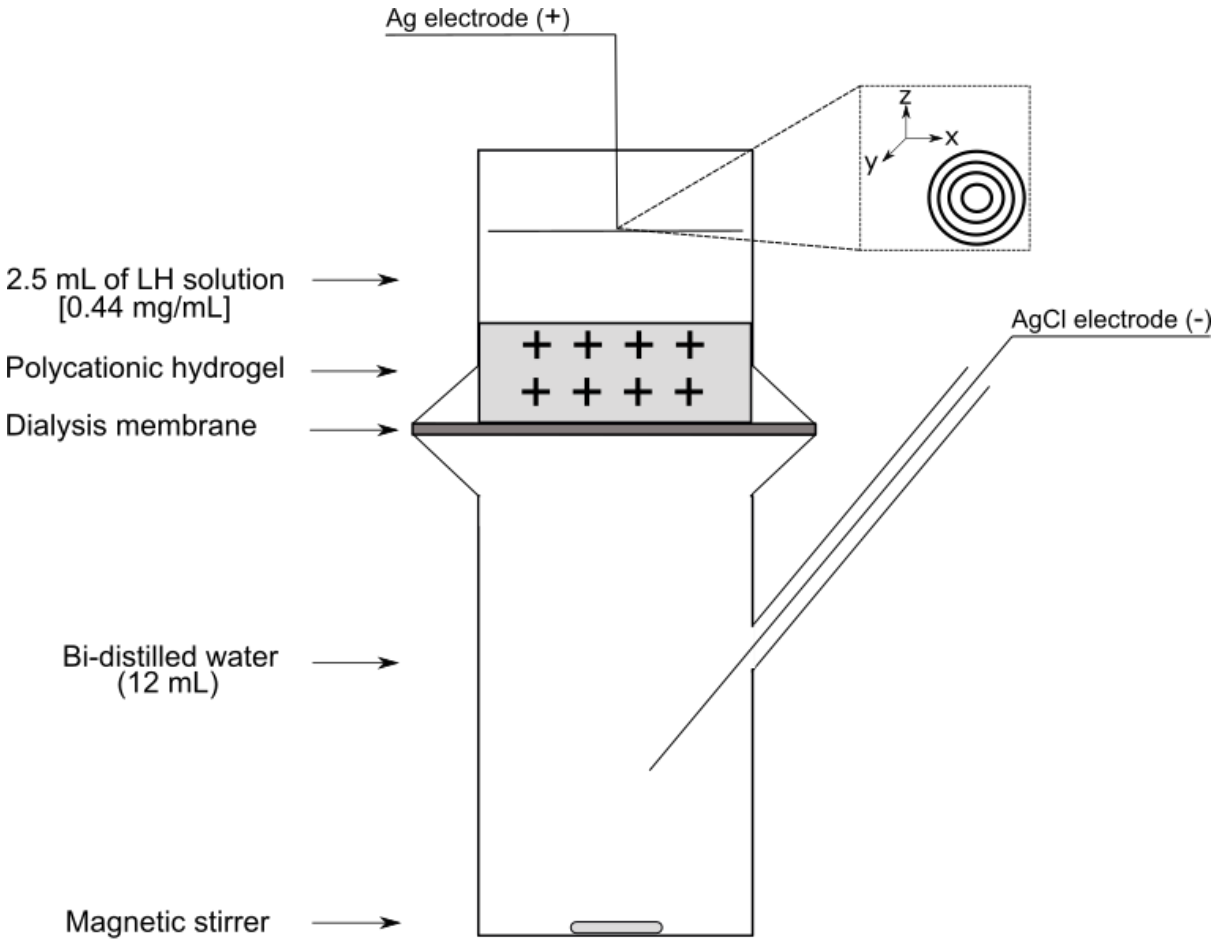

Figure S4.2 Schematic representation of the modified Franz cell unit employed for anodal permeation and lidocaine hydrochloride release experiments.

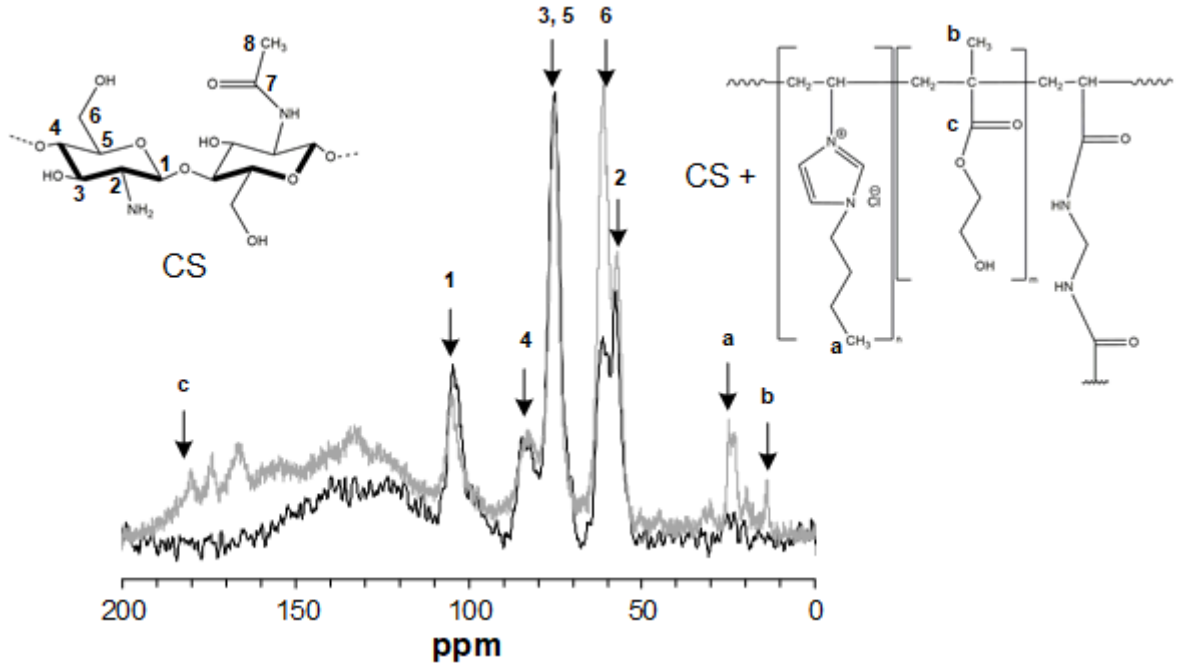

Figure S4.3 ^{13}C-CP/MAS solid state NMR spectra of deprotonated chitosan (DCS) (black line) and of s-IPN/CS/Co-PIL hydrogels (grey line). Represented spectra are normalized by the most intense peak of DCS at 74.85 ppm.

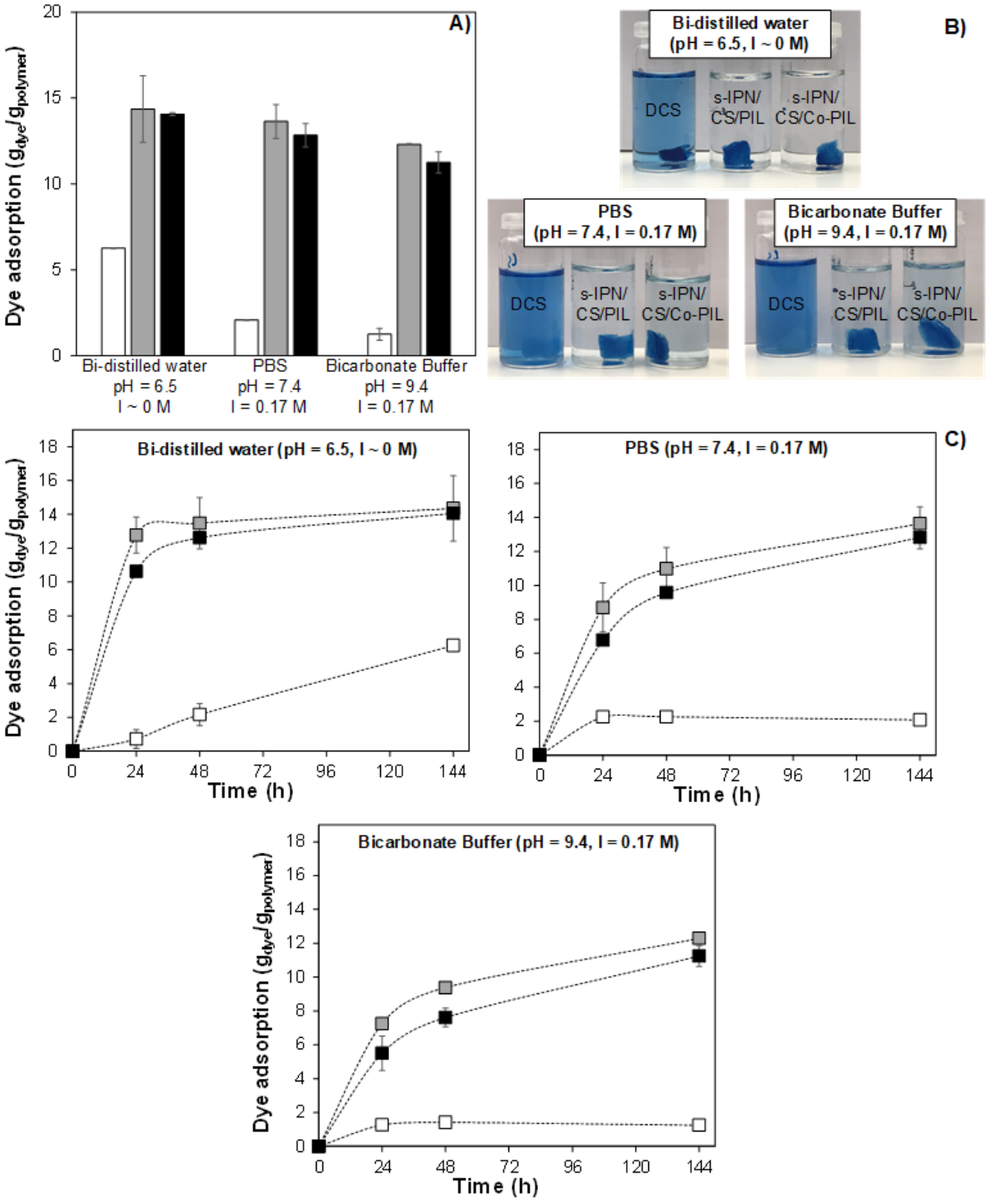

Figure S4.4 (A) Bromocresol green adsorption capacity up to 144 h of contact in different aqueous media: bi-distilled water (pH = 6.5, I ~ 0 M), PBS (pH = 7.4, I = 0.17 M) and Bicarbonate Buffer (pH = 9.3, I = 0.17 M). (B) Illustration of each aqueous media after 144 h of contact with the hydrogels. (C) Bromocresol green adsorption kinetics in different aqueous media. Samples were coded as: DCS (□), s-IPN/CS/PIL (■) and s-IPN/CS/Co-PIL (■). Experiments were conducted at room temperature (~ 23 ºC).

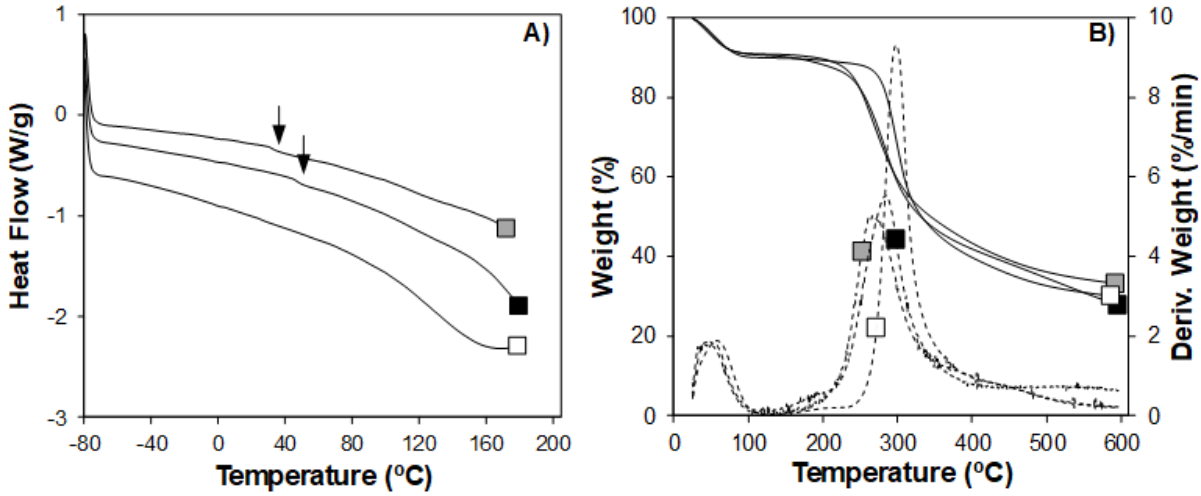

Figure S4.5 DSC thermograms (exothermal events oriented up) (A) and thermogravimetric (full line) and differential thermogram (DTG) (dashed line) profiles (B) of the prepared hydrogels. Samples were coded as: DCS (□), s-IPN/CS/PIL (■) and s-IPN/CS/Co-PIL (■).

Table S4.1 Average content (% w/w) of nitrogen (N), carbon (C) and hydrogen (H) in the synthesized hydrogels obtained from elemental analysis (after washing procedures).

Samples	N % (w/w)	C % (w/w)	H % (w/w)
DCS	6.15 ± 0.09	36.59 ± 0.12	7.61 ± 0.34
s-IPN/CS/PIL	7.12 ± 0.10	38.76 ± 0.03	7.64 ± 0.09
s-IPN/CS/Co-PIL	7.10 ± 0.01	39.23 ± 0.10	7.41 ± 0.34

Movie S4.1 Mechanical stability in bi-distilled water at room temperature (~ 23 ºC). of synthesized s-IPN hydrogels namely, s-IPN/CS/poly(HEMA), s-IPN/CS/PIL and s-IPN/CS/Co-PIL. (on-line link to be obtained)

Movie S4.2 Fast swelling/deswelling of IL-functionalized s-IPN hydrogels at room temperature (~ 23 ºC). (on-line link to be obtained)